Exergy-based performance assessment and optimization potential of refrigeration plants in air-conditioning applications

Lorenz Brenner

HAL Id: tel-03213647
https://theses.hal.science/tel-03213647

Submitted on 30 Apr 2021

N°d'ordre NNT : 2021LYSEI014

THESE de DOCTORAT DE L'UNIVERSITE DE LYON
opérée au sein de
L'INSA LYON

Ecole Doctorale N° 162
Mécanique, Énergétique, Génie civil, Acoustique

Spécialité / discipline de doctorat :

Thermique Énergétique

Soutenue publiquement le 24/02/2021, par :
Lorenz Hermann BRENNER

Exergy-based performance assessment and optimization potential of refrigeration plants in air-conditioning applications

Devant le jury composé de :

MME EICKER Ursula	Professeur des Universités Université Concordia, Canada	Présidente
M. BADEA Adrian	Professeur des Universités Université "Politehnica" Bucarest, Roumanie	Rapporteur
M. JOUBERT Patrice	Professeur des Universités Université de La Rochelle, France	Rapporteur
M. TILLENKAMP Frank	Professeur des Universités ZHAW, Suisse	Co-encadrant
M. GHIAUS Christian	Professeur des Universités INSA Lyon, France	Directeur de thèse
M. RUBINO Ruello	R&D Expert – Modeling Carrier scs, France	Invité

Département FEDORA – INSA Lyon - Ecoles Doctorales – Quinquennal 2016-2020

SIGLE	ECOLE DOCTORALE	NOM ET COORDONNEES DU RESPONSABLE
CHIMIE	**CHIMIE DE LYON** http://www.edchimie-lyon.fr Sec. : Renée EL MELHEM Bât. Blaise PASCAL, 3e étage secretariat@edchimie-lyon.fr INSA : R. GOURDON	**M. Stéphane DANIELE** Institut de recherches sur la catalyse et l'environnement de Lyon IRCELYON-UMR 5256 Équipe CDFA 2 Avenue Albert EINSTEIN 69 626 Villeurbanne CEDEX directeur@edchimie-lyon.fr
E.E.A.	**ÉLECTRONIQUE, ÉLECTROTECHNIQUE, AUTOMATIQUE** http://edeea.ec-lyon.fr Sec. : M.C. HAVGOUDOUKIAN ecole-doctorale.eea@ec-lyon.fr	**M. Gérard SCORLETTI** École Centrale de Lyon 36 Avenue Guy DE COLLONGUE 69 134 Écully Tél : 04.72.18.60.97 Fax 04.78.43.37.17 gerard.scorletti@ec-lyon.fr
E2M2	**ÉVOLUTION, ÉCOSYSTÈME, MICROBIOLOGIE, MODÉLISATION** http://e2m2.universite-lyon.fr Sec. : Sylvie ROBERJOT Bât. Atrium, UCB Lyon 1 Tél : 04.72.44.83.62 INSA : H. CHARLES secretariat.e2m2@univ-lyon1.fr	**M. Philippe NORMAND** UMR 5557 Lab. d'Ecologie Microbienne Université Claude Bernard Lyon 1 Bâtiment Mendel 43, boulevard du 11 Novembre 1918 69 622 Villeurbanne CEDEX philippe.normand@univ-lyon1.fr
EDISS	**INTERDISCIPLINAIRE SCIENCES-SANTÉ** http://www.ediss-lyon.fr Sec. : Sylvie ROBERJOT Bât. Atrium, UCB Lyon 1 Tél : 04.72.44.83.62 INSA : M. LAGARDE secretariat.ediss@univ-lyon1.fr	**Mme Sylvie RICARD-BLUM** Institut de Chimie et Biochimie Moléculaires et Supramoléculaires (ICBMS) - UMR 5246 CNRS - Université Lyon 1 Bâtiment Curien - 3ème étage Nord 43 Boulevard du 11 novembre 1918 69622 Villeurbanne Cedex Tel : +33(0)4 72 44 82 32 sylvie.ricard-blum@univ-lyon1.fr
INFOMATHS	**INFORMATIQUE ET MATHÉMATIQUES** http://edinfomaths.universite-lyon.fr Sec. : Renée EL MELHEM Bât. Blaise PASCAL, 3e étage Tél : 04.72.43.80.46 infomaths@univ-lyon1.fr	**M. Hamamache KHEDDOUCI** Bât. Nautibus 43, Boulevard du 11 novembre 1918 69 622 Villeurbanne Cedex France Tel : 04.72.44.83.69 hamamache.kheddouci@univ-lyon1.fr
Matériaux	**MATÉRIAUX DE LYON** http://ed34.universite-lyon.fr Sec. : Stéphanie CAUVIN Tél : 04.72.43.71.70 Bât. Direction ed.materiaux@insa-lyon.fr	**M. Jean-Yves BUFFIÈRE** INSA de Lyon MATEIS - Bât. Saint-Exupéry 7 Avenue Jean CAPELLE 69 621 Villeurbanne CEDEX Tél : 04.72.43.71.70 Fax : 04.72.43.85.28 jean-yves.buffiere@insa-lyon.fr
MEGA	**MÉCANIQUE, ÉNERGÉTIQUE, GÉNIE CIVIL, ACOUSTIQUE** http://edmega.universite-lyon.fr Sec. : Stéphanie CAUVIN Tél : 04.72.43.71.70 Bât. Direction mega@insa-lyon.fr	**M. Jocelyn BONJOUR** INSA de Lyon Laboratoire CETHIL Bâtiment Sadi-Carnot 9, rue de la Physique 69 621 Villeurbanne CEDEX jocelyn.bonjour@insa-lyon.fr
ScSo	**ScSo*** http://ed483.univ-lyon2.fr Sec. : Véronique GUICHARD INSA : J.Y. TOUSSAINT Tél : 04.78.69.72.76 veronique.cervantes@univ-lyon2.fr	**M. Christian MONTES** Université Lyon 2 86 Rue Pasteur 69 365 Lyon CEDEX 07 christian.montes@univ-lyon2.fr

*ScSo : Histoire, Géographie, Aménagement, Urbanisme, Archéologie, Science politique, Sociologie, Anthropologie

Acknowledgments

First of all, I would like to express my gratitude to Prof. Dr. Christian Ghiaus, who supervised the work, accompanied me throughout the PhD process and always supported me when it was necessary. I would also like to thank Prof. Dr. Frank Tillenkamp, who co-supervised the thesis. I am thankful for the opportunity that I could carry out the dissertation in parallel to my employment at the IEFE and for the freedom I had during my work. It was always a pleasure to work with both supervisors and I am grateful that they took time for discussions also in hectic moments as well as that they showed always trust in my work. I will definitely miss our collaboration.

The thanks for the valuable support during the course of the present work goes also to all participating experts and companies who took the time for a discussion and provided technical information, as well as to the Swiss Federal Office of Energy for partially funding the project.

Furthermore, I would like to thank all my friends and people I met during my time at the IEFE as well as during my studies. They made the last years a lot easier, be it through exciting discussions, sports activities (IEFE Sports) as well as the one or other beer including a game of *Jass*.

Ultimately, a very big thank you goes to my family, especially my parents, who have always supported and motivated me and never questioned any of my decisions. Most of all, I am extremely grateful for the support of my partner Lena and the patience she has shown. Thanks to her, I was always aware that there are other things in life than exergy analysis.

Lorenz Brenner

March 2021

Abstract

A significant amount of energy consumption in buildings is due to heating, ventilation and air-conditioning systems. Among other systems, refrigeration plants are subject of efficiency improvements. However, actual operating conditions of such plants and the performance must be known as well as any eventual optimization potential identified before enhancements can take place. Energy and exergy analyses have been widely used to assess the performance of refrigeration systems. Among others, exergy efficiency is used as an indicator to determine the system performance; however, the practical achievable values are unknown. Therefore, this work proposes a practice-oriented evaluation method for refrigeration plants, based on exergy analysis and technical standards as baseline. The identification of possible enhancements is highly relevant in practice, as measures which improve the system effectiveness most likely prevent frequent shortcomings during refrigeration plant operation. With the introduced optimization potential index (OPI), the achievable enhancements compared to the state of the art in technology and the performance are identified at a glance regardless the complexity of the system. By dividing the plant into different subsystems, each of them can be assessed individually. Laypersons can easily determine the system operating state and subsequently, if needed, initiate a detailed analysis as well as appropriate countermeasures by specialist. Moreover, modeling is seen as an appropriate method to determine additional reference values for refrigeration machines if none are available according to technical standards. Among different modeling techniques, artificial neural network models reveal the best performance for the present application. The application, functionality and purpose of the presented method is exemplified on two numerical test cases and on a real field plant as a case study. The investigation reveals an adequate operation of the studied field plant in general, where three out of seven cooling locations have performance issues. The reason should be identified in a subsequent detailed study. Overall, the auxiliary electrical exergy input shows the same magnitude as the thermal exergy input. This emphasizes the importance of minimizing the electrical energy usage, as it is the main overhead in the operating cost of refrigeration plants and also to achieve an increase in system performance. Moreover, measuring concepts of real systems are analyzed and the corresponding retrofitting costs for the application of the presented approach are identified. It is shown that a retrofit of the instrumentation can be worthwhile if the refrigeration plant already comprises a measuring concept close to the state of the art.

Keywords: optimization potential evaluation method, exergy analysis, vapor compression refrigeration plants, optimization potential index, OPI, free cooling

Résumé

Une grande partie de la consommation d'énergie dans les bâtiments est due aux systèmes de chauffage, de ventilation et de climatisation. Entre autres systèmes, les systèmes de réfrigération font l'objet de mesures d'amélioration de l'efficacité. Néanmoins, les conditions opérationnelles réelles de ces installations et leurs performances doivent être connues, ainsi que tout potentiel d'optimisation éventuel, avant que des améliorations puissent être réalisées. Les analyses exergétique et énergétiques ont été largement utilisées pour évaluer la performance des systèmes de réfrigération. Entre autres, l'efficacité exergétique est utilisée comme indicateur pour déterminer la performance du système, mais les valeurs réalisables dans la pratique sont inconnues. Par conséquent, ce travail propose une méthode d'évaluation pratique des systèmes de réfrigération basée sur une analyse exergétique et des normes techniques comme base de référence. L'identification des améliorations possibles est pertinente dans la pratique, car les mesures qui améliorent l'efficacité du système permettent probablement d'éviter de fréquentes déficiences pendant l'usage. Avec l'*optimization potential index* (OPI) introduit dans cet ouvrage, les améliorations réalisables par rapport à l'état de l'art de la technologie et la performance sont identifiées d'un seul coup d'œil, quelle que soit la complexité du système. En divisant l'installation en différents sous-systèmes, chacun peut être évalué individuellement. Les non-spécialistes peuvent facilement déterminer l'état de fonctionnement du système et ensuite, si nécessaire, lancer une analyse détaillée ainsi que des contre-mesures appropriées. De plus, la modélisation est considérée comme une méthode appropriée pour déterminer des valeurs de référence si aucune n'est disponible selon les normes techniques. Parmi les différentes techniques de modélisation, les modèles *artificial neural network* révèlent les meilleures performances pour l'application présentée. L'application, la fonctionnalité et l'objectif de la méthode présentée sont illustrés par deux cas numériques et sur une installation réelle. La recherche révèle un fonctionnement approprié de l'installation étudiée en général, où trois des sept espaces conditionnés ont des problèmes de performance. La raison devrait être identifiée dans une étude détaillée ultérieure. Dans l'ensemble, l'apport d'exergie électrique auxiliaire est du même ordre que l'apport d'exergie thermique. Cela souligne l'importance de réduire la consommation d'énergie électrique au minimum, car elle constitue le facteur principal dans le coût d'exploitation des installations de réfrigération et permet également d'augmenter la performance du système. En outre, les concepts de mesure des systèmes réels sont analysés et les coûts de mise à jour correspondants pour l'application de l'approche présentée sont identifiés. Il est démontré qu'une mise à jour de l'instrumentation peut être rentable, si l'installation frigorifique comprend déjà un concept de mesure proche de l'état de la art.

Mots-clés: méthode d'évaluation du potentiel d'optimisation, analyse exergétique, installations de réfrigération à compression de vapeur, *optimization potential index*, OPI, *free cooling*

Nomenclature

Abbreviations

AHU	air-handling unit
ANN	artificial neural network
C	condenser
CFC	chlorofluorocarbon
CHF	Swiss Franc
CL	subsystem cooling location
CPR	compressor
CST	subsystem cold water storage & transport
DC	subsystem dry cooler
E	evaporator
EF	equation fit
EU	European Union
EV	expansion valve
FC	subsystem free cooling
FV	finite volume
GWP	global warming potential
HCFC	hydrochlorofluorocarbon
HFC	hydrofluorocarbon
HFO	hydrofluoroolefins
HVAC	heating, ventilation and air-conditioning
IEA	International Energy Agency
IEFE	Institute of Energy Systems and Fluid Engineering
IHX	internal heat exchanger
MB	moving boundary
MID	magnetic-inductive flow rate sensor
ODP	ozone depletion potential
PC	precooler
PLP	physical lumped parameter
PSO	particle swarm optimization
RC	refrigeration cycle
RM	subsystem refrigeration machine
SC	subcooler
SFOE	Swiss Federal Office of Energy
SIA	Swiss Society of Engineers and Architects
SLHX	suction line heat exchanger
VDMA	Verband Deutscher Maschinen- und Anlagenbau
ZHAW	Zurich University of Applied Sciences

Variables

a	model coefficient	u	specific internal energy [J/kg]
A	heat exchanger surface area [m^2]	U	internal energy [J]
b	specific exergy [J/kg]	v	specific volume [m^3/kg]
B	exergy [J]	V	volume [m^3]
$\dot{B}$	exergy flow rate [W]	w	neuron output weighting [–]
c	specific heat capacity [J/(kg·K)]	W	electrical energy [J]
COP	coefficient of performance [–]	$\dot{W}$	electrical power [W]
CPI	control perfect index [–]	x	model input
CV	coefficient of variation [%]	y	exergy destruction ratio [–] /
E	energy [J]		measured output
EEI	energy efficiency index [–]	$\widehat{y}$	modeled / predicted output
EER	energy efficiency ratio [–]	α	neuron output
$ESEER$	European seasonal energy efficiency ratio [–]	ΔT	temperature difference [K]
f	amplification factor [–]	ε	heat exchanger effectiveness [–]
F	activation function	η	efficiency [–]
h	specific enthalpy [J/kg]	τ	exergetic temperature [–]
H	enthalpy [J]		
$\widehat{H}$	optimum potential [%]		
K	costs [CHF]		
KPI	key performance indicator [–]		
$\dot{m}$	mass flow rate [kg/s]		
MAE	mean absolute error		
MSE	mean-squared error		
n	number of data points / refrigeration machines [–]		
NTU	number of transfer units [–]		
OPI	optimization potential index [–]		
p	pressure [Pa]		
Q	thermal energy [J]		
$\dot{Q}$	heat flow rate (thermal power) [W]		
R^2	coefficient of determination [–]		
RI	relative irreversibility [–]		
$RMSE$	root-mean-squared error		
s	specific entropy [J/(kg·K)]		
S	entropy [J/K]		
$\dot{S}$	entropy production [W/K]		
SPF	seasonal performance factor [–]		
t	time [s]		
T	temperature [K]		
$\overline{T}$	logarithmic mean temperature [K]		
$TCOP$	total coefficient of performance [–]		
$TEPF$	total energy performance factor [–]		

Subscripts

0	reference state for exergy analysis		KC	cold production
act	actual		L	losses
amb	ambient		m	mass
aux	auxiliary		$meas$	measured
ANN	artificial neural network		$mech$	mechnical
c	condensation		out	component / system output
ch	chemical		p	potential / pressure
$cold$	cold side		ph	physical
$cool$	cooling		P	product
C	condenser		PLP	physical lumped parameter
Car	Carnot		Q_0	cold utilization
CL	cooling location		r	refrigerant
CP	circulating pumps		res	residual
CPR	compressor		rev	reversible
CST	cold water storage & transport		RC	refrigeration cycle based
$dest$	destroyed		RM	refrigeration machine
D	(cold water) distribution		sc	subcooling
DC	dry cooler		sh	superheating
DL	data logging		st	data storage
e	evaporation		sys	system
eff	effective		S	storage
el	electrical		th	thermal
en	energetic		tot	total
ex	exergetic		T	transmission
exh	exhaust		TLC	telecommunication equipment
E	evaporator		TS	temperature sensor
EF	equation fit based		un	unused
EM	electric meter		U	useful
FC	free cooling		w	work
FT	fluid transport		$waste$	waste
gen	generated		WT	heat transport
$guess$	guessed			
hot	hot side			
HE	heat exchanger			
HM	heat meter			
HW	hardware			
ihx	internal heat exchanger			
in	component / system input			
$inst$	installation			
$isen$	isentropic			
k	kinetic			

Superscripts

$*$	reference value for the OPI
acc	acceptable
act	actual
adq	adequate
AV	avoidable
EN	endogenous
EX	exogenous
id	ideal
UN	unavoidable

Table of contents

1 Introduction

The world faces an annual increase in energy consumption, which has risen noticeably in recent decades. According to the International Energy Agency (IEA), the total final energy consumption increased worldwide about 30% in the last 15 years [1]. The main reasons for the increasing demand are the advancements in technology, global population growth as well as economic development. A significant amount of the energy consumption in buildings is due to the heating, ventilation and air-conditioning (HVAC) systems. Depending on the climatic region, about 40-70% of the total energy consumption in air-conditioned buildings is due to systems for thermal comfort applications [2]. Thereby, up to 40% of this energy share is consumed by refrigeration machines and plants [3]. Ambient air temperature increase due to the global and local climate change is most likely the main reason for the increased demand of air-conditioning [4]. The growing implementation and dependence on refrigeration systems results in a significant increase in electricity consumption and consequently also in primary energy usage, especially during the warmer months over the year [2]. Consequently, additional power plants, ideally renewable energy sources, are needed in order to cover the increased electricity demand [4]. At the same time, efficient systems are needed in order to reduce the primary energy demand and correspondingly, to minimize the greenhouse gas emissions [2]. Santamouris identified the following possible countermeasures to decrease the cooling energy demand [4]:

- Initiate actions to reduce the effect of occuring climate change, e.g. increase the use of renewable energy sources.

- Enhance building structures and improve their effectiveness, e.g. reduce thermal losses.

- Improve the efficiency of mechanical air-conditioning systems and alternative cooling technologies.

In Switzerland, the Swiss Federal Council initiated a review of the existing energy strategies after the nuclear disaster in Fukushima (2011) [5]. A long-term sustainable energy policy should be evaluated, in which, among other measures, a stepwise reduction and finally a complete shutdown of the in Switzerland existing nuclear power plants is envisaged [5]. From this setting, the Energy Strategy 2050 was developed which contains the following three main strategies [6]:

- Increasing the energy efficiency of buildings, devices, etc.

- Increasing the use of renewable energy sources (hydro, geothermal, solar and wind power as well as biomass).

- Step-wise withdrawing from nuclear energy sources.

This set of measures was successfully approved by the Swiss population in a nationwide referendum in 2017 as new Energy Act (EnA) [7]. In line with the presented strategies, a technical report within the framework of the Swiss Federal Office of Energy (SFOE) program *EnergieSchweiz*[1] was elaborated. It evaluates measures and activities to achieve an increase in energy efficiency of refrigeration plants for air-conditioning applications [8]. There is currently no reliable market data on installed refrigeration plants in Switzerland, but according to estimations, around 30'000 air-conditioning refrigeration systems with more than 3 kg of refrigerant have been installed (status 2015), which have a total electrical power consumption of 1150 MW [8]. According to the authors and the involved experts in the study, a well-designed and correctly controlled refrigeration plant, which has a regular maintenance, can greatly reduce the energy consumption and the cooling costs. The consumers have also a significant influence through their behavior on energy consumption and expenses [8]. They state also, that reasons for efficiency deficits in refrigeration plants are manifold, which concern all the different actors in the field. As a consequence, the resulting action plan from the study includes projects to create tools and information bases for the various actors in the field of air-conditioning refrigeration and for implementation in the market [8]. The present operating conditions of refrigeration plants and the performance must be known as well as any eventual optimization potential identified before enhancements can take place.

At the Institute of Energy Systems and Fluid Engineering (IEFE) at the Zurich University of Applied Sciences (ZHAW) this led to the idea of developing a simple, practical and widely applicable approach for performance analysis and identification of possible optimization potentials of refrigeration plants with respect to the state of the art in technology. It should help actors in the industry to identify issues, and also, to raise awareness for an efficient refrigeration plant operation. If possible, the methodology should also serve as a preliminary tool to identify eventual problems already in the planning stage. Based on a preliminary study of Krütli *et al.* [9], the present work focuses on the further development of a goal-oriented assessment method for refrigeration plants in air-conditioning applications and to elaborate missing components. The following main objectives were considered during the development:

- Focus on water-water refrigeration plants (no devices with direct evaporation and condensation) including secondary hydraulic circuits with the corresponding auxiliary devices.

- Determining possible optimization potentials and system performance on a daily basis with respect to the state of the art in technology. If possible, based on enacted technical

---

1 *EnergieSchweiz* is since 2001 a platform initiated by the Federal Council, which unites all the activities of the SFOE in the fields of renewable energies and energy efficiency.

standards and regulations, as their fulfillment is mostly required and specified in tenders and contracts, respectively.

- Assessment of individual subsystems.

- Straightforward interpretation of the results. It should not require specialists to determine whether there is a need to take action on an installation.

- Wide applicability in practice. If possible, implementation with state-of-the-art measuring concepts of refrigeration plants.

- Low cost with acceptable compromises in accuracy.

- Possible application in monitoring systems.

Chapter 2 presents the state of the art of refrigeration systems and their performance evaluation. First, the typical structure of such systems is shown. Subsequently, existing energy- and exergy-based assessment approaches with corresponding performance key figures are presented and refrigeration system enhancements in this context discussed. Additionally, frequent shortcomings in refrigeration plant implementation and operation are revealed.

In chapter 3, the relevant principles and methods of the proposed exergy-based evaluation method are presented. Exergy analysis principles are discussed and the division of typical refrigeration plants into different subsystems is shown. Subsequently, novel key figures for the determination of eventual optimization potentials according to the state of the art in technology are proposed for two different operation modes of refrigeration plants (refrigeration machine and free cooling operation). As not all reference values can be determined by technical standards, the method comprises the modeling of refrigeration machines, especially to correctly determine the part load conditions of the latter for the evaluation. Accordingly, four different refrigeration machine models and the corresponding principles are presented as well as analyzed.

Chapter 4 presents the investigated systems and procedures in the study. This comprises two numerical test cases, a laboratory test rig at the IEFE and a real field plant located in Winterthur, Switzerland.

In chapter 5, the outcome of the whole analysis is elaborated and discussed. First, the modeling results are shown, where from the four different models the most promising one is identified. Subsequently, the application, functionality and purpose of the proposed evaluation method is exemplified with the numerical test cases and experimental data from the field plant as a case study.

Chapter 6 evaluates measuring concepts of real field plants and estimates eventual retrofitting costs for the application of the proposed evaluation method. The acquisition process of technical data of refrigeration plants from a variety of actors in the industry is presented and subsequently, where possible, their instrumentation is analyzed. Individual retrofitting cost estimates are carried out for each measuring equipment, and finally, an overall retrofitting expense for each investigated field plant is elaborated and discussed.

Finally, chapter 7 gives an overall conclusion of the present work, while further need of research is discussed and possible next steps are proposed in chapter 8.

All the presented methods, procedures and results are part of or a subsequent development of two journal publications and a technical report [10–12].

2 State of the art of performance evaluation of refrigeration systems

In the present chapter, the state of the art of assessment methods and key figures for determining the effectiveness, operating conditions and optimization potentials of refrigeration systems as well as analyses and performance enhancements in this context are presented (see section 2.3). Frequent problems in refrigeration plant implementation and operation are discussed (see section 2.4). Refrigeration systems for air-conditioning applications consist basically of vapor compression refrigeration machines, heat exchangers and secondary transport systems (pipes, circulating pumps), whose structures are elaborated subsequently in section 2.1 and 2.2.

2.1 Refrigeration machine

Next to ventilation or air-handling units, HVAC systems comprise usually a refrigeration system with a single or multiple refrigeration machines (depending on the system size) to generate the cooling. In such a device, thermal energy is transferred from a cold to a hot reservoir with a thermodynamic cycle by consuming electrical energy (see Fig. 2.1). If the main goal of the device is to generate usable heat from the cold source, e.g. the environment, one refers to a heat pump. If the device is used to generate cold, it is referred to a refrigeration machine. A distinction is made between absorption and vapor compression cycles. In absorption refrigeration processes, the working fluid is absorbed by a solvent in an absorber. Subsequently, it is pumped to a higher pressure level and expelled again with the supply of heat in a generator. In vapor compression processes, the pressure increase of the working fluid (also denoted refrigerant, see appendix A.1) is carried out with mechanical work of a compressor. In air-conditioning, about 90% of the employed devices are vapor compression refrigeration machines [13]. Therefore, the present work focuses on this technology. Fig. 2.2 shows schematically the vapor compression refrigeration cycle with the main components of the machine in its basic form, which are:

- the compressor,
- the condenser,
- the expansion valve,
- and the evaporator.

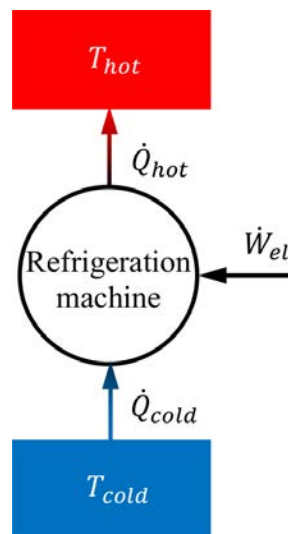**Figure 2.1** – Schematic of a refrigeration machine with a cold region at temperature T_{cold}, a hot region at temperature T_{hot}, the heat flow rates $\dot{Q}_{cold}$ and $\dot{Q}_{hot}$, as well as the electrical power input $\dot{W}_{el}$.

The compressor increases the pressure of the refrigerant, which is in superheated vapor state (see Fig. 2.2, process $1 \to 2$). The compression may be achieved with either displacement (reciprocating, screw, scroll or rotary) or dynamic (turbo) compressors [14]. Mostly, reciprocating compressors are used in air-conditioning refrigeration machines. There are three different compressor drive combinations, namely open, semi-hermetic and hermetic [15]. It is not related to the compression method but on their technical realisation. Open compressors have the compression unit and the motor physically separated, where the seal of the shaft guide separates the motor from the refrigerant circuit. They are typically used in large refrigeration systems, where the motor should be easy accessible for maintenance. Semi-hermetic compressors have both components integrated in the same housing. They are used in mid-range systems and maintenance is still possible, but are more sensible to contaminations. Hermetic compressors are used in small scale systems, e.g. refrigerators, and are hermetically sealed when mounted. Therefore, no maintenance is possible and in case of a failure the whole compressor has to be replaced.

In the next step (see Fig. 2.2, process $2 \to 3$), the heat is released over a heat exchanger, the condenser, at the high pressure level. The refrigerant is cooled down, liquefied and depending on the heat exchanger also subcooled. Typically, the condenser is designed as a tube bundle or plate heat exchanger. The heat dissipation can be achieved with several heat exchangers and thus on different temperature levels. If the temperature level of the condensation process is elevated, a portion of the released heat may be utilized further in heat recovery systems.
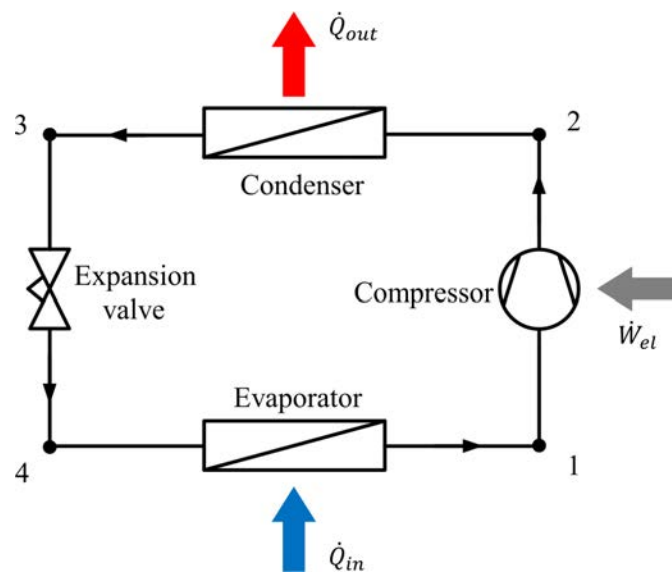

Figure 2.2 – Basic components of a vapor compression refrigeration machine (adapted from [16]).

Subsequently, the refrigerant is expanded with an expansion valve to a lower pressure and temperature level, respectively (see Fig. 2.2, process $3 \rightarrow 4$). After the process, the refrigerant is in vapor state and is supplied to the evaporator. The expansion is achieved with thermostatic or electronic expansion valves. Thermostatic expansion valves are low-priced and use the suction gas temperature and evaporation pressure as control variables. However, the correct adjustment is time-consuming and the needed level of superheating in the evaporator is usually elevated. Electronic expansion valves use several control variables (e.g. suction gas temperature, evaporation pressure, condensation pressure, subcooling temperature). Therefore, an exact adjustment of the superheating at the controller is feasible. This allows a decreased level of superheating, which is favorable for the refrigeration machine performance [17].

In the last step of the cycle (see Fig. 2.2, process $4 \rightarrow 1$), the cold production is achieved. Heat is removed from a medium to be cooled with a heat exchanger, the evaporator, at the low pressure level. During the process, heat is absorbed by the refrigerant, which evaporates. Similarly to the condenser, the evaporator is typically designed as a tube bundle or plate heat exchanger. It is distinguished between dry and flooded evaporators [14]. In dry evaporation processes, the refrigerant is in superheated (dry) vapor state at the exit. Therefore, it is important that the supplied liquid portion of the refrigerant by the expansion valve is only as large as the heat exchanger is able to fully evaporate under the operating conditions. Liquid refrigerant would damage the compressor (steam hammer effects). This is the reason why the superheating temperature is measured and used as a control variable for the expansion valve. In flooded evaporators, one portion of the refrigerant remains in liquid state in the lower region of the evaporator, while the superheated refrigerant is extracted in the upper area. This allows lower superheating temperatures, but increases the amount of refrigerant needed in the refrigeration machine.

2.2 Refrigeration plant

The refrigeration machine is the main component of refrigeration plants and generates the cooling. The cold water distribution and the heat rejection can be achieved differently, where refrigeration plants for air-conditioning applications are categorized into the following configurations:

- Air-air refrigeration system.
- Air-water refrigeration system.
- Water-water refrigeration system.

2.2.1 Air-air refrigeration system

Fig. 2.3 shows a simplified schematic of an air-air refrigeration system, which consists basically of a refrigeration machine with gas-liquid heat exchangers as evaporator and condenser (e.g. split devices). The room is directly cooled with the air passing the evaporator. Typically, the heat transfer is enhanced with a ventilator and a tube-fin configuration of the heat exchanger. On the hot side, the heat is rejected directly to the environment and has no further use. Such devices are suitable for low cooling loads and when single rooms have to be cooled. These systems have a close relationship to the room in which they are mounted and used. Ideally, they are only switched on when they are actually needed. In addition, they are an inexpensive solution, easy to use and uncomplicated to operate. However, the external devices may interfere with the architectural design of the building and the fan noise may disturb [17]. The air-air systems are generally employed in small scale air-conditioning systems and are not discussed further in the present work.
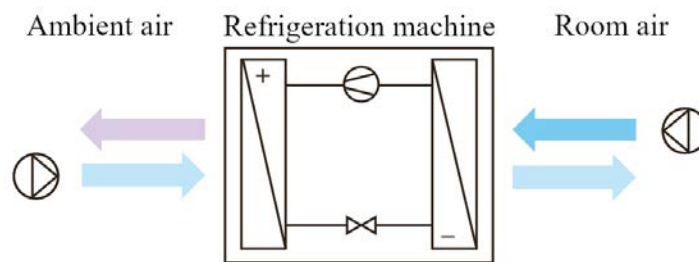
Figure 2.3 – Simplified schematic of an air-air refrigeration system (adapted from [17]).

2.2.2 Air-water refrigeration system

Fig. 2.4 shows schematically an air-water refrigeration plant. In comparison to air-air systems, a secondary hydraulic circuit is employed on the cold side of the refrigeration machine which is cooled down by the evaporator. The design of the chilled water distribution network is discussed

Figure 2.4 – Simplified schematic of a air-water refrigeration system (adapted from [17]).
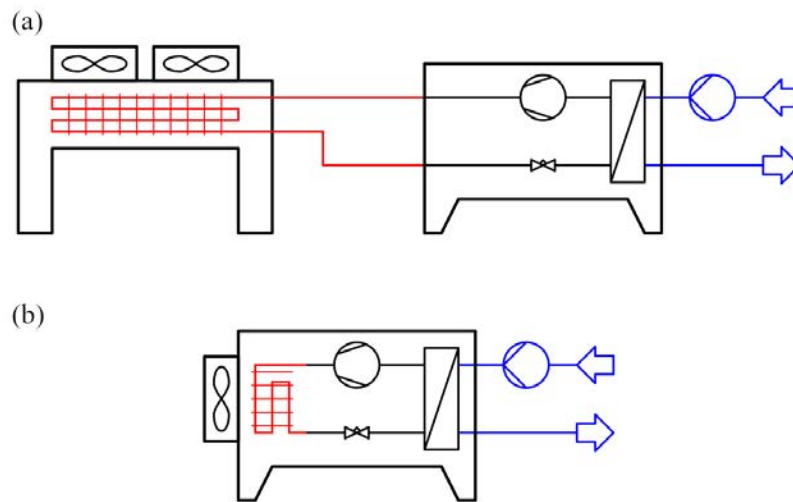
Figure 2.5 – Simplified schematic of air-cooled condensers: (a) separated and (b) integrated (adapted from [9]).

in subsection 2.2.3. In air-water refrigeration plants, the heat from the condenser is rejected directly to the environment, similarly to air-air systems. The heat rejection is achieved with air-cooled condensers and ventilators. They are either integrated in the refrigeration machine (e.g. in roof top units, see Fig. 2.5b) or installed separately (see Fig. 2.5a). If the condenser is deployed separately, e.g. on a roof, junction lines are necessary for the connection to the refrigeration machine. This has the disadvantage that depending on where the chiller is installed, e.g. in a technical room, the quantity of refrigerant required is significantly increased [17]. Air-water refrigeration systems with air-cooled condensers are commonly used for cooling capacities of up to 50 kW [9] and are not discussed further in the present work.

2.2.3 Water-water refrigeration system

Water-water refrigeration plants not only incorporate a secondary hydraulic circuit on the cold but also on the hot side of the refrigeration machine (see Fig. 2.6). They are usually deployed in mid to large scale refrigeration systems with a cooling capacity from 50 kW up to several megawatts, whose structure is explained subsequently.

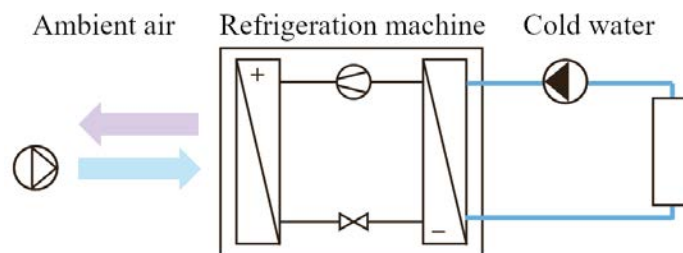**Figure 2.6** – Simplified schematic of a water-water refrigeration system (adapted from [17]).

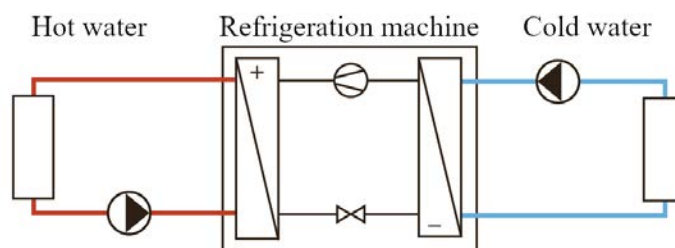**Figure 2.7** – Simplified schematic of the chilled water circuit with multiple cooling locations and an integrated cold water storage (adapted from [17]).

The chilled water distribution network is designed identically as in air-water refrigeration plants. Usually, water or a water-glycol mixture is used as working fluid. The chilled water is transported in the distribution network with the aid of circulating pumps up to the cooling location (see Fig. 2.7). The latter can be an air handling unit (AHU) of a heating, ventilation and air-conditioning (HVAC) system or the end-use location, e.g. a cooling coil in a chilled ceiling system. Depending on the size of the refrigeration plant, the cold water is delivered to multiple buildings or end-use locations. Furthermore, a cold water storage may be integrated to the system if a higher demand of system stability and supply security exists (see Fig. 2.7). The cold water storage can provide cooling capacity when a low cooling demand is present and the chiller is turned off. It serves also as an energy storage and safety reserve, e.g. in the event of a refrigeration machine failure. Moreover, the storage ensures the hydraulic decoupling in the distribution network to omit that different circulating pumps actively influence each other [17].

On the hot side, a water-cooled condenser with another secondary hydraulic circuit is present. The distribution network transports the hot water (also denoted cooling water) to a cooler, where the heat is dissipated to the environment (see Fig. 2.8). The heat rejection is usually carried out with dry coolers, hybrid dry coolers or cooling towers (evaporative coolers) [17]. Dry coolers mainly consist of heat exchangers and ventilators. They have low operating and maintenance

Figure 2.8 – Simplified schematic of the hot water circuit with coolers (adapted from [17]).

costs, but require a large surface area depending on the amount of heat which needs to be rejected. It is important that no recirculation of the heated air is present at the dry cooler. Such short circuits can compromise the heat transfer significantly [17]. Hybrid dry coolers have the same functionality but are additionally wetted, moisted or sprayed with water when higher ambient air temperatures are present. The evaporated water cools the air as well as the heat exchanger surface. This results in an increased heat transfer and a decreased temperature in the hydraulic circuit compared to conventional dry coolers. However, a water supply is necessary and the operating and maintenance costs are elevated [17]. In cooling towers, the hot water from the condenser is injected directly into the air flow of the cooler. This results in an air-water mixture (humidification), which is cooled by the air flow. The humidification with water enables adiabatic cooling, in which a part of the water evaporates. Therefore, the humidified air can be cooled below ambient air temperature. While this system is very effective regarding heat transfer and space requirements, the amount of supplied water is large and needs to be preconditioned. The system also needs frequent cleaning, and thus, the operation and maintenance costs are significantly elevated compared to the other cooling systems [17].

If the temperature level of the condenser side is sufficiently high, a part of the heat may be recovered, e.g. for space heating or domestic hot water (see Fig. 2.9). Similarly to the structure of the chilled water circuit, multiple heating locations and a heat storage may be integrated to the system [17]. The unusable heat is rejected conventionally with the aforementioned coolers.

The use of free cooling is feasible if the surrounding air temperature is substantially lower than at the cooling location. Therefore, this operating mode is mostly present in the colder months of the year. In the simplest form, free cooling is achieved with a heat exchanger arranged in parallel to the refrigeration machine (see Fig. 2.10). The heat exchanger couples both hydraulic circuits and allows an indirect cooling, where the heat is transferred from the cooling location

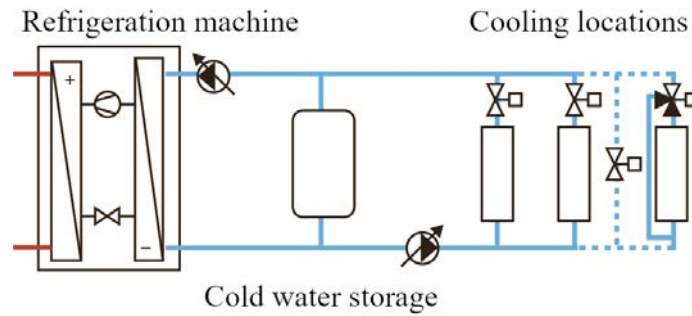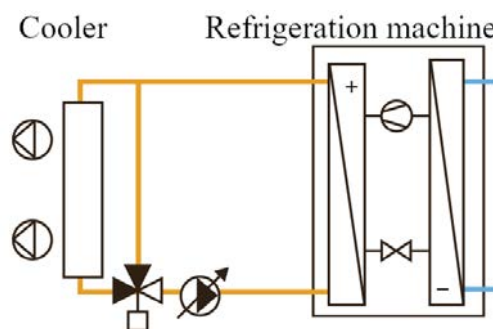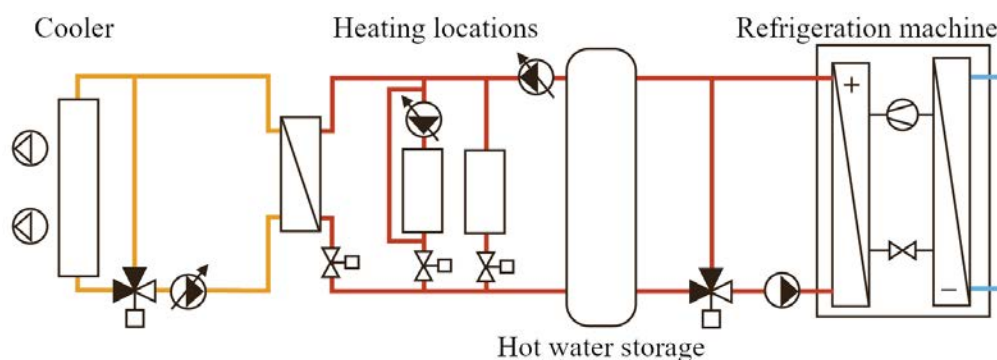**Figure 2.9** – Simplified schematic of the hot water circuit with multiple heating locations and a hot water storage (adapted from [17]).
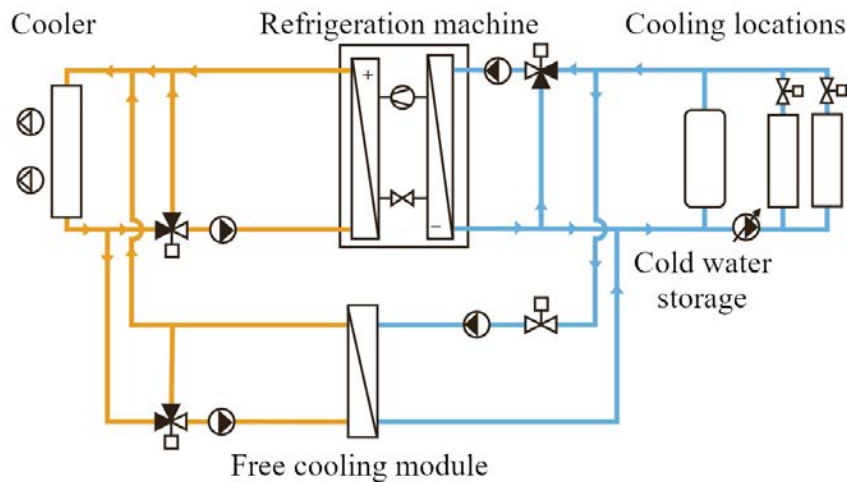
Figure 2.10 – Simplified schematic of a refrigeration plant with free cooling (adapted from [17]).

via the heat exchanger to the coolers and rejected to the environment. The refrigeration machine is usually turned off in free cooling operation and thus, the electrical energy of the compressor can be economized. An exception is a bivalent operation, where the free cooling module is used to precondition the cooling water before entering the evaporator. In order to make optimal use of free cooling, the hot side hydraulic circuit is designed for small temperature differences. This results in large volume flow rates and correspondingly large pipe diameters [17]. One of the main application for free cooling is in refrigeration plants of data centers. Since the chilled water temperature in such systems is elevated, the use of free cooling is economically reasonable and can be realized over longer periods during the year.

2.3 Assessment methods and performance of refrigeration systems

In order to increase the effectiveness of refrigeration systems, different key figures and procedures were applied or developed to examine the energy usage and to determine optimization potentials. In the following, evaluation methods and key figures are discussed, where it is distinguished between energy- and exergy-based approaches. In this context, analyses and performance enhancements of vapor compression refrigeration machines and plants are presented.

2.3.1 Energy-based approaches

The energy analysis is the most common method to evaluate thermodynamic systems involving energy transfer and conversion. It is based on the first law of thermodynamics, where energy is

conserved in every component or process. An energy balance is typically carried out to assess the corresponding incoming and outgoing energy flows of a system or component, while the performance evaluation is then realized in terms of key figures, e.g. ratios of energy output to input. Waste emissions, like heat transfer to the environment, may be determined and reduced accordingly, improving the effectiveness by still ensuring the desired initial task of the system.

The most applied performance indicator in this context is the energy efficiency η_{en}. It generally describes the ratio between the useful and supplied energy or power and is defined as [18, 19]:

$$\eta_{en} = \frac{E_{out}}{E_{in}} \tag{2.1}$$

with E_{in} and E_{out}, the energy input and output of the system, respectively. The key figure provides information on how much input is needed to achieve a desired output. In the context of refrigeration machines, the coefficient of performance COP is widely used as an indicator of performance, which is described as follows [14, 19, 20]:

$$COP = \frac{\dot{Q}_E}{\dot{W}_{CPR}} \tag{2.2}$$

where $\dot{Q}_E$ represents the cooling capacity of the evaporator and $\dot{W}_{CPR}$ the electrical power input of the compressor. Usually, the COP is larger than 1 and determined from data of stationary operating points. The parameters of these operating points, e.g. condensation or evaporation temperature, must be known accordingly to ensure an equitable comparison between different devices. If a whole refrigeration plant is examined, the energy consumption of all auxiliary devices, e.g. circulating pumps in the distribution network, should be considered. The system coefficient of performance is [21]:

$$COP_{sys} = \frac{\dot{Q}_U}{\dot{W}_{CPR} + \dot{W}_{aux}} \tag{2.3}$$

where $\dot{Q}_U$ is the useful thermal power at the cooling location and $\dot{W}_{aux}$ the electrical power input of the auxiliary devices. Another key figure used to determine the performance of refrigeration systems in air-conditioning applications is the energy efficiency ratio EER, which is given by [17, 22]:

$$EER = \frac{\dot{Q}_E}{\dot{W}_{eff}} \tag{2.4}$$

which describes the ratio of the cooling capacity to the effective electrical power input $\dot{W}_{eff}$ to

the refrigeration system. The latter includes the electrical power consumption of the compressor, all control, regulation and safety equipment as well as partially the electrical power consumption of ventilators and pumps. For water cooled refrigeration machines, the EER^+ is applied, where additionally the electrical power consumption of the coolers are considered [17, 22]. To determine the yearly performance of refrigeration systems, the ESEER (European seasonal energy efficiency ratio) finds application. As the cooling demand is usually depending on the season and the refrigeration systems may operate in part-load conditions, the year is divided into four cooling load ranges, whereas each of them is weighted according to an assumed operating time over the year. Consequently, the ESEER is defined as [17, 22]:

$$ESEER = 0.03 \cdot EER_{100\%} + 0.33 \cdot EER_{75\%} + 0.41 \cdot EER_{50\%} + 0.23 \cdot EER_{25\%} \quad (2.5)$$

where $EER_{25\%}$ to $EER_{100\%}$ denote the energy efficiency ratio at 25% to 100% load, respectively. Like the EER, the ESEER applies for refrigeration systems in air-conditioning applications and is not suitable for systems with high internal loads or heat utilization as they typically reveal a different operating scheme [17].

2.3.1.1 Technical standard VDMA 24247-2

A detailed assessment of the refrigeration machine is introduced in the technical standard VDMA 24247-2 [23]. It is mentioned that the influence on the COP due to temperature differences in heat exchangers, which affect the evaporation and condensation temperature, as well as the interaction between system components remains hidden. The key figure value is influenced by a diversity of parameters, and thus, a reliable comparison between refrigeration systems is only
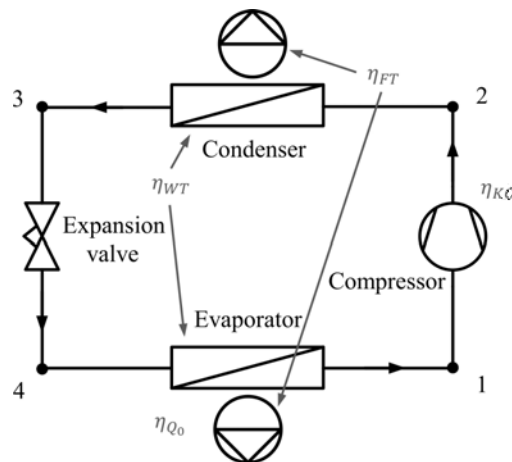

Figure 2.11 – Simplified schematic of a refrigeration machine with the different key figures: cold production efficiency η_{KC}, heat transport efficiency η_{WT}, fluid transport efficiency η_{FT} and cold utilization efficiency η_{Q_0} (adapted from [23]).

possible at the same operating conditions [23]. For those reasons, potentials for achieving the highest possible energy efficiency may remain unexploited. The following four key figures are proposed in the technical standard to allow a comprehensive assessment of the refrigeration machine performance (see Fig. 2.11) [23]:

- Cold production efficiency η_{KC}
- Heat transport efficiency η_{WT}
- Fluid transport efficiency η_{FT}
- Cold utilization efficiency η_{Q_0}

The cold production efficiency η_{KC} compares the real to the ideal refrigeration cycle [23]:

$$\eta_{KC} = \frac{\dot{Q}_E}{\dot{W}_{CPR}} \frac{T_c - T_e}{T_e} \tag{2.6}$$

with the cooling capacity of the evaporator $\dot{Q}_E$ and the electrical power input of the compressor $\dot{W}_{CPR}$. T_e and T_c correspond to the evaporation and condensation temperature, respectively. The performance indicator evaluates the influence of losses during the cold production and is also denoted Carnot quality grade [17]. The heat transport efficiency η_{WT} is defined as [23]:

$$\eta_{WT} = \frac{T_e}{T_U} \frac{T_0 - T_U}{T_c - T_e} \tag{2.7}$$

where T_U is the useful cooling temperature, e.g. of the cooling location, and T_0 the temperature of the heat sink, e.g. the environment. Unfavorable temperature differences in heat exchangers decrease the system performance. Therefore, the key figure evaluates the influence of these differences on the efficiency of the refrigeration machine [23]. The fluid transport efficiency η_{FT} is written as [23]:

$$\eta_{FT} = \frac{\dot{W}_{CPR}}{\dot{W}_{tot}} \tag{2.8}$$

where $\dot{W}_{tot}$ represents the total system power input. The performance indicator assesses the influence of the energy demand of auxiliary devices in the refrigeration machine, e.g. fans of an integrated air-cooled condenser [23]. The cold utilization efficiency η_{Q_0} is given by [23]:

$$\eta_{Q_0} = \frac{\dot{Q}_U}{\dot{Q}_E} \tag{2.9}$$

with the useful thermal power for cooling $\dot{Q}_U$ and the cooling capacity of the evaporator $\dot{Q}_E$. A larger cooling capacity is required to compensate for undesired heat flows. The latter can be

induced by unwanted heat transfer to the refrigeration machine from the environment, e.g. due to insufficient insulation of the pipes. The key figure assesses the influence of undesired heat supply on the cold side on the useful cooling capacity [23]. Further, the technical standard proposes an overall system efficiency, the energy efficiency level η_{tot}, by multiplying the aforementioned key figures with each other [23]:

$$\eta_{tot} = \eta_{KC}\eta_{WT}\eta_{FT}\eta_{Q_0} = \frac{\dot{Q}_U}{\dot{W}_{tot}}\frac{T_0 - T_U}{T_U} \tag{2.10}$$

The key figure can be interpreted as the ratio of the system COP and the COP of a reversible refrigeration cycle. Interestingly, the energy efficiency level corresponds to the definition of the exergy efficiency of a refrigeration plant if T_0 is chosen to be the temperature of the reference environment. However, this coherence is not mentioned in the norm.

2.3.1.2 Technical standard VDMA 24247-7

The assessment of refrigeration plants during operation is described in the technical standard VDMA 24247-7 [24]. The authors state that in order to measure and check the energy efficiency of plants during operation, a continuous monitoring is required, which should already be considered in the planning stage. Consequently, power and energy efficiency key figures can be determined from the measured and logged quantities (temperatures, volume flow rates, etc.) [24].

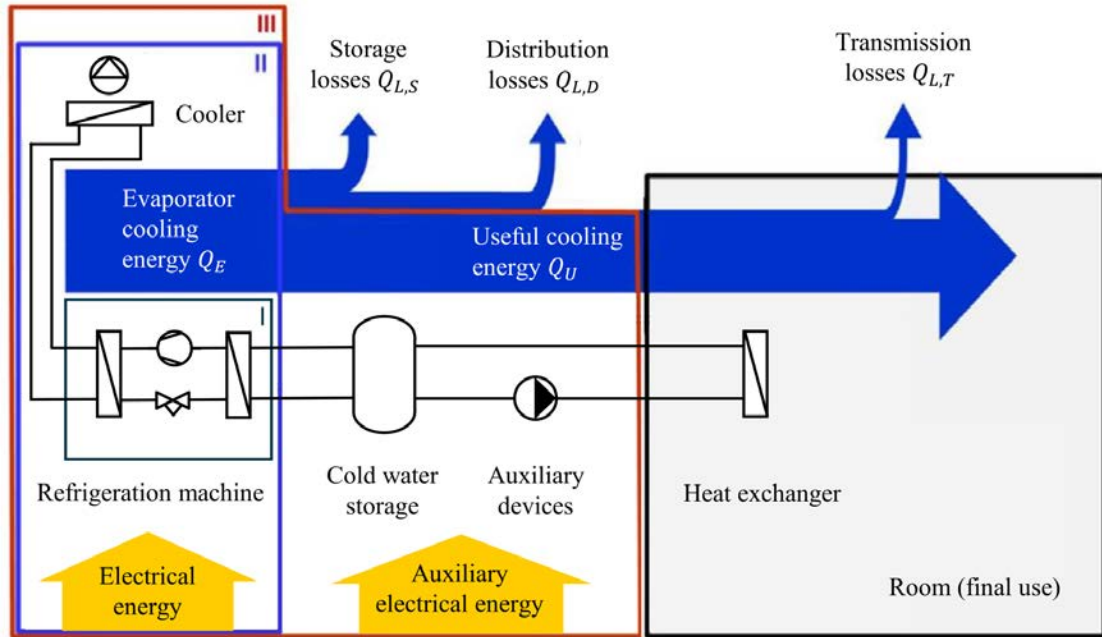

Figure 2.12 – Subsystem boundaries for assessing the refrigeration system: refrigeration machine (I), refrigeration machine including air-cooled condensers or hot side hydraulic circuit (II) and refrigeration plant (III) (adapted from [24]).

The technical standard suggests to use three different subsystems to assess the refrigeration plant (see Fig. 2.12). Subsystem I represents the refrigeration machine and subsystem II the refrigeration machine including air-cooled condensers or the hot side hydraulic circuit. Additionally, subsystem III represents the whole refrigeration plant including the distribution network with auxiliary devices and cold storages [24]. The first key figure defined in the technical standard is the total coefficient of performance TCOP [24]:

$$TCOP = \frac{\dot{Q}_{U,i}}{\dot{W}_{tot,i}} \tag{2.11}$$

where $\dot{Q}_{U,i}$ denotes the measured cooling power and $\dot{W}_{tot,i}$ the measured total electrical power consumption with respect to the selected system boundaries. If subsystem III is evaluated, the TCOP corresponds to the system COP defined in Eq. 2.3. The other key figure, the total energy performance factor TEPF, is given by [24]:

$$TEPF = \frac{\int_{t_1}^{t_2} \dot{Q}_{U,i} \, \mathrm{d}t}{\int_{t_1}^{t_2} \dot{W}_{tot,i} \, \mathrm{d}t} = \frac{Q_{U,i}}{W_{tot,i}} \tag{2.12}$$

with the cooling energy $Q_{U,i}$ and the total electrical energy input $W_{tot,i}$ according to the selected system boundaries as well as the evaluation start and end time, t_1 and t_2, respectively. The key figure describes the ratio of the measured cooling energy to the measured electrical energy consumption of all components related to a specific evaluation period and to the selected subsystem [24]. Therefore, the TEPF estimates the overall performance of the system and has a similar form as the cooling seasonal performance factor (CSPF) [25, 26]. The seasonal performance factor (SPF) is typically used for heat pumps, which is defined as the ratio of the useful heating energy to the total electrical energy input evaluated over a certain time period.

Field tests were carried out, in order to develop a standardized methodology to systematically monitor refrigeration systems and their efficiency [27]. The authors investigated the implementation of the energy efficiency rating approach of the standards VDMA 24247-2 [23] and VDMA 24247-7 [24] on four different field plants. As a result, a basic energy consumption monitoring was possible in most of the cases and potentials for optimization as well as efficiencies at different operating conditions were identified. However, difficulties occurred due to the measuring concepts of some field plants, as not all needed variables were available for monitoring. Thus, the implementation of the energy efficiency assessment for existing systems was difficult or impossible with the pursued method.

2.3.1.3 Reference-based performance indicators

Another approach for assessing a thermodynamic system is to define a key figure, where the actual performance or operating condition of a system is compared to a reference one. As an example, Sorrentino *et al.* introduced a model-based key performance indicator KPI in order to assess and monitor a telecommunication cooling system, where the key figure is defined as [28]:

$$KPI = \frac{EEI_{act}}{EEI_{ref}} \tag{2.13}$$

with the actual energy efficiency index EEI_{act} and the reference or desirable energy efficiency index EEI_{ref} of the investigated telecommunication cooling system. The energy efficiency index EEI is given by [28]:

$$EEI = \frac{\dot{W}_{TLC}}{\dot{W}_{TLC} + \dot{W}_{cool} + \dot{W}_{aux}} \tag{2.14}$$

where $\dot{W}_{TLC}$, $\dot{W}_{cool}$ and $\dot{W}_{aux}$ are the electrical power inputs of the telecommunication equipment, the cooling system and auxiliary devices, respectively. The authors mention two possible applications of the KPI. On the one hand, the key figure may be used to assess the cooling efficiency of the system, meaning to determine if the actual cooling strategy is convenient or not. On the other hand, the key figure may be used as a tool for model-based diagnostics. By comparing the measured (actual) cooling system power consumption to a simulated (reference) one, a faulty behavior may be detected. This reduces the risk of cooling device failure or an increased energy consumption can be avoided. The introduced method is applied for a single room as well as on a central office level. A lumped capacity model of the room developed by the authors was applied and run in parallel to the real system, in order to determine reference values resulting from different cooling strategies [28, 29].

2.3.1.4 Performance analysis and optimization of refrigeration machines

Among others, Gordon *et al.* investigated the behavior of a commercial R123 centrifugal chiller by varying the coolant flow on the secondary side of the condenser [30]. They determined, that an augmentation in coolant flow rate reduces the thermal lift in the compressor and therefore the power consumption decreases. A more significant change in the thermal lift was found at higher cooling loads and thus an improvement of the coefficient of performance COP from 1% in partial and up to 10% in full load operating conditions was observed. Zhao *et al.* carried out a model-based optimization of vapor compression refrigeration cycles [31]. By applying the found

optimized set point to an experimental test rig with R134a as refrigerant, they demonstrated an overall energy saving potential of around 9% compared to traditional on-off controlled systems.

Fritschi *et al.* conducted investigations in parallel compression cycles with carbon dioxide as refrigerant [32]. A numerical model was developed, which showed a good correlation to experimental data, in order to determine ideal operation conditions of the chiller. The conventional (single compressor) operation was compared with the parallel compression configuration, yielding an increase in COP value of up to 20%. Nevertheless, the biggest increases in efficiency are possible under circumstances that would, in any case, have a negative effect on the operation of any refrigeration system. An increase in efficiency of at least 10% is achievable, while still meeting the boundary conditions for an economical reasonable deployment. Refrigeration systems with parallel compressors are particularly well suited to systems with evaporating temperatures below or above 0 °C. However, based on the findings acquired in the study, the use of a parallel compressor in air-conditioning applications can be ruled out due to economic reasons. Furthermore, the study revealed a positive effect on the parallel compression circuit while having a low evaporation temperature and a high temperature at the gas cooler outlet. The latter is a critical factor in the refrigeration system, which determines the subcritical or transcritical operation of the system.

By replacing the conventional expansion valve with an expander, the cooling effect is enhanced by reducing the enthalpy at the evaporator inlet [33]. Also, the compressor power usage is decreased due to the recovery of expansion losses, which results in higher COP values. Expanders are typically used in CO_2 refrigeration cycles, because of the significant effects due to the large pressure differences [34–36]. Baek *et al.* developed a novel piston-cylinder expansion device, where they achieved an increase in system performance by up to 10.5% [37]. Gonçalves *et al.* determined a theoretical increase in COP of up to 5% by implementing an expander with realistic efficiencies in a R134a cycle [38]. The authors found that the efficiency improvement is more noticeable at higher condensing temperatures. Medium scale refrigeration machines with conventional refrigerants and expanders were investigated by Subiantoro *et al.* [39]. The authors showed an ideal COP increase of 19% by using an expander compared to a standard refrigeration cycle with R134a as refrigerant and a cooling capacity of 5.27 kW.

Similarly to expanders, expansion losses can be recovered with the use of ejectors [33]. However, they do not replace the expansion valve but are integrated additionally. With the use of an ejector, the pressure at the compressor suction line is increased. Therefore, the energy consumption of the compressor is reduced. Ersoy *et al.* achieved experimentally a COP increase of up
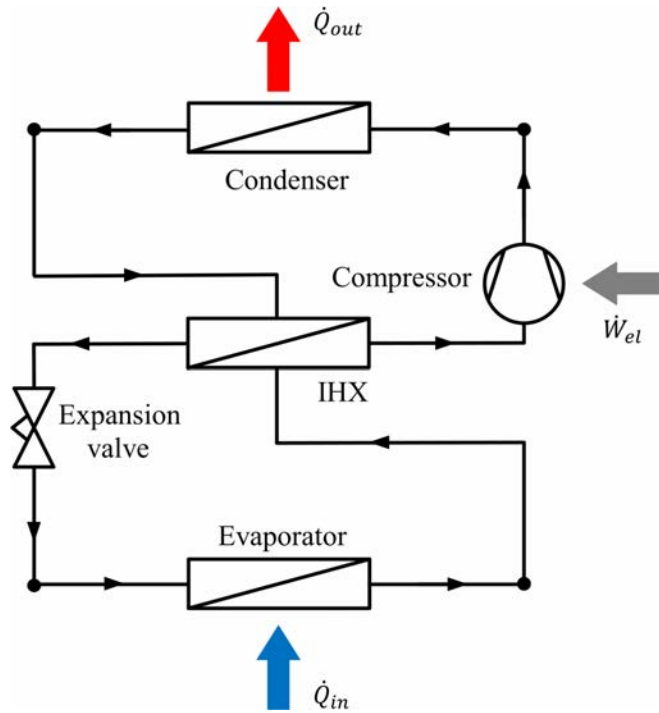
Figure 2.13 – Schematic of a vapor compression cycle with an IHX.

14.5% compared to a conventional refrigeration machine by integrating a two-phase ejector in a R134a refrigeration system [40]. Around 14-17% of the expansion work was recovered in the ejector. Furthermore, they determined a lower pressure drop over the evaporator in the ejector system with same external conditions.

By deploying an internal heat exchanger (IHX) in the compressor suction line, a so called suction line heat exchanger (SLHX), the subcooling on the high pressure and the superheating on the low pressure side is increased, respectively. This leads to a higher evaporator capacity and therefore to an extended cooling potential (see Fig. 2.13) [33]. Furthermore, the SLHX guarantees the supply of superheated steam to the compressor, which is important to omit any mechanical damages. The degree of subcooling might be enhanced as well within the condenser itself (condenser subcooling) or by applying an additional heat exchanger after the condenser in the cycle, the so called subcooler. Pottker *et al.* investigated in an experimental and theoretical study the effects of condenser subcooling and internal heat exchangers regarding the performance of an air-conditioning refrigeration machine with R134a as refrigerant [41, 42]. They demonstrated an increase in COP from 1.66 (near zero condenser subcooling) up to 1.96 (with condenser subcooling). Furthermore, they were able to maximise the COP value to 2.11 by using a SLHX. An increase in cooling capacity of around 8% was shown by Navarro-Esbrí *et al.* by applying an SLHX in a R1234yf refrigeration machine [43].

2.3.1.5 Performance analysis and optimization of refrigeration plants

Regarding the performance of refrigeration plants, Shan *et al.* proposed an improved chiller sequence control strategy for refrigeration plants with centrifugal chillers [3]. Typically, an optimal sequencing of the refrigeration machine operation can improve the plant efficiency and therefore, reduce the electrical energy consumption. The authors showed an energy saving potential of 3% in comparison to the original control strategy. Wei *et al.* investigated a chiller plant with four refrigeration machines, four cooling towers and two cold storages [44]. A data-driven approach was chosen to model the plant and subsequently, to ameliorate the operating conditions. A multi-layer perceptron model was used in order to optimize the on / off strategy of the different refrigeration machines and the temperatures in the plant. The model was applied with measurement data of two days, where the authors demonstrate an energy consumption reduction of approximately 14%. Another study focused on the energy optimization of a multi-chiller plant with cooling towers in a multistory office building [45]. The authors state that the total power consumption of such plants is significant and is increased due to mostly suboptimal plant operation. The refrigeration plants are either operated at design conditions or are only optimized locally. Energy models for the chillers, cooling towers and auxiliary devices were developed, in order to improve the energy utilization. For the optimization routine, the building load (chilled water mass flow rates and temperatures) and ambient conditions were used as inputs. The optimization delivered ideal on / off strategies of the equipment as well as chilled and cooling water conditions. By carrying out three case studies, the authors identified an average energy saving of 20% for small chiller plants and up to 40% for moderate sized refrigeration systems.

Next to the refrigeration machine, the cooler fans and circulating pumps can contribute significantly to the overall system energy consumption. A study was carried out in order to determine the energy savings if variable drives for cooling tower fans are implemented [46]. The system performance was compared to the dual speed mode, where the fan speed automatically switches between a low and a high rotational frequency depending on the needed water temperature leaving the cooling tower. Results showed that with a variable frequency drive, the water consumption was lowered by 13%. Furthermore, for the same cooling load, the overall energy consumption of the refrigeration plant was reduced by 5.8%. Mu *et al.* investigated in optimizations for the condenser water loop of a refrigeration system [47]. They proposed an extremum seeking control scheme which determines the ideal cooling tower fan speed as well as the ideal hot water distribution network mass flow rate. The power consumption of the chiller, the cooler fans and the circulating pumps were used as feedback signals. A simulation study of a virtual

refrigeration plant was carried out, where three different ambient conditions were applied. The authors showed an energy efficiency increase of up to 26% in comparison to fixed operating conditions of the auxiliary devices. Furthermore, they mentioned that model-based optimizations may increase the energy efficiency of refrigeration plants, but can be limited in practice due to sensor errors or model uncertainties.

To further reduce the energy consumption of the refrigeration plant, a free cooling system may be integrated. Yang *et al.* investigated in a refrigeration system with cooling towers and a parallel heat exchanger for free cooling operation in a data center [48]. Their analysis showed an operating cost reduction of the refrigeration plant by more than 50% in free cooling operation. In another study, free cooling for a data center in a hot summer and warm winter region with a cooling load of approximately 10 MW was evaluated [49]. The authors found an annual system COP increase from 5.9 to 7.3 and an energy saving rate of 19.2% if free cooling is fully utilized.

2.3.1.6 Limitations of energy analysis

As seen in the literature review, energy analysis is widely used to thermodynamically examine refrigeration systems and is particularly useful when investigating existing devices. Energy inputs and outputs can be assessed, where the latter can be split into useful and waste energy flows. The performance of refrigeration systems is usually determined and compared in terms of the COP. The latter is also often used in tenders for new plants and in the subsequent commissioning to verify whether the specified performance by the manufacturer is achieved. However, the influence of the operating conditions, e.g. temperatures, on the COP remains hidden. The reason is, that energy can be seen as a measure of quantity, which can neither be destroyed or produced, in accordance with the first law of thermodynamics. All the different forms of energy, e.g. thermal and mechanical energy, are considered to be equal. As a consequence, in energy analysis, the quality of different energy forms and the degradation of energy in a process due to irreversibilities are not considered. This results in some cases to a misleading interpretation of the system performance or wrong indications for optimization. To overcome this issues, the concept of exergy is applied, which is discussed in the subsequent section.

2.3.2 Exergy-based approaches

The exergy method has gained increased attention in the last decades. With the goal to reduce the energy demand of air-conditioning systems in buildings, exergy analyses were carried out for various applications in this context, such as the building envelope [50, 51], building energy systems [52, 53], photovoltaics [54–57], HVAC systems [58–61], heat pumps [62–66] and re-

frigeration systems [43, 67–76]. In general, exergy is defined as the unrestricted convertible portion of energy (maximum work) which can be obtained from any form of energy in a system by reversible interaction with a defined reference environment [77]. In other words, exergy can be seen as a measure of energy quality or useful energy which is fully transformable into any other form of energy and is the counterpart to the inconvertible portion, the anergy. In comparison to energy, exergy is a non conservative quantity. It is destroyed due to irreversibilities in real thermodynamic processes, e.g. in the compression process of a refrigeration machine, which represents a reduction in obtainable work or thermal potential. Such losses are related to the entropy production in the system [78], and thus, exergy analysis associates energy principles with the second law of thermodynamics. When considering solely heat transfer, where no work is obtained or consumed, exergy losses can be interpreted as a reduction in energy quality due to an inappropriate sizing of heat exchanger surfaces and the pumping of the heat transfer medium. Those losses are related to a certain temperature level, which allows an examination of the relationship between mass flow rate and temperature level of the investigated system. In exergy analysis, the quality of different energy flows and the respective losses as well as their magnitude can be identified throughout a system on a detailed level. This highlights different aspects of the energy usage, which are not visible in purely energetic considerations. Reducing exergy losses is the key for optimization, and thus, the exergy analysis is also useful when it comes to the subject of system improvement. Different forms of energy, e.g. electrical and thermal energy, are also comparable with the exergy method, as it is always referred to the same quantity. This enables a relative comparison between systems and processes.

Similarly to energy analysis, an exergy balance can be applied to determine the respective incoming and outgoing exergy flows as well as exergy losses of a system (see subsection 3.1.1.1). Likewise, one of the most applied key figure in exergy analysis is the exergy efficiency η_{ex}. In general it is defined as the ratio of the exergy output to the exergy input. It can also be written in function of the destroyed exergy in the system [19, 79–81]:

$$\eta_{ex} = \frac{\dot{B}_{out}}{\dot{B}_{in}} = 1 - \frac{\dot{B}_{dest}}{\dot{B}_{in}} \tag{2.15}$$

where $\dot{B}_{in}$ and $\dot{B}_{out}$ represent the total exergy input and ouput of the system, respectively. $\dot{B}_{dest}$ describes the destroyed exergy, also denoted exergy consumption or internal exergy losses, in the system due to irreversibilities, e.g. friction in a hydraulic circuit. The latter is related to the entropy production in the system (see subsection 3.1.1). The exergy efficiency can be determined for any arbitrary system without any additional information. It is a pure function of exergy

reduction due to irreversibilities. The key figure yields 1 when assessing a reversible process and 0 if the energy is completely degraded. It yields a realistic estimation of the system performance, meaning the ability to deliver a high quality energy output with a certain exergy input in a defined process, and thus, giving insight to the energy utilization. Eq. 2.15 is also referred to as total (overall) [79] or rational exergy efficiency [18]. However, there are different views how the exergy input and output is compounded, resulting in different definitions of the exergy efficiency depending on the investigated process [80]. As there is often a portion in the output exergy stream which is not utilized, another common definition of the exergy efficiency is [18, 80, 82]:

$$\eta_{ex} = \frac{\dot{B}_P}{\dot{B}_{in}} = 1 - \frac{\dot{B}_{waste} + \dot{B}_{dest}}{\dot{B}_{in}} = 1 - \frac{\dot{B}_L}{\dot{B}_{in}} \tag{2.16}$$

with $\dot{B}_P$ the amount of exergy in product outputs (useful output) and $\dot{B}_{waste}$ the waste exergy, also denoted external exergy losses, e.g. waste heat emissions to the environment. $\dot{B}_L$ represents the total exergy loss in the system (both waste and destroyed exergy). As an example, Simpson *et al.* investigated the hydrogen production via steam methane reforming, while defining the exergy efficiency accordingly [83]:

$$\eta_{ex} = \frac{\dot{B}_{H_2}}{\dot{B}_{in}} = 1 - \frac{\dot{B}_{un}}{\dot{B}_{in}} = 1 - \frac{\dot{B}_{exh} + \dot{B}_{dest}}{\dot{B}_{in}} \tag{2.17}$$

where $\dot{B}_{H_2}$ represents the exergy output of the hydrogen stream and $\dot{B}_{un}$ the unused exergy. $\dot{B}_{exh}$ depicts the exergy output of the exhaust stream and $\dot{B}_{dest}$ the destroyed exergy due to irreversibilities. For the investigated process, the exergy of the exhaust stream is not useful and is regarded as waste exergy, while theoretically it would be recoverable. The authors mention that if a bottoming cycle and a reactor would be implemented in the system to make use of the exhaust stream exergy, the exergy efficiency could theoretically be increased by 5% [83]. Therefore, the definition of the exergy efficiency from Eq. 2.16 considers the purpose of the system and that some exergy output streams are not utilized or valuable, resulting in a more meaningful estimation of the system performance. What all definitions have in common is, that the total exergy output and the destroyed exergy sums up to the total exergy input [19]. Electrical energy is per definition pure exergy, as it can be fully transformed into any other form of energy, e.g. heat. The exergy efficiency $\eta_{ex,RM}$ of a refrigeration cycle is therefore defined as [84]:

$$\eta_{ex,RM} = \frac{\dot{B}_E}{\dot{W}_{CPR}} = \frac{\dot{W}_{CPR,rev}}{\dot{W}_{CPR}} \tag{2.18}$$

which relates the thermal exergy output of the evaporator $\dot{B}_E$ to the compressor input $\dot{W}_{CPR}$.

The key figure can also be defined by the ratio of the ideal power input $\dot{W}_{CPR,rev}$ of a reversibly working machine (no losses) to the actual compressor effort, meaning that a reversibly operating refrigeration machine needs to supply at least the same amount of work as the cooling load exergy of the evaporator. If the whole refrigeration plant is considered, the exergy efficiency $\eta_{ex,sys}$ is defined as [21]:

$$\eta_{ex,sys} = \frac{\dot{B}_U}{\dot{W}_{CPR} + \dot{W}_{aux}} = \frac{\dot{B}_U}{\dot{W}_{tot}} \tag{2.19}$$

with $\dot{B}_U$ the useful thermal exergy at the cooling location, $\dot{W}_{aux}$ the electrical power input of the auxiliary devices and $\dot{W}_{tot}$ the total electrical power input of the refrigeration plant. Exergy loss ratios can be applied to compare components or subsystems in the overall process. The exergy destruction ratio y_i is described by [81,82]:

$$y_i = \frac{\dot{B}_{dest,i}}{\dot{B}_{in}} \tag{2.20}$$

where $\dot{B}_{dest,i}$ represents the exergy destruction in the ith component or subsystem of the investigated system. Alternatively, the exergy destruction ratio relates the exergy destruction of a component or subsystem to the total exergy losses in the system defined as [82,85]:

$$RI_i = \frac{\dot{B}_{dest,i}}{\dot{B}_{dest}} \tag{2.21}$$

where RI_i is the exergy destruction ratio, also denoted relative irreversibility [81]. This key figures are useful for the comparison of components and subsystems, indicating the contribution to the overall exergy losses due to irreversibilities. In comparison, such an evaluation is not possible in purely energetic considerations.

2.3.2.1 Advanced exergy analysis

Morosuk *et al.* showed the application of an advanced exergy analysis on refrigeration machines with different working fluids [86]. The study followed the approach to split the exergy destruction of every system component in endogenous and exogenous as well as avoidable and unavoidable portions (see Fig. 2.14). The same approach was used in other studies, e.g. for a refrigeration machine with parallel compression [69], for an ejector refrigeration cycle [87] or a ground source heat pump [88]. To consider the interaction between different system compo-

nents, the destroyed exergy in every i^{th} component $\dot{B}_{dest,i}$ is defined as [69, 86, 87]:

$$\dot{B}_{dest,i} = \dot{B}_{dest,i}^{EN} + \dot{B}_{dest,i}^{EX} \tag{2.22}$$

where $\dot{B}_{dest,i}^{EN}$ and $\dot{B}_{dest,i}^{EX}$ is the endogenous and exogenous exergy destruction, respectively. The endogenous part describes the exergy losses generated only in the ith component due to irreversibilities, while elsewhere ideal processes are considered. The exogenous portion describes the exergy loss in the ith component which is generated by imperfections of the remaining ones and the structure of the overall system. Such a distinction provides information about which components have the greatest influence on the efficiency. To consider technological limitations, the destroyed exergy in every i^{th} component $\dot{B}_{dest,i}$ can also be separated as follows [69, 86, 87]:

$$\dot{B}_{dest,i} = \dot{B}_{dest,i}^{UN} + \dot{B}_{dest,i}^{AV} \tag{2.23}$$

where $\dot{B}_{dest,i}^{UN}$ and $\dot{B}_{dest,i}^{AV}$ is the unavoidable and avoidable exergy destruction, respectively. The unavoidable exergy destruction represents the exergy loss which cannot be avoided due to the technological constraints. In contrast, the avoidable exergy destruction describes the exergy loss which can be minimized by optimizing the overall system and components, e.g. by enhancing the operating conditions. Coupling both splitting approaches, the destroyed exergy in every i^{th} component $\dot{B}_{dest,i}$ can be written as [69, 87]:

$$\dot{B}_{dest,i} = \dot{B}_{dest,i}^{UN,EN} + \dot{B}_{dest,i}^{UN,EX} + \dot{B}_{dest,i}^{AV,EN} + \dot{B}_{dest,i}^{AV,EX} \tag{2.24}$$

with $\dot{B}_{dest,i}^{UN,EN}$ the unavoidable endogenous exergy losses and $\dot{B}_{dest,i}^{UN,EX}$ the unavoidable exogenous exergy losses, which cannot be avoided in the respective component and overall system. $\dot{B}_{dest,i}^{AV,EN}$ represents the avoidable endogenous exergy loss which can be minimized by improving the considered component. $\dot{B}_{dest,i}^{AV,EX}$ describes the avoidable exogenous exergy loss which
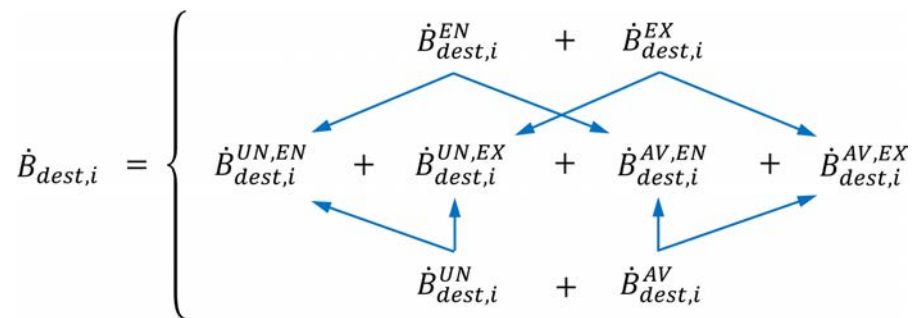

Figure 2.14 – Graphical representation of the exergy destruction splitting approach (adapted from [89]).

can be reduced by optimizing the remaining components and the system structure. The latter two parts are important parameters which represent the achievable improvement potential. Additionally, the mexogenous (mixed exogenous) exergy destruction is used in order to evaluate the simultaneous interaction between the system components [69, 87, 90].

Such advanced exergy analysis delivers a deepened insight into the exergy destruction and the interaction between system components, which provides a detailed understanding of the system irreversibilities. Accordingly, the potential for improvements and the priority which components should be mainly enhanced is revealed. This is helpful for a goal-driven system optimization. However, the determination of the different types of exergy losses is difficult and usually based on different assumptions and subjective decisions [91]. In the study of Morosuk *et al.* for example, an unavoidable and a theoretical refrigeration cycle is defined to split the exergy destruction [86]. For the unavoidable case it is assumed that the temperature differences in the heat exchangers (condenser and evaporator) between the refrigerant and the secondary side fluid is 0.5 K and that the compressor has an isentropic efficiency of 95%, which represents the technological limitation. The rest of the exergy destruction is assumed to be avoidable. To distinguish between endo- and exogenous exergy losses, four hybrid refrigeration cycles are conceived, where in each of them only one irreversible operating component is present [86]. The main conclusion of the authors is that an improvement in system performance would be achieved by first enhancing the evaporator and subsequently the compressor. Also, when considering the unavoidable refrigeration cycle, the interactions between the system components seem minor. Nevertheless, Byrne *et al.* mention in their study, that the above assumptions for the technological limitation seem not realistic and having a discrepancy from values obtained with their prototypes [21]. Furthermore, the authors found with their literature search that the exergy losses are influenced strongly by temperature and pressure differences in the system and indirectly by the operating conditions, which is linked to the sizing of the components.

2.3.2.2 Reference-based performance indicators

Similarly to energy analysis, the method to assess a system by applying reference-based key figures is also employed in exergy analysis. This approach was followed by Fan *et al.* in order to evaluate the performance of an HVAC system in an airport terminal building and to determine the influence of different control strategies [59]. Firstly, by means of a simulation model of the building and HVAC system as well as exergy analysis, the exergy efficiencies and exergy loss ratios were determined for every component in the system (cooling tower, chillers and AHU

with secondary pump). By investigating the yearly values, it was found that the AHU has the highest optimization priority, followed by the chillers. Furthermore, in order to evaluate the system performance over a certain time period in the setting of different control strategies with respect to an ideal operating level, the control perfect index CPI was introduced. It is defined as [59]:

$$CPI_{sys} = \frac{\sum\limits_{i=1}^{N} \dot{B}_{dest,sys,i}^{id}}{\sum\limits_{i=1}^{N} \dot{B}_{dest,sys,i}^{act}} \qquad (2.25)$$

where CPI_{sys} is the system control perfect index and N the number of operation conditions over the chosen period. $\dot{B}_{dest,sys,i}^{id}$ and $\dot{B}_{dest,sys,i}^{act}$ denote the ideal (i.e. lowest or minimal) exergy losses of the ideal operating level and the actual destroyed exergy of the system in the ith operation condition, respectively. The larger the key figure is, the more suitable is the control strategy and the better is the performance of the HVAC system. Furthermore, the optimum potential $\widehat{H}$ is defined as follows [59]:

$$\widehat{H}_{sys} = (1 - CPI_{sys}) \cdot 100\% \qquad (2.26)$$

where $\widehat{H}_{sys}$ represents the system optimum potential, which describes the degree of possible improvements with respect to the chosen control strategy and the ideal operating level. In the study, the ideal operating level was determined with a particle swarm optimization (PSO) algorithm and three different control strategies (original, optimal load allocation and optimal supply air temperature reset) were assessed. The highest yearly CPI value of 0.82 was reached with the optimal load allocation strategy in comparison to 0.77 with the original strategy. Another study applied the CPI on the same HVAC system, but considering 6 control strategies and two different ideal operating levels [60]. On the one hand, a limited-ideal operating level similar to the precedent study was considered, which represents the minimal exergy loss situation of the system at a specific operation condition. On the other hand, an ideal operating level was defined, which considers the minimal exergy losses over the year at various operation conditions [60]. As an outcome, control strategy 6 performed best, where the temperature level of the supplied cooling water and the supplied chilled water as well as the outdoor air flow rate is optimized at the same time. Also, the water side of the refrigeration system yields greater improvement potential compared to the air side, with respect to the chosen control strategies.

2.3.2.3 Evaluation of subsystems

Regarding refrigeration plants, the interest extents from the refrigeration machine itself to the neighboring components. It can be beneficial to partition the refrigeration plant into different subsystems. With this method, the exergy analysis reaches an increased level of detail. The key figures, e.g. the exergy efficiency, can be determined for every subsystem and each of them can be assessed individually. The approach to split the investigated system into subsystems was applied for a chilled water system of a campus [75]. It was divided into four subsystems (chilled water distribution, refrigeration, steam turbine drive and heat rejection), in order to carry out an energy-, exergy- and cost analysis of the plant. Fang *et al.* evaluated the operation performance of an HVAC system by partitioning it into three subsystems (cooling water, chilled water and air handling unit) and by applying ideal exergy flow models [61]. By minimizing the exergy destruction caused by the control system in each subsystem, the ideal operating level was defined. Five different control strategies were assessed, where the best strategy yields a performance improvement of 11.9 % compared to the most unfavorable one. Menberg *et al.* carried out a comprehensive exergy analysis of a ground-source heat pump in cooling and heating mode, where subsystems were chosen accordingly for a detailed evaluation of the plant (e.g. down to the detail of mixing valves) [66]. The exergy performance was analyzed by applying 6 different key figures in the form of exergy efficiencies, e.g. the ratio of exergy output to non-natural exergy input, or exergy ratios, e.g. the ratio of natural exergy input to total exergy input. The investigation discovered different exergy losses in the components with respect to the operating mode. The exergy performance in heating mode is mentioned to be twice as high as in cooling operation. The authors state the need of additional research regarding variable boundary conditions as well as the study of alternative reference environment definitions, in order to allow an analysis under real operation conditions. Another study presents the framework of an international collaboration regarding low exergy systems for buildings [92]. The use of exergy analysis is emphasized to capture all the relevant aspects of the energy usage and to decrease further the exergy demand of buildings as well as reducing the primary energy demand. To optimize the energy usage and therefore reducing the exergy losses, the exergy path was followed within the whole energy chain from the conversion of primary energy up to the building envelope through different subsystems. Likewise, when assessing refrigeration plants, the exergy flows can be followed through the whole system from the input to the output. Thus, the location as well as the magnitude of the losses can be identified in every subsystem.

2.3.2.4 Evaluation of hydraulic circuits

By considering the exergy input of auxiliary devices, such as circulating pumps, the configuration of hydraulic networks in the refrigeration plant can be evaluated. An unfavorable design of the hydraulic circuit provokes additional losses in the piping, e.g. due to wall friction or unnecessary mixing valves. A low amount of thermal exergy transferred in the subsystems implies also a higher mass flow rate of the fluid in the distribution networks in order to deliver the desired amount of useful energy to the cooling locations. Both phenomena cause an elevated power consumption of the circulating pumps. This plays an important role in practice, as a well-suited hydraulic integration of the refrigeration machine or free cooling module (coupling of the consumer and dry cooler circuits by means of a heat exchanger arranged in parallel to the refrigerating machine, see subsection 2.2.3) is crucial in order to achieve a highly performing plant. Kazanci *et al.* carried out exergy analyses of different space heating [93] and cooling systems [94], while considering the exergy input of auxiliary devices. The authors mention in both studies, that the exergy input of such devices may strongly influence the system performance. When considering air cooling cases, where ventilation systems are used to remove the heat, large ventilation rates were observed [94]. As a consequence, an increased energy consumption was present. This is eventually also the case for coolers in refrigeration plants. Moreover, the authors mention that a low electrical exergy consumption of auxiliary devices is important for systems with a low temperature difference between the supply and return flow [93], which can be present in hydraulic circuits of refrigeration plants.

2.3.2.5 Performance analysis and optimization of refrigeration machines

An experimental study analyzed a small scale vapor compression refrigeration machine with three different refrigerants [67]. An exergy analysis was carried out in order to determine the exergy losses in each component and the exergy efficiency η_{ex} of the system. For all refrigerants, major exergy losses were revealed in the compressor, followed by the evaporator and condenser. The highest exergy efficiency of approximately 0.1 was achieved with the refrigerant R12. Ahamed *et al.* carried out a review of existing exergy analyses regarding vapor compression refrigeration machines [68]. Among others, they investigated the influence of the evaporation and condensation temperature on the total exergy losses. Taking existing studies into account, they found that higher evaporation and lower condensation temperatures yielded the lowest exergy losses in the refrigeration machine, regardless which refrigerant was used.

Gullo *et al.* carried out an advanced exergy analysis of a commercial R744 refrigeration machine with parallel compression from subcritical to transcritical operation [69]. The system behaviour

at two outdoor temperatures of 25 and 35 °C was evaluated. Most of the exergy losses are present in the gas cooler, the medium temperature evaporator and the high stage compressor at an outdoor temperature of 25 °C. Moreover, the contribution of the high pressure expansion to the total exergy losses in the system increased from 8.8% to 13.5% at an outdoor temperature of 35 °C. Exergy efficiencies of 0.176 and 0.133 were found at 25 and 35 °C outdoor temperature, respectively. Consequently, they state that a performance increase of the low stage compressor is achievable if the irreversibilities of the components associated with the gas cooler are reduced. Also, the interaction between the different system components on the total irreversibilities is minor, except for the gas cooler. Another study evaluated the effect if two separate refrigeration machines are coupled together by means of a heat exchanger (cascade machine) [70]. The latter serves as a superheater in the primary and as a condenser in the secondary loop, respectively. The COP of the combined cycles is up to 3.7% higher compared to the separated systems and reaches a value of up to 3.65 at an evaporator temperature of 0 °C. The exergy losses in the coupled system were all the time lower than in the separated systems regardless the evaporating temperature. Similarly to the COP, an increase in exergy efficiency of 3.5% was found when employing the coupled system. The highest exergy efficiency of 0.32 was reached at an evaporation temperature of 0 °C.

Bilir Sag *et al.* demonstrated an increase in COP from 3.17 to 3.537 with an ejector cycle compared to a basic R134a vapor compression refrigeration machine at a cooling load of 4.55 kW [71]. Further, the authors found an increase in exergy efficiency of up to 11% at the same operating conditions, yielding an exergy efficiency of 0.21. Another study focused on energy and exergy analysis of a bi-evaporator compression / ejection refrigeration cycle [72]. The performance of the ejector cycle was compared to a conventional system, where an increase in COP of up to 30% and exergy efficiency of up to 28% was found, depending on the evaporator and condenser inlet temperatures. Major exergy destruction was discovered in the compressor and evaporator for the conventional system and in the ejector of the modified cycle.

Another study carried out a performance and exergy analysis of a refrigeration machine with an additional subcooler and four different refrigerants R134a, R22, R410A and R717 [73]. They state that the COP of the refrigeration machine is increased with the subcooler due to the increased cooling capacity without an increase in compressor work. Moreover, they found an ideal degree of subcooling of 4 to 7 K regarding the total exergy destruction.

2.3.2.6 Performance analysis and optimization of refrigeration plants

Zhang *et al.* carried out an analysis of a complex cascade refrigeration system with multiple refrigerants and supply temperature levels ranging from -100 to 23 °C [74]. They developed a general exergy-based synthesis model based on mixed-integer nonlinear programming (optimization of nonlinear problems) to determine the ideal retrofit solution. The method comprises an exergy analysis of the existing or retrofit refrigeration plant, the maximization of the system exergy efficiency with the model considering all refrigerants and temperature levels simulataneously, and in the end, the validation and evaluation of the found solution. As a result, the pressure levels and the positioning of some evaporators in the system were adjusted. By comparing the original and the optimized refrigeration plant, they found electrical energy and cost savings of up to 19%. Harrell *et al.* carried out an energy, exergy and cost analysis of a campus chilled water system [75]. They found the highest system exergy efficiency of 0.13 at an evaporator cooling load of 70%. By dividing the refrigeration plant into four different subsystems (heat rejection, steam turbine drive, refrigeration machine and chilled water distribution) they were able to determine the exergy loss ratio in each of them. The most significant exergy losses of 42 and 31% were discovered in the stream turbine drive and refrigeration machine, respectively. Hui *et al.* carried out an exergy analysis of cooling towers at different outdoor air humidities [76]. A typical HVAC system in an office building located in Hong Kong was considered in the investigation. Monthly exergy efficiencies were calculated, where the highest exergy efficiency of the system was found in May with a value of 0.252. The authors state, that the exergy efficiency highly depends on the wet-bulb temperature of the surrounding air. The highest exergy efficiency of the cooling tower with a value of 0.287 is reached at a relative outdoor air humidity of 50%.

An adequate measuring concept is needed in refrigeration plants to check whether the planning specifications are met. Such measurements should in addition enable an energy controlling and provide necessary data for operational optimization. This is typically important for larger refrigeration plants with an elevated electricity consumption. However, such measuring concepts require a fixed installation of the instrumentation and should be given special attention during the planning process. The application of measurement concepts for efficiency investigations of refrigeration plants with an exergy based approach was investigated by Eisenhauer *et al.* [95]. A complete exergy analysis of refrigeration plants requires a large number of measured variables. In order to reduce these, the authors suggest to extend the chosen system boundaries, with the drawback of decreasing the level of detail, or to use thermodynamic relations and assumptions to determine the missing quantities. The authors state also that the method from the

standard VDMA 24247-2 is well suited for a relative comparison of similar refrigeration plants, but reaches its limitation when a deviation from the reference process is present. Moreover, the determination of typical reference values for system components is difficult, which is necessary for an absolute comparison.

2.3.2.7 Difficulties in exergy analysis

It has been shown that exergy analysis is a useful tool to determine the magnitude as well as the location of losses due to irreversibilities in a thermodynamic system, which is not possible in purely energetic considerations. With this information efficiency limiting components or operating conditions may be discovered, optimization potentials revealed and systems enhanced accordingly. One difficulty which arises in a detailed exergy analysis is that an increased number of measured variables is needed and that the corresponding thermodynamic properties must be known accordingly. In the present day, this is not considered as a crucial limiting factor. What is more challenging, is the definition of a sound reference environment, which is a prerequisite to carry out a reliable exergy analysis. The choice of the reference state influences the absolute exergy values, and thus, determines the outcome of the analysis. This topic is addressed in detail in subsection 3.1.1.2.

2.4 Frequent problems in refrigeration plant implementation and operation

It is apparent that the planning process, the technical realization and the operation of water-water refrigeration plants is challenging due to the increased complexity. A market survey among actors in the refrigeration industry was carried out by Rohrer *et al.* in order to determine the most frequently occurring deficiencies [96]. The most mentioned problem is an insufficient coordination of the overall system, due to a faulty interaction of individual system components. In this context, increased demands for control and regulation systems are present. Moreover, a wrong dimensioning of cold storages and auxiliary devices can contribute significantly to inadequate operating conditions of the refrigeration system. Another mentioned reason is a poor commissioning of the refrigeration plant and subsequently, a lack of optimization during operation. The authors state that the implementation and extension of optimization measures, which increase the efficiency of refrigeration systems, helps to prevent the identified problems. They mention also the need of research for a consistent evaluation of refrigeration plant performance and a reliable determination of optimization potentials.

Lang *et al.* elaborated a technical report regarding measures and activities to achieve an increase in energy efficiency of refrigeration plants for air-conditioning applications. Among others, they identified the following manifold and also economic reasons for efficiency deficits of refrigeration systems [8]:

- The additional costs that are caused by an inefficient refrigeration system are not relevant for most operators or tenants. Air-conditioning refrigeration is rarely a budget item and the annual electricity costs for cooling remain hidden in the total energy and ancillary costs.

- The company, i.e. tenant, who ultimately has to pay the electricity costs of the air-conditioning system has normally no influence on the building, the chosen cooling solution and its energy efficiency.

- For new buildings, the investor is usually only interested in the investment costs. Solutions with lower initial expenses are preferred, even if these subsequently cause higher energy costs.

- The time and cost pressure during planning leads the plant engineer to rely on his standard solution concepts or to outsource the planning completely to the component supplier. Both methods involve the risk that compromises regarding energy efficiency are made.

- New plants are usually designed according to best conscience and then commissioned. What remains hidden in the planning stage, is the actual use of the building and the air-conditioning system. After a certain time of operation, the entire system would have to be adjusted to the actual requirements. However, in practice this readjustment rarely takes place. As a consequence, a large number of air-conditioning systems have been operated for years with the commissioning settings, without taking into account the real conditions of use. The latter may change also over time or are unintentionally changed.

- The suppliers offer the plant engineers an all-round service in which the suppliers also take over the design of the refrigeration system.

- In the case of optimization, the expert cannot guarantee to the plant operator a successful operational optimization of an existing system. Experience shows that there are refrigeration systems in which the power consumption can be considerably reduced with a few new settings. In other systems, not even a comprehensive analysis does reveal significant saving potentials.

- The system operator is usually overwhelmed with the technical questions. He is satisfied

when the air-conditioning system runs smoothly and provides the desired indoor climate.

- The concept of an air-conditioning refrigeration plant is decisive for the future energy consumption. However, the concepts implemented in practice show that not all plant engineers are familiar with energy-efficient concepts.

- An optimization of a refrigeration system always includes the risk of malfunction after the manipulations during operation. Therefore, many operators prefer not to make any major changes to the system in order to minimize the risk.

- Often, data of the electrical power consumption, the cooling capacity and other operating states are missing, which would allow conclusions regarding the effectiveness of the system. On the one hand such data must be collected for a certain period of time, and on the other hand there are not always measuring devices installed to acquire the data.

2.5 Conclusions

In air-conditioning refrigeration, mostly vapor compression refrigeration systems are deployed. They come in different forms, such as small devices with direct evaporation and cooling for single rooms or large refrigeration plants with several megawatts cooling power and separate distribution networks. Where possible, free cooling is utilized to economize the electrical power consumption of the refrigeration machine. The planning process, the technical implementation and the operation of refrigeration plants in air-conditioning applications is challenging due to the increased complexity, where reasons for an inefficient operation are manifold, concerning various actors in the sector (e.g. plant operators, plant engineers a well as refrigeration machine resellers and manufacturers). The interest extents from the refrigeration machine itself to the neighboring subsystems. In practice, a well-suited hydraulic integration of the chiller or free cooling module is crucial in order to achieve a highly performing plant. Energy and exergy analysis are widely used tools to assess the performance and to enhance refrigeration systems involving transport and conversion of energy. Exergy analysis allows a more comprehensive study of systems, as the high quality energy and its degradation can be examined throughout the system from the input to the output, from which possible measures can be derived to increase the efficiency. This is not feasible in purely energetic considerations, but is especially important for refrigeration plants, as the electrical (high quality) energy is the main expense during operation. In most cases the effectiveness is determined and compared by means of key figures, such as COP or exergy efficiency. More detailed analyses comprise the definition of subsystems or the

evaluation of single components. In this context, the occurring exergy losses are determined and related to the total exery losses or exergy input of the system to provide additional information for possible optimization. Besides to the common performance indicators, further key figures are elaborated in order to compare the investigated refrigeration system with an occurring or modeled reference process. Studies of refrigeration machines focus mostly on performance improvements by enhancing the basic refrigeration cycle with additional components, e.g. internal heat exchangers or subcoolers. The performance of refrigeration plants is rather enhanced by improving the operation conditions, e.g. optimizing the chiller on/off strategy or temperature levels in the system.

According to the reviewed literature and with considerations regarding the practical relevance, research is on the one hand needed in the development of efficiency assessment procedures considering the whole refrigeration system. The methods should be consistently applicable in practice with the most common measuring concepts of real field plants, while still ensuring a sufficient level of detail. On the other hand, the determination of typical reference values is required in order to allow an absolute comparison of different refrigeration plants under real operating conditions. Due to the increased complexity of such systems, not only the refrigeration machine itself, but also the cold and hot water distribution circuits should be considered in order to evaluate the hydraulic integration of the refrigeration machine. Optimization potentials should be revealed, as measures which improve the system effectiveness most likely prevent frequent shortcomings during refrigeration plant operation.

3 Principles and methods of the proposed assessment approach

Together with the findings highlighted in chapter 2, a novel and general applicable assessment approach for vapor compression refrigeration plants with cold water distribution is developed. It enables the determination of the performance as well as possible optimization potentials with respect to the state of the art in technology. The proposed assessment approach for refrigeration plants is introduced in section 3.1. As certain reference values cannot be determined with technical standards, the work comprises the modeling of refrigeration machines, which is discussed separately in section 3.2.

3.1 Novel exergy-based evaluation approach for refrigeration plants

To overcome the mentioned disadvantages of energy analysis (see subsection 2.3.1.6), an exergy-based approach[2] is regarded as appropriate and is applied in the present work. The electrical energy consumption of the refrigeration machines and auxiliary devices is the main expense in refrigeration plant operation. This represents high quality energy which is degraded along the processes in the whole system. Therefore, the evaluation method involves a comprehensive exergy analysis of the system, where the exergy flow is examined from the input to the output. The refrigeration plant is split into reasonable subsystems, which leads to a reduction of the required measurement variables by still ensuring a sufficient level of detail. Furthermore, the optimization potential index (OPI, see subsection 3.1.3) for a daily evaluation is introduced, which is based on the actual and an achievable reference exergy input with technical standards as baseline. This reveals the improvement potential in each subsystem with respect to the state of the art in technology at a glance, which is of great importance in practice. The quantity exergy is seen as an appropriate measure to evaluate each subsystem, as different energy forms are comparable with each other. Consequently, the heat transfer and temperature levels in the system as well as the energy consumption of the auxiliary devices can be evaluated simultaneously, which results in one single key figure per subsystem. Two different operating modes are then considered, namely refrigeration machine (see subsection 3.1.2.1) and free cooling operation (see subsection 3.1.2.2).

3.1.1 Exergy principles

The exergy of a system consists of different components which can be described accordingly [82]:

$$B_{sys} = B_{ph} + B_k + B_p + B_{ch} \tag{3.1}$$

with B_{ph} the physical, B_k the kinetic and B_p the potential exergy, respectively, where the sum of these terms is also denoted thermo-mechanical exergy. B_{ch} represents the chemical exergy.

---

2 *Remark:* Exergy and entropy analysis theoretically offer the same in-depth insight into energy utilization, because both originate from the second law of thermodynamics, where irreversibilites of processes are considered. Also, the exergy destruction of a process is proportional to its entropy production. The ranking between systems resulting from an exergy or entropy analysis will thus be the same. However, due to the lack of measurement data and missing thermodynamic quantities, entropy analysis was discarded as an approach for the present investigation of refrigeration plants.

The physical exergy is defined as [82]:

$$
\begin{aligned}
B_{phys} &= (U - U_0) + p_0(V - V_0) - T_0(S - S_0) \\
&= (H - H_0) - T_0(S - S_0)
\end{aligned}
\tag{3.2}
$$

where U denotes the internal energy, V the volume, S the entropy and H the enthalpy at a specific system state. The same variables with the subscript 0 indicate the properties of the reference environment (separately discussed in subsection 3.1.1.2) in which the system is placed, where p_0 and T_0 represent the reference pressure and temperature, respectively. The kinetic and potential exergy of a system correspond to the kinetic and potential energy, as the latter two are fully convertible into any other form of energy. If the system is at rest and at the same position relative to the reference environment, both terms vanish. In that case, the physical exergy describes the theoretical maximum amount of work which can be extracted when the system is brought into thermodynamic and mechanical equilibrium with the reference environment. The chemical exergy is the theoretical maximum amount of work which can be extracted, if the system is further brought into chemical (or total) equilibrium with the reference environment [18]. The chemical exergy is primarily relevant when chemical reactions, e.g. in combustion processes, or mixing and separation processes of different components are considered. If no such processes are present, an evaluation of the chemical exergy is usually not required. The reason is, that it cancels out when differences in exergy values at different system states are evaluated, e.g. in control volume investigations [82]. Therefore, the chemical exergy is out of scope of the present work and not further considered.

3.1.1.1 Exergy balance

Similarly to energy, exergy transfer is realised by heat, work and mass flow. By applying an exergy balance over a control volume (see Fig. 3.1), e.g. a complete system or one single component, the rate of change of exergy $\mathrm{d}B/\mathrm{d}t$ can generally be expressed as [16]:

$$
\frac{\mathrm{d}B}{\mathrm{d}t} = \underbrace{\sum_i \left(1 - \frac{T_0}{T_i}\right)\dot{Q}_i}_{\dot{B}_{th}} - \underbrace{\left(\dot{W} - p_0\frac{\mathrm{d}V}{\mathrm{d}t}\right)}_{\dot{B}_w} + \underbrace{\sum_j \dot{m}_{in,j}b_{in,j} - \sum_k \dot{m}_{out,k}b_{out,k}}_{\dot{B}_m} - \dot{B}_{dest}
\tag{3.3}
$$

where $\dot{B}_{th}$ represents the thermal exergy transfer rate associated with the transfer of energy by heat with a heat flow rate $\dot{Q}_i$ at the temperature level T_i with respect to the reference temperature T_0. $\dot{B}_w$ denotes the exergy transfer accompanying work with the actual mechanical or electrical power $\dot{W}$ and surroundings work, where p_0 is the reference pressure and $\mathrm{d}V/\mathrm{d}t$ the rate of
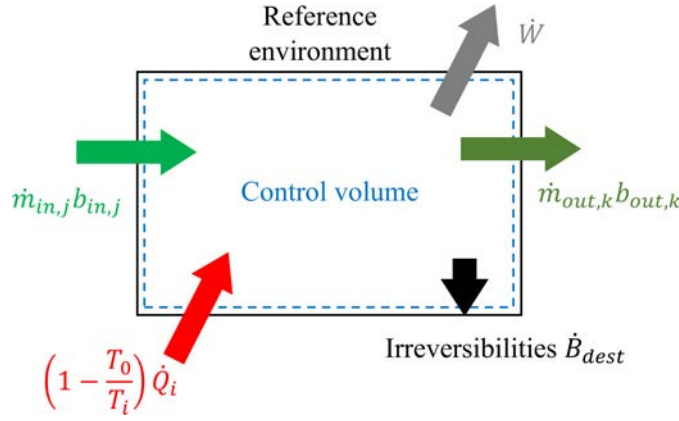
Figure 3.1 – General control volume for an exergy balance.

change of the control volume. Electrical, as well as mechanical, energy is high quality energy and by definition pure exergy, while heat is low quality energy and therefore only contains a certain amount of exergy. By heat transfer processes, e.g. heat conduction through a wall, the work potential of the heat, and therefore the exergy, decreases due to irreversibilities. According to the second law of thermodynamics, any irreversible process produces entropy due to losses, e.g. friction. The exergy destruction $\dot{B}_{dest}$ quantifies the loss in work potential and is related to the generated entropy at a constant reference temperature [19, 82]:

$$\dot{B}_{dest} = T_0 \dot{S}_{gen} \geq 0 \tag{3.4}$$

where $\dot{S}_{gen}$ represents the entropy production in the process. Eq. 3.4 is also referred to as the Gouy-Stodola theorem [82]. Any real process generates entropy and therefore exergy is destroyed. The term $\dot{B}_m$ in Eq. 3.3 indicates the exergy transfer rate in and out of the system by mass flow, where $\dot{m}_{in,j}$ and $\dot{m}_{out,k}$ are the incoming and outgoing mass flow rates, respectively. $b_{in,j}$ and $b_{out,k}$ denote the associated specific flow exergies, which can be described as [16]:

$$b = (h - h_0) - T_0(s - s_0) + b_k + b_p \tag{3.5}$$

where h and s is the specific enthalpy and entropy, respectively. h_0 and s_0 represent the reference values at the reference environment with temperature T_0 and pressure p_0. b_k denotes the specific kinetic and b_p the specific potential exergy. If a closed system is considered, the term $\dot{B}_m$ in Eq. 3.3 vanishes. By assuming steady-state, negligible kinetic and potential exergy differences as well as incompressible flow (liquid in the hydraulic circuits), Eq. 3.3 can be expressed as [53,97]:

$$0 = \sum_i \left(1 - \frac{T_0}{T_i}\right) \dot{Q}_i - \dot{W} + \sum_l \left(1 - \frac{T_0}{T_l}\right) \dot{Q}_l - \dot{B}_{dest} \tag{3.6}$$

where the exergy transfer by mass flow is now expressed by the net heat $\dot{Q}_l$ transported over the control volume boundary with the incoming and outgoing mass flow (derivation see appendix A.2) and the logarithmic mean temperature $\overline{T}_l$ defined as:

$$\overline{T}_l = \frac{T_{in,l} - T_{out,l}}{\ln\left(\dfrac{T_{in,l}}{T_{out,l}}\right)} \tag{3.7}$$

with $T_{in,l}$ the temperature of the incoming and $T_{out,l}$ the temperature of the outgoing mass flow, respectively. The simplifications in Eq. 3.6 are justifiable with the intention of ensuring a broad applicability of the presented method and to require as few as possible measuring locations. In that way, the required number of sensors are kept as low as possible and eventual retrofitting costs are reduced. While the pressure losses are not explicitly treated for the exergy transfer between the subsystems, they are indirectly considered on subsystem level by assessing the exergy input of the circulating pumps in the exergy analysis. A detailed hydraulic evaluation could be carried out in a further evaluation step, assuming that the required technical data would be available. The thermal exergy flow rate has the property of changing its flow direction with respect to the heat flow rate, depending on the system temperature. If $T > T_0$, the Carnot factor [84]:

$$\eta_{Car} = \left(1 - \frac{T_0}{T}\right) \tag{3.8}$$

is positive and the exergy flow rate has therefore the same direction as the heat flow rate. η_{Car} is also denoted exergetic temperature factor τ [18]. Conversely, the exergy flow rate has the opposite direction of the heat flow rate if $T < T_0$, as the Carnot factor is negative [18,84,98]. In other words, thermal exergy is always transferred towards the reference environment. Regarding the thermal exergy, Shukuya introduced the concept of warm and cool exergy, depending on whether the system temperature is higher or lower than the reference [99].

3.1.1.2 Reference environment

Two different general reference environment definitions can be identified, the so called restricted and unrestricted dead state [18, 82, 100]. The unrestricted dead state, also simply denoted dead state, is the state of thermal, mechanical and chemical equilibrium between the investigated system and the environment. The restricted dead state describes the state of thermal and mechanical equilibrium. As no chemical exergy is considered, the restricted dead state, in the present work termed reference environment, is used. Different theoretical requirements of the latter are mentioned in literature:

- The reference environment is in thermodynamic equilibrium and its properties (i.e. temperature and pressure) remain unchanged despite the consumption or release of energy and matter [84].

- The reference environment is infinitely large and in stable equilibrium, with all parts at rest relative to each other. Processes within the reference environment are reversible and do not affect it [18].

- The thermodynamic properties of the reference environment must not be influenced by the system under consideration [101].

- The reference environment must be available and ready to be used by the system under consideration (e.g. available as a sink) [98].

It is evident that a sound definition of the reference environment is challenging, which is often seen as the weak point of exergy analysis. Nevertheless, it is crucial in order to carry out reliable evaluations. In comparison to energy analysis, the chosen reference values, e.g. reference temperature, do not level out in an exergy balance. Therefore, the choice of the reference environment may influences the results. Mostly, for simplicity, a model of the natural environment (actual physical world) with typical ambient conditions is applied, where a constant pressure and temperature of 101'325 Pa (1 atm) or 100'000 Pa and 25 °C (298.15 K) is defined, respectively [16, 19, 82, 89, 102–104]. This choice may be justified by the fact that the surrounding of the system usually is the actual physical world, which is available as a sink and unnoticeably influenced by the process. In comparison to the investigated system, it can also be regarded as unlimited. However, it is inarguably that the ambiant air temperature fluctuates on a daily and yearly basis in most climate regions, which raises the question, whether to use a static or variable reference temperature. The choice of a sound reference temperature is especially important in the building environment, which concerns also refrigeration plants. As the system temperature is usually close to the environment and may fluctuate across the reference, the results of such exergy analyses are difficult to interpret and may be perplexing. Accordingly, different studies have addressed this problem.

Torío *et al.* examined different reference environments for buildings and their energy supply systems: the universe, the indoor air inside the building, the undisturbed ground and the ambient air surrounding the building [98]. They recommend to use the current surrounding outdoor air as a variable reference state, which is not affected by the processes under consideration and available. The variable (e.g. hourly averaged) outdoor temperature was also applied in other studies, e.g. in the case of a ventilation heat recovery exchanger [105], an HVAC system [61],

an air cooling system [106] or a building heating and cooling system [107]. Not all authors justify their choice, but one mentioned assumption is that because the real ambient temperature is always changing, it leads to errors in an analysis with a static reference state.

Moreover, Bonetti investigated the exergy stored in the building envelope and in a domestic hot water tank as a case study [101]. A fixed reference temperature based on thermal comfort is proposed and the results compared with a variable reference equal to the hourly averaged outdoor air temperature. Contradictive findings were observed if a variable reference was used for the case of exergy storage. In the case of the domestic hot water tank, for example, the exergy of the tank remains constant over the day using a fixed reference temperature, which is in line with the occupant and water heating control. On the contrary, the exergy fluctuates considerably if a variable reference temperature is applied. It is mentioned, that this behavior only reflects the external variations, which are not observed by the occupant or the water heating system in the building itself. Similarly, a constant reference temperature representing the comfort-zone upper limit was applied in another study concerning the thermal storage of the building envelope [51].

Another study evaluated the effect of hourly, monthly and yearly averaged ambient air temperatures as reference in a thermal exergy analysis of a building [108]. The findings are, that the resulting exergy destruction is not significantly influenced by the reference choice in the investigated system. However, the exergy values of flows are more affected, if the system temperature is close to that of the reference environment. Averaged ambient air temperatures (monthly, yearly or over the investigated time period) were also applied in other studies [52, 109–111].

Furthermore, Pons demonstrated that the reference state temperature must be fixed and constant also for dynamic analysis [112]. Only if the reference temperature T_0 is constant (e.g. in Eq. 3.2), then exergy is a function of state which results from a linear combination of energy and entropy. It is also mentioned that the full significance of exergy is obtained when the reference environment consists of the ambient air properties, which are the most favorable for the process considered. When investigating a refrigeration machine, which rejects heat to the environment, and considering the fluctuating ambient air temperature as the reference, the lowest ambient air temperature in the investigated time period would be applied [113]. This framework was among others adopted in a case study for a heat pump [113], for exergy optimization of a hybrid photovoltaic/thermal collector [114] or in the case of a building energy systems [115].

As shown, the choice of the reference environment, especially the reference temperature, is a highly controversial issue. In the present work, the standard model of the natural environment

mentioned above, with the constant averaged ambient air temperature over the investigated time period, i.e. over all investigated days, will be applied as an approach. This fulfills with good approximation the theoretical requirements of the reference environment as well as the consistent definition of exergy as a linear combination of energy and entropy. Also, the results are straightforward to interpret, which is one of the mentioned objectives for the evaluation method, as the system temperatures do not fluctuate across the reference. However, the most favorable ambient air temperature for the process, as proposed by Pons, cannot be applied in the present work for the refrigeration machine operating mode. The reason is that the temperatures at the cooling locations in the investigated system would be greater than the reference in certain situations. This contradicts the actual circumstances in reality, where a refrigeration machine is needed for cooling, because the ambient air temperature is elevated compared to the cooling location. Theoretically speaking, an exergy flow rate would be extracted from the cooling location, instead of being supplied by the refrigeration machine. Baehr *et al.* mention, that an exergy flow rate must be supplied to the cooling location by a refrigeration machine, in order to maintain the desired temperature [84]. The approach of using the most favorable ambient air temperature for the process, however, would be possible for the free cooling operating mode, where the cooling location temperature is in reality higher than the environmental temperature. Nevertheless, for consistency, the averaged ambient air temperature over the investigated time period is applied for both present operating modes.

3.1.2 Typical refrigeration plants and subsystem definition

In the present work, piping & instrumentation diagrams of 24 real systems for air-conditioning applications with a cooling power ranging from 20 up to 5252 kW are studied, where mostly multiple refrigeration machines are set up in parallel (e.g. redundancy) and multiple cooling locations are present. The refrigeration machines consist usually of the four main components compressor, evaporator, condenser and expansion valve. Only in 4 out of 24 field plants the refrigeration machine includes additional components, e.g. a subcooler, or it is not mentioned in the technical data sheets. 11 field plants make use of free cooling and heat utilization on the hot side hydraulic circuit is implemented in 17 systems. The latter is however not investigated in the present work due to missing measurement data. Therefore, it is distinguished between refrigeration machine (see subsection 3.1.2.1) and free cooling operation (see subsection 3.1.2.2) of refrigeration plants in the present work. In refrigeration machine operation, the temperature level of the system is higher than the environment on the hot side side, while being lower on the cold side. In free cooling operation, the temperatures in the whole refrigeration plant are higher

than the environment. From measurement data, both operating modes can be distinguished: if the electrical power consumption of the compressor is larger zero ($\dot{W}_{el,CPR} > 0$) and the heat flow rate at the free cooling module zero ($\dot{Q}_{FC} = 0$), refrigeration machine operation mode is present. Conversely, there is free cooling operation if $\dot{W}_{el,CPR} = 0$ and $\dot{Q}_{FC} > 0$. The parallel operation of the refrigeration machine and free cooling module (e.g. pre-cooling of the cold side) is not considered in the present work. Subsequently, the common structure of refrigeration plants for air-conditioning applications (compare subsection 2.2.3) in both operating modes and their separation into subsystems for the evaluation is elaborated in detail.

3.1.2.1 Refrigeration machine operation

A refrigeration plant with cold water distribution in refrigeration machine operating mode is depicted schematically in Fig. 3.2. The cooling is generated by vapor compression refrigeration machines (see Fig. 3.2, subsystem refrigeration machine, RM), which cool down the secondary side liquid, consisting typically of a water-glycol mixture. The cold water is stored and transported (see Fig. 3.2, subsystem cold water storage & transport, CST) to the cooling locations (see Fig. 3.2, subsystem cooling location, CL), e.g. to an air handling unit (AHU), while consuming electrical energy to drive the circulating pumps. To remove the heat of the condensers, another secondary cycle with dry coolers (as a first approach, all coolers are considered as dry coolers in the present work) and circulating pumps is present (see Fig. 3.2, subsystem dry cooler, DC). As the aim of the present work is to evaluate refrigeration plants, the cooled room itself and the building envelope are not considered. Furthermore, the subsystem DC and CST occur usually only once per system, while they absorb the exergies of all RM and feed all CL subsystems, respectively.

The definition of the subsystems is based on considerations regarding the exergy analysis and the study of piping & instrumentation diagrams of real systems. A compromise between level of detail and required measurement equipment (with considerations regarding state-of-the-art measuring concepts) was applied as an approach. On subsystem level, a performance evaluation and the determination of an eventual optimization potential is possible, which is the main goal of the presented method. However, with the definition of subsystem boundaries, the fineness of the evaluation is specified. Where and why exergy losses occur in the subsystems itself cannot be determined. A more detailed analysis would be necessary if the responsible component for an unfavorable operation needs to be identified. Nevertheless, first indications may be found by comparing the transferred exergy with a defined reference. The hydraulic circuit in Fig. 3.2
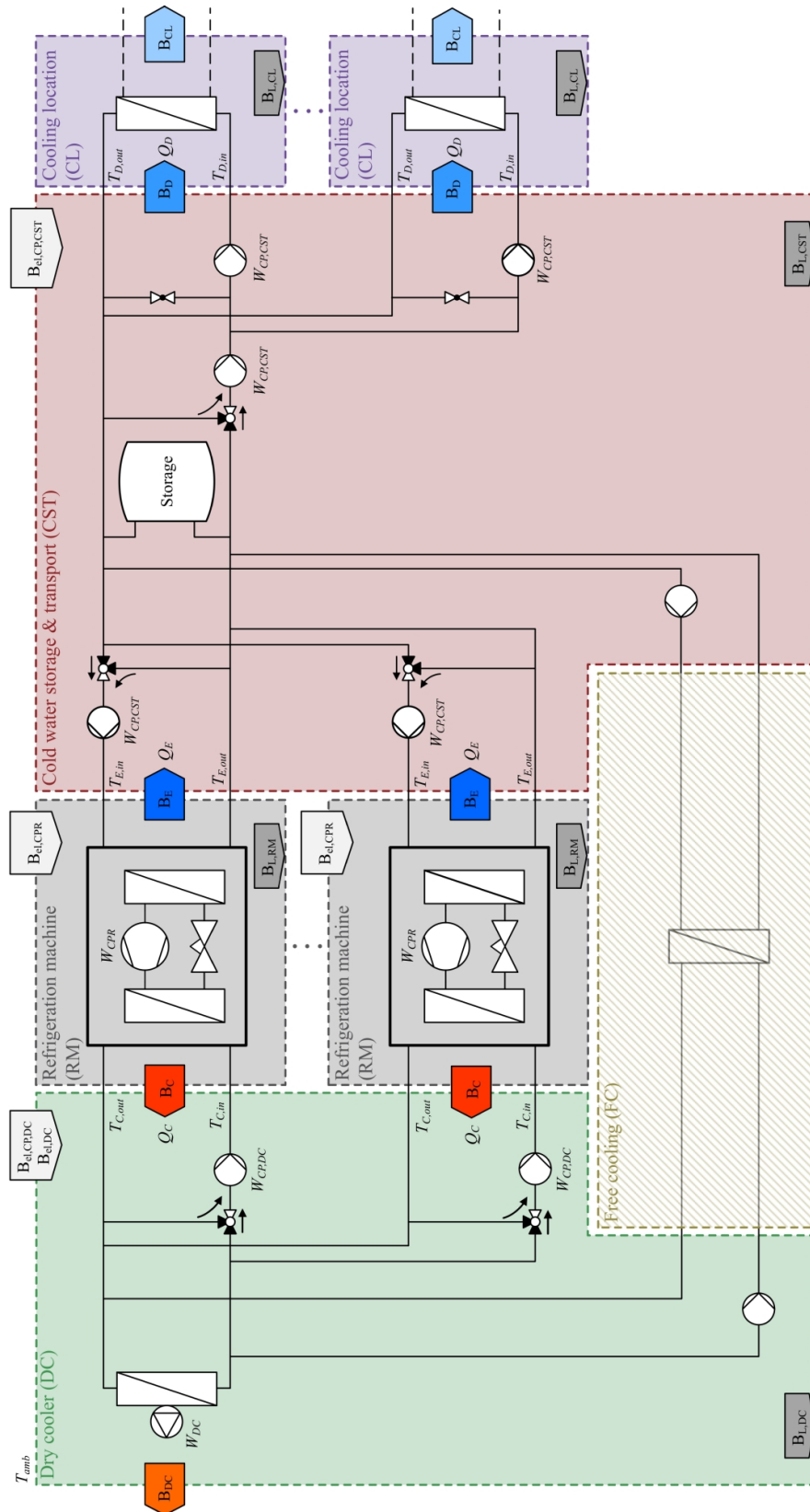
Figure 3.2 – Generalized schematic of a typical vapor compression refrigeration plant with cold water distribution and its subsystems in refrigeration machine operating mode (adapted from [11]). Arrows indicate the exergy inputs and outputs of each subsystem, where the blue and red color depicts the cold and hot side of the plant, respectively. Variables in italic indicate measured quantities for the exergy calculation (see Tab. 3.1 and 3.2 for details).

is not intended to represent the optimum solution, but to illustrate the assignment of pumps, valves, etc. to the subsystems. It is important to notice, that in the present study the auxiliary units are clearly assigned to the secondary hydraulic circuits. When defining the subsystems in a real installation, certain degrees of freedom are acceptable. An additional subsystem could be defined, e.g. if two hydraulic circuits on a different temperature level for the cold water distribution are present. However, it must be ensured that no components lie on the chosen subsystem boundary, for example T-connections, 3-way valves, etc. They must be completely assigned to a subsystem, as it is presented in the schematic. While such components are hardly important for energetic evaluations, exergy losses are present, which must be taken into account. Moreover, it must be ensured that all needed quantities to calculate the exergies are measured or derivable with thermodynamic relations or models. With this considerations, every subsystem may be evaluated individually.

Furthermore, Fig. 3.2 shows the measured quantities in every subsystem in order to determine the corresponding exergy in- and outputs, which are indicated with arrows (see Tab. 3.1 and 3.2 for details). The B_L arrows indicate the internal and external exergy losses of the respective subsystems. The exergy input is generated on the one hand by electrical energy of the compressor, circulating pumps as well as dry cooler fans and on the other hand by thermal and

Table 3.1 – Measured variables for the exergy computation according to Fig. 3.2.

Subsystem	Measured variables	
dry cooler	Q_C	condenser thermal energy
	$T_{C,in}$	condenser secondary side inlet temperature
	$T_{C,out}$	condenser secondary side outlet temperature
	$W_{CP,DC}$	cirulating pump electrical energy
	W_{DC}	dry cooler fan electrical energy
refrigeration machine	W_{CPR}	compressor electrical energy
cold water storage & transport	Q_E	evaporator thermal energy
	$T_{E,in}$	evaporator secondary side inlet temperature
	$T_{E,out}$	evaporator secondary side outlet temperature
	$W_{CP,CST}$	cirulating pump electrical energy
cooling location	Q_D	cold water distribution thermal energy
	$T_{D,in}$	cold water distribution inlet temperature
	$T_{D,out}$	cold water distribution outlet temperature
all subsystems	T_{amb}	ambient air temperature

Table 3.2 – Exergy inputs and outputs of the subsystems according to Fig. 3.2.

Subsystem	Exergy input		Exergy output	
dry cooler	$B_{el,CP,DC}$	circulating pump exergy	B_{DC}	dry cooler exergy
	$B_{el,DC}$	dry cooler fan exergy		
	B_C	condenser exergy		
refrigeration machine	$B_{el,CPR}$	compressor exergy	B_C	condenser exergy
			B_E	evaporator exergy
cold water storage & transport	$B_{el,CP,CST}$	circulating pump exergy	B_D	cold water distribution exergy
	B_E	evaporator exergy		
cooling location	B_D	cold water distribution exergy	B_{CL}	cooling location exergy

flow exergy exchange over the subsystem boundaries. Considering the electrical power input of the compressor and auxiliary units is plausible from a theoretical and functional point of view. The electrical power consumption of the circulating pumps, for example, is a necessary expense for the functioning of the subsystem CST and DC. The exergy input is needed in order to push the fluid through the piping in the secondary hydraulic cycle while overcoming the wall friction. Furthermore, a portion of the supplied electrical energy is converted into heat, which increases the temperature of the fluid. Both processes are associated with exergy losses. Consequently, a system with a well designed hydraulic circuit requires a lower exergy input of the circulating pumps. The same applies to the dry coolers, as they allow an increased heat transfer by forced convection. The exergy input of auxiliary devices was also included in other studies [66, 93, 94, 116].

3.1.2.2 Free cooling operation

A refrigeration plant with cold water distribution in free cooling operating mode is depicted schematically in Fig. 3.3. If the surrounding air temperature is substantially lower than the temperature in the refrigeration plant, the use of free cooling is feasible, which is mostly the case in the colder months over the year. Typically, a free cooling module (see Fig. 3.3, subsystem free cooling, FC) in the form of a heat exchanger, is arranged in parallel to the chillers. In free cooling operation, the coupling of both hydraulic circuits (see Fig. 3.3, subsystem dry cooler, DC and cold water storage & transport, CST) allows an indirect cooling of the cooling locations (see
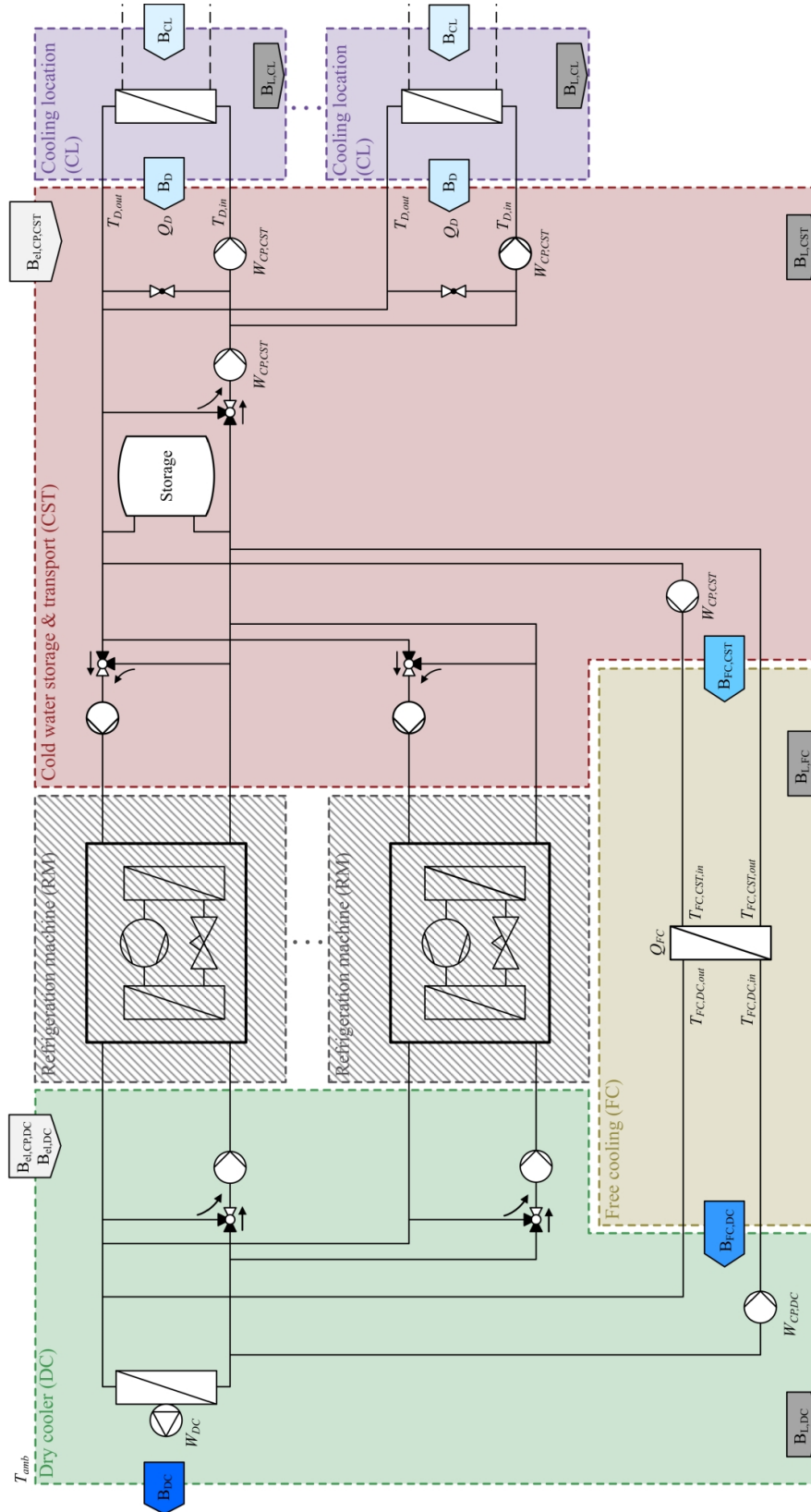
Figure 3.3 – Generalized schematic of a typical vapor compression refrigeration plant with cold water distribution and its subsystems in free cooling operating mode (adapted from [11]). Arrows indicate the exergy inputs and outputs of each subsystem. Variables in italic indicate measured quantities for the exergy calculation (see Tab. 3.1 and 3.2 for details).

Table 3.3 – Measured variables for the exergy computation according to Fig. 3.3.

Subsystem	Measured variables	
dry cooler	$W_{CP,DC}$	cirulating pump electrical energy
	W_{DC}	dry cooler fan electrical energy
free cooling	Q_{FC}	free cooling thermal energy
	$T_{FC,DC,in}$	free cooling inlet temperature DC side
	$T_{FC,DC,out}$	free cooling outlet temperature DC side
	$T_{FC,CST,in}$	free cooling inlet temperature CST side
	$T_{FC,DC,out}$	free cooling outlet temperature CST side
cold water storage & transport	$W_{CP,CST}$	cirulating pump electrical energy
cooling location	Q_D	cold water distribution thermal energy
	$T_{D,in}$	cold water distribution inlet temperature
	$T_{D,out}$	cold water distribution outlet temperature
all subsystems	T_{amb}	ambient air temperature

Table 3.4 – Exergy inputs and outputs of the subsystems according to Fig. 3.3.

Subsystem	Exergy input		Exergy output	
dry cooler	$B_{el,CP,DC}$	circulating pump exergy	B_{DC}	dry cooler exergy
	$B_{el,DC}$	dry cooler fan exergy		
	$B_{FC,DC}$	free cooling exergy DC side		
free cooling	$B_{FC,CST}$	free cooling exergy CST side	$B_{FC,DC}$	free cooling exergy DC side
cold water storage & transport	$B_{el,CP,CST}$	circulating pump exergy	$B_{FC,CST}$	free cooling exergy CST side
	B_D	cold water distribution exergy		
cooling location	B_{CL}	cooling location exergy	B_D	cold water distribution exergy

Fig. 3.3, subsystem cooling location, CL). In this operating mode, the refrigeration machines are turned off, and thus, the otherwise required electrical energy of the compressors is economized. As in the simplified schematic of the refrigeration machine operating mode, the hydraulic circuit is not intended to represent the optimum solution, but to illustrate the assignment of the auxiliary devices to the subsystems, whereby the same considerations regarding the subsystem definition

as in refrigeration machine operating mode are applied. Accordingly, the exergies of every subsystem in free cooling operating mode as well as the measured quantities for the computation are depicted in Fig. 3.3 (for details see Tab. 3.3 and 3.4).

3.1.3 Optimization potential index (OPI)

As shown in subsection 2.3.2, various key figures are applied in literature to evaluate the performance of thermodynamic systems. Mostly, the energy efficiency (compare Eq. 2.1), the coefficient of performance (compare Eq. 2.2 and 2.3) in the case of refrigeration systems and heat pumps, as well as exergy efficiencies (compare Eq. 2.15 to 2.19) are applied. The latter account for losses due to irreversibilites, and thus, giving insight into the energy utilization. Since every real process is irreversible, exergy losses are to be expected and the need to know the best process possible is appearing. The exergy efficiency allows a comparison of the performance between similar systems, although it is usually less meaningful when intrinsically different systems are considered [82]. With this indicator, the performance of systems is determined with regard to the thermodynamic ideal (e.g. in the case of refrigeration machines the actual compressor effort is compared with the one of a reversibly operating cycle), but there are no reference values available stating which exergy efficiency should be achieved in a certain process. Thus, the quantification of the performance and possible optimization potentials according to the state of the art in technology is difficult. Assuming two refrigeration plants A and B with $\eta_{ex,A} = 0.1$ and $\eta_{ex,B} = 0.15$, it is obvious that plant B is more efficient than plant A. Nevertheless, there is no evidence that plant B possesses further optimization potential comparing to the state of the art in technology, which is of greater importance in practice. This lets us introduce a complementary key figure, denoted optimization potential index OPI [10]:

$$OPI = 1 - \frac{\eta_{ex}}{\eta_{ex}^*} = 1 - \frac{\dfrac{\dot{B}_{out}}{\dot{B}_{in}}}{\dfrac{\dot{B}_{out}}{\dot{B}_{in}^*}} = 1 - \frac{\dot{B}_{in}^*}{\dot{B}_{in}} \tag{3.9}$$

where η_{ex} represents the actual exergy efficiency of the system and η_{ex}^* a reference or baseline exergy efficiency. The key figure describes the behavior of the real system in comparison with a reference system under identical operation conditions, while the same exergy output $\dot{B}_{out}$ is achieved. Thus, the evaluation of a subsystem is carried out with the assumption that the adjacent subsystems perform identically. $\dot{B}_{in}$ and $\dot{B}_{in}^*$ describe the actual exergy input according to measurements and the reference exergy input, respectively. As a first approach, the reference

values are defined according to technical standards. This represents an achievable technological baseline, where the specified conditions can be fulfilled or exceeded if the refrigeration plant is properly engineered and maintained. Typically, such standards are specified in tenders or contracts and should be fulfilled at the stage of commissioning. Any other appropriate standards or limits (e.g. performance parameters) could find application, i.e. the baseline can depend on the technological requirements in different countries or regions. This is important in practice, as technologies are constantly evolving. In the present work, all reference exergies which are not solely computed with measured quantities but calculated with technical reference values, are marked with an asterisk. Furthermore, the OPI represents a reference-based indicator (see subsection 2.3.1.3 and 2.3.2.2), which differs from conventional performance key figures such as COP or exergy efficiency. The latter relate the system output to the input, while the OPI relates the technological reference input to the actual measured input. This helps to reduce the needed number of measuring locations for the evaluation, as the exergy outputs of the subsystems DC and CL do not need to be determined, and allows a separate evaluation of the subsystems. As a consequence however, the key figures of all subsystems cannot be mathematically combined to an overall system OPI, which represents a possible drawback of the proposed method. The OPI may also indicate that a subsystem performs unfavorably, while the neighboring subsystems still fulfill the technical requirements, which may seem inconsistent with conventional performance key figure definitions. The reason is that each subsystem is evaluated individually with the appropriate technical baseline and the useful output is assumed to be identical in the actual and reference situation. To the best of our knowledge, the proposed OPI definition is justifiable, as the purpose of the method is the independent evaluation of each subsystem and the determination of eventual optimization potentials on subsystem level.

The systematic approach to determine the OPI is based on a balance of the exergy transfer over the subsystem boundaries. For the analysis of refrigeration machines, data from a steady operating phase is usually averaged and evaluated. The latter is problematic for refrigeration plants, as possibly not enough stationary phases over the evaluation period are present, which fulfill the selection criteria. With a dynamic approach, additional difficulties arise in the evaluation of the instationary exergy balance. Therefore, a quasi-stationary approach is proposed in the present work, where steady-state is assumed over the measurement interval. Consequently, the electrical power and heat flow rates are integrated over each measurement interval, and subsequently, the respective exergy inputs are computed. As the cooling load in refrigeration plants usually follows a daily rhythm, it is proposed to evaluated the OPI on a daily basis. It is assumed, that any accumulated exergy (or energy), e.g. in storages, will be consumed the same day (no seasonal

storages present). The optimization potential index is then formed with the sum of the calculated exergy inputs of every measurement interval over the day, where the number of summands varies depending on the present measurement interval:

$$OPI = 1 - \frac{\sum\limits_{t=0\,h}^{24\,h} B_{in}^*}{\sum\limits_{t=0\,h}^{24\,h} B_{in}} \tag{3.10}$$

This definition depicts an averaged performance indicator, similarly to the cooling seasonal performance factor (CSPF) [25] or total energy performance factor (TEPF, see Eq. 2.12) [24], which accounts for the overall behaviour of the system in a specific evaluation period by using the respective integral values of energy or exergy flow rates. A similar approach was also applied to determine the exergy efficiency over a longer period [116].

The interpretation of the results becomes straightforward when evaluating the OPI and the performance as well as optimization potential of the refrigeration plant is visible at a glance (see Fig. 3.4). No specialists are required to reveal eventual issues or improvement potentials, which is of great importance in practice. For example, plant operators can easily evaluate the system operation by tracking the key figure over time, e.g. with a daily check. If the actual exergy input of the subsystem is larger than the reference (meaning an increased input is required to achieve
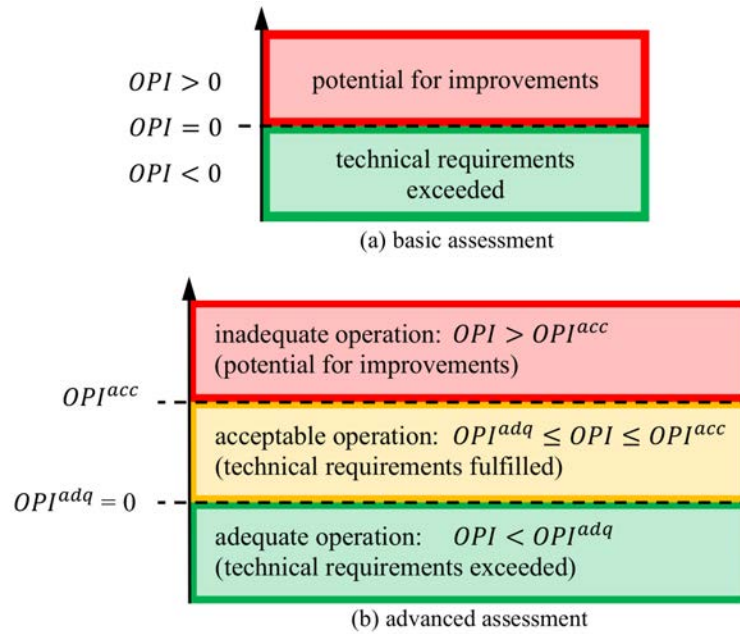
Figure 3.4 – Optimization potential index scale for determining the operating condition of the refrigeration plant and revealing improvement capabilities with (a) a basic and (b) a detailed assessment (adapted from [10]).

the same output), the OPI is larger than 0 and indicates potential for improvements. Conversely, the OPI delivers a value inferior to 0 if the actual exergy input is lower than the reference. Thus, no optimization potential according to the state of the art in technology is present, as the technical requirements are exceeded. An OPI ≈ 0 is achieved with good engineering and indicates that the technical requirements are met (see Fig. 3.4a). Making an example: assuming the OPI of every subsystem is below 0 and therefore, the refrigeration plant operates according to the technical requirements. Then, due to a malfunction of a circulating pump in the subsystem CST, the energy consumption is increased. The issue is revealed with an increased value of the OPI in the mentioned subsystem and points out an optimization potential. Therefore, the OPI delivers a first localization of eventual issues and optimization potentials on subsystem level. In a second evaluation step, the malfunction can be further narrowed down with a more detailed energy or exergy analysis. Eventually, by including a cost analysis, it is revealed if adjustments to the system are worthwhile, not only from a technical but also an economical aspect. Plant operators can then initialize the appropriate corrective measures by specialists to increase the performance of the refrigeration plant.

With the basic assessment (see Fig. 3.4a and results published [10, 11]), the boundary between favorable and unfavorable operation is sharp and it is unknown which values close to 0 still represent a permissible operation. Therefore, the interpretation of the results becomes clearer by defining a further acceptable limit OPI^{acc} to allow an advanced assessment (see Fig. 3.4b). A colored indicator with the different operating states can be realized and implemented in monitoring systems, which helps also to raise awareness for an efficient refrigeration plant operation. Ideally, these limits are specified with statistically sound, representative measurements and with the help of experts. Not only technical and methodical but also strategic aspects have to be considered together with all actors in the industry. This involves long term investigations of different real systems with varying size and cooling loads, which is out of scope of the present work. Nevertheless, as an approach and to exemplify the method, additional limits are derived from technical standards with certain assumptions or thermodynamic models to simulate the different operating states in the present work.

3.1.3.1 Refrigeration machine operation

In the present subsection, the evaluation method of the OPI in each subsystem in refrigeration machine operating mode is elaborated.

3.1.3.1.1 Subsystem dry cooler

The optimization potential index of the subsystem DC (see Fig. 3.2) is:

$$OPI_{DC} = 1 - \frac{\sum\limits_{t=0\,h}^{24\,h} \left(\sum\limits_{i} B^*_{C,i} + \sum\limits_{j} B^*_{el,CP,DC,j} + \sum\limits_{k} B^*_{el,DC,k} \right)}{\sum\limits_{t=0\,h}^{24\,h} \left(\sum\limits_{i} B_{C,i} + \sum\limits_{j} B_{el,CP,DC,j} + \sum\limits_{k} B_{el,DC,k} \right)} \tag{3.11}$$

where the exergy input is summed up over all refrigeration machines and auxiliary devices, which feed the subsystem. The actual condenser exergy B_C is given by:

$$B_C = Q_C \left(1 - \frac{T_0}{\overline{T}_C} \right) \tag{3.12}$$

with the condenser thermal energy Q_C, the reference environment temperature T_0 and the secondary side logarithmic mean temperature of the condenser $\overline{T}_C$ expressed by:

$$\overline{T}_C = \frac{T_{C,in} - T_{C,out}}{\ln \left(\dfrac{T_{C,in}}{T_{C,out}} \right)} \tag{3.13}$$

where $T_{C,in}$ and $T_{C,out}$ are the secondary side condenser in- and outlet temperatures, respectively. Electrical energy is per definition pure exergy, and therefore, the exergy input of circulating pumps $B_{el,CP,DC}$ is defined as follows:

$$B_{el,CP,DC} = W_{CP,DC} \tag{3.14}$$

where $W_{CP,DC}$ represents the circulating pump electrical energy. Similarly, the exergy input of dry cooler fans $B_{el,DC}$ corresponds to:

$$B_{el,DC} = W_{DC} \tag{3.15}$$

with W_{DC}, the respective electrical energy of the dry cooler fans. The reference condenser exergy B^*_C is expressed by the following equation:

$$B^*_C = Q_C \left(1 - \frac{T_0}{T^*_C} \right) \tag{3.16}$$

Table 3.5 – Temperature differences in the dry cooler heat exchanger according to VDMA 24247-8 [117].

	Adequate	Acceptable
ΔT_{HE}	≤ 6 K	≤ 8 K

where T_C^* describes the reference secondary side temperature of the condenser. As no reference temperatures for the inlet and outlet of the condenser according to technical standards are available, a definition similarly to Eq. 3.13 is not possible. Therefore, a calculation with the ambient air temperature as a basis and temperature differences according to technical standards as well as available measurements is proposed as a first approach. The following relation is introduced:

$$T_C^* = T_{amb} + \Delta T_{HE} + \frac{T_{C,out} - T_{C,in}}{2} \tag{3.17}$$

where ΔT_{HE} represents the temperature difference in the dry cooler heat exchanger, meaning the heat transfer medium outlet to ambient air inlet temperature difference. Target values of the latter are reported by the technical standard VDMA 24247-8 [117] (see Tab. 3.5). For the OPI_{DC} the stricter value of 6 K is applied. The necessary electrical energy of the auxiliary devices should not exceed a certain percentage of the total condenser or evaporator thermal energy of the installed refrigeration machines. In the technical standard SIA 382/1 [22] this portion is defined with the electro-thermo amplification factor $f_{el,th}$ (see Tab. 3.6). The total electrical energy consumption of the circulating pumps should not exceed $\approx 1.5\%$ of Q_C on the hot side and $\approx 1.2\%$ of Q_E on the cold side of the refrigeration plant, respectively. The total electrical energy consumption of the cooler fans should not exceed $\approx 3.5\%$ of Q_C. Additionally, a stricter uniform value of $\leq 1\%$ for circulating pumps is mentioned in the technical standard VDMA 24247-8. As no stricter limit is available for the energy consumption of the cooler fans, a factor of 37 is defined as a first approach, which represents proportionally the same increase as between the values of the two technical standards for circulating pumps. The limiting values are summarized in Tab. 3.6. It is proposed to calculate the reference exergy input of circulating pumps $B_{el,CP,DC}^*$ according to:

$$B_{el,CP,DC}^* = \frac{1}{f_{el,th,CP,DC}} \sum_i Q_{C,i} \tag{3.18}$$

where $f_{el,th,CP,DC}$ represents the electro-thermo amplification factor for circulating pumps. For the OPI_{DC} a value of 100 is specified, which respresents the stricter limit. Correspondingly, it

is proposed to compute the reference exergy input of dry cooler fans with the following equation:

$$B_{el,DC}^* = \frac{1}{f_{el,th,DC}} \sum_i Q_{C,i} \tag{3.19}$$

where $f_{el,th,DC}$ is the associated electro-thermo amplification factor for dry cooler fans. Like for the circulating pumps the stricter value is applied, which is 37.

The boundary between adequate and acceptable operation OPI_{DC}^{adq} is 0 with the given definition of the key figure. If the actual exergy input is lower than the stricter reference value according to the technical standards, the technical requirements are exceeded and the key figure is lower than 0. If the OPI is higher than 0, it has to be evaluated if the acceptable boundary is exceeded or not. The latter can be determined likewise to Eq. 3.11. Instead of using actual exergy values in the denominator, acceptable values are applied. They are calculated similarly as in Eq. 3.16 to 3.19, whereby the less strict limiting values according to technical standards are specified. Consequently, OPI_{DC}^{acc} is defined with:

$$OPI_{DC}^{acc} = 1 - \frac{\sum\limits_{t=0\,h}^{24\,h} \left(\sum\limits_i B_{C,i}^* + \sum\limits_j B_{el,CP,DC,j}^* + \sum\limits_k B_{el,DC,k}^* \right)}{\sum\limits_{t=0\,h}^{24\,h} \left(\sum\limits_i B_{C,i}^{acc} + \sum\limits_j B_{el,CP,DC,j}^{acc} + \sum\limits_k B_{el,DC,k}^{acc} \right)} \tag{3.20}$$

where B_C^{acc} is the acceptable condenser exergy, calculated similarly to Eq. 3.16 and 3.17, but applying the less strict temperature difference ΔT_{HE} of 8 K. The acceptable circulating pump exergy $B_{el,CP,DC}^{acc}$ is defined according to Eq. 3.18 by applying the acceptable limit value of 85 for the amplification factor. Moreover, the acceptable dry cooler fan exergy $B_{el,DC}^{acc}$ is determined with Eq. 3.19, whereby a value of 28 is applied for $f_{el,th,DC}$.

Table 3.6 – Electro-thermo amplification factors in each subsystem for dry cooler fans and circulating pumps according to the technical standard VDMA 24247-8 [117] and SIA 382/1 [22].

Subsystem	Electro-thermo amplification factor		Adequate (VDMA 24247-8)	Acceptable (SIA 382/1)
dry cooler	dry cooler fans	$f_{el,th,DC}$	$\geq 37^3$	≥ 28
	circulating pumps	$f_{el,th,CP,DC}$	≥ 100	≥ 85
cold water storage & transport	circulating pumps	$f_{el,th,CP,CST}$	≥ 100	≥ 65

---

3 *Remark:* As mentioned, no stricter limit is available for $f_{el,th,DC}$ in the standard VDMA 24247-8. As an approach the factor of 37 is defined, which represents proportionally the same increase as between the values for the circulating pumps.

3.1.3.1.2 Subsystem refrigeration machine

The optimization potential index proposed for the subsystem RM (see Fig. 3.2) is:

$$OPI_{RM} = 1 - \frac{\sum\limits_{t=0\,h}^{24\,h} B_{el,CPR}^*}{\sum\limits_{t=0\,h}^{24\,h} B_{el,CPR}} \tag{3.21}$$

where the exergy input of the compressor $B_{el,CPR}$ is given by:

$$B_{el,CPR} = W_{CPR} \tag{3.22}$$

with the compressor electrical energy W_{CPR}. Correspondingly, the reference exergy input of the compressor $B_{el,CPR}^*$ is:

$$B_{el,CPR}^* = W_{CPR}^* \tag{3.23}$$

with the reference compressor electrical energy W_{CPR}^*. To the best of our knowledge, no specific values for the latter are available because it depends on a variety of variables (e.g. part load conditions, refrigeration machine size, refrigerant, etc.). As a first approach, the reference compressor electrical energy W_{CPR}^* is determined with a model of the refrigeration machine (see section 3.2). Since the assessment method should be widely applicable, the model should require few and easily obtainable data. While the refrigeration machine is typically well instrumented to provide pressures and temperatures to the control system, the variables are however rarely logged in external monitoring or management systems. Therefore, secondary side temperatures and the evaporator thermal energy are specified as input variables. The reference secondary side temperature T_C^* of the condenser (see Eq. 3.17) is used together with the cooling load and cold water temperatures of the actual situation. A similar approach is applied to determine $B_{el,CPR}^{acc}$ (for the boundary OPI_{RM}^{acc}), by using the acceptable temperature differences according to the technical standards (see Tab. 3.5) for the computation of the corresponding condenser secondary side temperatures.

3.1.3.1.3 Subsystem cooling location

The optimization potential index of the subsystem CL (see Fig. 3.2) is:

$$OPI_{CL} = 1 - \frac{\sum\limits_{t=0\,h}^{24\,h} B_D^*}{\sum\limits_{t=0\,h}^{24\,h} B_D} \tag{3.24}$$

where the cold water distribution exergy B_D is calculated according to:

$$B_D = Q_D \left(1 - \frac{T_0}{\overline{T}_D} \right) \tag{3.25}$$

with the cold water distribution thermal energy Q_D and the logarithmic mean temperature $\overline{T}_D$ expressed by:

$$\overline{T}_D = \frac{T_{D,in} - T_{D,out}}{\ln \left(\dfrac{T_{D,in}}{T_{D,out}} \right)} \tag{3.26}$$

where $T_{D,in}$ and $T_{D,out}$ are the cold water distribution in- and outlet temperatures, respectively. The same procedure is applied for the reference cold water distribution exergy:

$$B_D^* = Q_D \left(1 - \frac{T_0}{T_D^*} \right) \tag{3.27}$$

with the reference temperature $\overline{T}_D^*$ expressed by:

$$\overline{T}_D^* = \frac{T_{D,in}^* - T_{D,out}^*}{\ln \left(\dfrac{T_{D,in}^*}{T_{D,out}^*} \right)} \tag{3.28}$$

where $T_{D,in}^*$ and $T_{D,out}^*$ represent the reference in- and outlet temperatures, respectively. It is proposed to define the reference values for the cold water distribution inlet temperature depending on the air-conditioning application according to the technical standard SIA 382/1 [22] listed in Tab. 3.7, where a temperature difference to the outlet of 6 K is specified (according to literature a common value [17]). As an approach, a tolerance of ± 1 K is defined for the adequate (reference) and acceptable boundary, which represents the allowed temperature variation for a functional measurement of water temperatures according to the technical standard SIA 382/1 [22]. Correspondingly, the temperatures with the upper and lower limit are applied in Eq. 3.28 for the reference B_D^* and acceptable exergy input B_D^{acc}, respectively.

Table 3.7 – Reference inlet and outlet cold water distribution temperatures for defined air-conditioning applications according to the technical standard SIA 382/1 [22].

Air-conditioning application	Reference inlet temperature $T_{D,in}^*$	Reference outlet temperature $T_{D,out}^*$
no dehumidification	14 °C $\pm$ 1 °C	20 °C $\pm$ 1 °C
partial dehumidification	10 °C $\pm$ 1 °C	16 °C $\pm$ 1 °C
controlled dehumidification	6 °C $\pm$ 1 °C	12 °C $\pm$ 1 °C

3.1.3.1.4 Subsystem cold water storage & transport

The optimization potential index proposed for the subsystem CST (see Fig. 3.2) is:

$$OPI_{CST} = 1 - \frac{\sum\limits_{t=0\,h}^{24\,h} \left(B_E^* + \sum\limits_{j} B_{el,CP,CST,j}^* \right)}{\sum\limits_{t=0\,h}^{24\,h} \left(\sum\limits_{i} B_{E,i} + \sum\limits_{j} B_{el,CP,CST,j} \right)} \qquad (3.29)$$

where the exergy input is summed up over all present refrigeration machines and auxiliary devices, which supply the subsystem. An exception is the reference evaporator exergy B_E^*, as it is determined over an exergy balance (see Eq. 3.33) for all present chillers and can therefore not be allocated to each one individually. The evaporator exergy is given by:

$$B_E = Q_E \left(1 - \frac{T_0}{\overline{T}_E} \right) \qquad (3.30)$$

with the evaporator thermal energy Q_E and the logarithmic mean temperature of the evaporator $\overline{T}_E$ expressed by:

$$\overline{T}_E = \frac{T_{E,in} - T_{E,out}}{\ln \left(\dfrac{T_{E,in}}{T_{E,out}} \right)} \qquad (3.31)$$

where $T_{E,in}$ and $T_{E,out}$ correspond to the secondary side evaporator in- and outlet temperature, respectively. Identically to the subsystem DC, the exergy of circulating pumps is:

$$B_{el,CP,CST} = W_{CP,CST} \qquad (3.32)$$

with $W_{CP,CST}$, the corresponding electrical energy of the circulating pumps. As an approach, the reference evaporator exergy input B_E^* is computed with an exergy balance over the cold storage & transport boundaries as follows:

$$B_E^* = \sum\limits_{k} B_{D,k}^* + B_{L,CST} - \sum\limits_{j} B_{el,CP,CST,j}^* \qquad (3.33)$$

where B_D^* is the reference exery output of the cold distribution (reference situation of the subsystem CL) and $B_{el,CP,CST}^*$ the reference circulating pump exery input. Similarly to the subsystem DC, it is proposed to calculate the reference exergy input of circulating pumps with:

$$B_{el,CP,CST}^* = \frac{1}{f_{el,th,CP,CST}} \sum\limits_{i} Q_{E,i} \qquad (3.34)$$

where $f_{el,th,CP,CST}$ represents the average electro-thermo amplification factor of 100 between the acceptable and adequate limit according to Tab. 3.6. The exergy loss $B_{L,CST}$ is assumed to be identical as in the actual situation, which results in a stricter assessment and is defined as:

$$B_{L,CST} = \sum_i B_{E,i} + \sum_j B_{el,CP,CST,j} - \sum_k B_{D,k} \tag{3.35}$$

The acceptable boundary OPI_{CST}^{acc} is calculated analogously with Eq. 3.29. Instead of using the actual exergy input, the acceptable exergy input applies. The latter is determined by specifying the acceptable limiting values in Eq. 3.33 and 3.34.

3.1.3.2 Free cooling operation

In this subsection, the evaluation method of the OPI in each subsystem in free cooling operating mode is presented.

3.1.3.2.1 Subsystem dry cooler

The optimization potential index of the subsystem DC (see Fig. 3.3) in free cooling operation is derived similarly as in refrigeration machine operation with:

$$OPI_{DC} = 1 - \frac{\sum\limits_{t=0\,h}^{24\,h} \left(B_{FC,DC}^* + \sum\limits_j B_{el,CP,DC,j}^* + \sum\limits_k B_{el,DC,k}^* \right)}{\sum\limits_{t=0\,h}^{24\,h} \left(B_{FC,DC} + \sum\limits_j B_{el,CP,DC,j} + \sum\limits_k B_{el,DC,k} \right)} \tag{3.36}$$

where the electrical exergy input of each present circulating pump and dry cooler ventilator is summed up. The free cooling exergy on the DC side $B_{FC,DC}$ is defined as:

$$B_{FC,DC} = Q_{FC} \left(1 - \frac{T_0}{\overline{\overline{T}}_{FC,DC}} \right) \tag{3.37}$$

where Q_{FC} represents the free cooling thermal energy and $\overline{\overline{T}}_{FC,DC}$ the logarithmic mean temperature of the free cooling heat exchanger according to:

$$\overline{\overline{T}}_{FC,DC} = \frac{T_{FC,DC,in} - T_{FC,DC,out}}{\ln\left(\dfrac{T_{FC,DC,in}}{T_{FC,DC,out}}\right)} \tag{3.38}$$

with the inlet and outlet temperature $T_{FC,DC,in}$ and $T_{FC,DC,out}$ of the heat exchanger on the dry cooler side. As in refrigeration machine operation, the exergy of the dry cooler fans $B_{el,DC}$ is given by:

$$B_{el,DC} = W_{DC} \tag{3.39}$$

with the dry cooler ventilator electrical energy W_{DC}. Correspondingly, the exergy of circulating pumps $B_{el,CP,DC}$ is defined by:

$$B_{el,CP,DC} = W_{CP,DC} \tag{3.40}$$

with $W_{CP,DC}$, the respective electrical energy input of the circulating pumps. The reference exergy of the free cooling module on the DC side is given by:

$$B_{FC,DC}^* = Q_{FC} \left(1 - \frac{T_0}{T_{FC,DC}^*} \right) \tag{3.41}$$

where $T_{FC,DC}^*$ represents the reference temperature of the free cooling module. For the latter, the following approach is proposed:

$$T_{FC,DC}^* = T_{amb} + \Delta T_{HE} + \frac{T_{FC,DC,out} - T_{FC,DC,in}}{2} \tag{3.42}$$

where ΔT_{HE} denotes the temperature difference between the secondary hydraulic circuit medium outlet and the ambient air inlet of the dry cooler heat exchanger according to Tab. 3.5. Similarly to refrigeration machine operation, a value of 6 K is applied. The reference exergy of the dry cooler fans $B_{el,DC}^*$ is defined as follows:

$$B_{el,DC}^* = \frac{1}{f_{el,th,DC}} Q_{FC} \tag{3.43}$$

with the electro-thermo amplification factor for dry cooler fans $f_{el,th,DC}$ (see Tab. 3.6). Similarly, the reference exergy of the circulating pumps $B_{el,CP,DC}^*$ is given by:

$$B_{el,CP,DC}^* = \frac{1}{f_{el,th,CP,DC}} Q_{FC} \tag{3.44}$$

where $f_{el,th,CP,DC}$ represents the electro-thermo amplification factor for circulating pumps (see Tab. 3.6). A value of 37 and 100 is specified for the dry cooler fans and circulating pumps, respectively. As mentioned, the amplification factors are defined with respect to the thermal energy of the condenser and evaporator of the integrated refrigeration machine. As an approach, the thermal energy of the free cooling module is used for the computation of the reference exergies of the auxiliary devices, as the refrigeration machines are turned off in free cooling operation. The acceptable optimization potential index is calculated according to Eq. 3.36, where the actual exergies are replaced with the corresponding acceptable ones. The latter are determined

with Eq. 3.41 to 3.44, by applying the acceptable technological limits according to Tab. 3.5 and 3.6.

3.1.3.2.2 Subsystem cold water storage & transport

The optimization potential index proposed for the subsystem CST (see Fig. 3.3) in free cooling operation is:

$$OPI_{CST} = 1 - \frac{\sum\limits_{t=0\,h}^{24\,h} \left(\sum\limits_i B^*_{D,i} + \sum\limits_j B^*_{el,CP,CST,j} \right)}{\sum\limits_{t=0\,h}^{24\,h} \left(\sum\limits_i B_{D,i} + \sum\limits_j B_{el,CP,CST,j} \right)} \tag{3.45}$$

where the exergy input is summed up over all present cooling locations and circulating pumps, which supply the subsystem. Identically as in refrigeration machine operating mode, the cold water distribution exergy B_D is calculated according to:

$$B_D = Q_D \left(1 - \frac{T_0}{\overline{T}_D} \right) \tag{3.46}$$

with the cold water distribution thermal energy Q_D and the logarithmic mean temperature $\overline{T}_D$ expressed by:

$$\overline{T}_D = \frac{T_{D,in} - T_{D,out}}{\ln \left(\dfrac{T_{D,in}}{T_{D,out}} \right)} \tag{3.47}$$

where $T_{D,in}$ and $T_{D,out}$ are the cold water distribution in- and outlet temperatures, respectively. The exergy of circulating pumps is:

$$B_{el,CP,CST} = W_{CP,CST} \tag{3.48}$$

with $W_{CP,CST}$, the corresponding electrical energy of the circulating pumps. The reference cold water distribution exergy is proposed by:

$$B^*_D = Q_D \left(1 - \frac{T_0}{\overline{T}^*_D} \right) \tag{3.49}$$

with the reference temperature $\overline{T}^*_D$ expressed by:

$$\overline{T}^*_D = \frac{T^*_{D,in} - T^*_{D,out}}{\ln \left(\dfrac{T^*_{D,in}}{T^*_{D,out}} \right)} \tag{3.50}$$

where $T^*_{D,in}$ and $T^*_{D,out}$ represent the reference in- and outlet temperatures according to Tab. 3.7, respectively. Similarly to the subsystem DC, it is proposed to calculate the reference exergy input of circulating pumps with:

$$B^*_{el,CP,CST} = \frac{1}{f_{el,th,CP,CST}} Q_{FC} \tag{3.51}$$

where $f_{el,th,CP,CST}$ represents the electro-thermo amplification factor for circulating pumps of 100 according to Tab. 3.6. The acceptable boundary $OPI^{acc}_{CST,FC}$ is calculated similarly to Eq. 3.45 by applying Eq. 3.49 to 3.51 with the corresponding acceptable limiting values from Tab. 3.6 and 3.7.

3.1.3.2.3 Subsystem free cooling

The optimization potential index for the subsystem FC (see Fig. 3.3) is proposed according to:

$$OPI_{FC} = 1 - \frac{\sum\limits_{t=0\,h}^{24\,h} B^*_{FC,CST}}{\sum\limits_{t=0\,h}^{24\,h} B_{FC,CST}} \tag{3.52}$$

where the free cooling exergy on the CST side $B_{FC,CST}$ is given by:

$$B_{FC,CST} = Q_{FC} \left(1 - \frac{T_0}{\overline{T}_{FC,CST}} \right) \tag{3.53}$$

with $\overline{T}_{FC,CST}$ the logarithmic mean temperature of the free cooling heat exchanger according to:

$$\overline{T}_{FC,CST} = \frac{T_{FC,CST,in} - T_{FC,CST,out}}{\ln\left(\dfrac{T_{FC,CST,in}}{T_{FC,CST,out}}\right)} \tag{3.54}$$

where $T_{FC,CST,in}$ and $T_{FC,CST,out}$ represent the inlet and outlet temperature of the heat exchanger on the cold water storage & transport side, respectively. The reference free cooling exergy input $B^*_{FC,CST}$ is given by:

$$B^*_{FC,CST} = Q_{FC} \left(1 - \frac{T_0}{T^*_{FC,CST}} \right) \tag{3.55}$$

Table 3.8 – Temperature differences in the free cooling module according to VDMA 24247-8 [117].

	Adequate	Acceptable
ΔT_{FC}	$\leq 1...2$ K	≤ 3 K

with $T^*_{FC,CST}$ the reference temperature of the free cooling module on the CST side. For the latter, the following approach is proposed:

$$T^*_{FC,CST} = \overline{T}_{FC,DC} + \Delta T_{FC} \tag{3.56}$$

where ΔT_{FC} represents the temperature difference in the free cooling heat exchanger between the two working fluids of the subsystem DC and CST. Target values of the latter are reported by the technical standard VDMA 24247-8 [117] (see Tab. 3.8). For the OPI_{FC} a value of 1 K is specified. The acceptable boundary OPI^{acc}_{FC} is determined analogously to Eq. 3.52 by replacing the actual with the acceptable values in the denominator and using the less strict temperature difference ΔT_{FC} of 3 K in Eq. 3.56 for the calculation of $B^{acc}_{FC,CST}$.

3.1.3.2.4 Subsystem cooling location

For technical reasons, typically two different monitoring systems are present in the refrigeration plant and the cooled room or the ventilation system itself. Therefore, no physical data is available for the calculation of B_{CL} (see Fig. 3.3) in the subsystem CL. For the latter, an alternative OPI definition is proposed as a first approach in free cooling operation. Namely, the exergy input is set to be the same in the actual and in the reference condition, while the exergy output varies according to the technical standards. The latter is plausible from a thermodynamic viewpoint, as it is favorable for the subsystem, if more exergy is extracted compared to the reference operating condition. As an outlook, it should be considered to link the monitoring systems and to measure the corresponding temperatures and heat flow rates at the cooling location for future investigations (e.g. in the AHU system or the cooled room itself, depending on how the cooling location is realized). In the present work, the optimization potential index for the subsystem CL is proposed with:

$$OPI_{CL} = 1 - \frac{\sum\limits_{t=0\,h}^{24\,h} B_D}{\sum\limits_{t=0\,h}^{24\,h} B^*_D} \tag{3.57}$$

The calculation of the cold water distribution exergy is carried out analogously to subsection 3.1.3.2.2. The adequate (reference) and acceptable limiting values according to Tab. 3.7 are applied.

3.2 Refrigeration machine modeling

In order to investigate and optimize an energy system, the behavior at various operating conditions must be known or determined. In the case of vapor compression refrigeration machines, generally the power consumption of the compressor, the heat fluxes over the heat exchangers as well as the thermodynamic properties (temperature, pressure, enthalpy, etc.) of the refrigerant in the various states of the thermodynamic cycle and of the secondary side working fluid are of interest. Basically, there are two different ways to obtain the desired data. One possibility is the experimental approach, in which measurements are carried out; the other is the development and use of models to determine the system behavior. The experimental approach is difficult for the situation of refrigeration machines in field plants. Installing measurement equipment is always bound to investment costs, and therefore, most of the devices are only instrumented with the indispensable sensors necessary for the operation (e.g. overheating temperature sensor, low and high pressure side sensors etc.). Also, those variables are rarely logged for monitoring purposes, as the secondary side temperatures and cooling load is of main interest for the plant operators. As mentioned by Wang [118], in most of the buildings, real-time measuring of the refrigeration machine power consumption is not very common. The latter is one reason, why much attention was paid to refrigeration machine models. According to Rasmussen *et al.*, they are most likely worthwhile for [119]:

- system analysis, design and optimization,

- model-based control design,

- control tuning and commissioning,

- fault detection and diagnosis.

Each of this tasks may require a different modeling approach, where the purpose of the model should be considered before developing or employing it. While a detailed model might be the best choice regarding accuracy, its usefulness can be reduced e.g. due to additional difficulties during model set-up, calibration and simulation or by requiring an increased amount of input variables [119].

In the present work, the model should be applicable to determine additional reference values for the subsystem RM (see subsection 3.1.3.1.2). Therefore, the purpose is to predict the compressor electrical power consumption at different operating conditions. To account for the latter and to ensure the application with state-of-the-art measuring concepts of refrigeration plants, secondary side temperatures and the evaporator cooling load should be used as input parameters. Those

values are either measured or determined with technical standards. In the following, different modeling approaches from literature review are discussed (see subsection 3.2.1), and subsequently, the models applied in the present study are elaborated in detail (see subsection 3.2.2).

3.2.1 Modeling approaches

In general, mathematical models can be categorized into white-, grey- and black-box models. White-box models, also referred to as physics based models, require the fundamental knowledge of the physical laws of the process under investigation. If the corresponding equations as well as parameters are known, they have a high generalization ability, meaning that they perform well even if a data set not used for the model development is applied. However, such analytical models are difficult to generate when complex phenomena or systems are studied and if required data is unknown. In that case, they generally reveal an inferior accuracy compared to black-box models [120–122]. In contrast, black-box models, also referred to as data-driven or empirical models, do not require any knowledge of the physics governing the evaluated process and are built with less effort compared to white-box models. With collected data from the investigated system, a mathematical relationship between the in- and output variables can be determined. While such models usually reveal an increased accuracy, the extrapolating capabilities are limited if processes outside the learning domain are considered [120–122]. The third modeling approach, the grey-box models, also denoted semi-empirical models, involve physical laws to build the basic model structure, where certain model parameters are identified from measurement data. Therefore, such models profit from the qualities of the other two approaches: they show generally a better generalization ability compared to the data-driven models and reveal an increased accuracy compared to the analytical ones [120–122].

The modeling topic was addressed by several authors in the case of vapor compression refrigeration machines. A review study of Rasmussen covers alone over 100 related investigations [122]. At the present day, refrigeration machines are commonly modeled with the grey- or black-box approach. In the following, a selection of refrigeration machine models are presented, where it is distinguished between:

- equation-fit based models,

- physical lumped parameter models,

- refrigeration cycle (physical component) based models,

- artificial neural network models.

Equation-fit based (EF) models are purely empirical and do not aim to fully characterize each component in the refrigeration machine, but to predict certain key performance parameters such as the COP, the cooling load or the compressor power consumption. As an example, a first-order linear model for the refrigeration machine COP has the following form [123]:

$$COP = a_1 + a_2 T_{C,in} + a_3 T_{E,in} + a_4 \dot{Q}_E \tag{3.58}$$

where $T_{C,in}$ is the condenser secondary side inlet temperature, $T_{E,in}$ the evaporator secondary side inlet temperature and $\dot{Q}_E$ the cooling load. All the model coefficients a_i have no physical meaning and are identified from experimental or manufacturer data. Many other equation-fit based models have been developed, which are mostly second-order polynomials. Yik *et al.* developed a bi-quadratic model by curve-fitting manufacturer performance data of air- and water-cooled reciprocating, screw and centrifugal chillers [124]. The model predicts the normalized chiller electricity demand in function of the condenser secondary side inlet temperature and the normalized evaporator cooling load. Stoecker *et al.* proposed a second-order polynomial model with 9 coefficients to determine the power required by the compressor of reciprocating chillers and the refrigerating capacity in function of the evaporating and condensing temperature, respectively [125]. Chang *et al.* developed a model for determining the chiller power consumption in function of the temperature difference between the condenser and evaporator secondary side inlet temperature as well as the part load ratio of the compressor [126]. The authors state that the model is accurate, especially in short-term prediction. Wang conceived a novel power consumption model for multi-parallel centrifugal chillers [118]. The model uses the evaporator secondary side temperature difference, the cooling water outlet temperature as well as the pressure difference between the parallel chilled water pipes as input parameters. The authors found that the model is slightly more accurate in comparison to four existing empirical models (among others the mentioned Yik [124] and Chang [126] models).

Physical lumped parameter (PLP) models are grey-box models and make use of thermodynamic or heat transfer relations to build the model structure based on semi-empirical equations and require experimental data to obtain missing parameters e.g. with regression. They generally have a similar form as the equation-fit based models, but the parameters reveal a physical characteristic. Some of the most popular physical lumped parameter models are the Gordon-Ng models. Gordon *et al.* developed a chiller performance model for centrifugal refrigeration machines [127], where in a subsequent work by Ng *et al.* a model for reciprocating chillers was conceived [128]. Further investigations resulted in the fundamental Gordon-Ng model, which is valid for a large

range of mechanical refrigeration machine types and sizes [20]. It is a three-parameter model which relates the refrigeration machine COP to the secondary side inlet temperatures as well as evaporator heat flow rate and has the following structure [20]:

$$\frac{T_{E,in}}{T_{C,in}}\left(1+\frac{1}{COP}\right)=1+a_1\frac{T_{E,in}}{\dot{Q}_E}+a_2\frac{T_{C,in}-T_{E,in}}{T_{C,in}\dot{Q}_E}+a_3\frac{\dot{Q}_E}{T_{C,in}}\left(1+\frac{1}{COP}\right) \quad (3.59)$$

where the regression parameters a_i reveal the physical characteristics of the refrigeration machine: a_1 represents the entropy generation in the refrigeration cycle, a_2 the heat losses or gains from the refrigeration machine and a_3 the total heat exchanger thermal resistance. Foliaco *et al.* modified the Gordon-Ng model to determine the compressor power consumption of a water-cooled centrifugal refrigeration machine, by maintaining the physical parameters [129]. The latter were estimated with a steady-state refrigeration cycle analysis and compared with the values obtained by regression, where the estimated values revealed a relative error below 20%. Another physical lumped parameter model for screw compressor refrigeration machines was developed by Lee (Lee simplified model), which is based on the first and second law of thermodynamics as well as the NTU-ε effectiveness method of heat exchangers [130, 131]. The performance of different models was assessed by Lee *et al.* on the basis of 11 different chillers [130], where the Lee model revealed an overall coefficient of variation of the root-mean-squared error (CV, compare subsection 3.2.3) of 5.32%.

Refrigeration cycle (RC) based models, also denoted physical component based models, aim to evaluate and predict the evolution of the refrigerant and its thermodynamic states during the passage through each refrigeration machine component, where it is exposed to compression, expansion as well as heat gains and losses. Usually, the nodal approach is applied, where the main components (compressor, evaporator, condenser and expansion valve) are modeled separately and then connected to each other in order to simulate the whole refrigeration cycle. For such models, the thermo-physical properties (enthalpy, entropy, etc.) of the refrigerant in function of the occuring conditions (pressure, temperature, etc.) must be known and are determined from tables or by equations of state (EOS). As an example, Browne *et al.* developed a steady-state model for centrifugal refrigeration machines, while applying 5 submodels and considering heat gains or losses from the environment [132]. They applied the NTU-ε effectiveness method (compare subsection 3.2.2.3) to model the heat transfer in the condenser as well as the evaporator (both shell-and-tube heat exchangers) and to determine the refrigerant saturation temperatures, where different correlations are applied to compute the respective heat transfer coefficients. The pressure drop is assumed to be 10 and 5% of the saturation pressure in the con-

denser and evaporator, respectively. Moreover, the expansion valve is modeled as an isenthalpic expansion process (same specific enthalpy before and after the expansion) [132]. Multiple equations are applied to describe the behaviour of the centrifugal compressor for computing the refrigerant mass flow rate. The latter is determined in function of the impeller pressure ratio, the angle of the impeller, the impeller exhaust area, the mean isentropic coefficient, the volume flow rate of the refrigeration at the impeller outlet as well as the pressure and specific volume at the compressor inlet [132]. The whole model is able to predict the condenser and evaporator heat flow rate, the COP as well as the refrigerant mass flow rate and the thermodynamic states in the refrigeration cycle. The results were validated with experimental data in part and full load, where the prediction error is found to be in the range of approximately ±10% [132]. Accurate modeling of expansion valves and compressors is relatively simple compared to modeling the heat exchangers. Capturing accurately the behavior of evaporators and condensers considering phase change (also with start-up and shut-down conditions with appearing and vanishing fluid phases) is a complex task [133]. Therefore, other RC based models use the fundamental equations for conservation of mass, momentum and energy to characterize the behavior of the heat exchangers in detail and to capture the transition between the subcooled, two-phase and superheated refrigerant states [134–136]. The best know methods to discretize and solve these equations are the moving boundary (MB) and finite volume (FV) approaches [133, 137].

Artificial neural networks (ANNs) are black-box models, which are inspired by the biological nervous system. The ANNs comprise a set of simple elements in parallel, the so called neurons, which have a weighted connection between each other in different layers. This results in a construct of multiple mathematical functions, which relates a set of inputs to certain outputs [138]. Depending on the application, ANNs can be composed of any number of neurons and arranged in different structures. Some may also include so called bias neurons which have a constant input of 1 in order to account for the invariant part of the prediction. As an example, Fig. 3.5 shows a three-layer feed-forward neural network, where x_n are the input parameters, y_m the network outputs as well as $w_{j,n}$ and $w_{m,j}$ the weighted connections between the neurons in the different layers. Each neuron has weighted inputs which are summed up in a first step. Subsequently, the obtained value is passed through an activation function, weighted again and passed to the next neurons [138]. In the case of the presented neural network structure, the output α_j (also called activation) of each neuron in the hidden layer is defined by [138]:

$$\alpha_j = F \left(\sum_{i=1}^{n} x_i w_{j,i} \right) \tag{3.60}$$
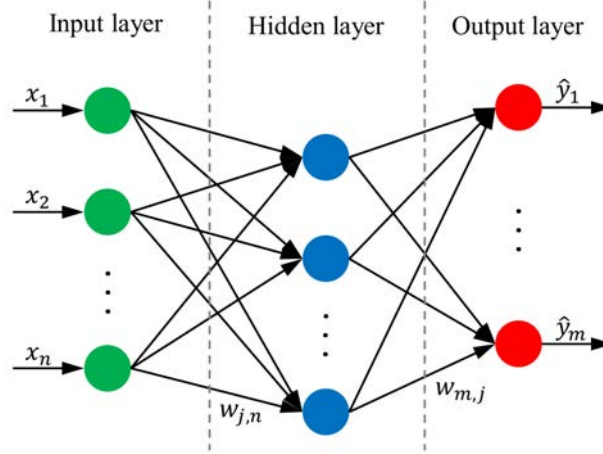
Figure 3.5 – Topology of a three-layer feed-forward neural network (adapted from [139]). The variables represent the inputs x, the outputs $\widehat{y}$ and the weightings w.

with the activation function F, where mostly a sigmoid function is applied. The activation function has the purpose to define if a neuron is activated or not and brings non-linearity to the system. Also, the function should be differentiable, as during training of the ANN gradients of the error with respect to each weight are computed. One of the most popular learning method is the back-propagation, which is a gradient-descent based procedure [138]. With this method, the error between the predicted and given output is minimized by iteratively adapting the weightings of the neurons. The error is usually expressed in terms of root-mean-squared (RMSE, compare subsection 3.2.3) or mean-squared error (MSE), where the latter is defined with [120]:

$$MSE = \frac{1}{n} \sum_{i=1}^{n} (\widehat{y}_i - y_i)^2 \tag{3.61}$$

where $\widehat{y}_i$ is the predicted and y_i the measured value, respectively. n denotes the number of data points. Şahin evaluated the performance of a refrigeration machine with internal heat exchanger and three different refrigerants by using ANNs [140]. Five input parameters (cooling capacity as well as condenser, evaporator, superheating and subcooling temperature) are used to compute the refrigeration machine COP. Depending on the refrigerant, the ANN comprises one hidden layer with 7 to 11 neurons. The author reports an excellent agreement of the predicted compared to the actual values, where the coefficient of determination (R^2, compare subsection 3.2.3) is mentioned to be at least 0.99. Another study used an ANN to predict the power consumption of 6 refrigeration machines in order to optimize the on-off sequencing in a refrigeration plant [141]. The model uses four input neurons (evaporator and condenser secondary side temperatures), one output neuron (refrigeration machine power consumption) as well as 20 and 40 neurons in the first and second hidden layer, respectively. The simulation errors are mentioned to be

below 0.52%. Kim *et al.* applied an ANN model to determine the energy consumption of a chiller in a HVAC system [142]. The model uses 8 input parameters to consider outside conditions, operation conditions, the seasonality and the historical energy use, where 60% of the measurement data was used for training the ANN and 40% for testing. Among others, the influence of the number of hidden neurons on the prediction accuracy was investigated. The number was varied between 2 to 20, where no significant improvement was found if more then 12 neurons were applied. According to the findings, the ANN model predicts the monthly chiller energy consumption with an accuracy of approximately 99.1%.

3.2.2 Investigated models

In the present work, each presented modeling approach is investigated, namely an equation-fit based model, a physical lumped parameter model, a simple refrigeration cycle based model and an ANN model. All models are steady-state, but are evaluated with the corresponding input variables and boundary conditions at every time step i.e. measurement interval. With this quasi-stationary approach (assuming steady-state over the measurement interval, similarly to the OPI evaluation), the temporal behavior of the refrigeration machine can be characterized with good approximation (see section 5.1). Moreover, since the best performing model is applied in the proposed exergy-based evaluation method, which should be generally applicable and where a daily assessment of the OPI is carried out, the quasi-stationary approach is considered acceptable. For preliminary tests, the models are first applied with experimental data of a laboratory test rig (see section 4.3), and subsequently, with experimental data of a field plant (see section 4.2) to determine their applicability for the exergy-based evaluation method. The experimental data is split into training / validation (also denoted internal) and testing (also denoted external) data sets. The latter is applied in order to evaluate the performance of the models when data excluded from training is utilized. In the internal data sets, 60% of the measurements are randomly assigned for training. All models are then compared in terms of model performance indicators (see subsection 3.2.3) to determine the best suiting model for the exergy-based evaluation approach.

3.2.2.1 Equation-fit based model

The Comstock model has been chosen as an equation-fit based model representative in the present work, as it uses commonly measured quantities in field plants as input variables. It is a second-order polynomial fitting model with 7 fitting parameters a_i to determine the compressor

electrical power consumption $\dot{W}_{CPR}$, which has the following form [118]:

$$\dot{W}_{CPR} = a_1 + a_2 T_{E,in} + a_3 T_{C,in} + a_4 \dot{Q}_E + a_5 T_{E,in} \dot{Q}_E + a_6 T_{C,in} \dot{Q}_E + a_7 \dot{Q}_E^2 \quad (3.62)$$

with $T_{E,in}$ the evaporator secondary side inlet temperature, $T_{C,in}$ the condenser secondary side inlet temperature and $\dot{Q}_E$ the evaporator heat flow rate as input parameters. The coefficients a_i reveal no physical characteristic and are determined from measurement data with a non-linear curve fitting algorithm pre-implemented in MATLAB [143].

3.2.2.2 Pyhsical lumped parameter model

In the present work, the modified Gordon-Ng model by Folicao *et al.* is applied [129], as like the Comstock model, it uses commonly measured quantities in field plants as input variables. Even if the model is conceptualized for centrifugal chillers, it is investigated in the present analysis. The reason is that it bases on the Gordon-Ng model, which is applicable for a wide range of different refrigeration machine types and sizes. It is a three-parameter model which has the following form [129]:

$$\dot{W}_{CPR} - \left(\frac{T_{C,in} - T_{E,out}}{T_{E,out}} \right) \dot{Q}_E = a_1 T_{C,in} + a_2 \left(\frac{T_{C,in} - T_{E,out}}{T_{E,out}} \right) \\ + a_3 \left(\frac{\dot{Q}_E^2 + \dot{Q}_E \dot{W}_{CPR}}{T_{E,out}} \right) \quad (3.63)$$

with $T_{E,out}$ the evaporator secondary side outlet temperature, $T_{C,in}$ the condenser secondary side inlet temperature and $\dot{Q}_E$ the evaporator heat flow rate as input parameters. The fitting parameters are determined with a regression routine pre-implemented in MATLAB [143], where a_1 denotes the entropy generation in the refrigeration cycle, a_2 the heat losses or gains from the refrigeration machine and a_3 the total heat exchanger thermal resistance. By rearranging Eq. 3.63, the electrical power consumption of the compressor $\dot{W}_{CPR}$ is then determined with:

$$\dot{W}_{CPR} = \frac{a_1 T_{C,in} + a_2 \left(\frac{T_{C,in} - T_{E,out}}{T_{E,out}} \right) + \left(\frac{T_{C,in} - T_{E,out}}{T_{E,out}} \right) \dot{Q}_E + a_3 \frac{\dot{Q}_E^2}{T_{E,out}}}{1 - a_3 \frac{\dot{Q}_E}{T_{E,out}}} \quad (3.64)$$

3.2.2.3 Refrigeration cycle based model

A simplified RC based model has been applied in the present work, which considers the four main refrigeration machine components (evaporator, compressor, condenser and expansion valve) in terms of thermodynamic and heat transfer relations. Fig. 3.6 shows a schematic of the considered refrigeration cycle as well as the corresponding log(p)-h-diagram with the different refrigerant states. The model uses secondary side temperatures as well as the evaporator cooling load as input variables and incorporates 6 physical parameters (see Tab. 3.9 for details), which are identified from measurement data. To reduce the number of unknown parameters, the following assumptions apply for the model:

- steady-state operation,

- negligible heat exchange with the environment,

- negligible pressure losses,

- isenthalpic expansion.

The evaporator and condenser are modeled with the NTU-ε effectiveness method and are considered as heat exchangers with phase change on the primary side. This represents a special case, where the heat capacity rates of the condensing vapor or evaporating liquid tends towards infinity

Table 3.9 – Inputs, outputs and parameters of the RC based model.

Type	Variables	
input	$T_{E,in}$	evaporator secondary side inlet temperature
	$T_{E,out}$	evaporator secondary side outlet temperature
	$T_{C,in}$	condenser secondary side inlet temperature
	$T_{C,out}$	condenser secondary side outlet temperature
	$\dot{Q}_E$	evaporator heat flow rate
output	$\dot{W}_{CPR}$	compressor electrical power
parameter	η_{isen}	compressor isentropic efficiency
	$\eta_{el,mech}$	compressor electro-mechanical efficiency
	ΔT_{sh}	superheating temperature difference
	ΔT_{sc}	subcooling temperature difference
	$(UA)_E$	evaporator surface dependent overall heat transfer coefficient
	$(UA)_C$	condenser surface dependent overall heat transfer coefficient
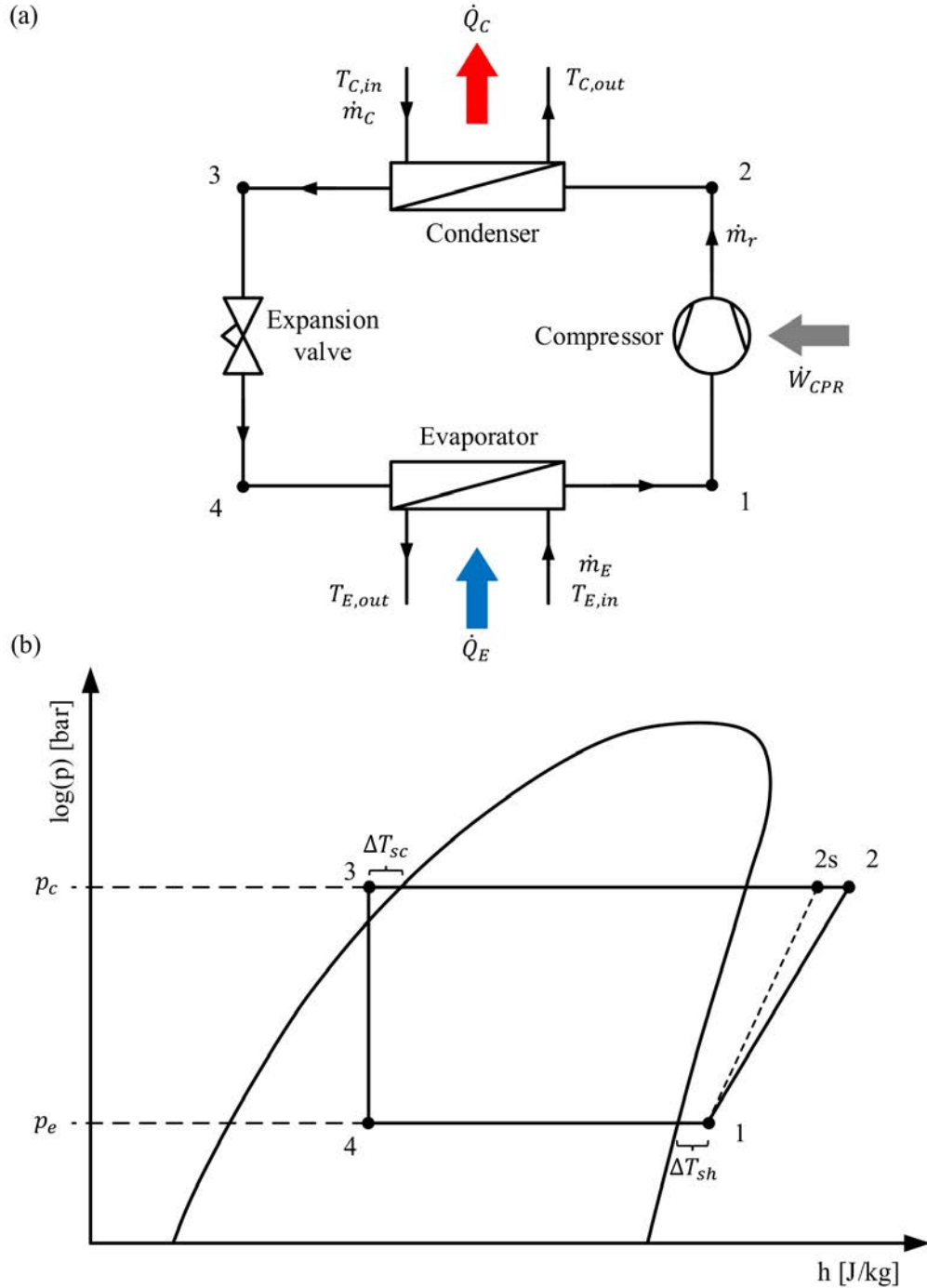
Figure 3.6 – Simplified schematic of (a) the considered refrigeration cycle and (b) the corresponding log(p)-h-diagram with the different refrigerant states 1 to 4 and 2s.

(nearly isothermal processes). The evaporator effectiveness ε_E is then given by [144, 145]:

$$\varepsilon_E = 1 - e^{-NTU_E} \tag{3.65}$$

where NTU_E denotes the dimensionless parameter *number of transfer units* of the evaporator, which is defined as [144]:

$$NTU_E = \frac{(UA)_E}{c_{p,E}\dot{m}_E} \tag{3.66}$$

with $(UA)_E$ the overall heat transfer coefficient times the heat transfer area of the evaporator as well as $c_{p,E}$ and $\dot{m}_E$ the specific heat capacity and the mass flow rate of the secondary side chilled water, respectively. As the heat capacity and mass flow rate of the secondary side are unknown, they can be determined with:

$$c_{p,E}\dot{m}_E = \frac{\dot{Q}_E}{T_{E,in} - T_{E,out}} = \frac{\dot{Q}_E}{\Delta T_E} \tag{3.67}$$

with the temperature difference between the evaporator secondary side inlet and outlet ΔT_E. The evaporation temperature of the refrigerant is then given with [144, 145]:

$$T_e = T_{E,in} - \frac{\Delta T_E}{\varepsilon_E} \tag{3.68}$$

Analogously, Eq. 3.65 to 3.68 apply also for the condenser by utilizing the corresponding quantities. With the chosen NTU-ε effectiveness approach, the superheating and subcooling effects in the heat exchangers are not explicitly treated. However, the error is assumed negligible, as it is presumably compensated with the UA parameter when calibrating the model. With the evaporation and condensation temperature, the low and high pressure level, p_e and p_c (see Fig. 3.6b), can be determined[4]. The refrigerant temperature T_1 at state 1 after the evaporator (see Fig. 3.6) is determined with:

$$T_1 = T_e + \Delta T_{sh} \tag{3.69}$$

where ΔT_{sh} represents the superheating temperature difference. Similarly, the refrigerant temperature T_3 at state 3 after the condenser (compare Fig. 3.6) is given by:

$$T_3 = T_c - \Delta T_{sc} \tag{3.70}$$

where ΔT_{sc} is the subcooling temperature difference. Together with the found pressures, the specific enthalpies and entropies (h_1, h_3, s_1, s_3) of the refrigerant can be identified at state 1 and 3. After the condenser, the refrigerant passes through an expansion valve and expands from the

---

[4] *Remark:* As mentioned, refrigeration cycle based models require the knowledge of the thermo-physical properties of the refrigerant, which have to be determined from tabulated data or with equations of state (EOS). In the first version of the model, the properties were computed with the Soave-Redlich-Kwong (SRK) EOS [146], to fully understand the evaluation procedure. The SRK EOS was conceptualized for real gases and is still of interest at the present day due to its simple form compared to other EOS. In the final model however, to accurately capture the liquid state after the condenser, the thermodynamic properties are computed with the tool REFPROP (Reference Fluid Thermodynamic and Transport Properties Database), which has implemented the NIST (National Institute of Standards and Technology) EOS for a broad range of fluids [147].

condensing to the evaporating pressure. While beeing in liquid phase after the condenser, the refrigerant exhibits a change to liquid-vapor phase when expanding. By assuming an isenthalpic expansion process, the specific enthalpy h_4 at state 4 after the expansion valve (see Fig. 3.6) is equivalent to the specific enthalpy h_3 at state 3. With an energy balance, the evaporator heat flow rate $\dot{Q}_E$ is given by [14, 16]:

$$\dot{Q}_E = \dot{m}_r(h_1 - h_4) \tag{3.71}$$

from which the refrigerant mass flow rate $\dot{m}_r$ can be determined. The actual compressor input $\dot{W}_{CPR,act}$ is defined according to [14, 16]:

$$\dot{W}_{CPR,act} = \dot{m}_r(h_2 - h_1) \tag{3.72}$$

where the enthalpy h_2 at state 2 after the compressor must be known (see Fig. 3.6). The compressor isentropic efficiency η_{isen} is given by [14, 16]:

$$\eta_{isen} = \frac{\dot{W}_{CPR,isen}}{\dot{W}_{CPR,act}} = \frac{\dot{m}_r(h_{2s} - h_1)}{\dot{m}_r(h_2 - h_1)} = \frac{h_{2s} - h_1}{h_2 - h_1} \tag{3.73}$$

which relates the isentropic compressor input $\dot{W}_{CPR,isen}$ with the actual compressor power $\dot{W}_{CPR,act}$, where h_{2s} represents the specific enthalpy at state 2s resulting from an isentropic (i.e. reversibel) compression (see Fig. 3.6). h_{2s} can be determined, as the specific entropy s_{2s} at state 2s equals the specific entropy s_1 at state 1. From Eq. 3.73 it follows for h_2:

$$h_2 = \frac{(h_{2s} - h_1)}{\eta_{isen}} + h_1 \tag{3.74}$$

Finally, the compressor electrical power $\dot{W}_{CPR}$ is determined with [148]:

$$\dot{W}_{CPR} = \frac{\dot{W}_{CPR,act}}{\eta_{el,mech}} \tag{3.75}$$

where $\eta_{el,mech}$ represents the compressor electro-mechanical efficiency to account for mechanical as well as electrical losses e.g. in the frequency converter. The condenser heat flow rate $\dot{Q}_C$ is given with an overall energy balance over the refrigeration cycle [14]:

$$\dot{Q}_C = \dot{Q}_E + \dot{W}_{CPR,act} \tag{3.76}$$
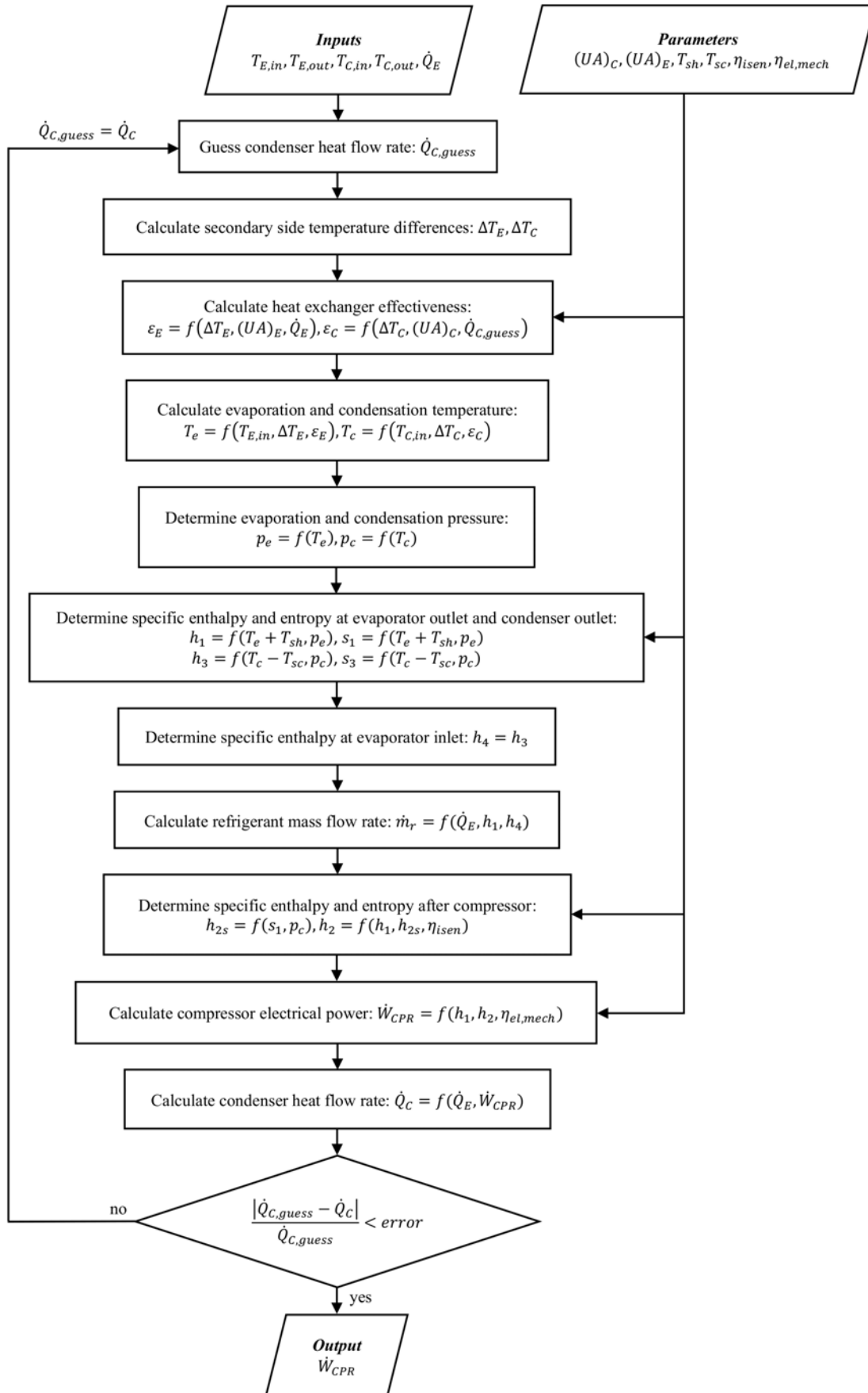
Figure 3.7 – Algorithm flow chart of the RC based model with the corresponding inputs, parameters and output.

A flow chart of the algorithm is shown in Fig. 3.7. The condenser heat flow rate is unknown in the beginning and guessed for the initial iteration. Subsequently, $\dot{Q}_C$ is iteratively computed with the described procedure, compared with the guessed value and applied in the next iteration step, until the relative error is lower than 0.1%. Then, the model yields the corresponding compressor electrical power. To accurately determine the latter with a given data set of inputs, the model parameters (see Tab. 3.9) must be known and are identified from measurements. Therefore, the following cost i.e. objective function is minimized [118]:

$$RMSE = \sqrt{\frac{1}{n} \sum_{i=1}^{n} \left(\widehat{\dot{W}}_{CPR,i} - \dot{W}_{CPR,i} \right)^2} \qquad (3.77)$$

which represents the root-mean-squared error (RMSE, compare subsection 3.2.3) with $\widehat{\dot{W}}_{CPR,i}$ and $\dot{W}_{CPR,i}$ the simulated and measured compressor electrical power of each data set, respectively. n denotes the number of measurement points used for training. The parameters are initially identified with a batch gradient-descent routine [149] and then iteratively optimized with a pre-implemented minimization algorithm in MATLAB [143], until the RMSE is minimized. All parameters reveal a physical characteristic and defining them as constants is physically not correct (except in steady-state). The overall heat transfer coefficient, for example, is dependent on the heat exchanger configuration and the present flow conditions. However, to the best of our knowledge, this simplification is reasonable with the goal of generating a widely applicable model which can be employed independently of the compressor and heat exchanger design, even if no technical details of the refrigeration machine are available.

3.2.2.4 Artifical neural network model

In the present work, a feed-forward ANN model is applied with one input layer, one ouput layer and one hidden layer (see Fig. 3.8), which has been determined by trial and error. Like the RC based model, the ANN has 5 input parameters (secondary side temperatures as well as evaporator cooling load) and one output parameter, the compressor electrical power $\dot{W}_{CPR}$. A tan-sigmoid and a linear activation function is used for the hidden and output layer, respectively. The hidden layer consists of 21 and 25 neurons (with bias) when applied on the laboratory test rig and the field plant, respectively. The amount of neurons was identified by iteratively increasing the number until the performance function, chosen to be the mean-square error (MSE), converged. The number of neurons is substantially lower than the number of training data points, which reduces the risk of overfitting. The ANN is designed, set-up and trained with the neural network
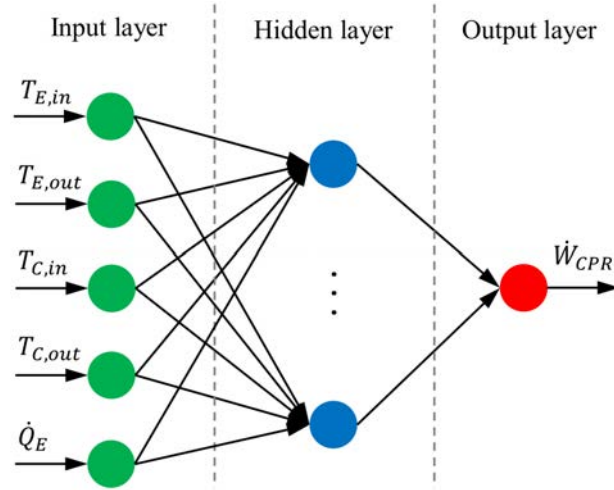
Figure 3.8 – Topology of the applied feed-forward neural network with the corresponding input and output variables.

toolbox pre-implemented in MATLAB [143], where the Levenberg-Marquardt back-propagation algorithm is applied for training [150]. This algorithm is a combination of the Newton and gradient-descent method, which is particularly useful for moderate-sized ANNs with the MSE as performance function [151].

3.2.3 Model performance metrics

Many different performance indicators exist, which can be applied to evaluate the model accuracy. In the present work, the following indicators are applied, where y_i represents the measured value, $\widehat{y}_i$ the predicted value and n the number of data points. One of the most applied index is the root-mean-squared error (RMSE) defined as [140]:

$$RMSE = \sqrt{\frac{1}{n}\sum_{i=1}^{n}\left(\widehat{y}_i - y_i\right)^2} \tag{3.78}$$

The second index is the mean-absolute error (MAE) which has an increased interpretability compared to the RMSE, which is given by [118]:

$$MAE = \frac{1}{n}\sum_{i=1}^{n}|\widehat{y}_i - y_i| \tag{3.79}$$

The coefficient of variation of the root-mean-squared error (CV or CV-RMSE), also denoted relative root-mean-squared error (R-RMSE), indicates if the model has a satisfactory prediction ability, where a small value indicates a high predictive accuracy. The indicator is defined with [118]:

$$CV = \frac{RMSE}{\overline{y}_i} \cdot 100\% \tag{3.80}$$

where $\overline{y}_i$ is the average of the measured values. Additionally, the coefficient of determination (R^2) is applied, which is given by [140]:

$$R^2 = 1 - \frac{SS_{res}}{SS_{tot}} = 1 - \frac{\sum\limits_{i=1}^{n} (y_i - \widehat{y}_i)^2}{\sum\limits_{i=1}^{n} (y_i - \overline{y}_i)^2} \tag{3.81}$$

This indicators relates the sum of the squared residuals (deviation from the predicted and measured value) SS_{res} with the total sum of squares SS_{tot}. The closer the value of R^2 is to 1, the more accurate are the modeled values.

4 Investigated systems and procedures

This chapter presents the examined systems and procedures. In order to exemplify the proposed exergy-based evaluation method and to demonstrate the functionality, the rating system is applied on two numerical test cases (see section 4.1) as well as on a case study, while for the latter, experimental data gained from a field installation is used (see section 4.2). Besides the field plant, a laboratory test rig is utilized for preliminary refrigeration machine model evaluations, which is elaborated in section 4.3.

4.1 Test cases

Two numerical test cases, representing a field plant in refrigeration machine operating mode as shown in Fig. 3.2 with one refrigeration machine and one cooling location, are analyzed in the present study. The first case represents an adequate operating refrigeration plant, while the second simulates a faulty operation due to a fouled condenser and dry cooler heat exchanger. Therefore, a larger temperature difference between the condenser in- and outlet as well as an increased inlet temperature is assumed (due to an increased temperature difference in the dry cooler heat exchanger). As a consequence, an increased electrical energy consumption of the dry cooler fans as well as of the circulating pumps in subsystem DC and of the compressor in subsystem RM is present. For both cases the same cooling load and temperature levels in the subsystem CST and CL are assumed. A steady-state operation of the refrigeration system with daily values according to Tab. 4.1 is considered. The computation of the corresponding exergies and the OPI is then carried out according to the described method in subsection 3.1.3.1.

Table 4.1 – Defined daily values of temperatures, thermal and electrical energies for both evaluated test cases in each subsystem.

Subsystem	Variables	Values test case 1 (adequate operation)	Values test case 2 (faulty operation)
dry cooler	Q_C	3196.8 MJ	3283.2 MJ
	$T_{C,in}$	27 °C (300.15 K)	29 °C (302.15 K)
	$T_{C,out}$	30 °C (303.15 K)	35 °C (308.15 K)
	$W_{CP,DC}$	27.8 MJ	46.9 MJ
	W_{DC}	71.0 MJ	78.2 MJ
refrigeration machine	W_{CPR}	518.4 MJ	604.8 MJ
cold water storage & transport	Q_E	2678.4 MJ	2678.4 MJ
	$T_{E,in}$	18 °C (291.15 K)	18 °C (291.15 K)
	$T_{E,out}$	12 °C (285.15 K)	12 °C (285.15 K)
	$W_{CP,CST}$	21.4 MJ	21.4 MJ
cooling location	Q_D	1944.0 MJ	1944.0 MJ
	$T_{D,in}$	13 °C (286.15 K)	13 °C (286.15 K)
	$T_{D,out}$	17 °C (290.15 K)	17 °C (290.15 K)
all subsystems	T_0	22 °C (295.15 K)	22 °C (295.15 K)

4.2 Field plant

An existing refrigeration plant located in the city of Winterthur, Switzerland is investigated in the present work as a case study. The field plant consists of five parallel refrigeration machines with 950 kW cooling power each and ammonia (R717) as refrigerant. Additionally, one free cooling heat exchanger is integrated to the system and the refrigeration machines as well as the distribution networks are located underground. The hydraulic circuit supplies seven different buildings with cold water, where the cooling locations represent air-handling units of ventilation systems in the different buildings. The main application is for office space cooling, where the temperature level of the cold water distribution corresponds to an air-conditioning application with partial dehumidification. Three rooftop coolers with a nominal power of 2000 kW and 12 circulating pumps with a nominal volume flow rate ranging from 52.2 to 485 m^3/h are present. Two of which are winter pumps for the free cooling module and one winter pump substitutes the others in the subsystem CST when the cooling load is low. Moreover, two cold storages with a capacity of 3.5 m^3 are integrated to the refrigeration system.

As a result, the refrigeration plant is split into 14 and 10 different subsystems, according to the considerations in subsection 3.1.2, in refrigeration machine and free cooling operating mode, respectively. A piping & instrumentation diagram of the field plant with the corresponding subsystems is depicted in Fig. 4.1. Each of them is assessed individually in both operating modes according to the described evaluation method in subsection 3.1.3. Measurement data of the field plant over the entire year 2018 was collected by the plant operator (energy contractor), where no detailed information about the measurement equipment is available. The data was recorded at an interval of 5 minutes, which results in 288 summands for the daily assessment of the OPI in the present evaluation. In a first step, the measurement data was reviewed and prepared for the evaluation. Two cooling locations were inoperative until April 2018 and one until May 2018. Additionally, one of the five refrigeration machines was commissioned in April 2018, most probably to cover the increased cooling load of the additional cooling locations. Four measurement points of one operating cooling location were missing from 12.04.2018 13:40 to 12.04.2018 13:55, which were approximated by linear interpolation. No data was registered in the monitoring system of the winter pumps, which are active in free cooling operation as well as in refrigeration machine operation when then cooling load is low. As an approach, the electrical energy input is calculated under the assumption that they behave similarly as the circulating pumps which were monitored.
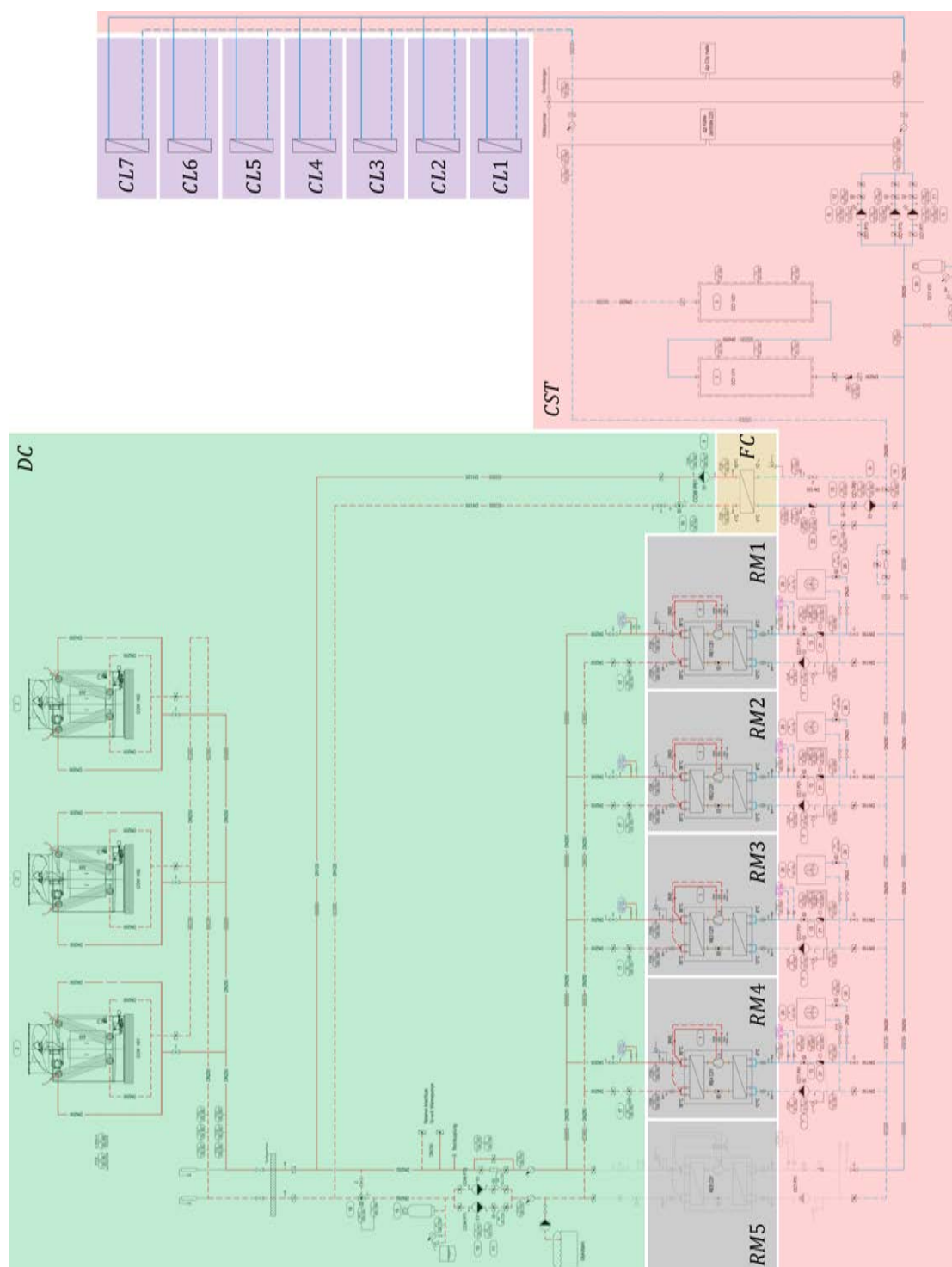
Figure 4.1 – Piping & instrumentation diagram of the investigated field plant (copyright Leplan AG, Switzerland) with the definition of the different subsystems (compare Fig. 3.2 and 3.3).

For the investigation of the different refrigeration machine models according to subsection 3.2.2, measurement data of refrigeration machine 1 (RM1) is used for training and validation. Subsequently, measurements from refrigeration machine 2 (RM2) are applied as testing data set, to determine the generalization quality of each modeling approach. The data sets are prepared in a

way, that only measurement points are considered if the cooling load is larger than zero, i.e. the refrigeration machines are running.

4.3 Laboratory test rig

The test facility is located at the refrigeration laboratory of the Institute of Energy Systems and Fluid Engineering at the Zurich Unversity of Applied Sciences in Winterthur, Switzerland and includes two refrigeration machines. The first refrigeration cycle operates with R134a as refrigerant, whereas the second one works with R744 (CO_2). Latter was successfully operated by Fritschi *et al.* [32] in order to carry out investigations regarding the efficiency in carbon dioxide refrigeration technology with parallel compression. Within the scope of the present work, experimental investigations are carried out with the R134a machine. Coupled to the chillers, two secondary hydraulic circuits with a water-glycol mixture as working fluid are present. Two 3 m^3 storage tanks, from which the liquid is pumped to the refrigeration machines and the corresponding heat exchangers, serve as the heating and cooling source.

4.3.1 R134a vapor compression refrigeration machine

The R134a vapour compression refrigeration machine (see Fig. 4.2) consists of the following main components:

- compressor (CPR),

- precooler (PC),

- condenser (C),

- subcooler (SC),

- expansion valve (EV),

- evaporator (E),

- internal heat exchanger (IHX).

A simplified piping & instrumentation diagram of the full test setup is shown in Fig. 4.3 and the main component details are listed in Tab. 4.2. The test rig was designed to investigate different machine configurations and situations, e.g. to simulate an undersized heat exchanger. For this reason, each heat exchanger may be enabled / disabled on demand, relatively simple by opening / closing the corresponding valves. Consequently, every heat exchanger has its own

Figure 4.2 – Overview of the R134a refrigeration machine test rig.

bypass piping. All external heat exchangers (precooler, condenser, subcooler and evaporator) are connected to the secondary hydraulic circuits. The liquid flow is generated by a glandless pump located at each heat exchanger. The volume flow rates and the inlet temperatures can be dynamically regulated as desired. The flow rates are measured with MID (magnetic-inductive) flow meters at the heat exchanger outlet (see Fig. 4.3, location $\dot{V}_E$, $\dot{V}_C$, $\dot{V}_{SC}$ and $\dot{V}_{PC}$), whereas the temperatures are directly metered in the water-glycol mixture (*in-situ*) with Pt100 sensors at the heat exhanger in- and outlet, respectively (see Fig. 4.3, location $T_{C,in}$, $T_{E,in}$, $T_{E,out}$, $T_{C,in}$, $T_{C,out}$, $T_{SC,in}$, $T_{SC,out}$ and $T_{PC,in}$, $T_{PC,out}$). With the obtained data, the in- and outgoing heat fluxes of the refrigeration machine can be determined.

The refrigeration cycle itself is completely instrumented with 8 Pt100 temperature sensors (see Fig. 4.3, location T_1 to T_8), 2 pressure taps for the absolute pressure before and after the compressor (see Fig. 4.3, location p_e and p_c), as well as 2 pressure sensors to determine the pressure drop over the precooler / condenser and the internal heat exchanger (see Fig. 4.3, location Δp_c and Δp_{ihx}), respectively. The maximum operating pressure of the R134a refrigeration machine is 10 and 24 bar on the low and high pressure side, respectively. The Pt100 sensors are coupled
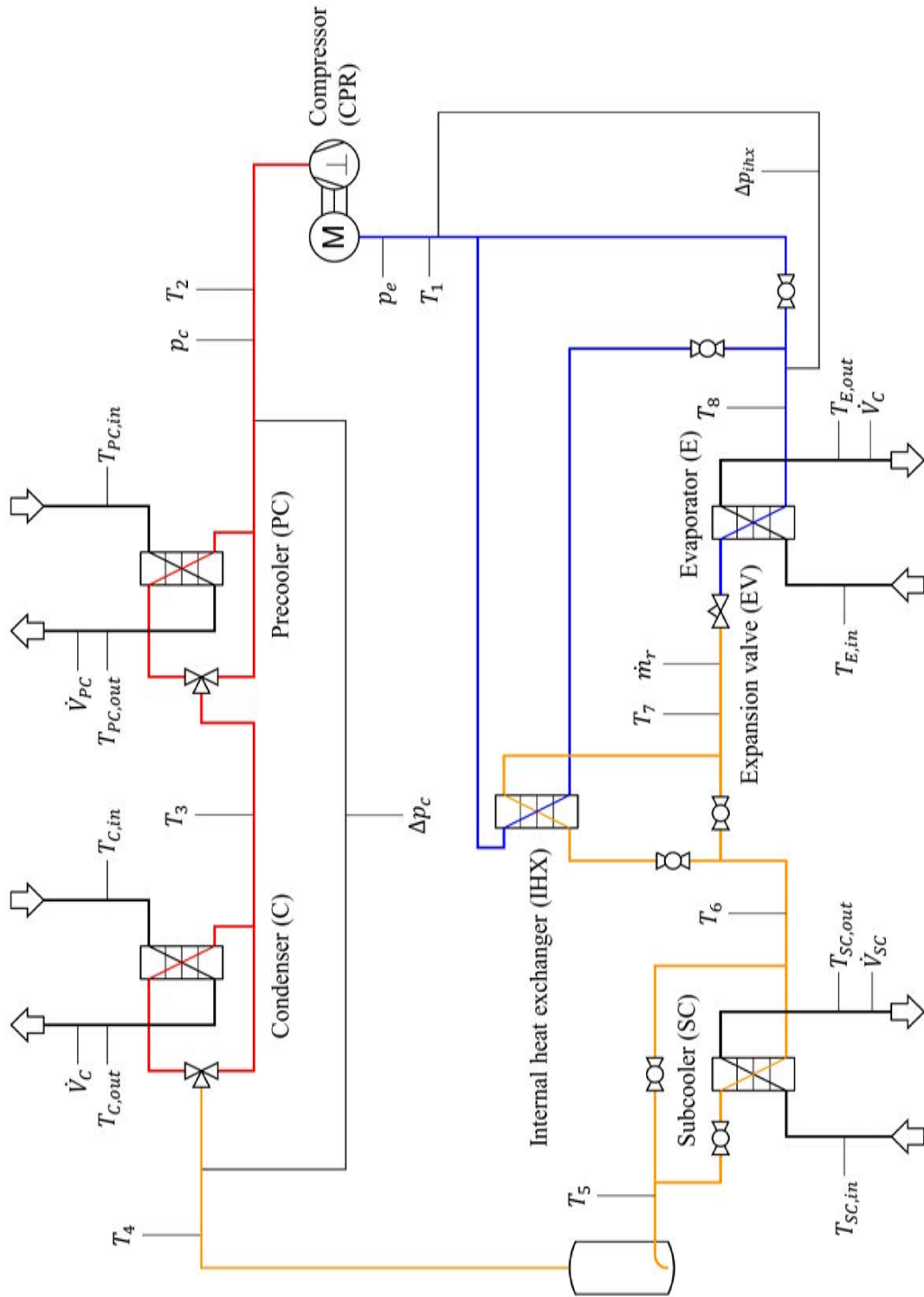
Figure 4.3 – Simplified schematic of the test setup with the corresponding components and measurement locations.

on the tubing with a thermal compound (*ex-situ* measurement) and are well insulated in order to minimize any external effects. Moreover, the mass flow rate is determined directly in front of the expansion valve (see Fig. 4.3, location $\dot{m}_r$) with a coriolis flow meter. The electrical power of the compressor is measured as well.

Table 4.2 – List of the installed components in the R134a refrigeration machine.

Component	Type	Model	Nominal capacity [kW]
compressor (CPR)	reciprocating compressor	Bitzer 4TES-12Y-40P	13.8
precooler (PC)	plate heat exchanger	SWEP B25Tx30	20
condenser (C)	plate heat exchanger	SWEP B25Tx60	30
subcooler (SC)	plate heat exchanger	SWEP B8Tx14	3.4
expansion valve (EV)	electronic expansion valve	Siemens MVL661.15-0.4	-
evaporator (E)	plate heat exchanger	SWEP V120Tx60	17.2
internal heat exchanger (IHX)	plate heat exchanger	SWEP B12Lx30	-

With the present setup, the cooling load and the corresponding operating state of the refrigeration machine is defined by the temperature level and the throughput of the secondary side, as well as the evaporating temperature. The operating point of the compressor and the expansion valve is regulated by an integrated control system (proportional-integral-derivative controller), which can be overwritten to specify a manually defined compressor frequency. However, any changes in the control system are delicate and need to be carried out cautiously in order to avoid any damage to the machine. The worst-case scenario would be an incomplete evaporation of the refrigerant, which results in liquid slugging and the subsequent mechanical failure of the compressor.

4.3.2 Measurement configurations

For investigating the refrigeration machine models, measurements with the basic refrigeration machine configuration (pre- and subcooler deactivated) are carried out. Different compressor load conditions and chilled water set-point temperatures are considered (see Tab. 4.3), which results in 9 measurement configurations. To force the compressor in a constant part load condition, the present control system was deactivated. The compressor frequency was then set to a constant value directly at the frequency inverter. For all measurements, the condenser secondary side inlet temperature $T_{C,in}$ is maintained at approximately 35 °C and the measurement interval is set to 1 s. The evaporator and condenser secondary side volume flow rate, $\dot{V}_E$ and $\dot{V}_C$, is set to 51 and 69 l/min, respectively. The minimal part-load condition is given by the test

rig (lower values are not feasible) and the cold water temperatures are chosen with regard to the practical relevance. A set-point of 6 °C is widely used in refrigeration plants for air-conditioning applications, although the cold water temperature should be chosen as high as possible.

For the evaluation of the different refrigeration machine models according to subsection 3.2.2, data set no. 2 to 4 and 6 to 8 are applied for training / validation (internal data set), where a share of 60% is randomly assigned for training. Correspondingly, the data sets 1, 5 and 9 are applied for testing (external data set). Data set 1 and 9 should reveal the extrapolating and data set 5 the interpolating qualities of each modeling approach.

Table 4.3 – List of the investigated measurement configurations with the corresponding size of the registered data set.

Data set no. [–]	Compressor load [%]	Chilled water set-point temperature ($T_{E,out}$) [°C]	Data set size [–]
1	50	1	647
2	75	1	611
3	100	1	561
4	50	6	647
5	75	6	633
6	100	6	717
7	50	10	601
8	75	10	783
9	100	10	569

5 Results and discussion of the modeling and proposed assessment approach

In the present chapter, the results of the described methods (see section 3.1 and 3.2) are presented and discussed. First, the outcome of the different modeling approaches is shown in section 5.1, where from the four different models the most promising one is identified. Subsequently, the analysis results of the proposed exergy-based assessment approach are presented in section 5.2. To exemplify the practical application, functionality and purpose of the method, it is applied on the numerical test cases and experimental data from the field plant as a case study.

5.1 Refrigeration machine modeling

The goal of the present section is to analyze the performance of each investigated model as preliminary test applied with measurement data of the laboratory test rig (see subsection 5.1.1) and subsequently with measurements of refrigeration machines in the field plant (see subsection 5.1.2). The study should reveal the most promising modeling approach for the application in the exergy-based assessment method to determine reference values for the subsystem RM.

5.1.1 Laboratory test rig

Fig. 5.1 shows the measured and modeled compressor electrical power consumption (y-axis) of the laboratory refrigeration machine in function of the corresponding measuring point (x-axis). The measured compressor electrical power ranges from approximately 5100 to 7980 W (see Fig. 5.1a) and from 4750 to 8500 W (see Fig. 5.1b) in the training / validation and testing data set, respectively. Fig. 5.2 depicts the modeled compressor electrical power consumption of each modeling approach (y-axis) in function of the measured compressor electrical power consumption (x-axis) with a $\pm 10\%$ error band. Furthermore, Tab. 5.1 lists the values of the different performance indicators for each model with respect to the internal (training / validation) and external (testing) data.

To begin with, the predicted compressor electrical power $\dot{W}_{CPR,EF}$ by the equation-fit based (EF) model shows qualitatively a good agreement with measurements $\dot{W}_{CPR,meas}$ when using internal data (see Fig. 5.1a). The model reveals a root-mean-squared (RMSE) and mean-absolute error (MAE) of approximately 165 and 140 W (see Tab. 5.1), respectively, which are the second lowest values among the investigated approaches. When applying the model to the testing data set, the interpolation quality is adequate (see Fig. 5.1b, data point no. 648 to 1280) and a slight overprediction of approximately 4% is present when extrapolating (see Fig. 5.1b, data point no. 1 to 647 as well as 1281 to 1849). Consequently, the RMSE and MAE increase by 29.04 and 14.53 W, respectively. The model reveals an adequate generalization (i.e. extra- and interpolation) ability, where all simulated values are inside of the $\pm 10\%$ error band (see Fig. 5.2a). This is also demonstrated by coefficient of determination (R^2) values close to one and low coefficient of variation (CV) values, respectively. This outcome is interesting, as according to the literature search, empirical models usually reveal an inferior generalization quality.

The physical lumped parameter (PLP) model reveals a similar behaviour, where the simulated compressor electrical power $\dot{W}_{CPR,PLP}$ fits qualitatively well the experimental results

$\dot{W}_{CPR,meas}$ with both the internal and external data (see Fig. 5.1). With the training / validation data set, the RMSE and MAE is 173 and 143 W (see Tab. 5.1), respectively. As expected, the values are larger than for the black-box models. Nevertheless, the model performance is still reasonable, which is shown by adequate R^2 and CV values. Also, all the predicted values lie inside of the $\pm 10\%$ error band (see 5.2b). Similarly to the EF model, a slight overprediction is present with the external data set (see Fig. 5.1b, data point no. 1 to 647 as well as 1281 to 1849 and Fig. 5.2b, testing data set).

(a) Training / validation data set (60% used for training)

(b) Testing data set (not used for training)
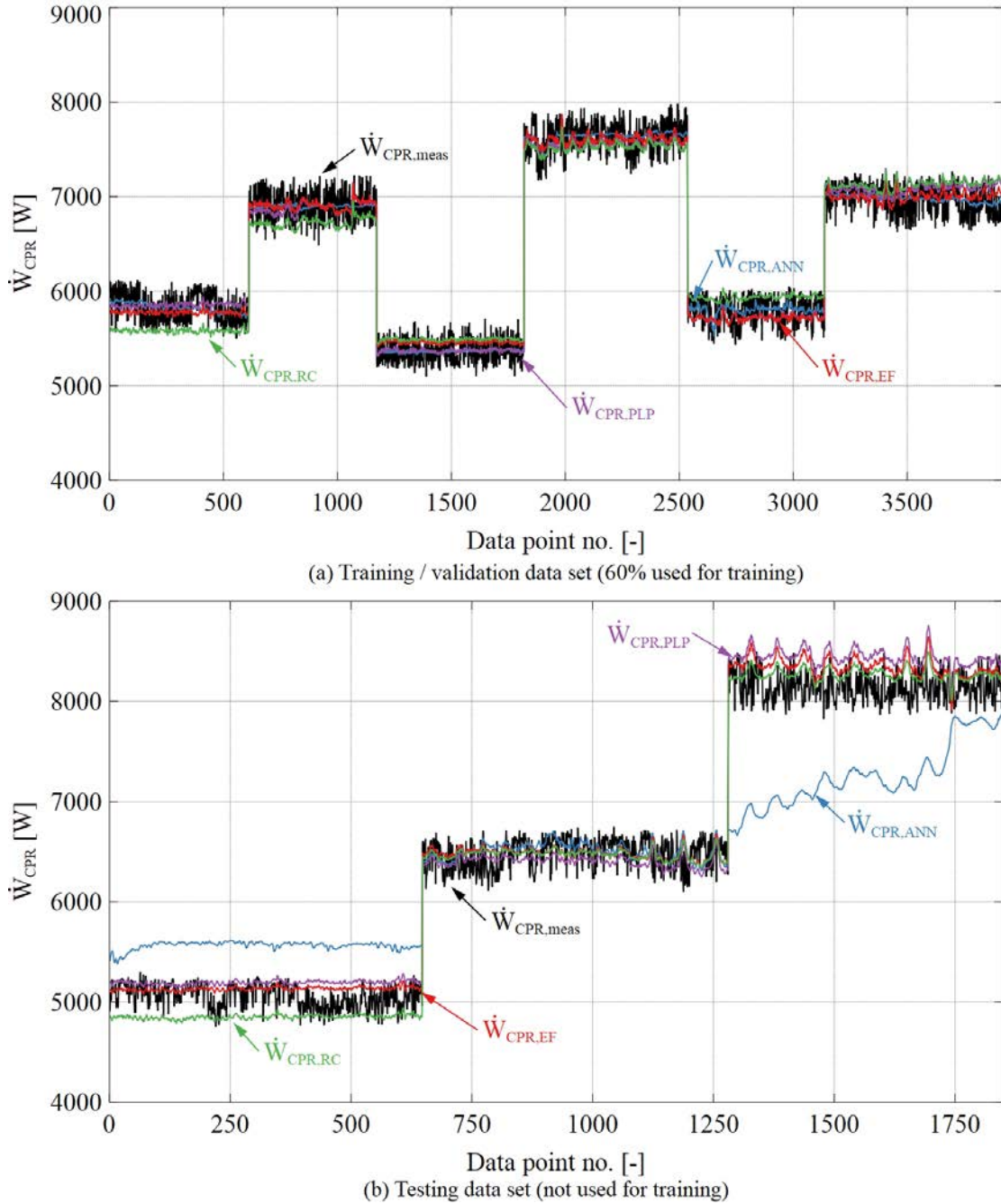
Figure 5.1 – Comparison of the measured and predicted compressor electrical power consumption for the laboratory test rig with (a) the training / validation data set and (b) the testing data set.

Moreover, the refrigeration cycle (RC) based model shows a differentiated behavior. With the internal data set, the model yields a RMSE and MAE of approximately 222 and 179 W (see Tab. 5.1), respectively, which are the highest values among the investigated approaches. Depending on the operating state an over- or underprediction of the compressor electrical power compared to the experimental data is present (see Fig. 5.1a, $\dot{W}_{CPR,RC}$). The same behavior is observed with the external data (see Fig. 5.1b), where the RMSE and MAE decreases by approximately 18 and 7 W, respectively. It is assumed that this result is caused by the constant model parameters, which are determined with an optimization procedure. On the one hand, it is un-
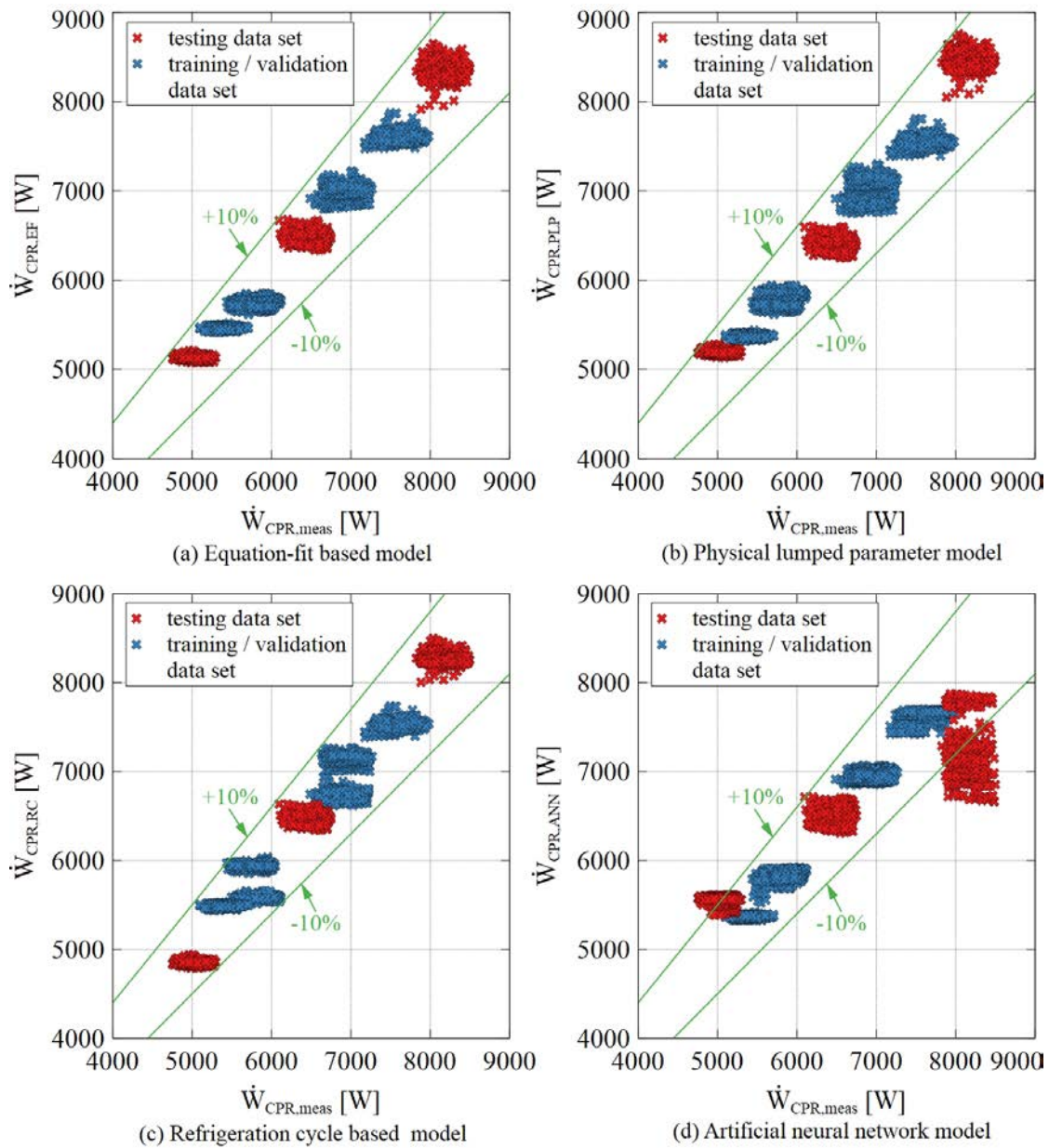
Figure 5.2 – Comparison of the experimental and modeling results of the compressor electrical power consumption for the laboratory test rig: (a) equation-fit based model, (b) physical lumped parameter model, (c) refrigeration cycle based model and (d) artifical neural network model.

known if the global minimum of the cost function is reached during training. On the other hand, the model parameters, e.g. the overall heat transfer coefficient, would in reality vary depending on the operating state. Nevertheless, like the other models, the performance is reasonable, which is revealed with adequate R^2 and CV values. Also, all predicted values are within the ±10% error band (see Fig. 5.2c) and the model is second best in terms of extrapolation.

The artificial neural network (ANN) model simulates the compressor electrical power accurately when using internal data (see Fig. 5.1a, $\dot{W}_{CPR,ANN}$), where no overprediction is present. Among the investigated models, it yields the lowest RMSE and MAE values with 143 and 120 W (see Tab. 5.1), respectively. As suspected, the interpolation quality is adequate, where however, the model fails to correctly extrapolate (see Fig. 5.1b). With the testing data set, approximately 37% of the predicted values lie outside the ±10% error band (see Fig. 5.2d). As a consequence, the ANN model yields the highest RMSE, MAE and CV values as well as the lowest R^2 value with the external data set. This result reveals that ANNs extrapolate poorly and the model performance decreases significantly when input data outside the learning domain is considered.

When comparing the different modeling approaches, the ANN model performs best when using the internal data and the EF model when using the external data. The reason for the adequate performance of the EF model when extrapolating can finally not be determined. One possibility

Table 5.1 – List of the RMSE, MAE, R^2 and CV values for each modeling approach with respect to the internal (training / validation) and external (testing) data of the laboratory test rig.

Performance indicator	Equation-fit based model		Phyiscal lumped parameter model	
	internal	external	internal	external
root-mean-squared error (RMSE) [W]	165.05	194.09	172.79	244.58
mean-absolute error (MAE) [W]	139.84	154.37	143.21	197.80
coefficient of determination (R^2) [–]	0.960	0.976	0.956	0.962
coefficient of variation (CV) [%]	2.55	2.99	2.67	3.77
	Refrigeration cycle based model		Artificial neural network model	
	internal	external	internal	external
root-mean-squared error (RMSE) [W]	221.99	203.66	142.90	625.77
mean-absolute error (MAE) [W]	178.92	171.89	120.00	500.41
coefficient of determination (R^2) [–]	0.928	0.974	0.970	0.752
coefficient of variation (CV) [%]	3.44	3.14	2.21	9.64

is that the operating points used in the testing data set are not far of the training / validation operating points. As expected, both physical models reveal an inferior performance with the internal data set compared to the empirical models. As mentioned, the most probable reason is the constant model parameters, which would in reality vary with respect to the operating conditions. All investigated modeling approaches, except the ANN model when applying the external data set, yield a CV value of 2.21 to 3.77% and a R^2 value of 0.928 to 0.976. As mentioned in literature, a CV value of less than 5% is acceptable for practical applications when models are applied for predicting the compressor power consumption [118, 152]. Therefore, no modeling approach can be excluded preliminarly when calibrated with an appropriate data set.

5.1.2 Field plant

Fig. 5.3 and 5.4 show the measured and modeled compressor electrical power consumption (y-axis) in function of the corresponding measuring point (x-axis) with respect to the training / validation and testing data set. For the former, measurement data of refrigeration machine 1 (RM1) and for the latter, measurement data of refrigeration machine 2 (RM2) installed in the investigated field plant are applied. The measured compressor electrical power ranges from 1 to 195 kW (see Fig. 5.3a) and from 1 to 184 kW (see Fig. 5.4a) in the training / validation and testing data set, respectively, where mostly part load conditions are present. Moreover, Fig. 5.5 depicts the modeled compressor electrical power consumption of each modeling approach (y-axis) in function of the measured compressor electrical power consumption (x-axis) with a ±10% error band and Tab. 5.2 lists the values of the different performance indicators for each model with respect to the internal (training / validation) and external (testing) data.

To start with, the equation-fit based (EF) model reveals with the internal data an RMSE and MAE value of 3.23 and 2.36 kW (see Tab. 5.2), respectively, where the values are reasonable with the given range of the compressor electrical power. Similar values are achieved with the testing data set. This outcome is probably due the large training domain, where all kind of part and full load conditions are covered. Also, all refrigeration machines in the field plant are of the same type and size, whereby most likely all of them reveal a similar operating behavior. In comparison to the other models, the EF model data scatters the most overall (see Fig. 5.5a), where approximately 29% of the simulated values lie outside of the ±10% error band. Correspondingly, it has the tendency for under- and overprediction in part as well as full load conditions. This behaviour is also visible when qualitatively comparing the modeling results $\dot{W}_{CPR,EF}$ with the experimental data $\dot{W}_{CPR,meas}$, with both the internal and external data set (see Fig. 5.3b and 5.4b).

The physical lumped parameter (PLP) model reveals a similar performance as the EF model, where the RMSE and MAE values range depending on the data set from 3.15 to 3.2 kW and 2.44 to 2.55 kW, respectively (see Tab. 5.2). The predicted values scatter less in a compressor electrical power range of 50 to 130 kW and approximately 32% of the simulated values lie outside of the $\pm 10\%$ error band (see Fig. 5.5b). When comparing qualitatively the simulated values $\dot{W}_{CPR,PLP}$ with the measurements $\dot{W}_{CPR,meas}$, a slight underprediction is present in part load conditions of the refrigeration machines (see Fig. 5.3b and 5.4b).

(a) Training / validation data set (overview)

(b) Training / validation data set (detail view)
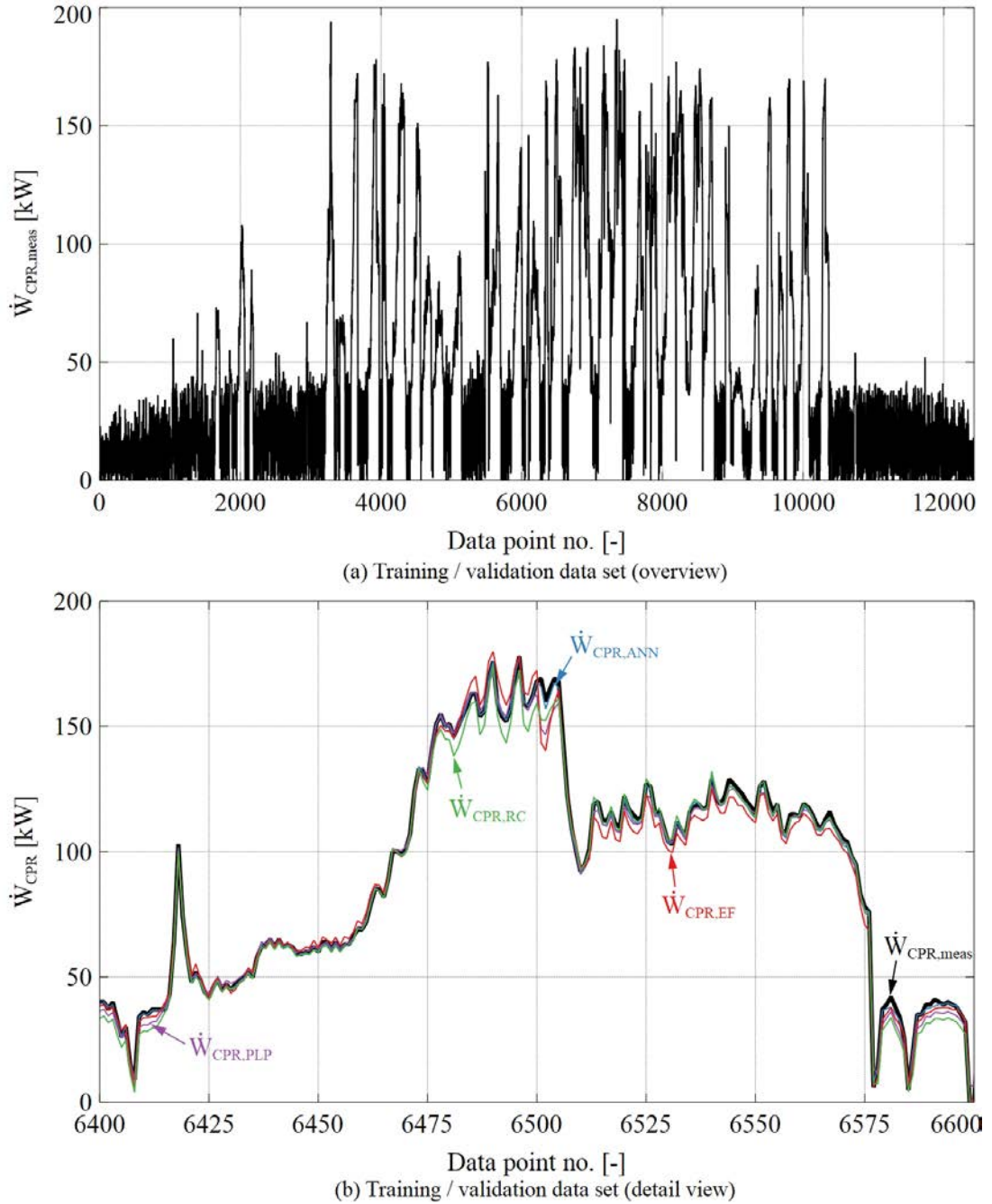
Figure 5.3 – Range of measured compressor electrical power of RM1 in the field plant (training / validation data set): (a) overview and (b) detail view with comparison of the measured and predicted compressor electrical power consumption.

Furthermore, the refrigeration cycle (RC) based model performs worst among the investigated modeling approaches when appling the internal data set, which is revealed with an RMSE and MAE value of 4.02 and 3.16 kW (see Tab. 5.2), respectively. With the external data, the RMSE increases by 0.22 kW and the MAE by 0.24 kW. As mentioned in subsection 5.1.1, this outcome is most likely due to the constant model parameters, which would vary in reality. Also, a large range of different operating states is present in the experimental data of the field plant, which
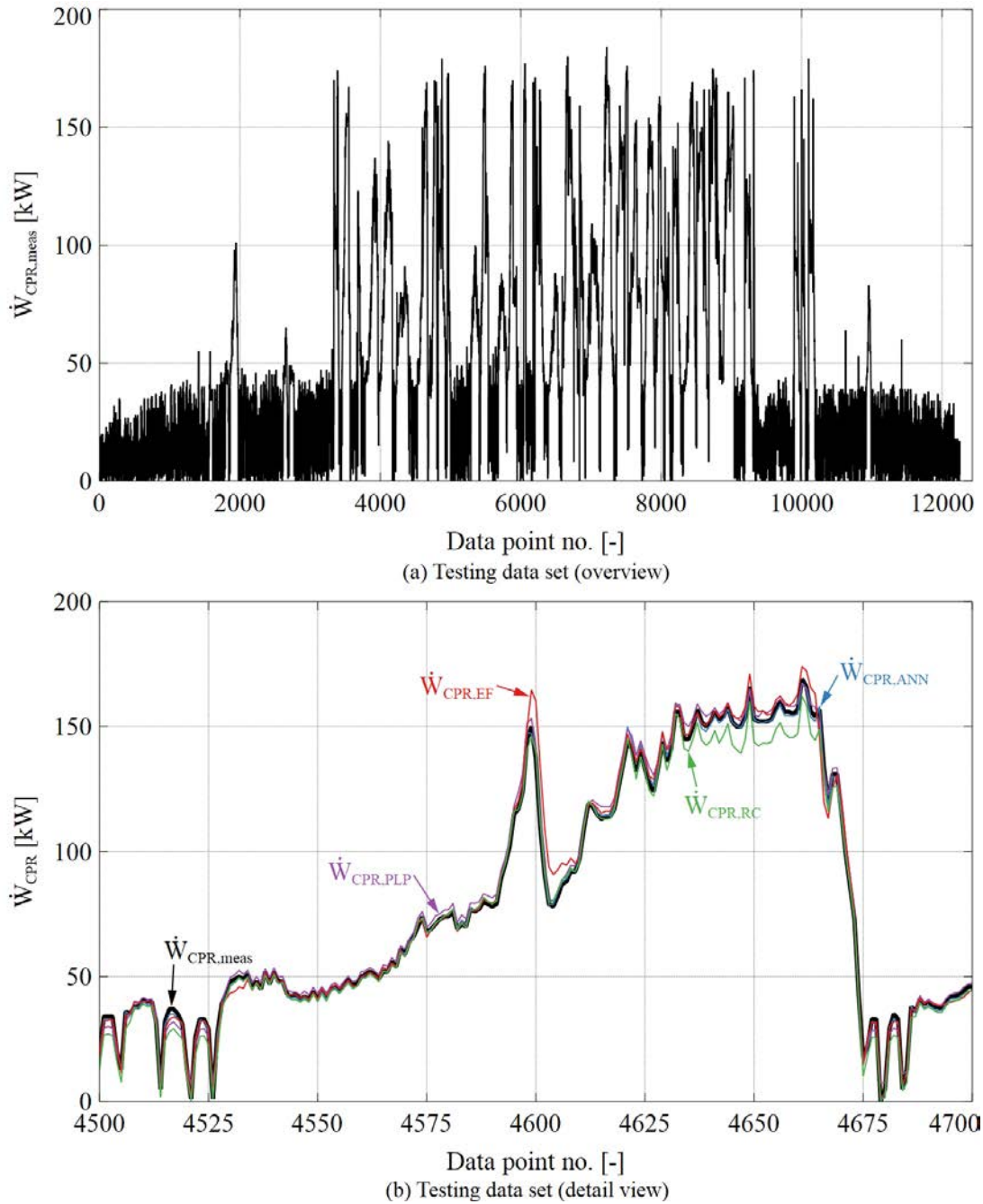
Figure 5.4 – Range of measured compressor electrical power of RM2 in the field plant (testing data set): (a) overview and (b) detail view with comparison of the measured and predicted compressor electrical power consumption.

complicates the identification of valid parameters for all part and full load conditions. The model has the overall tendency to underpredict the compressor electrical power, which is qualitatively shown when comparing the modeled $\dot{W}_{CPR,RC}$ with the experimental data $\dot{W}_{CPR,meas}$ (see Fig. 5.3b and 5.4b). Also, approximately 51% of the predictions lie outside of the $\pm 10\%$ error band, especially at a compressor power consumption lower than 50 kW (see Fig. 5.5c).

The predicted compressor electrical power $\dot{W}_{CPR,ANN}$ by the artificial neural network (ANN) model shows qualitatively a good agreement with measurements $\dot{W}_{CPR,meas}$ when using inter-
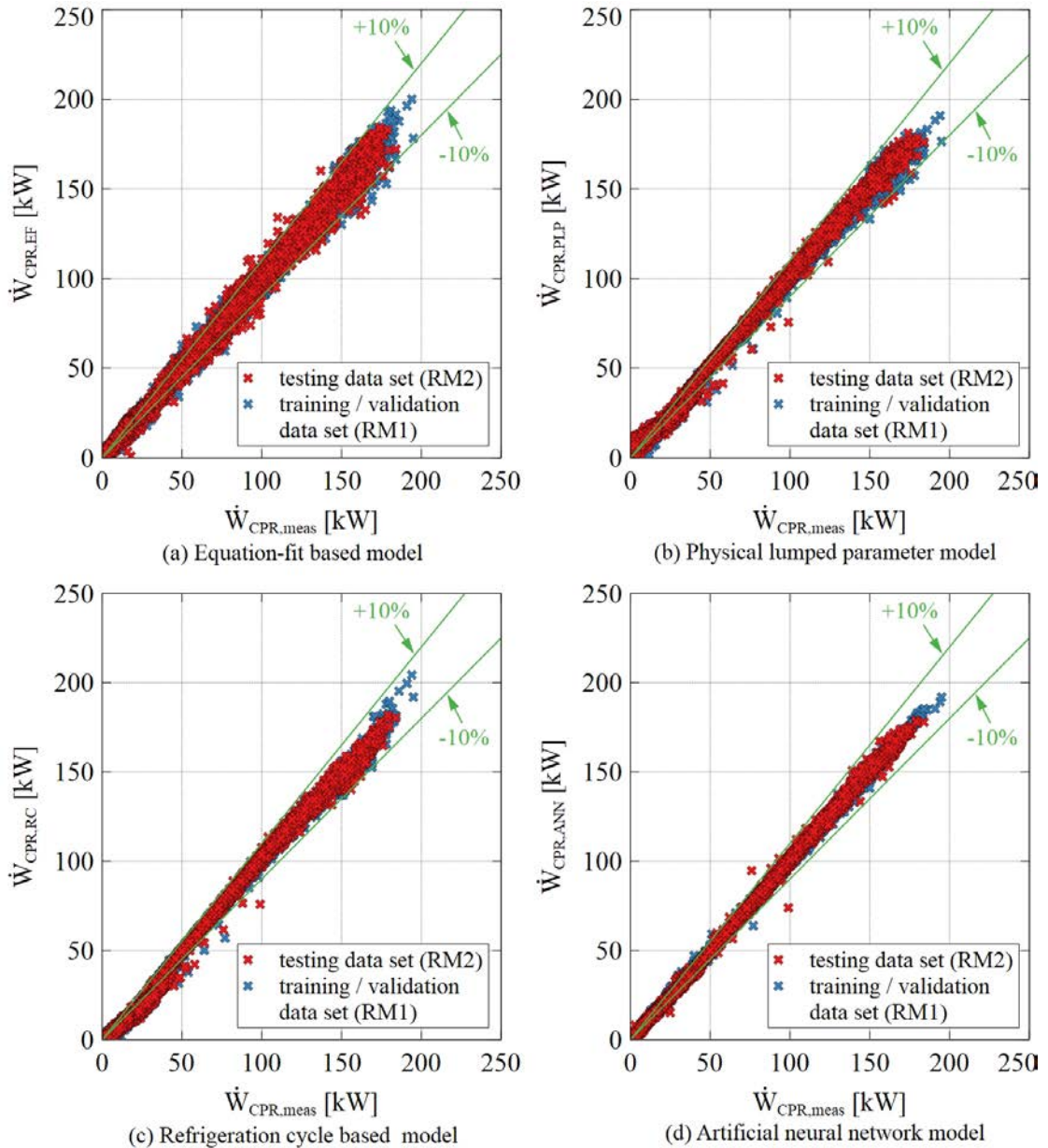
Figure 5.5 – Comparison of the experimental and modeling results of the compressor electrical power consumption for the field plant: (a) equation-fit based model, (b) physical lumped parameter model, (c) refrigeration cycle based model and (d) artifical neural network model.

nal and external data (see Fig. 5.3b and 5.4b). As mentioned for the EF model, this result is most likely due the large training domain, where all kind of part and full load conditions are covered and the similar operating behavior of both refrigeration machines. The ANN model reveals RMSE and MAE values of 1.12 to 1.45 kW and 0.8 to 1.07 kW (see Tab. 5.2), respectively, which are the lowest values among the investigated approaches. The adequate performance is also demonstrated with R^2 values close to 1 and CV values below 3%, where only approximately 10% of the simulated values are outside of the $\pm 10\%$ error band (see Fig. 5.5d).

When comparing the different models, the ANN performs best when using the internal as well as external data. All models perform only slightly worse with the testing data set, which is most likely due to the similar behavior of the two simulated refrigeration machines. The EF and PLP model reveal a similar performance, where the RC model underpredicts the compressor power significantly in part load conditions. The latter contributes to the highest RMSE, MAE and CV as well as lowest R^2 values compared to the other investigated models. All performance indicators reveal acceptable values except the CV, where only the ANN model reaches values lower than 5%, which is adequate for a practical application of the model [118, 152].

Consequently, the ANN model is applied for the exergy-based assessment system, which is a black-box model based on measurements of the existing system. By using reference tempera-

Table 5.2 – List of the RMSE, MAE, R^2 and CV values for each modeling approach with respect to the internal (training / validation) and external (testing) data of the field plant.

Performance indicator	Equation-fit based model		Phyiscal lumped parameter model	
	internal	external	internal	external
root-mean-squared error (RMSE) [kW]	3.23	3.26	3.15	3.20
mean-absolute error (MAE) [kW]	2.36	2.34	2.44	2.55
coefficient of determination (R^2) [–]	0.995	0.994	0.995	0.995
coefficient of variation (CV) [%]	6.36	6.34	6.20	6.22
	Refrigeration cycle based model		Artificial neural network model	
	internal	external	internal	external
root-mean-squared error (RMSE) [kW]	4.02	4.24	1.12	1.45
mean-absolute error (MAE) [kW]	3.16	3.40	0.80	1.07
coefficient of determination (R^2) [–]	0.992	0.991	0.999	0.999
coefficient of variation (CV) [%]	7.91	8.25	2.21	2.82

tures on the condenser secondary side according to technical standards, the reference compressor power consumption can be simulated. In order to increase the accuracy, the ANN is retrained for the other four present refrigeration machines in the field plant. As a result, the RMSE and MAE values range from 1.07 to 1.14 kW and 0.77 to 0.81 kW, respectively. The CV ranges from 1.62 to 2.21%, where the R^2 is 0.999 for all refrigeration machines.

5.2 Exergy-based evaluation approach

This section presents the results of the proposed exergy-based evaluation method for determining the performance and optimization potentials of refrigeration plants. First, the outcome of the application on two numerical test cases is shown and discussed to exemplify the approach and its functionality (see subsection 5.2.1). Subsequently, the results of the case study are presented in subsection 5.2.2.

5.2.1 Test cases

By applying the method described in subsection 3.1.3.1 and using the test case data of Tab. 4.1, the corresponding exergy values and the OPI of each subsystem are determined. To exemplify the method, a basic assessment (no additional acceptable operation boundary) is carried out, where the stricter, adequate technical standards are applied for the reference values. Fig. 5.6a depicts the optimization potential index of every subsystem in the two investigated test cases. It is apparent, that in adequate operation (test case 1) all the OPI values are below 0. Thus, the technical requirements are met. In test case 2, a fouled condenser and dry cooler heat exchanger is assumed, which results in a faulty operation of the refrigeration plant. The issue is revealed with an OPI of 0.06 in the subsystem DC and 0.017 in the subsystem RM, indicating potential for improvement.

A first detailed analysis is feasible by investigating the exergy inputs of every component in the subsystem DC (see Fig. 5.6b). In test case 1, all the actual exergies B are inferior to the references B^*, resulting in an OPI_{DC} of –0.18. In test case 2, an increased exergy input of the circulating pumps is observed, in order to overcome the additional pressure drop in the fouled heat exchangers. Likewise, the dry cooler fan exergy input is increased to ensure a sufficient heat transfer, while still being approximately 7 MJ below the reference. The condenser exergy input is elevated compared to the reference due to the given increased secondary side temperature and heat exchanger temperature difference, which also affects the subsystem RM, resulting in an OPI value superior to 0.

(a) OPI of the different subsystems in adequate (test case 1)
and faulty operation (test case 2)

(b) Actual and reference daily exergy sum of the subsystem DC
in adequate (test case 1) and faulty operation (test case 2)
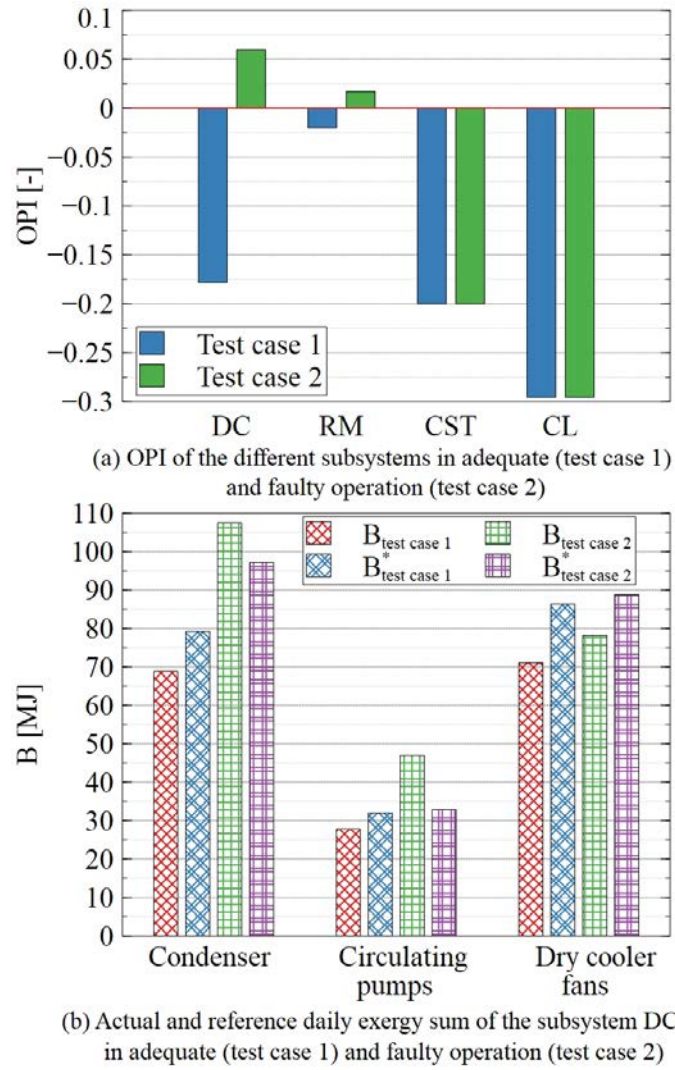
Figure 5.6 – Results of the test case 1 (adequate operation) and test case 2 (faulty operation): (a) optimization potential index of the subsystems dry cooler, refrigeration machine, cold water storage & transport and cooling location, (b) actual and reference daily exergy sum of the different components in the subsystem DC.

The numerical test cases demonstrate the functionality of the method, where the OPI delivers information about the refrigeration plant performance and indicating potential for improvement compared to the state of the art in technology if a faulty operation is present. Consequently, the location of the malfunction can be identified on subsystem level. While the evaluation of the exergies helps to determine possible reasons for the malfunction in a first step, a more detailed study should be carried out to clearly identify the faulty components, unfavorable control settings or any other issue.

5.2.2 Case study

In the following, the outcome of the case study is elaborated. By applying the method described in subsection 3.1.3.1 and 3.1.3.2, together with the acquired data from the field plant, the corresponding exergy values and the optimization potential indices of each subsystem are determined. The results in refrigeration machine and free cooling operation are presented and discussed in subsection 5.2.2.1 and 5.2.2.2, respectively. The analysis should further demonstrate the usage of the evaluation approach and reveal the performance as well as eventual optimization potentials of the field plant.

5.2.2.1 Refrigeration machine operation

According to the available experimental data, refrigeration machine operation occurred from begin of April to end of October and on few days in November as well as December. The exergy reference environment temperature T_0 applied in refrigeration machine operation is 18.07 °C. Figs. 5.7, 5.9 to 5.14 and 5.16 show the daily optimization potential index (OPI, y-axis) in refrigeration machine operation of every subsystem in the field plant under investigation in function of the date (x-axis) in the mentioned time period. The daily OPI is indicated with data points, where the 14-days moving average is represented by a solid line to evaluate the OPI tendency over time. The green, yellow and red zone depicts the adequate (technical requirements exceeded), acceptable (technical requirements fulfilled) and inadequate (potential for improvement) operation condition, respectively. In Fig. 5.16 the adequate and acceptable boundary is indicated with a green and red dashed line, respectively. The adequate boundary is always at OPI = 0 according to the key figure definition (the actual exergy value B is compared with the reference $B^* = B^{adq}$), while the acceptable limit (the acceptable exergy value B^{acc} is compared with the reference $B^* = B^{adq}$) may fluctuate due to dependencies of various measured parameters at the different operating points, e.g. the acceptable circulating pump exergy depends on the electro-thermal amplification factor and the variable measured thermal energy. Additionally, missing data points for the acceptable limit were determined by interpolation. An exception is the subsystem CL, where the acceptable limit is constant over the whole operation range due to the constant and independent reference values (cold water distribution temperatures). Furthermore, Fig. 5.8 and 5.15 shows the actual, reference (adequate) and acceptable daily exergy sum (y-axis) of each component in the subsystem DC and CST, respectively, in function of the date (x-axis) in the mentioned time period.

5.2.2.1.1 Subsystem dry cooler

To begin with, the subsystem dry cooler has an average OPI_{DC} of approximately 0.05 and fluctuates strongly within a range of –0.36 to 0.57 (see Fig. 5.7). In 82.5 % of the time, the optimization potential index is below the acceptable boundary OPI_{DC}^{acc}, where the technical requirements are fulfilled and exceeded in 39.2 and 43.3% of the time, respectively. Single outliers should not be overly considered, as only a constant elevated key figure indicates potential for improvement. By investigating the moving average OPI_{DC}^{avg}, it is evident that the subsystem performs well except in the beginning to mid October, where the key figure exceeds the acceptable boundary, indicating potential for improvements. Similarly to the investigated test case 2 in section 5.2.1, a high key figure is an indicator for an elevated condenser secondary side temperature or an elevated electrical power consumption of the auxiliary devices, compared to the technical standards. Possible reasons are a temperature rise through mixing circuits, an increased dry cooler fan speed (e.g. unfavorable control settings for the present operation), ambient air recirculation at the dry cooler which compromises the heat transfer or fouled heat exchangers. The latter can be excluded as a reason for the unfavorable operating condition, because otherwise OPI_{DC} would generally be higher over the whole time period.
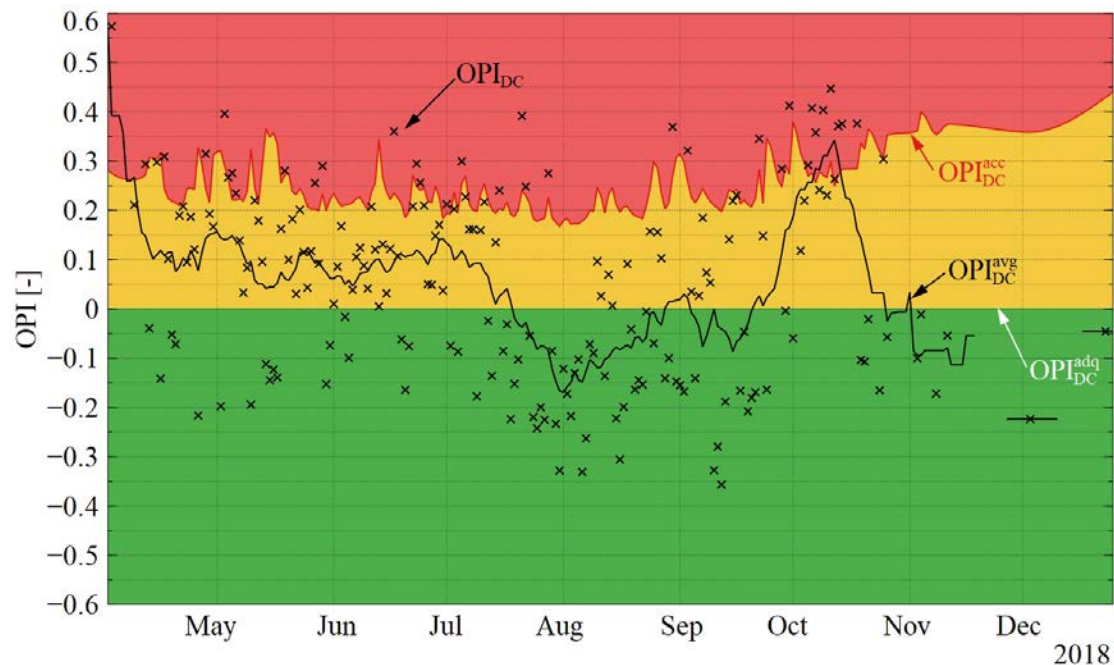
Figure 5.7 – Optimization potential index OPI_{DC} of the subsystem DC in refrigeration machine operation with adequate (green), acceptable (yellow) and inadequate (red) operation range. The data points (black crosses) represent the daily OPI values and the black solid line indicates the 14-days moving average of the OPI.

To investigate these unfavorable operating conditions, the daily exergy inputs can be analyzed as a next step. By examining the exergy of the condenser B_C (see Fig. 5.8a) and the circulating pumps $B_{el,CP,DC}$ (see Fig. 5.8b) it is apparent, that the actual exergy input is generally lower or exhibits the same magnitude as the reference, which is favorable for the refrigeration plant operation. However, the actual dry cooler fans exergy $B_{el,DC}$ (see Fig. 5.8c) is mostly elevated compared to the adequate and acceptable values. This contributes to an increase of
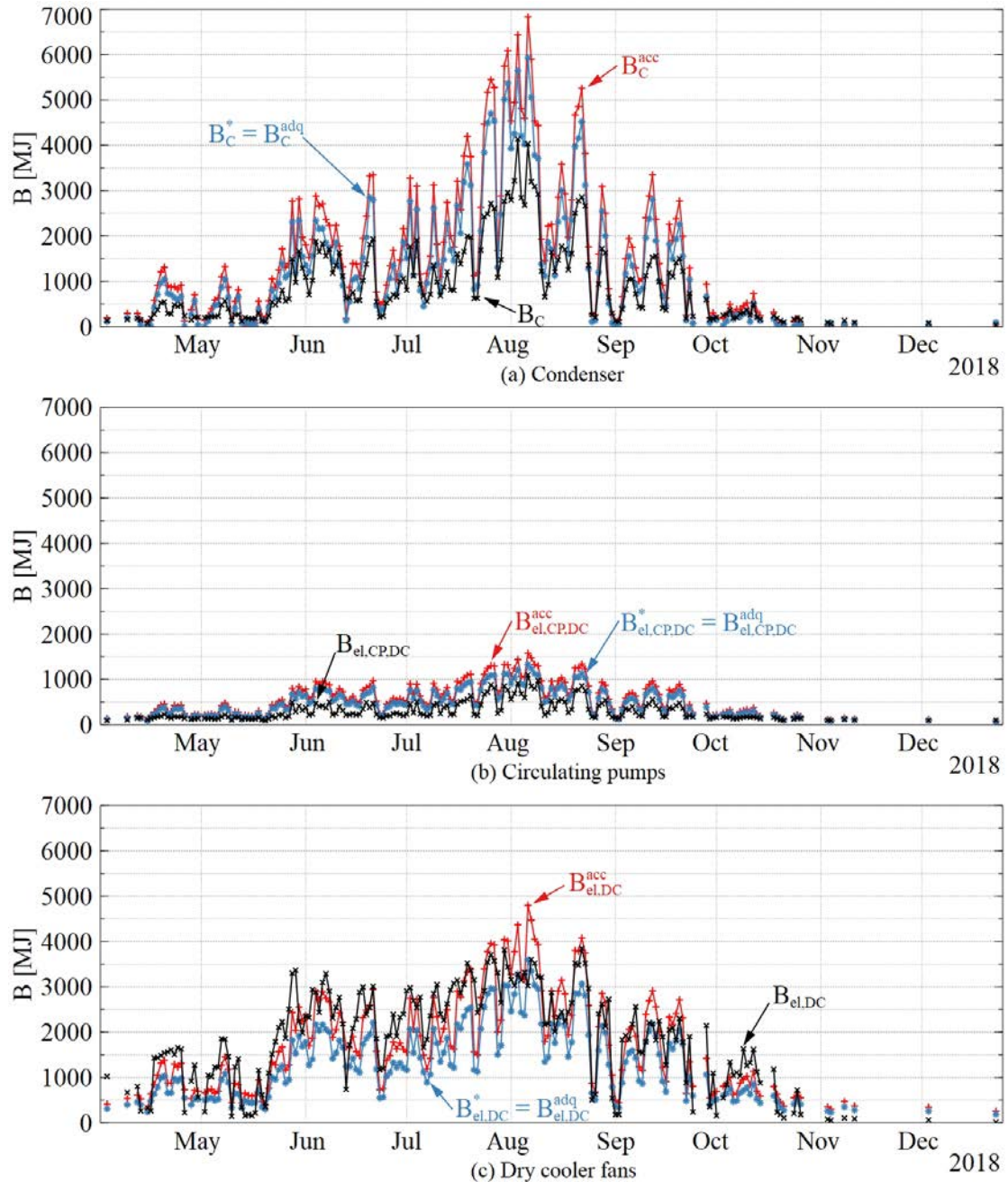
Figure 5.8 – Actual, reference (adequate) and acceptable daily exergy sum in refrigeration machine operation of the different components in the subsystem DC: (a) condenser, (b) circulating pumps and (c) dry cooler fans.

the OPI, eventually indicating potential for improvement. A similar behaviour was shown by the circulating pumps exergy in test case 2 (see section 5.2.1). Moreover, the actual dry cooler fans exergies reveal generally a higher magnitude compared to the condenser exergies. In October for example, the actual dry cooler fans exergy is approximately up to 3 times higher as the condenser and circulating pumps exergy. Therefore, the dry cooler fans electrical exergy is the driving quantity in this time period and has the most impact on OPI_{DC}. As a consequence, the key figure yields values which lie in the inadequate operation range, regardless how well the condenser and the circulating pumps perform. Thus, the reason for the inadequate performance of the subsystem DC in October are most likely the dry coolers, where the exact reason for the unfavorable operation would need to be determined in a subsequent detailed analysis. This behavior is not only observed in October, but also on several other days during the year (when OPI_{DC} is superior to OPI_{DC}^{acc}). Taking May 29th as an example, the actual dry cooler fans exergy effort is roughly twice as high as determined by the stricter technical standards, which corresponds to an exergy difference of approximately 1800 MJ. The latter value is 1.6 times the exergy sum of the condenser and circulating pumps, and thus determines the outcome. However, as mentioned, daily outliers are not necessarily an indication of a malfunction, but if the key figure continuously and significantly increases, the subsystem would need inspection.

Interestingly, in exergetic considerations, the electrical exergy plays a substantial role in comparison to the thermal exergy input. In energetic considerations, the electrical energy input only accounts for 1 to 3.5% of the thermal energy according to the technical standards. This relationship underlines the importance of minimizing the electricity consumption of auxiliary devices where possible in order to achieve an adequate system performance, which was also stated in other research [93].

5.2.2.1.2 Subsystem refrigeration machine

The optimization potential index of the five different refrigeration machines lies in the range of –0.47 to 0.44 (see Fig. 5.9 to 5.13), whereas the maximum difference in OPI of 0.43 between two chillers (RM4 and RM5) is reached on June 15th. As the cooling load varies depending on the weather condition and building occupancy or for maintenance purposes, not all chillers were operating daily and thus in some situations, e.g. on August 4th, not all key figures are present. Refrigeration machine 2 yields the lowest average optimization potential index OPI_{RM2} of –0.03 (see Fig. 5.10), while the key figure scatters the least among the remaining refrigeration machines. The chiller operates approximately 80% of the time below the acceptable boundary

OPI_{RM2}^{acc}, where 60 and 20% of the time an adequate and acceptable operation of the subsystem is achieved, respectively. Conversely, refrigeration machine 5 yields the highest average key figure among all refrigeration machines of 0.02 (see Fig. 5.13). In 44 and 29% of the time in the investigated period the technical requirements are exceeded and fulfilled, respectively. The refrigeration machine was commissioned on April 13th, and therefore, no key figures are present before that day. Overall, OPI_{RM1} to OPI_{RM5} are at least 73% of the time in adequate and acceptable operation range. This indicates a reasonable performance of all refrigeration machines and their hydraulic integration, where mostly little to no optimization potential compared to the technical standards is present.

Interestingly, by examining the moving average OPI_{RM}^{avg} of all refrigeration machines, they reveal a similar operation. Analogue tendencies of an increasing and decreasing OPI are observed, where a slight shift in the y-axis between the different chillers is present. Presumably, this is due to the same type and size of all installed refrigeration machines, e.g. redundancy purposes, where each of them are operated comparably with a certain sequence control strategy. Moreover, it is revealed that during the warmer months over the year (where the most cooling is necessary), i.e. June to end of August, all refrigeration machines exceed and fulfill the technical requirements. This leads to the assumption that the chillers are working near to or at the design point and that the hot side hydraulic circuit is properly operating (see subsection 5.2.2.1.1). The
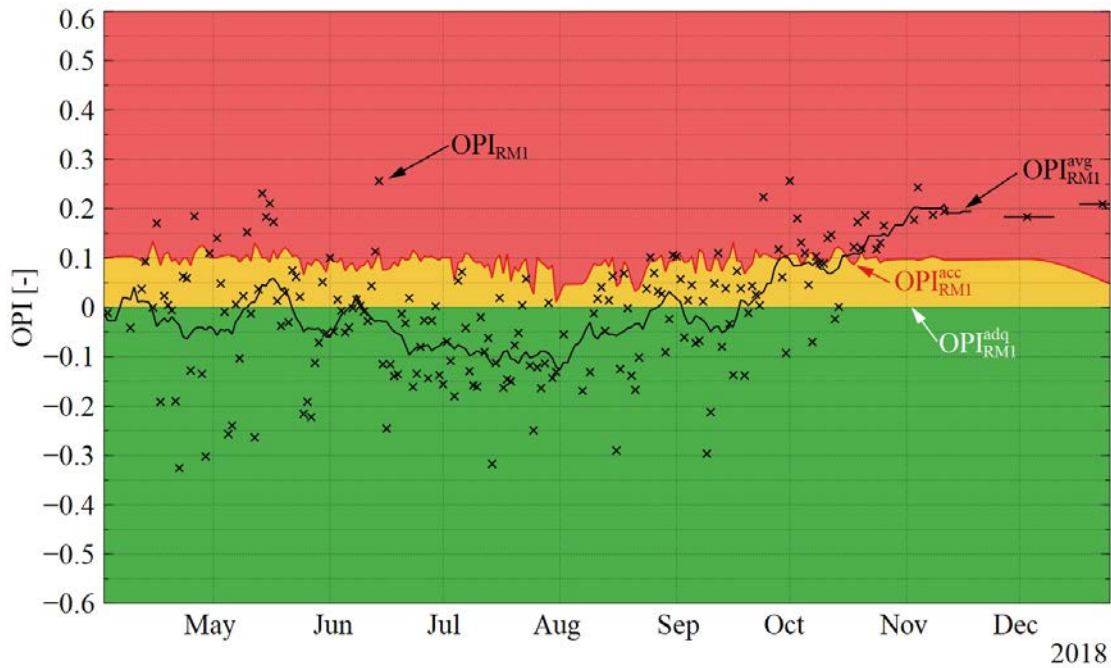
Figure 5.9 – Optimization potential index OPI_{RM1} of the subsystem RM (refrigeration machine 1) with adequate (green), acceptable (yellow) and inadequate (red) operation range. The data points (black crosses) represent the daily OPI values and the black solid line indicates the 14-days moving average of the OPI.
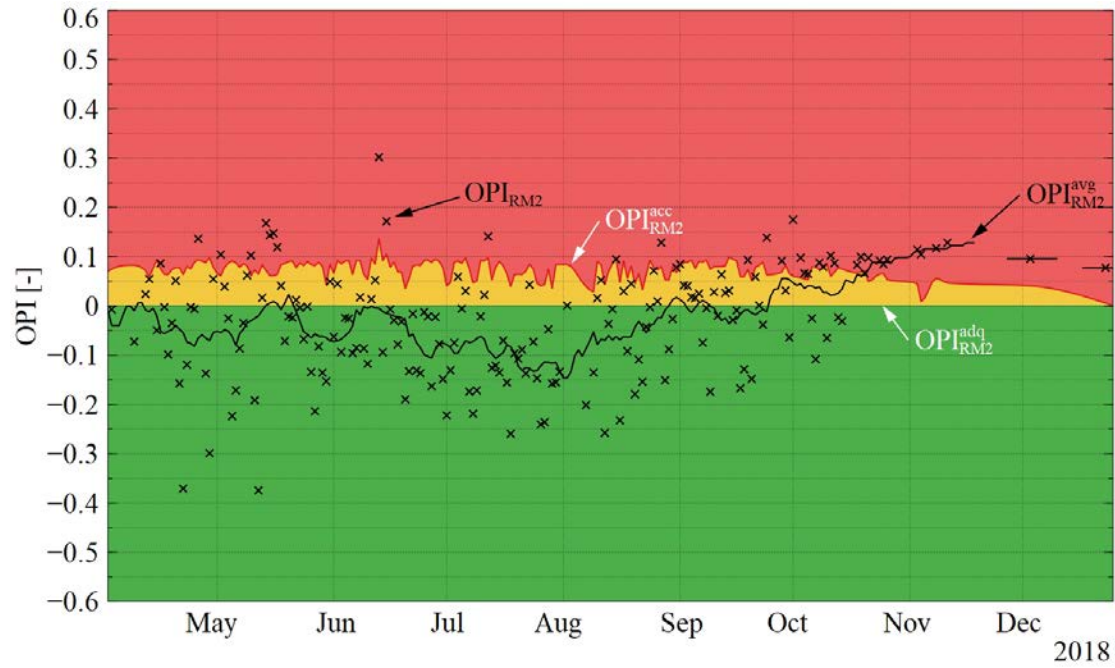
Figure 5.10 – Optimization potential index OPI_{RM2} of the subsystem RM (refrigeration machine 2) with adequate (green), acceptable (yellow) and inadequate (red) operation range. The data points (black crosses) represent the daily OPI values and the black solid line indicates the 14-days moving average of the OPI.
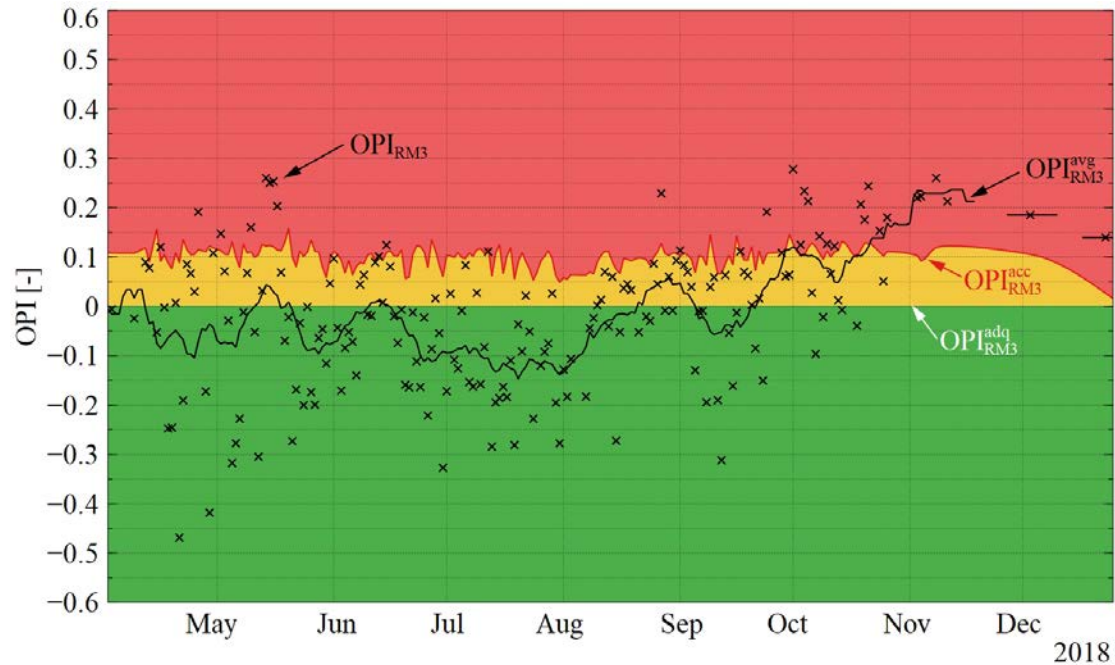
Figure 5.11 – Optimization potential index OPI_{RM3} of the subsystem RM (refrigeration machine 3) with adequate (green), acceptable (yellow) and inadequate (red) operation range. The data points (black crosses) represent the daily OPI values and the black solid line indicates the 14-days moving average of the OPI.

refrigeration machines reveal an increase of the OPI in the transition period, i.e. April, May and September, where mostly an acceptable operation is present. A further noticeable increase in OPI is observed in the colder months October to December, where generally an inadequate operation is present. Most likely, the refrigeration machines are not operating at the design point in the mentioned time period or the temperature level on the hot side hydraulic circuit is not ideal, where the latter can result in an increased electrical power consumption of the compressors. According to literature, lowering the condensing temperature (which is highly influenced by the hot side hydraulic circuit) by 1 K, can reduce the energy consumption of the refrigeration plant by up to 2.5% as a rule of thumb [17]. Consequently, a high OPI value does not necessarily indicate a malfunction of the refrigeration machine itself and its components, but additionally an inadequate integration into the hydraulic circuits, e.g. due to unfavorable control system settings. The increased OPI values in the colder months can also be an indicator to make use of free cooling, which is typically active in this period (see subsection 5.2.2.2). Furthermore, to the best of our knowledge, errors resulting from the ANN model are possible but assumed negligible (according to the model performance, see subsection 5.1.2). To finally determine the issues in the subsystem RM in the mentioned time period a detailed analysis would be necessary, assuming the needed experimental data is available.
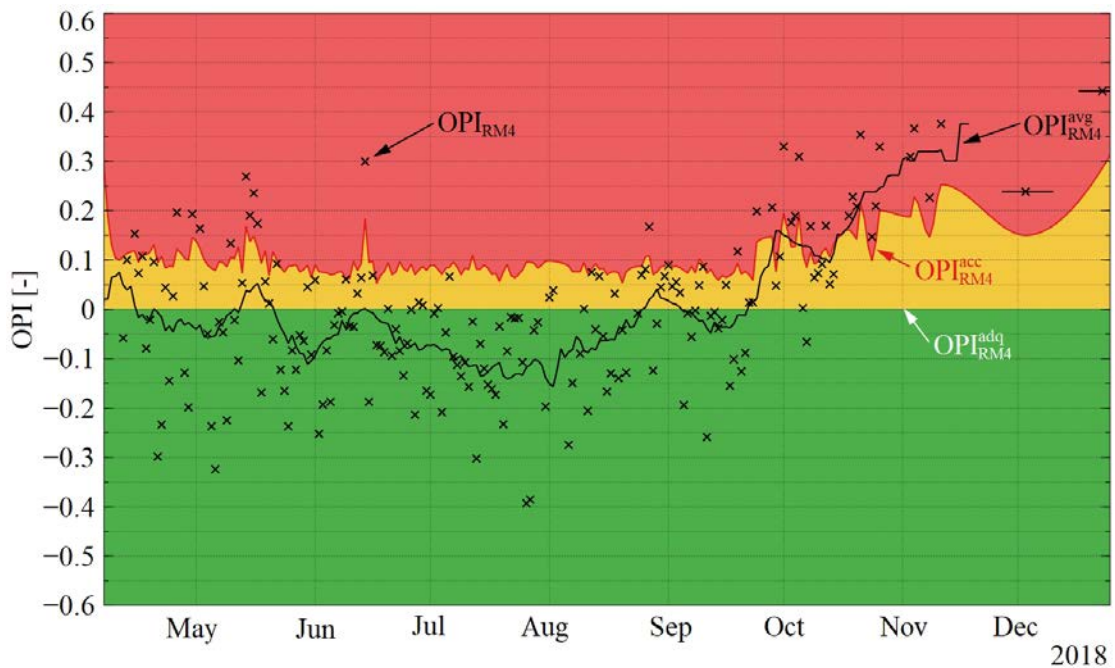
Figure 5.12 – Optimization potential index OPI_{RM4} of the subsystem RM (refrigeration machine 4) with adequate (green), acceptable (yellow) and inadequate (red) operation range. The data points (black crosses) represent the daily OPI values and the black solid line indicates the 14-days moving average of the OPI.
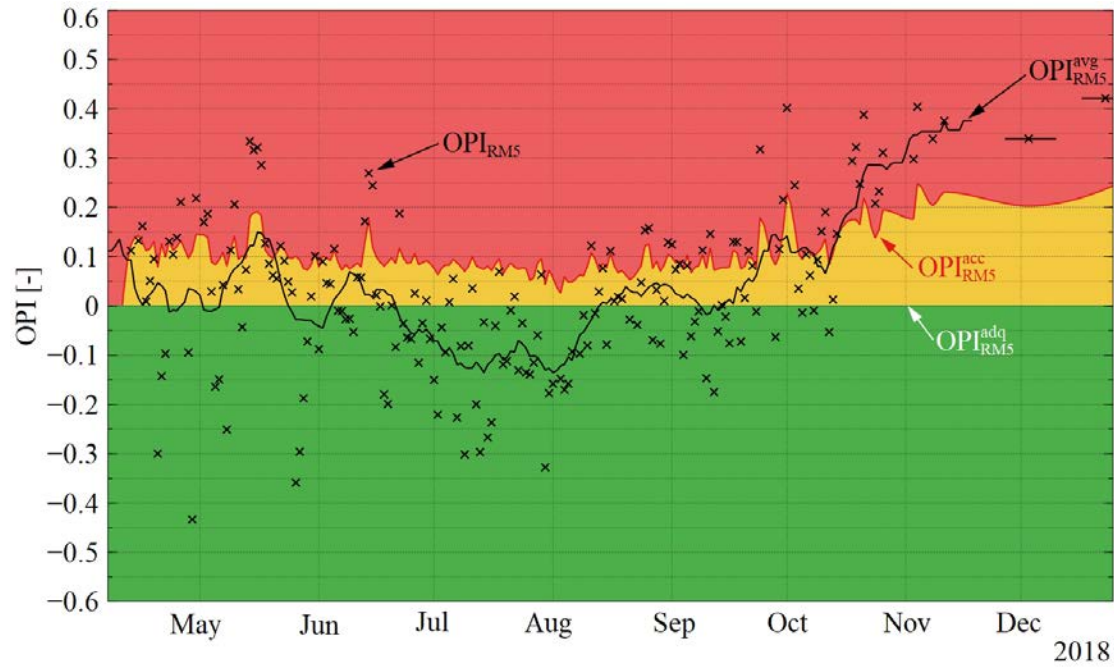
Figure 5.13 – Optimization potential index OPI_{RM5} of the subsystem RM (refrigeration machine 5) with adequate (green), acceptable (yellow) and inadequate (red) operation range. The data points (black crosses) represent the daily OPI values and the black solid line indicates the 14-days moving average of the OPI.

5.2.2.1.3 Subsystem cold water storage & transport

The optimization potential index of the subsystem CST fluctuates less compared to the other subsystems (see Fig. 5.14). The index reaches its minium of –0.03 on June 30th and its maximum of 0.25 on September 29th. The OPI_{CST} is approximately 97% of the time between the acceptable OPI_{CST}^{acc} and adequate boundary OPI_{CST}^{adq}, revealing an average value of 0.11. Also, when observing the moving average OPI_{CST}^{avg}, no significant increase over time is visible. Therefore, the technical requirements are fulfilled and no to little optimization potential according to the technical standards is present. This outcome leads to the assumption that the hydraulic circuit is well designed, correctly maintained and the circulating pumps well controlled, yielding an electrical energy consumption of the circulating pumps below the limit of 1 to 1.5% of the evaporator thermal energy Q_E.

The latter is verifiable by assessing the daily exergy inputs of the subsystem. As suspected, the actual exergy input of the circulating pumps $B_{el,CP,CST}$ (see Fig. 5.15b) is significantly (approximately up to a factor of 2) lower than the acceptable exergy input $B_{el,CP,CST}^{acc}$ and reveals similar magnitudes compared with the adequate (reference) exergy input $B_{el,CP,CST}^{adq}$. This has a positive impact on the operation conditions, which contributes to a low OPI as the technical
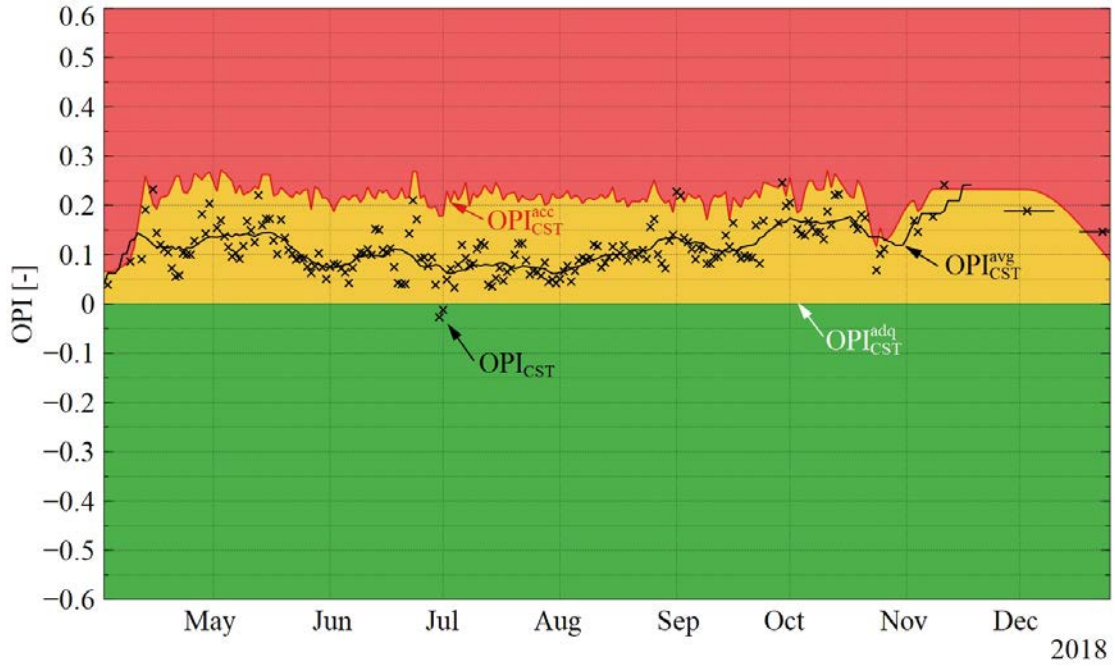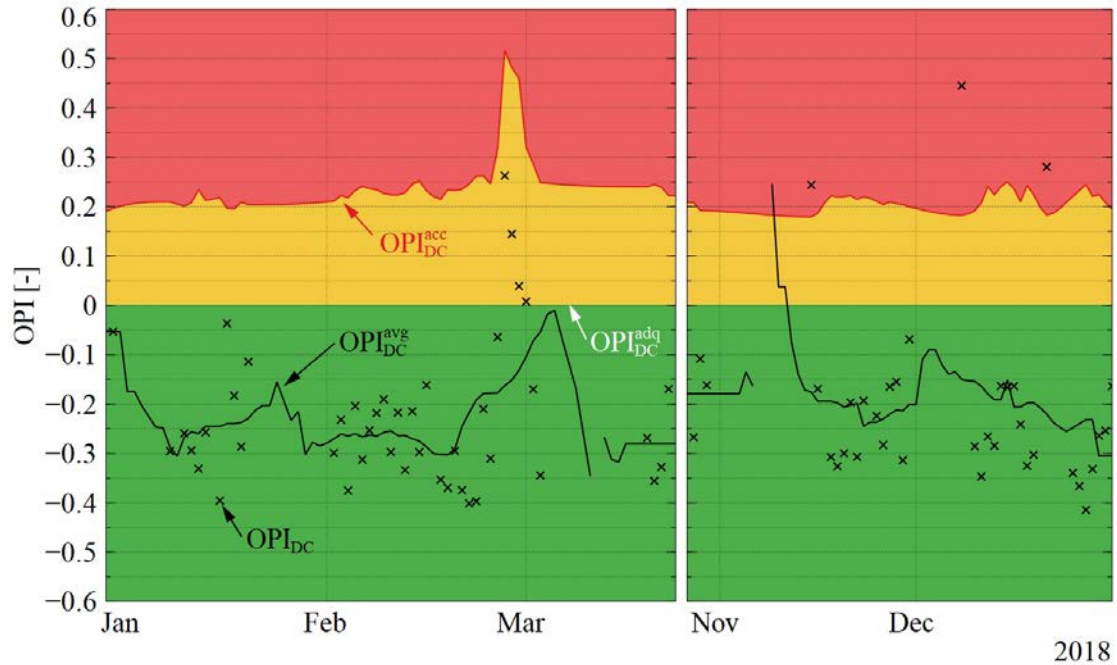
Figure 5.14 – Optimization potential index OPI_{CST} of the subsystem CST in refrigeration machine operation with adequate (green), acceptable (yellow) and inadequate (red) operation range. The data points (black crosses) represent the daily OPI values and the black solid line indicates the 14-days moving average of the OPI.

requirements are fulfilled and mostly exceeded. Conversely, when examining the daily evaporator exergy input (see Fig. 5.15a), it is evident that the actual daily exergy input B_E is most of the time in the range of the acceptable B_E^{acc} and higher than the adequate (reference) exergy input B_E^{adq}. The latter contributes to an increase of the key figure. This result is possibly caused by the approach to determine the evaporator reference values with an exergy balance (because no reference values in technical standards were available), where the same exergy losses are assumed for all operation conditions. This yields a rather strict assessment, because the exergy losses would in reality generally be lower in adequate and acceptable operation. Nevertheless, the subsystem fulfills the technical requirements, which underlines the fact that it is well designed, operated and maintained.

Similarly to the subsystem DC, the electrical exergy input has a substantial impact on the subsystem performance. This underlines again the importance of reducing the electricity demand of auxiliary devices where possible, e.g. by employing pumps with a variable-frequency drive for an adaptive speed control and proper control system settings, to achieve a favorable refrigeration plant operation.
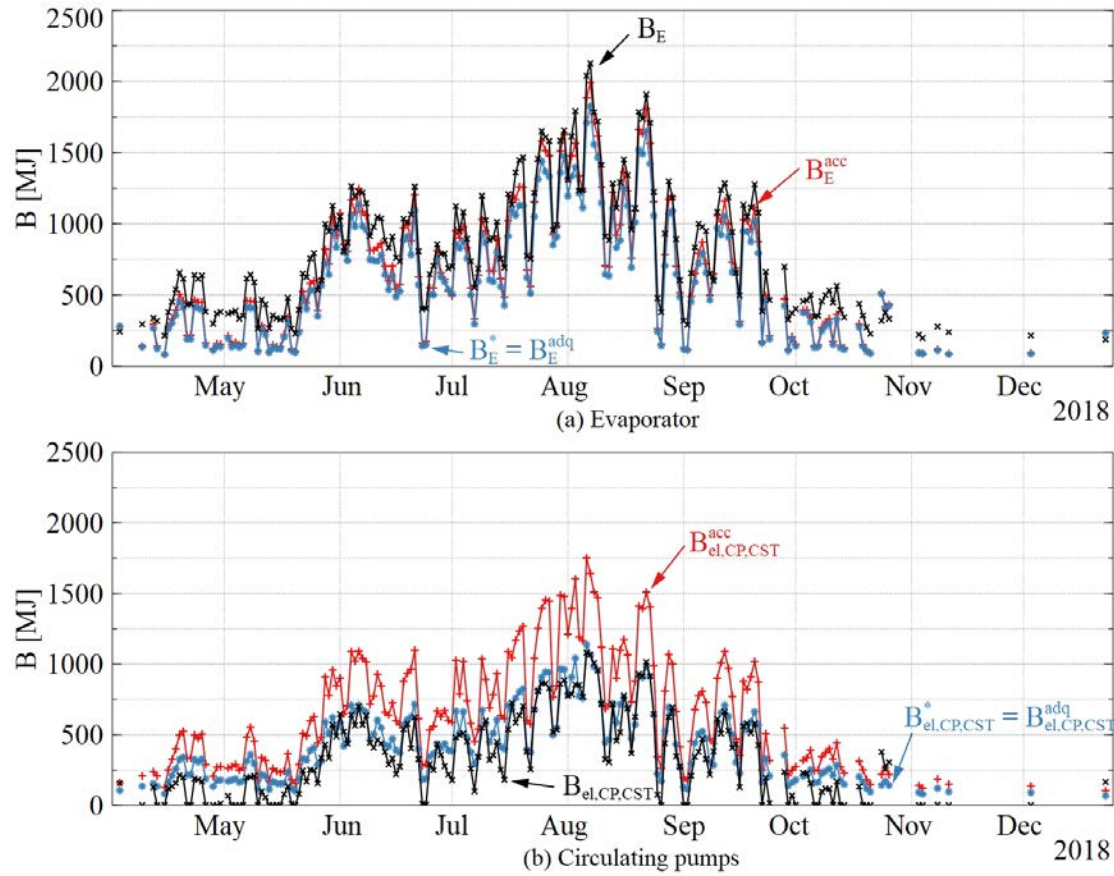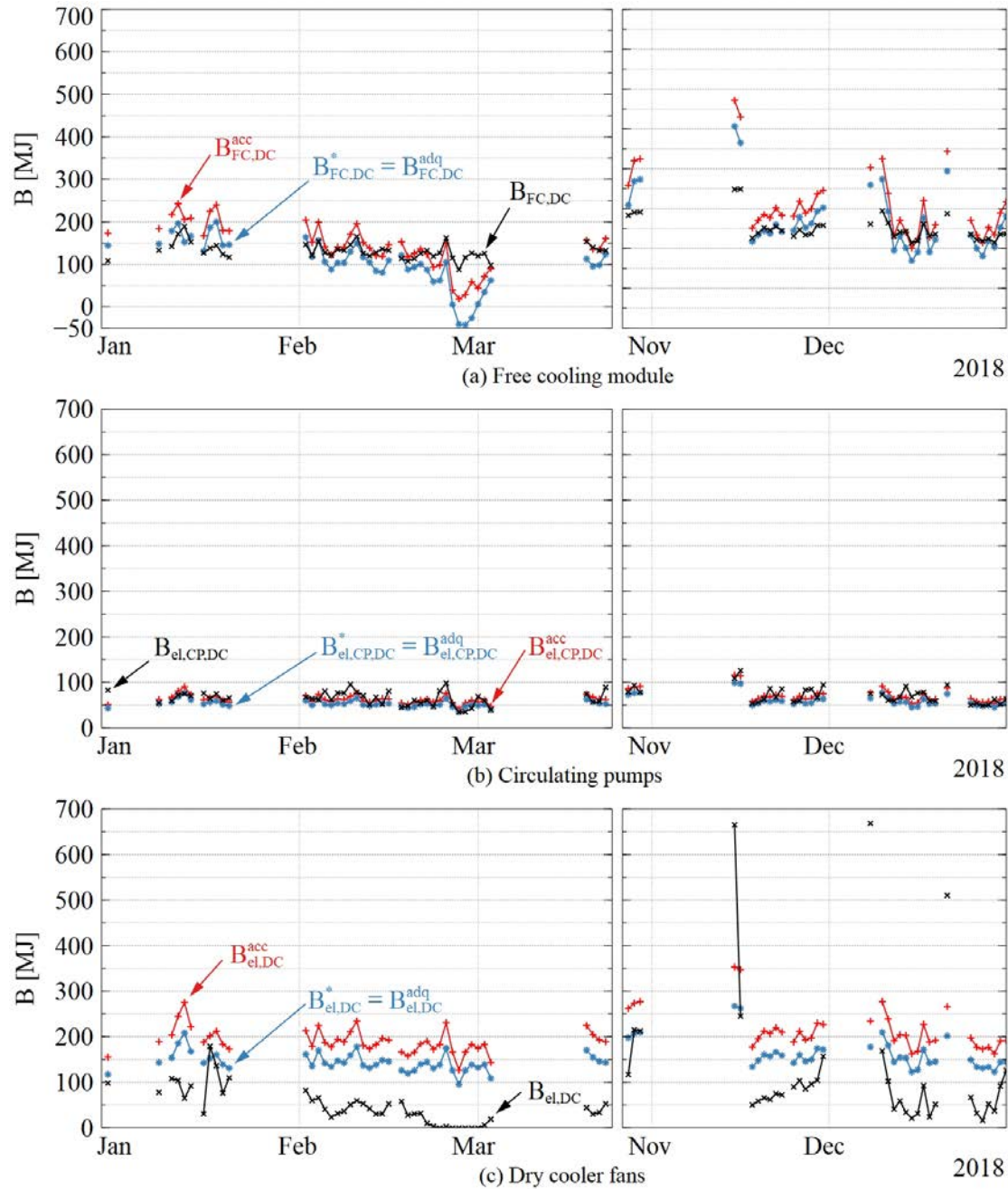
Figure 5.15 – Actual, reference (adequate) and acceptable daily exergy sum in refrigeration machine operation of the different components in the subsystem CST: (a) evaporator and (b) circulating pumps.

5.2.2.1.4 Subsystem cooling location

The optimization potential index in the subsystem CL exhibits a differentiated behavior depending on the cooling location (see Fig. 5.16). All locations have an adequate (reference) and acceptable average temperature of the cold water distribution between the in- and outlet of ≈ 12 and 14 °C, respectively, according to the technical standards. Cooling location 3 performs best with an average OPI_{CL3} of –0.81 (see Fig. 5.16a), where 79% of the time adequate operation is present. The mean cold water distribution temperature reaches ≈ 14.3 °C in the warmer months over the year, which is elevated compared to the design point. Therefore, the actual supplied exergy is lower as the references, which is favorable for the subsystem operation and the technical requirements are exceeded. Nevertheless, in the colder months (April, May, November and December) the OPI increases over the acceptable boundary OPI_{CL}^{acc}. This represents a reduction of the cold water distribution temperature compared to the design point, where finally the reason cannot be determined with the available experimental data. One possibility is that unfavorable control settings are present, which influence the behavior of mixing valves near the
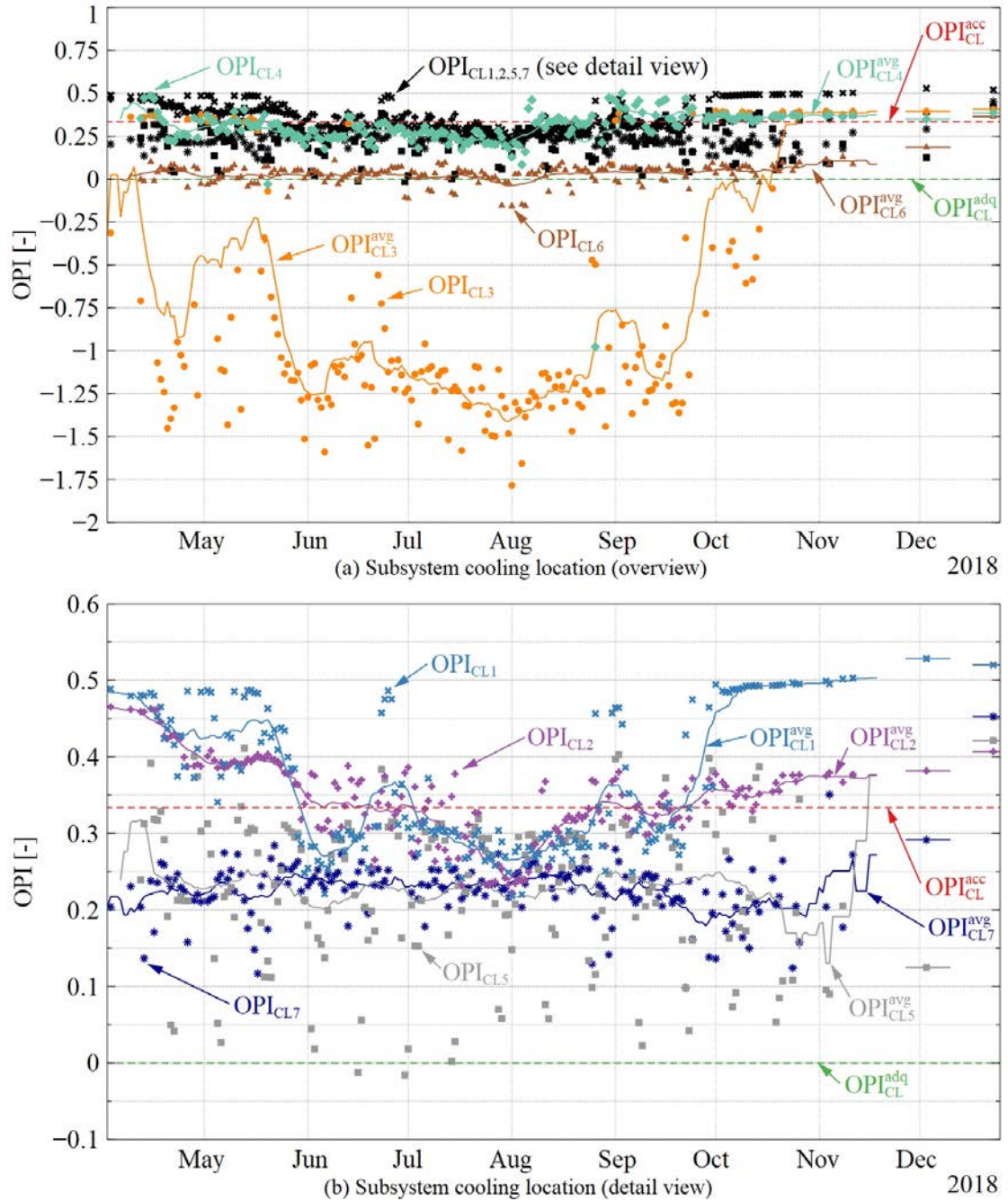
Figure 5.16 – Optimization potential index OPI_{CL} of the subsystem CL in refrigeration machine operation with adequate (green dashed line) and acceptable (red dashed line) boundary: (a) overview and (b) detail view representation. The data points represent the daily OPI values and the solid lines indicate the 14-days moving average of the OPI.

cooling location. Another reason could be a significantly reduced or even inexistent cooling demand in that time period. CL6 performs second best (see Fig. 5.16a) followed by CL5 and CL7 (see Fig. 5.16b) with an average $OPI_{CL6} = 0.03$ and $OPI_{CL5} = OPI_{CL7} = 0.23$, respectively. When examining the moving average OPI_{CL}^{avg} of the mentioned cooling locations, it is evident that all of them reveal no significant de- or increase of the key figure. Over the whole

examined period, the OPI is at least 91% of the time below the acceptable boundary OPI_{CL}^{acc}. Consequently, the technical requirements are fulfilled and no to little optimization potential is present.

Conversely, the optimization potential index of the other cooling locations is only approximately 40 (CL2) to 58% (CL4) of the time below the acceptable boundary OPI_{CL}^{acc}. This is mostly present in July to September, where the cooling locations reveal an acceptable operation. This indicates, that if a higher cooling demand is present, the temperature level of the cold water distribution is correctly controlled and no to little optimization potential is present. Similarly to CL3, the OPI increases in the colder months over the year, visible with both the daily values and the moving average, indicating potential for improvement. Again, the reason for this behavior can finally not be determined. A detailed analysis of the mentioned cooling locations should be carried out, in order to determine any faulty components or control settings. However, a fouled heat exchanger, which would result in an elevated temperature difference in order to ensure the heat transfer, can be excluded as a possible malfunction. If not, the OPI would generally be higher and not only in the transition period.

5.2.2.2 Free cooling operation

According to the available experimental data, free cooling operation occurred from January to March and from end of October to December. The exergy reference environment temperature T_0 applied in free cooling operation is 2.49 °C. Figs. 5.17, 5.19, 5.20 and 5.22 show the daily optimization potential index (OPI, y-axis) in free cooling operation of every subsystem in the field plant under investigation in function of the date (x-axis) in the mentioned time period. Identically to the refrigeration machine operation, the daily OPI is indicated with data points, where the 14-days moving average is represented by a solid line to evaluate the OPI tendency over time. The green, yellow and red zone depict the adequate (technical requirements exceeded), acceptable (technical requirements fulfilled) and inadequate (potential for improvement) operation condition, respectively. In Fig. 5.22 the adequate and acceptable boundary is indicated with a green and red dashed line, respectively. Furthermore, Fig. 5.18 and 5.21 shows the actual, reference (adequate) and acceptable daily exergy sum (y-axis) of each component in the subsystem DC and CST, respectively, in function of the date (x-axis) in the mentioned time period.

5.2.2.2.1 Subsystem dry cooler

To begin with, the subsystem DC operates according to the technical requirements, where in 96 and 91% of the time these are fulfilled or exceeded, respectively (see Fig. 5.17). Also, the OPI_{DC} reveals an average value of –0.22 and no significant optimization potential with respect to the technical standards is therefore present. Nevertheless, when observing the 14-days moving average OPI_{DC}^{avg} an increase of the key figure is apparent in end of February, also of the acceptable boundary. Three outliers with a value superior to OPI_{DC}^{acc} are present on November 15th as well as December 8th and 21st. However, such outliers should not be overly considered, as only a constantly high or rising key figure is a possible indication of a faulty operation. By investigating the daily exergy sums, the reason for the adequate performance of the subsystem DC is revealed (see Fig. 5.18).

On the one hand, the daily exergy input of the free cooling module $B_{FC,DC}$ (see Fig. 5.18a) and the circulating pumps $B_{el,CP,DC}$ (see Fig. 5.18b) has mostly a similar magnitude as the adequate B^{adq} or acceptable B^{acc} values. On the other hand, the daily exergy input of the dry cooler fans (see Fig. 5.18c) is substantially, around factor 2, lower than the adequate values. This is favorable for the subsystem operation and contributes to a low OPI. However, the actual dry cooler fan input is increased by approximately a factor of 6 the same days the OPI reveals potential for
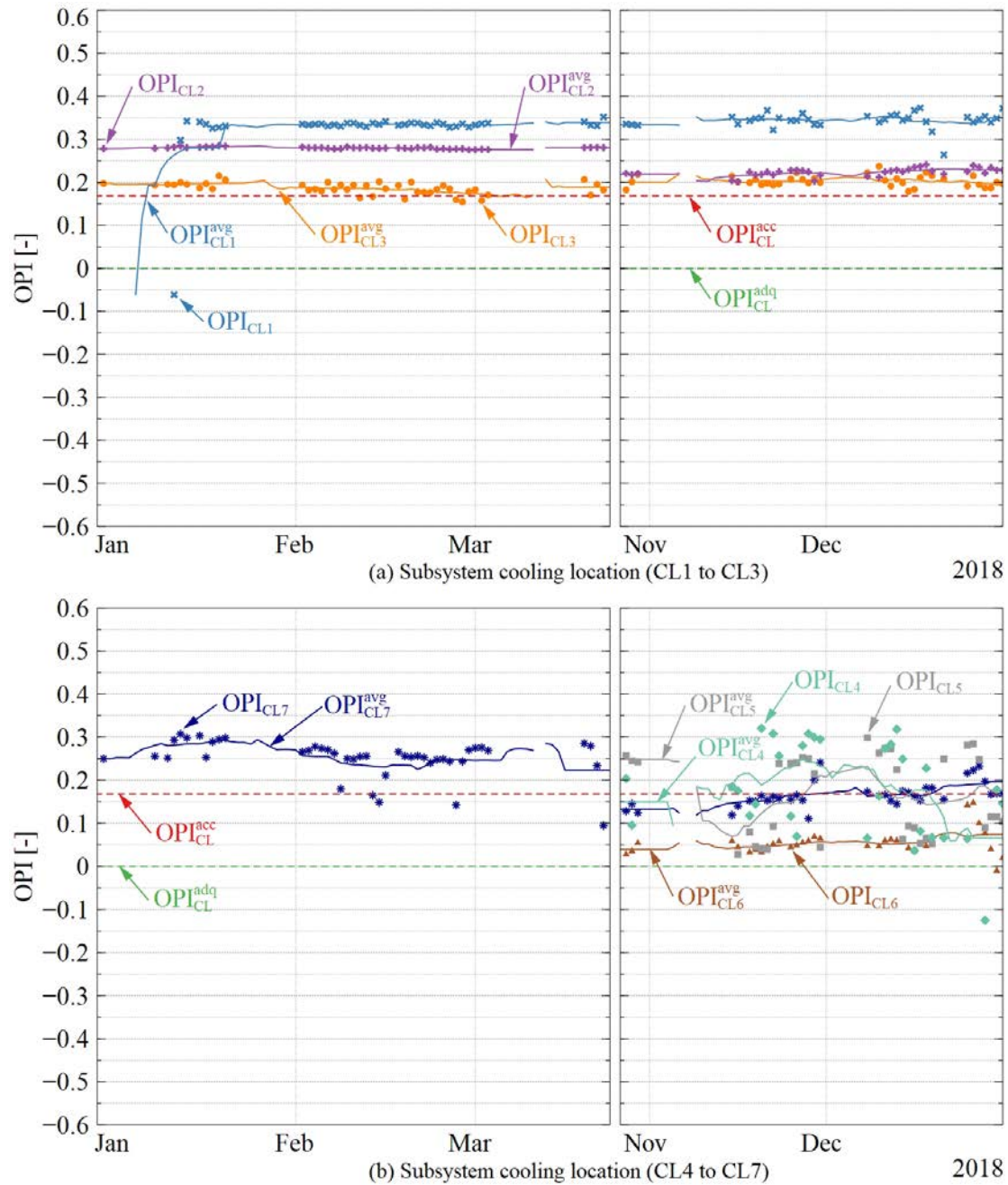

Figure 5.17 – Optimization potential index OPI_{DC} of the subsystem DC in free cooling operation with adequate (green), acceptable (yellow) and inadequate (red) operation range. The data points (black crosses) represent the daily OPI values and the black solid line indicates the 14-days moving average of the OPI.

improvement. As in refrigeration machine operation, the daily exergy input of the auxiliary devices have a similar magnitude compared to the thermal exergy of the free cooling module. Likewise, the dry cooler fans electrical exergy is one driving quantity, where it determines the outcome on the mentioned days where outliers are present. Again, this emphasizes to the reduce the auxiliary electrical energy consumption where possible.

Figure 5.18 – Actual, reference (adequate) and acceptable daily exergy sum in free cooling operation of the different components in the subsystem DC: (a) condenser, (b) circulating pumps and (c) dry cooler fans.

Moreover, from February 26th to 28th, the adequate free cooling module exergy $B_{FC,DC}^{adq}$ is negative, which would theoretically represent a subsystem output and reveals a possible drawback of the method. Due to significantly low ambient air temperatures in this time period and with the given definition of the adequate and acceptable temperature in the subsystem DC, they are at times lower than the exergy reference environment temperature T_0. As a consequence, the thermal exergy transfer direction is reversed, resulting in negative free cooling module exergy values. These are responsible for the increase of the OPI_{DC} and OPI_{DC}^{acc} in end of February (see Fig. 5.17). This outcome emphasizes the adequate choice of the reference environment temperature for the exergy analysis, in order to avoid perplexing results (see subsection 3.1.1.2). To the best of our knowledge, the chosen constant reference temperature reduces such outliers to a minimum, where the explained behavior is only observed on the mentioned days in the whole analysis. If the latter would fail with different experimental data, a possible workaround could be to carry out the analysis with absolute exergy values or to introduce a limiting function.

5.2.2.2.2 Subsystem free cooling

The subsystem FC shows an average OPI_{FC} of 0.05 and exhibits almost a steady-state behavior over the investigated time period (see Fig. 5.19). The minimum of 0.02 is achieved on January 21st and the maximum of 0.09 on November 16th. When analyzing the moving average OPI_{FC}^{avg},
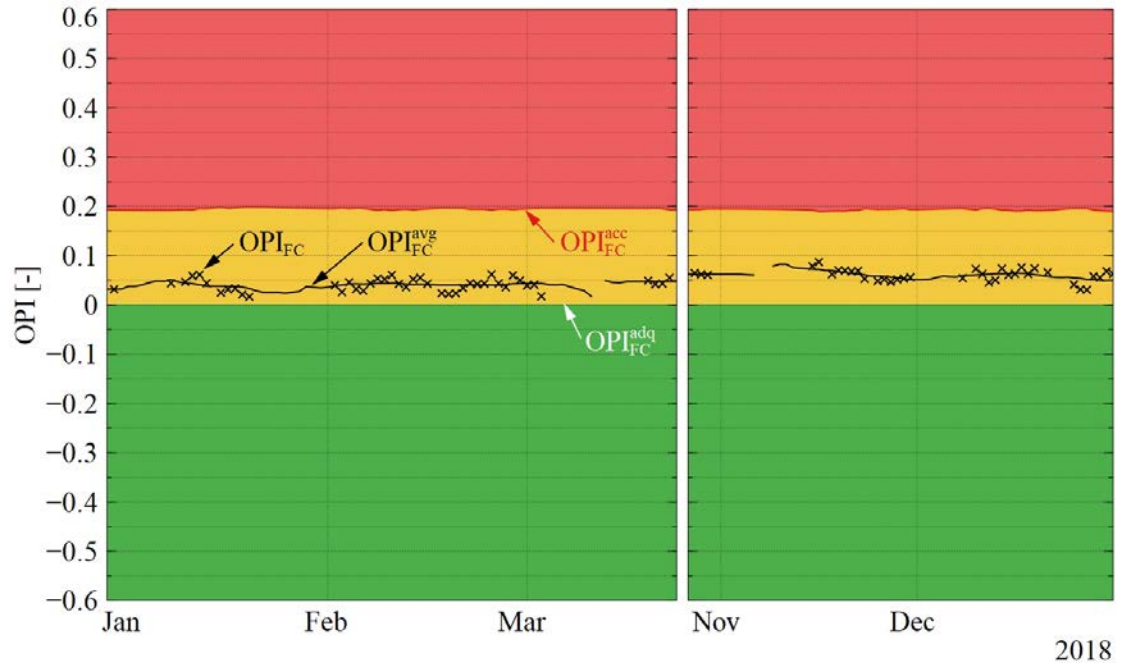
Figure 5.19 – Optimization potential index OPI_{FC} of the subsystem FC (free cooling module) with adequate (green), acceptable (yellow) and inadequate (red) operation range. The data points (black crosses) represent the daily OPI values and the black solid line indicates the 14-days moving average of the OPI.

no significant increase is observed, which would indicate a malfunction. The key figure is 100% of the time between the acceptable OPI_{FC}^{acc} and adequate OPI_{FC}^{adq} boundary and the technical requirements according to the applied technical standards are fulfilled. This leads to the assumption that the implemented free cooling module is well designed according to the needed specifications. Consequently, no to little optimization potential is present. Possibly, the temperature difference in the heat exchanger could be further decreased. Whether such an intervention is worthwhile, also from an economic point of view, would need to be determined in a detailed analysis (assuming experimental data would be available).

5.2.2.2.3 Subsystem cold water storage & transport

The subsystem CST reveals a similar behavior compared the subsystem dry cooler (see subsection 5.2.2.2.1), where the OPI_{CST} fluctuates in the range of –0.57 to 0.13 and reveals an average value of –0.15 (see Fig. 5.20). Also, the technical requirements are exceeded in 89% of the time which results in an adequate subsystem operation. This leads to the same assumption as in refrigeration machine operation (see subsection 5.2.2.1.3), where the hydraulic circuit is apparently well designed and controlled as well as the circulating pumps correctly operated, resulting in a low electrical power consumption and a low exergy input compared to the references, respectively. Consequently, no improvment potential according to the technical standards
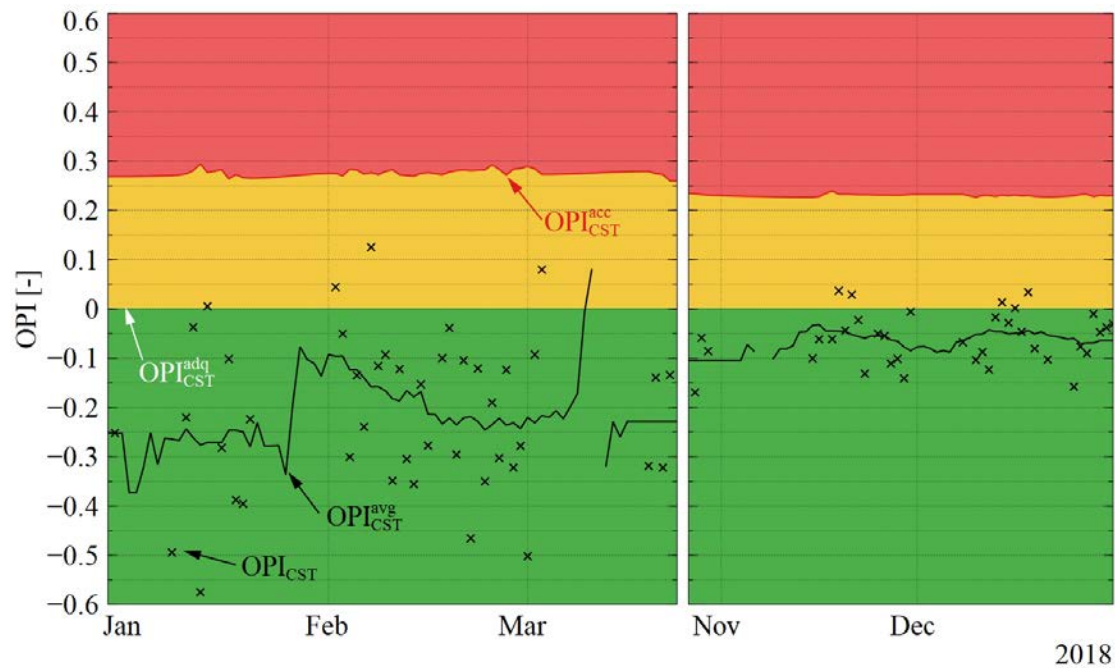
Figure 5.20 – Optimization potential index OPI_{CST} of the subsystem CST in free cooling operation with adequate (green), acceptable (yellow) and inadequate (red) operation range. The data points (black crosses) represent the daily OPI values and the black solid line indicates the 14-days moving average of the OPI.
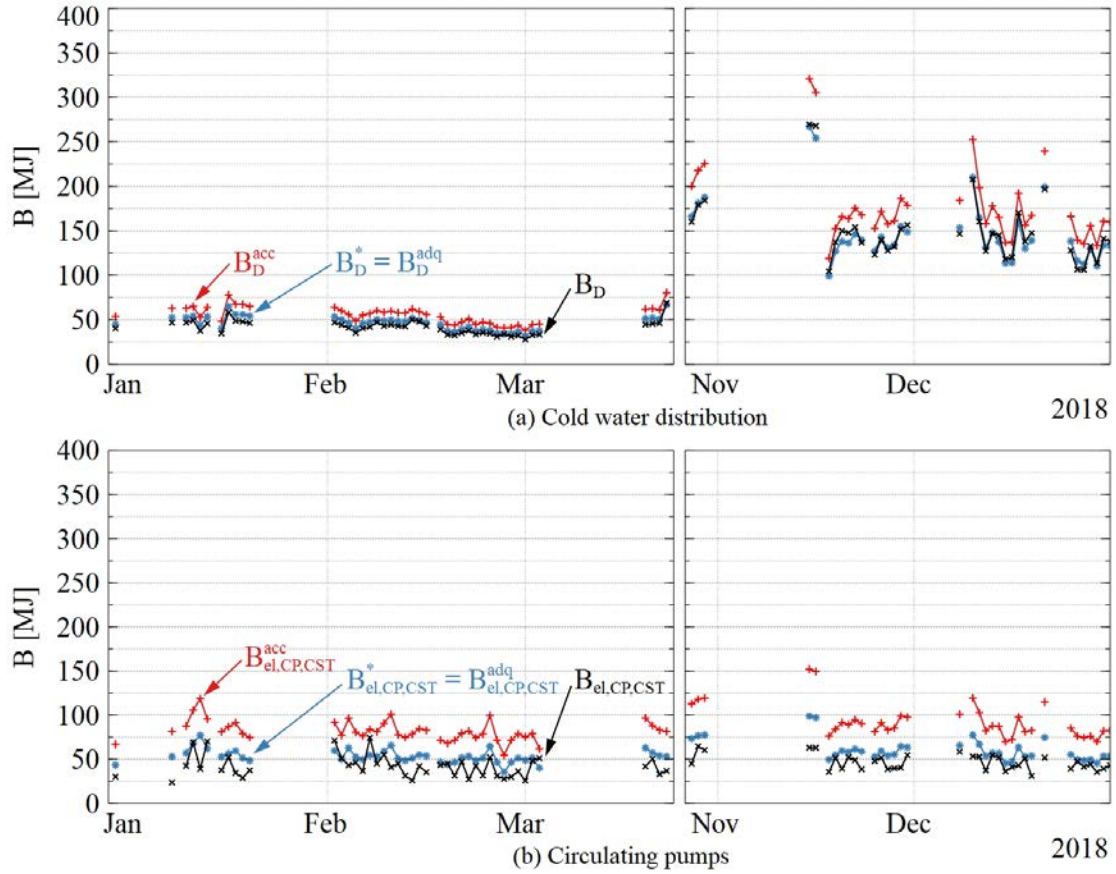
Figure 5.21 – Actual, reference (adequate) and acceptable daily exergy sum in free cooling operation of the different components in the subsystem CST: (a) cold water distribution and (b) circulating pumps.

is present. Interestingly, when observing the moving average OPI_{CST}^{avg}, the performance indicator reveals an increase of approximately 0.1 from mid-March to end of October. A possible reason are the three additional cooling locations which were integrated at the end of April to May, and thus, the actual exergy input of the subsystem is increased.

By investigating the actual, reference and acceptable daily exergy sum of the subsystem, the reason for the adequate performance is determined (see Fig. 5.21). Both, the actual cold water distribution B_D and circulating pumps exergy $B_{el,CP,CST}$, is generally (except on some days, e.g. December 19th) lower than the reference B^{adq} and acceptable exergy B^{acc}, respectively. Evidently, this contributes to a low OPI in the whole time period. As suspected, the cold water distribution exergy input is increased in the end of the year due to the additionally commissioned cooling locations.

5.2.2.2.4 Subsystem cooling location

The cooling locations reveal a differentiated behavior compared to the other subsystems in free cooling operation (see Fig. 5.22). As mentioned, cooling location 4, 5 and 6 were commissioned

in April and May, where no key figures are present before that time. When analyzing the 14-days moving average OPI_{CL}^{avg}, it is shown that the key figure of all cooling locations except CL4 and CL5 are almost in steady-state. The OPI_{CL4} and OPI_{CL5} fluctuates in a range of –0.13 to 0.32 and 0.03 to 0.30, respectively. Cooling location 6 performs best (see Fig. 5.22b), has an averaged OPI_{CL6} of approximately 0.06 and is 100% of the time between the adequate OPI_{CL}^{adq} and acceptable OPI_{CL}^{acc} boundary. Therefore, the technical requirements are fulfilled and no to

(a) Subsystem cooling location (CL1 to CL3)

(b) Subsystem cooling location (CL4 to CL7)

Figure 5.22 – Optimization potential index OPI_{CL} of the subsystem CL in free cooling operation with adequate (green dashed line) and acceptable (red dashed line) boundary: (a) CL1 to CL3 and (b) CL4 to CL7. The data points represent the daily OPI values and the solid lines indicate the 14-days moving average of the OPI.

little optimization potential according to the applied technical standards is present. CL4 and CL5 are 47% of the time in acceptable operation, where they have an average OPI_{CL4} and OPI_{CL5} of 0.18 and 0.17, respectively. Therefore, the mentioned cooling locations reveal most of the time an acceptable cold water distribution temperature, which is also observed in refrigeration machine operation (see subsection 5.2.2.1.4).

Cooling location 3 operates over the whole time period and cooling location 7 in November and December close to the technical requirements, which is indicated with an average OPI_{CL3} and OPI_{CL7} of 0.19 and 0.21, respectively. Furthermore, CL1 and CL2 reveal all the time an inadequate temperature level of the cold water distribution, which is revealed by an averaged OPI of 0.33 and 0.25. The key figure is all the time, except one outlier of CL1 on January 13$^{\text{th}}$, above the acceptable boundary OPI_{CL}^{acc}. Consequently, the mentioned subsystems are most of the time in inadequate operating conditions, which indicates potential for improvements. The reason for the unfavorable operation can finally not be determined with the available experimental data. As in refrigeration machine operation, possible reasons are unfavorable control settings of mixing valves close to the cooling locations or a significantly reduced cooling load in the investigated time period. The latter imposes maybe a different cold water distribution temperature level compared to full load condition design point, which is applied for the computation of the reference values. Therefore, the cooling locations should be inspected to determine eventual issues and to initiate countermeasures in order to achieve an increased performance.

5.2.2.3 Comparison of refrigeration machine and free cooling operation

Fig. 5.23 summarizes the monthly averaged optimization potential index (y-axis) as a function of the date (x-axis) of each subsystem in refrigeration machine (RM) and free cooling (FC) operation mode. To facilitate the comparison, the OPI of the subsystem RM and CL is averaged over all refrigeration machines and cooling locations, respectively. Since there were only six days of refrigeration machine operation in November and December as well as three days of free cooling operation in October, these values have to be considered with reservations.

The subsystem dry cooler (DC) shows a reduced performance in refrigeration machine operation compared to free cooling mode (see Fig. 5.23a), where the technical requirements are fulfilled in the whole time period. The highest averaged values of $OPI_{DC,RM}$ and $OPI_{DC,FC}$ is reached in October with 0.19 and –0.18, respectively. The adequate performance in free cooling operation is most likely due to the reduced power consumption of the cooler fans. Since there is a sufficiently large temperature difference between the system and ambient air in the winter months, the dry
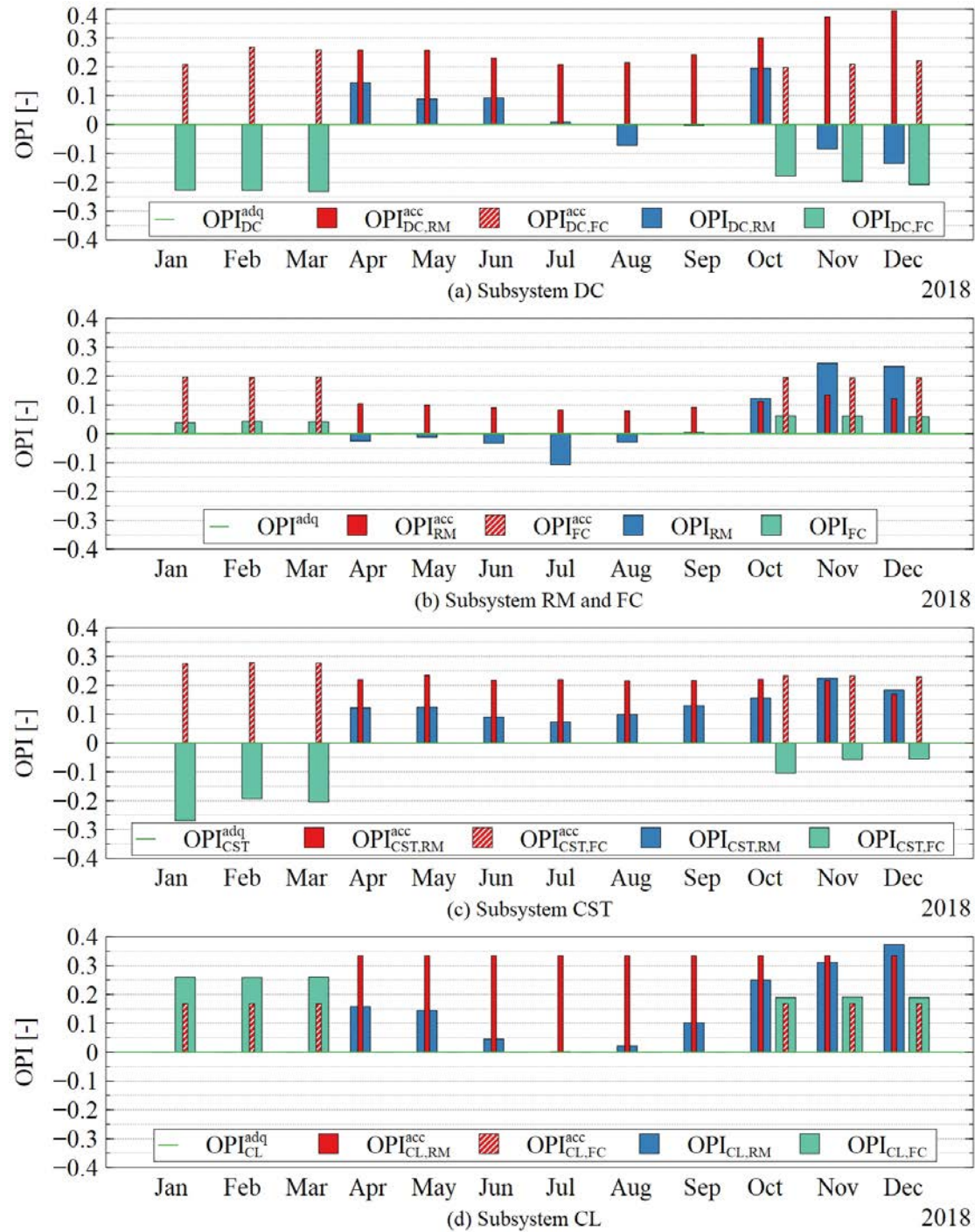
Figure 5.23 – Monthly averaged optimization potential index of all subsystems in refrigeration machine and free cooling operation: (a) dry cooler, (b) refrigeration machine / free cooling, (c) cold water storage & transport and (d) cooling location. Acceptable values (OPI^{acc}) are indicated with red / dashed red bars and the adequate value (OPI^{adq}) with a green solid line, respectively.

cooler can dissipate the thermal energy produced presumably with a reduced fan speed. Also, as the reference electrical energy consumption of the auxiliary devices is determined with the free cooling thermal energy as an approach, the reference exergy values may turn out to be less strict compared to refrigeration machine operation.

The subsystem free cooling (FC) shows a slightly worse performance than the subsystem RM over the period considered, except in October to December (see Fig. 5.23b). The former is over the whole year in acceptable operation, where the subsystem refrigeration machine (RM) reveals optimization potential especially in the months November and December. As already mentioned, this can be an indicator to make use of free cooling. This assumption is also consistent with experimental data of the free cooling operation, which mainly occurs in the winter months.

Similarly to the subsystem DC, subsystem cold water storage & transport (CST) reveals a better performance in free cooling operation (see Fig. 5.23c). The highest averaged values of $OPI_{CST,RM}$ and $OPI_{CST,FC}$ is reached in November and December with 0.22 and –0.06, respectively. The technical requirements are fulfilled or exceeded in every month over the year, which leads to the mentioned assumption that the hydraulic circuit is well designed and the auxiliary devices favorably operated.

By observing the monthly averaged OPI values of the subsystem cooling location (CL) over the whole year, it is visible that the technical requirements are fulfilled in the warmer months in refrigeration machine operation (see Fig. 5.23d). This leads to the conclusion, that the cold water distribution temperature is correctly controlled according to the design (application with partial dehumidification). Conversely, optimization potential is indicated in the colder month over the year, in both, refrigeration machine and free cooling operation. Over the year, the subsystem CL reveals a better performance in refrigeration machine operation than in free cooling mode. As mentioned, the reasons for an inadequate operation can finally not be determined with the available experimental data, where a detailed analysis would be necessary for further clarifications.

5.2.2.4 Comparison of OPI with COP and exergy efficiency

In order to further demonstrate the purpose and practical usability of the proposed method, the daily OPI is compared with the daily COP and exergy efficiency in refrigeration machine operation of each subsystem where possible. To simplify the comparison, the key figures are averaged over all refrigeration machines and cooling locations, resulting in one key figure per subsystem. In all calculations, the daily exergy or energy sum of the respective in- and ouputs is applied. The COP_{RM} is calculated according to Eq. 2.2, while for the subsystem DC the respective electrical energy consumption of the auxiliary devices is additionally included as effort. For the COP_{CST}, the cold distribution thermal energy Q_D and the additional electrical energy input of the circulation pumps in the subsystem are considered. With this definitions, the

COP should deliver information about the performance with respect to the defined subsystems as close as possible to the OPI. The exergy efficiencies of the subsystem RM $\eta_{ex,RM}$ and CST $\eta_{ex,CST}$ are computed according to Eq. 2.18 and 2.15, respectively. Due to missing measured quantities, the exergy efficiency of the subsystem DC and CL as well as the COP of subsystem CL could not be calculated. For completeness, the system COP and exergy efficiency (up to the cold water distribution) is computed according to Eq. 2.3 and 2.19, respectively. For the comparison, measurement data of the field plant on July 15th and July 18th is used. The daily OPI, COP and exergy efficiency values are listed in Tab. 5.3, where an adequate or acceptable operation of the refrigeration plant subsystems is present on July 18th. Conversely, on July 15th, the dry cooler fans electrical energy consumption is increased (see Fig. 5.8), which represents an unfavorable operation of the subsystem DC with potential for improvement.

First of all, it is apparent that the refrigeration machines perform well on both days, which is revealed with a low OPI and a high COP, respectively. While the COP is rather elevated, the exergy efficiency is approximately in the range of findings in performance investigations of vapor compression refrigeration machines [67, 71, 153]. The same behavior is observed in the subsystem CST (where the technical requirements are fulfilled, compare Fig. 5.14), which is consistent with the general findings of the field plant analysis (see subsection 5.2.2). A performance increase or decrease is revealed with an increase or decrease in COP and exergy efficiency value, respectively. However, a high COP or exergy efficiency does not exclude an OPI indicating potential for improvements. In the case of the subsystem CST for example, the circulating pumps exergy input is generally lower and the evaporator exergy input generally higher as compared with the reference. This results in a value above the adequate but below acceptable boundary,

Table 5.3 – OPI, COP and η_{ex} values in the different subsystems as well as of the overall system on July 15th (unfavorable operation of the dry cooler fans) and July 18th (technical requirements fulfilled or exceeded).

Subsystem	July 15th			July 18th		
	OPI [–]	COP [–]	η_{ex} [–]	OPI [–]	COP [–]	η_{ex} [–]
dry cooler (DC)	0.24	5.36	–	–0.22	5.90	–
refrigeration machine (RM)	–0.16	9.63	0.17	–0.12	8.17	0.15
cold water storage & transport (CST)	0.05	8.80	0.67	0.07	7.43	0.60
cooling location (CL)	–0.01	–	–	–0.01	–	–
overall system	–	4.99	0.08	–	5.45	0.09

indicating an acceptable operation where the technical requirements are fulfilled. Consequently, the absolute values of the OPI are less important compared to the other key figures, as it is of main interest if the technical requirements are fulfilled or not and if optimization potential is present, i.e. if the adequate or acceptable boundary is exceeded or not. Moreover, the exergy efficiency of the cold water distribution subsystem is close to findings in literature [75]. This exergy efficiency is significantly higher as compared to the subsystem RM, which leads to the conclusion that the exergy losses in the subsystem CST are correspondingly low. It is assumed that processes in the cold water distribution, which have a small temperature difference, exhibit a minor exergy destruction, which is favorable for the effectiveness. While this behavior cannot be confirmed through a calculation due to missing measured quantities, this correlation was also stated in literature [66]. Conversely, the COP_{CST} and COP_{DC} reveal lower values compared to the COP_{RM}, which is due to the additionally included effort of the auxiliary devices.

Furthermore, with the given definition of the OPI, only the subsystem inputs are considered (actual input compared to a reference input according to technical standards), where it is assumed that each adjacent subsystem of the investigated one perform identically in the present situation. As mentioned in subsection 3.1.3, the key figures of all subsystems cannot be mathematically combined to an overall system OPI, which represents a possible drawback of the proposed method. This is considered acceptable however, as the purpose of the method is to reveal eventual optimization potentials compared to the state of the art in technology on subsystem level independently of the overall system performance. By evaluating the overall system COP and exergy efficiency, the values are lower than of the single subsystems and are approximately in a similar range as found in literature [49, 75, 154]. Both key figures reveal a decrease of 0.46 and 0.01 between July 18th and July 15th, respectively. This indicates a performance reduction of the refrigeration plant, where the reason for this behavior is not evident. The possible issue is revealed when evaluating the subsystem DC. Comparing the COP_{DC} on both days, a decreases of 0.54 is present. This reveals a performance reduction of the subsystem due to the present increase in electrical energy consumption of the dry cooler fans. However, by only considering the COP, in this case a value of 5.36, it is not apparent if any optimization potential with respect to the technical standards is present. By analyzing the OPI_{DC}, an increase from –0.22 to 0.24 is observed. Therefore, the inadequate operation is indicated with a positive OPI value above the acceptable boundary (see Fig. 5.7). This represents a potential for improvement, in the present case reducing the power consumption of the cooler fans. This relationship reveals the purpose and the significance of the optimization potential index. While the COP and exergy efficiency deliver adequate information about the refrigeration plant performance, the OPI re-

veals any eventual optimization potential of each subsystem with respect to the state of the art in technology, which is highly relevant in practice. To the best of our knowledge, a combined analysis with the proposed method (revealing possible optimization potentials in a first step) together with conventional energy and exergy analysis (identifying the malfunction in detail in a second step and evaluate if adjustments are worthwhile) delivers a target-oriented procedure to analyze the refrigeration plant behavior and to optimize the system efficiency.

6 Evaluation of measuring concepts in real field plants and retrofitting costs

The main goal of the work presented in this chapter is to acquire technical data of 15 – 20 real field plants and to evaluate their existing measuring concept as well as to determine eventual retrofitting costs for the application of the proposed evaluation method. Correspondingly, the acquisition process to receive technical data of real field plants and the analysis of their measuring concepts is elaborated and discussed in section 6.1. Eventual retrofitting costs of the investigated field plants are estimated and discussed in section 6.2.

6.1 Measuring concepts in real field plants

As mentioned in the standard VDMA 24247-7, an adequate measuring concept and monitoring system is a necessary prerequisite for a target-oriented evaluation of refrigeration systems and their efficiency during operation [24]. Within the scope of the present work, the typical structure of real refrigeration plants in air-conditioning applications and the state-of-the-art measuring concepts are of interest. It is relevant if existing field plants already incorporate an adequate measuring and logging concept for the application of the proposed exergy-based evaluation method (see section 3.1).

Before contacting the actors in the industry, selection criteria are elaborated to determine whether a refrigeration plant is suitable for further investigations. In order to avoid a too strong restriction in the selection of systems in advance, only the following two criteria are defined as mandatory:

- The field plant is mainly used for air-conditioning applications (i.e. refrigeration applications for thermal comfort).

- The refrigeration system incorporates secondary hydraulic circuits for the cold water distribution (no direct evaporating systems).

The following criteria are desirable:

- The cooling capacity of the field plant is greater than 50 kW ($\dot{Q}_{E,sys} > 50\,kW$)[5].

- The field plant incorporates all basic subsystems (refrigeration machine, dry cooler, cold water storage & transport, cooling locations) as well as additional components (heat utilization, free cooling).

6.1.1 Acquisition of technical information

A contact list of companies in the refrigeration industry serves as a working basis to obtain information of existing air-conditioning refrigeration systems, which are suitable for evaluation (according to selection criteria). The companies were divided into the following sub-groups according to their areas of expertise and should have access to the appropriate facilities:

- plant engineer / designer,

- plant operator,

---

5 Frequency of refrigeration plants for air-conditioning applications with the corresponding cooling capacity according to statistics [155]:
- 20 to 50 kW (13 %)
- 50 to 100 kW (39 %)
- 100 to 300 kW (40 %)
- over 300 kW (8 %)

- refrigeration machine importer / supplier,

- refrigeration machine manufacturer.

The synthesis of existing company lists and the integration of new companies according to inputs from experts in the industry as well as the execution of a targeted market research completed the contact list, which comprises a total of 69 contacts. A final assessment of the suitability of a plant can only be clarified after a first contact. For this reason, the contact list is rather comprehensive. It can be assumed that there are refrigeration plants which do not meet the mandatory criteria or that the contacted companies decline to collaborate.

In order to make the process of acquisition and the related telephone inquiries of companies more efficient, a contacting guide and an information leaflet with the most important facts about the project are developed. The latter serves as an information basis for the responsible persons of the companies in case of an existing interest in a collaboration. By logging the inquiries and partially contacting the companies again, the receipt of sufficient technical information is ensured. The instrumentation level is then determined based on received piping & instrumentation schematics of field plants with the help of a checklist. In addition, open questions and ambiguities are clarified by means of plant visits or meetings with plant engineers. In a few individual cases, where the plants were not actively supported, the best possible estimate of measuring point availability is made in discussions with plant engineers.
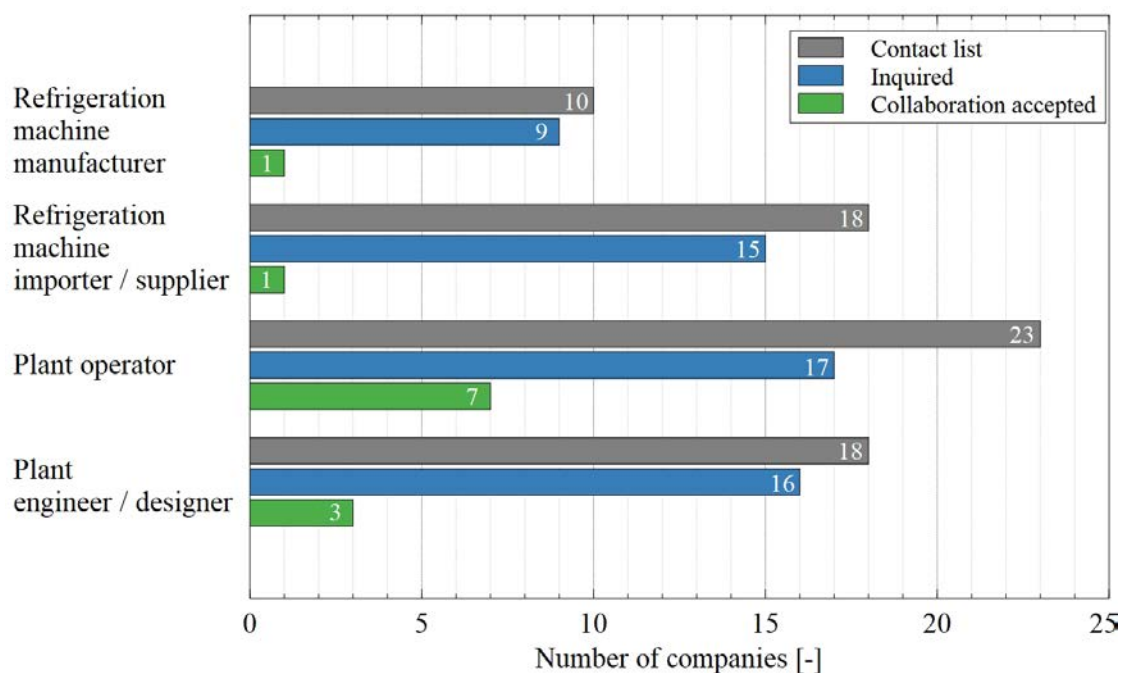
Figure 6.1 – Response rate of the inquired companies divided into the different fields of expertise (adapted from [12]).

Based on the contact list created, a total of 57 of 69 companies were contacted. As the target of 15 – 20 plants was exceeded and a wide range of refrigeration plants was available, a further inquiry of the 12 remaining companies was not carried out. In some cases, one company provided technical data of several refrigeration plants. In Fig. 6.1 the results of the inquiry are shown, broken down by field of expertise. For each area, it is evident how many companies are on the contact list, were inquired and accepted a collaboration. In general, the number of cancellations in each expertise field is relatively high (response rate of 6 – 40%), where mostly plant operators pledge a collaboration. One of the most frequently cited reasons for a rejection is that no suitable system or no access to the overall system is available. A lack of time resources is also an obstacle for many. For some companies, a reply was still outstanding even after the third contact. Consequently, these were no longer inquired.

Table 6.1 – Overview and key data of the investigated refrigeration plants for air-conditioning applications (adapted from [12]).

Field plant no.	Cooling capacity [kW]	Refrigerant	Field of application	Site (city)	Build year
1	200	R134a	air-conditioning	Cham ZG	2016
2	128	R410a	air-conditioning	Zürich ZH	2017
3	4750	R717	air-conditioning	Winterthur ZH	2014
4	5252	R717	air-conditioning	Luzern LU	2016
5	573	R410a	air-conditioning	Zürich ZH	2016
6	449	R410a	air-conditioning	Zürich ZH	2012
7	189	R410a	air-conditioning	Zürich ZH	2012
8	519	R410a	air-conditioning	Zürich ZH	2012
9	570	R134a	air-conditioning	Zürich ZH	2014
10	988	R134a	air-conditioning	Opfikon ZH	2011
11	1320	R717	air-conditioning / fabrication	Schaffhausen SH	2017
12	867	R134a	air-conditioning / server	Bern BE	2007
13	158	R134a	air-conditioning	Rothrist AG	2014
14	214	R410a	air-conditioning	Winterthur ZH	2016
15	141	R410a, R744	air-conditioning	Uster ZH	2017
16	190	R410a	air-conditioning / sale	Zürich ZH	2018
17	612	R407c, R134a	air-conditioning / sale	Bülach ZH	2015
18	900	unknown	air-conditioning / sale	Zürich ZH	2015
19	20	R744	air-conditioning	Eglisau ZH	2015
20	250	R134a	air-conditioning / sale	Uster ZH	2016
21	25	R744	air-conditioning / sale	Jona SG	2018
22	50	R410a	air-conditioning / sale	Wollerau SZ	2018
23	800	R134a	air-conditioning / server	Bern BE	2012
24	288	R407c	air-conditioning / server	Liebefeld BE	2006
25	43	R410a	air-conditioning / sale	Zumikon ZH	2014
26	194	R410a	air-conditioning / fabrication	Netstal GL	2012
27	unknown	unknown	air-conditioning / sale	Zürich ZH	unknown
28	unknown	unknown	air-conditioning	Wädenswil ZH	unknown

From the response of 12 companies in total, it was possible to evaluate technical information of 28 different refrigeration plants and to partially inspect them on site. Tab. 6.1 shows an overview of the field plants investigated, listing the cooling capacities, the refrigerants used, the fields of application and the site (for the evaluation of the instrumentation see subsection 6.1.2). All field plants are located in Switzerland. The cooling capacities of the systems vary from 20 to 5'252 kW, which is desirable for the present study. More than half of the refrigeration plants are less than four years old, with systems built between 2006 – 2018. In addition, the majority of the refrigeration machines use the refrigerants R410a and R134a. Most of the listed refrigeration plants are installed in shopping malls or office buildings, where some of them have two fields of application (with air-conditioning as the main purpose).

6.1.2 Evaluation of measuring concepts

Of the 28 field plants from the acquisition, the instrumentation of four systems (plant no. 25 to 28) cannot be examined due to insufficient information (e.g. incomplete schematics). For the evaluated refrigeration plants, according to technical documentation and on-site clarifications or

Table 6.2 – Summary of the installed measuring equipment in the examined field plants (adapted from [12]).

Field plant no.	n_{RM}	$\dot{Q}_{E,sys}$ [kW]
1	1	200
2	1	128
3	5	4750
4	4	5252
5	2	573
6	2	449
7	1	189
8	2	519
9	2	570
10	2	988
11	2	1320
12	4	867
13	1	158
14	1	214
15	2	141
16	3	190
17	2	612
18	2	900
19	1	20
20	1	250
21	1	25
22	1	50
23	2	800
24	3	288

Column groups: Refrigeration machine (W_{CPR}, Q_E, $T_{E,out}$, $T_{E,in}$, Q_C, $T_{C,out}$, $T_{C,in}$, Q_{HU}, $T_{HU,out}$, $T_{HU,in}$); Dry cooler ($W_{CP,DC}$, W_{DC}, Q_C, $T_{C,out}$, $T_{C,in}$, T_{amb}); Cold water storage & transport ($W_{CP,CST}$, Q_E, $T_{E,out}$, $T_{E,in}$, Q_D, $T_{D,out}$, $T_{D,in}$); Cooling location (W_{CL}, Q_D, $T_{D,out}$, $T_{D,in}$); Heat utilization (W_{HU}, Q_{HU}, $T_{HU,out}$, $T_{HU,in}$); Free cooling (W_{FC}, Q_{FC}, $T_{FC,out}$, $T_{FC,in}$); Logging.

Legend:
- Measurement equipment present, logged or derivable
- Measurement equipment present, not logged
- Measurement equipment present, measurement subpar or not finally determinable
- Measurement equipment not present
- Subsystem not included

meetings with plant engineers, the instrumentation status is summarized in Tab. 6.2. The number of refrigeration machines installed in the system and the total cooling capacity is described by n_{RM} and $\dot{Q}_{E,sys}$, respectively. The remaining variables in the table correspond to the individual measuring points in the various subsystems (compare subsection 3.1.2.1 and 3.1.2.2). This summary is also applied to estimating the individual retrofitting costs to allow an application of the proposed exergy-based evaluation method (see section 6.2).

The overview of the assessed field plants reveals that there are great differences in measuring equipment. Some plants have a comprehensive instrumentation as well as an overall system data logging. Accordingly, field plant no. 12 incorporates a state-of-the-art measuring concept. Also, field plant no. 3, 4, 9 to 11 as well as 20 and 21 are instrumented close to the state of the art, where only a minor amount of sensors are missing. In comparison, other systems such as field plant no. 5 have only a basic instrumentation (mostly temperatures) and no data acquisition. Field plant no. 15 to 24 incorporate no overall monitoring system, but quantities are logged individually. Field plant no. 24 has hardly any measurement equipment installed, where only the compressor electrical power is logged. 11 field plants incorporate a free cooling module and 17 make use of heat utilization. Furthermore, the following trends are observed:

- In general, the plants are sparingly equipped with electric meters. For cost reasons, the electrical power consumption of the cooler fans $\dot{W}_{DC}$ and circulation pumps $\dot{W}_{CP}$ is, with some exceptions, never recorded individually. The compressor electrical power consumption $\dot{W}_{CPR}$ is measured in half of all investigated systems. This reveals the typical pattern of energy efficiency evaluations: key figures such as COP, EER or SPF are important in practice for efficiency assessments of refrigeration systems, also to determine if the technical specifications are met after the commissioning of the plant. Using the compressor electrical power together with the evaporator $\dot{Q}_E$ or cold water distribution thermal power $\dot{Q}_D$ the key figures can be determined on refrigeration machine or overall system level, respectively. Consequently, the energetic performance of the refrigeration plant can be evaluated.

- In most systems, the cooling capacity of the cold water distribution $\dot{Q}_D$ to the cooling locations is of interest (e.g. for the account of charges of the users connected to the refrigeration system). 18 out of 24 systems are equipped accordingly with heat meters at the cooling locations, either individually per consumer or at least as a combined meter across all consumer groups.

- The best-equipped field plants are from companies with energy contracting.

- Temperatures are measured or logged in all field plants, however not always at every metering location.

- An adequate monitoring system should be state of the art nowadays (topic of digitization), but is however often not installed. A comprehensive data logging and evaluation is of particular interest to companies in the energy contracting sector or those who operate their own facilities. All examined refrigeration plants are controlled by a guidance system and would be able to record data. Only in 7 field plants data is effectively registered and stored on a server for a longer period of time. Another 9 plants have an insufficient monitoring and logging system. Most of them have a circular buffer with storage space for measuring periods from a few hours up to several weeks. These are used for efficient troubleshooting. In the remaining 8 plants a guidance system is available, but no data is registered.

6.2 Retrofitting costs for the application of the proposed assessment approach

The basis to determine the retrofitting costs of each field plant is, on the one hand, knowledge from a preliminary study [9] and, on the other hand, active contact with plant engineers and manufacturers of measuring equipment. For the calculation, the approach was followed to determine separately the costs for each measuring equipment in function of the cooling capacity, as generally valid as possible, based on measuring equipment manufacturer and plant engineer data. In order to ensure a uniform cost estimate for a subsequent comparison of the different field plants, the subsystems free cooling and heat utilization were not considered in the calculation, as they are not present in all refrigeration systems (compare Tab. 6.2). It is important to notice, that the number of retrofit measuring locations not necessarily results in the highest overall retrofitting costs. Heat meters and their installation, for example, are more expensive than temperature sensors. Therefore, if one plant requires the installation of one additional heat meter and a second plant the integration of several additional temperature sensors, the former eventually still reveals a higher overall retrofitting cost (see subsection 6.2.3).

6.2.1 Specifications and assumptions for the retrofit of measuring equipment

To ensure same boundary conditions for all offer requests at measuring equipment manufacturers as well as to assure a uniform cost estimate, specifications and assumptions are defined for the examined measuring instruments with the help of experts in the field:

- General:
    - Suboptimal placed measuring points are completely replaced by new ones. For example, a heat meter measuring location incorporates two temperature sensors, but no flow sensor. In this case, the existing instrumentation would be replaced by a heat meter with integrated temperature sensors.

- Heat meter:
    - The heat meter should be offered as a package with flow sensor, temperature sensors (immersed sensor) and controller for each measuring point.
    - The accuracy of the heat meters should comply with accordance to standard market use.
    - If possible, magnetic inductive flow sensors (MID) should be used.
    - It is assumed that the measuring equipment can be installed without great additional effort. This means that among others no lifting platforms are necessary, insulation can be easily removed and no special welding techniques are required.
    - The flow sensors are installed flanged or welded (all measuring points have a pipe diameter larger than DN50).
    - The heat meter is commissioned by the manufacturer at the field plant.
    - If possible, the measurement data is transmitted via Modbus[6].

- Electric meter:
    - Electrical consumers (e.g. compressor, auxiliary devices, etc.) are measured summarized per subsystem if possible and the corresponding electrical meters are offered based on the total power consumption. If, for example, four circulating pumps are installed in the cold water distribution subsystem, they are grouped together on one line, where then the power is measured.
    - For a power consumption of up to 4 kW at the measuring point, direct measuring meters are applied. For higher powers, additional current transformers are installed.
    - If possible, the measurement data is transmitted via Modbus.
    - It is assumed that the wiring can be carried out without great additional expenditure. This means that among others risers and cable trays are available, no unproportional long lines are to be installed and that the existing switchboard has space reserves for the planned enhancements.

---

6 Modbus is a communication protocol that enables data exchange between a master and several slaves. This is the industry standard for connecting computers to measurement and control systems.

- Temperature sensors:
    - Only immersed sensors are applied.

    - State of the art sensor types are used (often Pt100).

- Monitoring and data logging:
    - A common control system (SPS, SAIA, or similar) is available, which is known to the provider of the data acquisition.

    - Up to 100 measuring points, i.e. 100 sensors, are to be recorded simultaneously and their data stored continuously. The measuring interval should be practicable.

    - Offers should include the costs for setting up and programming a data logging with storage. The sensor wiring shall not be offered (assuming the data can eventually be captured by the control or guidance system).

The field plant documentation serves as a data basis for offer requests. Wherever possible, necessary information for the sizing of measuring locations is taken and summarized in a table. For heat meters, the nominal diameters, working fluids, flow rates and temperatures are collected at the corresponding measuring points. For electric meters, where possible, the electrical power consumption of the measuring point is identified from technical data. Additionally, one manufacturer requested the nominal electric current of the devices to be metered.

In discussions with plant engineers, various manufacturers or suppliers of measuring equipment and data logging systems were identified. The companies were contacted by phone to get a first impression of the sensor possibilities as well as important information from manufacturer experience. Based on these conversations, it was able to gain further insights which were later used to calculate installation costs. In case of a present interest from the manufacturer side, the corresponding summarizing tables with the needed technical data were delivered to receive an offer or a completed cost table.

6.2.2 Retroffiting costs for the measuring equipment

Four out of five heat meter manufacturers as well as two out of three contacted electric meter manufacturers answered with an offer for the measuring equipment. For the data logging system, only one supplier was able to provide a cost estimate by telephone. Based on the information obtained, specific retrofitting costs are defined for the individual components in order to determine the total retrofitting costs of each field plant. For this purpose, the offers of the manufacturers or suppliers are carried together and averaged with respect to the system cooling

capacity. Also, with the known expense per measuring instrument, retrofitting costs of any other arbitrary refrigeration system could be easily evaluated. All in the following mentioned costs are reported in Swiss Francs (CHF)[7].

6.2.2.1 Heat meter

Fig. 6.2 shows the average hardware costs for heat meters from manufacturer and supplier offers (y-axis) as a function of the system cooling capacity (x-axis). It is revealed, that higher cooling capacities lead to higher hardware costs, most probably due to the increased pipe diameters in the system. The estimation of the hardware expense $K_{HM,HW}$ for a heat meter to be retrofitted is proposed as follows:

$$K_{HM,HW} = 2.9114 \cdot \dot{Q}_{E,sys} + 2632.8 \tag{6.1}$$

where $\dot{Q}_{E,sys}$ represents the system cooling capacity. The linear function was fitted from the available data. It is worth mentioning that Eq. 6.1 only includes the price of the flow and temperature sensor as well as controller. The installation is calculated separately. The cost function was randomly compared at various heat meter measuring points with the available values from the offers. It was found that $K_{HM,HW}$ can deviate between 2.5 to 23.2% from the actual of-
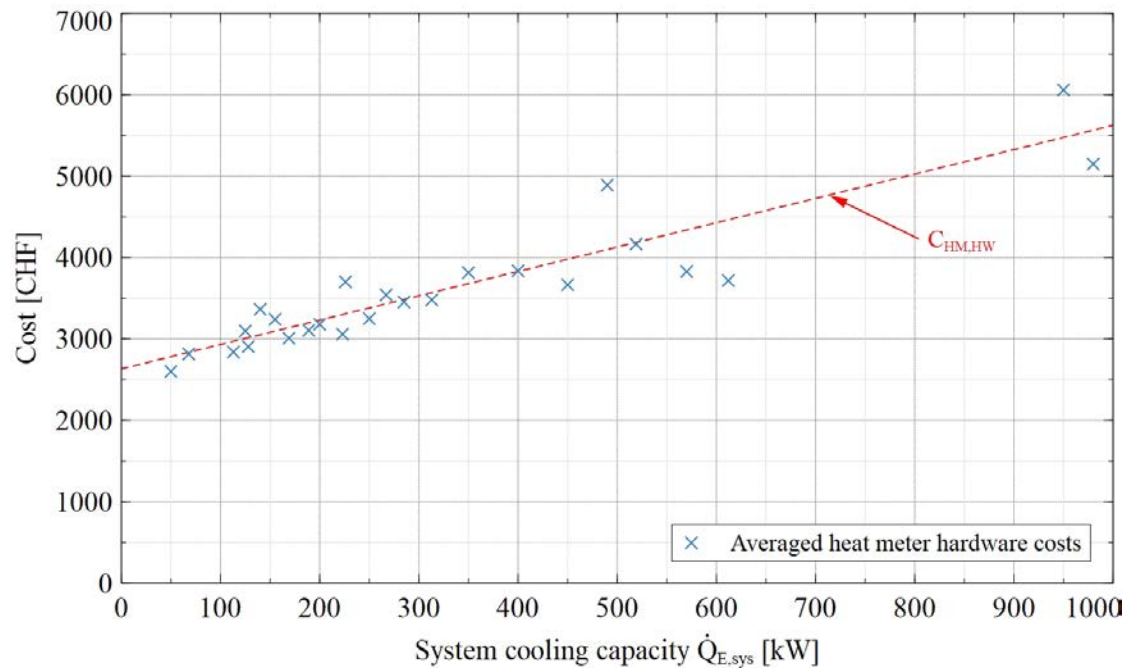
Figure 6.2 – Hardware cost for heat meters in function of the cooling capacity of the system. Blue crosses indicate the individual averaged cost estimate from manufacturers and suppliers. The red dashed lines indicates the fitted linear cost function (adapted from [12]).

---

7   1 CHF $\approx$ 0.92 EUR (state 17th December 2020)

---

fers, which is regarded as a reasonable range. In that way, by applying the cost function, the retrofitting expense of any other refrigeration plant investigated in the future can be determined with a reasonable effort. Three field plants in the investigated portfolio (compare Tab. 6.2) have a cooling capacity above 1 MW. Of these, only plant no. 4 lacked a heat meter, whose price for the total retrofitting cost is directly determined from the manufacturer offers.

Each manufacturer or supplier inquired stated that the calculation of the total expense depends strongly on the design of the respective refrigeration plant. Accordingly, the installing costs are difficult to estimate. One manufacturer stated that several years of experience have shown that the installing costs range between 1 to 2 times the purchase price of the hardware. Latter statement was applied as an approach for the estimation and the following relationship applies to the heat meter installation costs $K_{HM,inst}$:

$$K_{HM,Inst} = 1.5 \cdot K_{HM,HW} \tag{6.2}$$

Consequently, by combining Eq. 6.1 and 6.2, the total retrofit costs K_{HM} for a heat meter measuring point in function of the cooling capacity is given by:

$$K_{HM} = K_{HM,HW} + 1.5 \cdot K_{HM,HW} = 7.2785 \cdot \dot{Q}_{E,sys} + 6582 \tag{6.3}$$

6.2.2.2 Electric meter

According to discussions with manufacturers, the present electrical current is the decisive factor for the hardware costs of electric meters. Above a certain device size, current transformers must be installed, which can double the expense. Also, in comparison to the heat meters, the costs depend minimally on the system cooling capacity and are significantly lower. According to the information of manufacturers, a total hardware cost $K_{EM,HW}$ for electric meters including current transformers of CHF 400 is defined, which is up to 15 times lower than heat meter hardware costs.

Again, the installation effort is difficult to estimate. This was also confirmed by statements of the measuring equipment manufacturers. According to the latter, the wiring may require one hour of work up to a whole working day. A workload of 5 hours was considered as an adequate estimate for the average installation time. At an hourly rate of CHF 120, it corresponds to an installation cost $K_{EM,inst}$ of CHF 600 per electric meter. The retrofitting costs for electric meters K_{EM} are thus:

$$K_{EM} = K_{EM,HW} + K_{EM,inst} = 1000 \tag{6.4}$$

This number is also in line with a statement of one supplier. Furthermore, a total retrofitting cost for electric meters of CHF 960 was estimated in a preliminary study [9].

6.2.2.3 Temperature sensor

For the retrofitting of temperature sensors, a cost K_{TS} of CHF 250 for the purchase and 1 hour of installation was defined according to experience from experts in the field.

6.2.2.4 Data logging

For a monitoring and data logging system, the costs behave similarly to electric meters in a way that they are constant over the entire system cooling capacity range. The available information reveals that the costs for a data logging system only increase noticeably if a large number of data points (in the order of 2000 measuring points) is involved. None of the plants investigated would exceed that number, even if the largest plant would be completely uninstrumented. The costs for a separate data acquisition system K_{DL} are:

$$K_{DL} = K_{DL,sys} + K_{DL,st} = 8000 \tag{6.5}$$

with $K_{DL,sys}$ the intial costs for a data monitoring system (approximately CHF 6'000, incl. programming, commissioning etc.) and $K_{DL,st}$ the costs for a local storage infrastructure (approximately CHF 2'000). These costs apply for the data collection according to the assumptions mentioned in subsection 6.2.1 as well as to the local storage of data. As an approach, a local data storage is assumed, because renting external servers would yield increased costs. Also, an external connection to the local server is simple to realize with current technology.

6.2.3 Field plant retrofitting needs and costs

Fig. 6.3 reveals the number of missing or subpar measuring locations (y-axis) for each investigated field plant (x-axis). Refrigeration plant no. 12 and 22 are the best- and worst-case regarding the missing instrumentation, where half of the field plants have 7 or more missing measuring devices. However, this number does not necessarily result in high retrofitting costs, as the heat meters are by far the most expensive. If the missing locations are temperature sensors, the expense is minor.
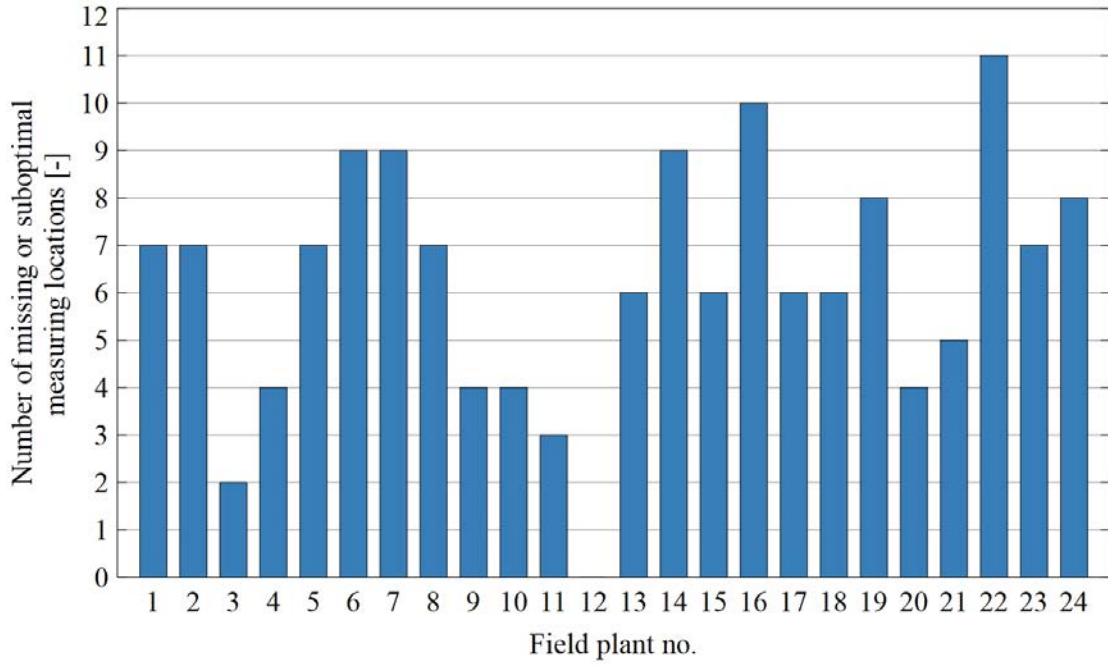
Figure 6.3 – Number of missing or suboptimal measuring locations of each refrigeration plant investigated (adapted from [12]).

On the basis of Tab. 6.2 and the determined individual sensor expense, a cost estimate is conducted for each field plant. The price for missing heat and electric meters as well as temperature sensors are considered, whereby the total retrofitting effort K_{tot} is:

$$K_{tot} = \sum_i K_{HM} + \sum_j K_{EM} + \sum_k K_{TS} \tag{6.6}$$

The monitoring and data logging is considered as state of the art and could be realized as an interim solution with the included control or guidance system in most of the field plants. Also, at least a temporal data storage is present in 16 of 24 field plants, e.g. for maintenance purposes. The cost estimate is intended to reflect the essential retrofits to capture the thermo-physical quantities to implement the exergy-based assessment approach, and accordingly, the cost of the data registration K_{DL} was not included.

Often, a heat meter measuring point is missing, while the temperature sensors are present (e.g. field plant no. 1: $\dot{Q}_E$, $T_{E,in}$ and $T_{E,out}$). In these cases no flow sensor is present, and thus, the heat flow rate cannot be determined. As described in subsection 6.2.1, such measuring equipment would be completely replaced. This over-instrumentation has hardly any influence on the total costs.
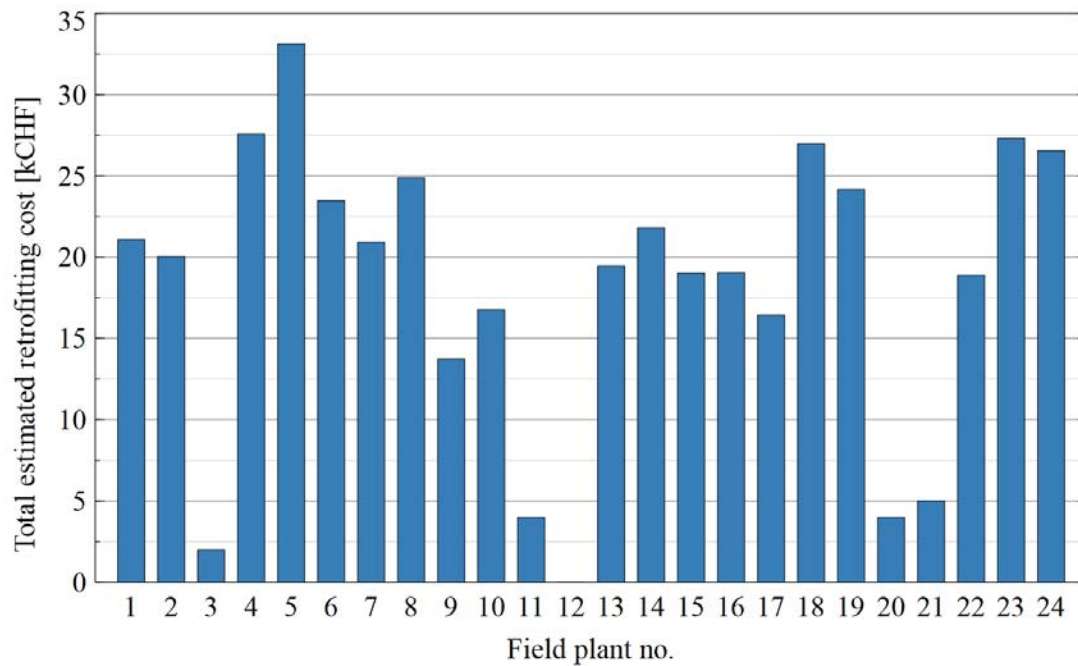
Figure 6.4 – Estimated total retrofitting costs for each refrigeration plant investigated (adapted from [12]).

Fig. 6.4 reveals the total estimated retrofitting cost (y-axis) for each investigated field plant (x-axis), where the average of all retrofitting costs is CHF 18'100. Refrigeration plant no. 12 and 5 are the best- and worst-case regarding the total expense. In the former no measuring equipment needs to be retrofitted (no additional costs). Meanwhile, the retrofitting costs of field plant no. 5 are CHF 33'101. This reveals that depending on the instrumentation status and the type of missing measuring equipment, contrasting expenses can arise. If systems built in 2016 or newer are considered, the average retrofitting costs are approximately CHF 14'300. In contrast, especially older plants have a limited instrumentation. As already mentioned, refrigeration plants are best instrumented in the energy contracting sector, whereby the average retrofitting costs for these plants are about CHF 9'500. For plants equipped with an acceptable measuring concept for conventional efficiency monitoring, e.g. the electrical power consumption of the compressors and the heat flow rates are measured, the average retrofitting costs are approximately CHF 7'700. Presumably, new refrigeration plants will be significantly better instrumented in the future, also in connection with the topic industry 4.0 and rising interest in online monitoring. It can also be noted that each plant engineer has different priorities regarding the measuring concept. If a standard instrumentation would be specified and defined, the retrofitting costs could be further reduced.

It can be concluded that the retrofitting costs are rather elevated for the application of the proposed exergy-based evaluation method in older field plants, where an enhancement of the in-

strumentation must be examined in detail and is probably only worthwhile in individual cases. However, if field plants with a measuring concept close to the state of the art are considered, the average retrofitting costs are low. If a large part of the measurement equipment is already available and, for example, only the data monitoring and storage is missing, a retrofit can be worthwhile to assess the field plant with the proposed exergy-based evaluation method.

7 Conclusions

The present work introduces a novel key figure, the optimization potential index (OPI), which is based on technical standards and exergy analysis. It enables the determination of the performance and corresponding improvement potential of vapor compression refrigeration plants with cold water distribution. Splitting the analysis into refrigerating machine and free cooling operation allows a target-oriented evaluation of the entire system. By dividing the plant into different subsystems, each one can be assessed individually and the location of eventual problems are identified on subsystem level. To the best of our knowledge, the proposed exergy-based method enables an absolute comparison of different refrigeration plants with defined reference values according to the state of the art in technology. Modeling is seen as an appropriate method to determine additional reference values for refrigeration machines if none are available according to technical standards. Among different modeling techniques, ANN models reveal the best performance for the present application. Presumably, this approach is also applicable to other existing systems if sufficient measurement data is available to fit the model parameters. Ultimately, the functionality and purpose of the assessment method has been successfully demonstrated by applying it on two numerical test cases and on a real field installation as a case study.

Furthermore, with the presented method, the optimization potential is revealed at a glance regardless the complexity of the system. The identification of possible enhancements is highly relevant in practice, as measures which improve the system effectiveness most likely prevent frequent shortcomings during refrigeration plant operation. Laypersons can easily determine the system operating state and subsequently, if needed, initiate a detailed analysis as well as appropriate countermeasures by specialist. To the best of our knowledge, a combined analysis with the proposed method (revealing possible optimization potentials in a first step) together with conventional energy and exergy analysis (identifying the malfunction in detail in a second step and evaluate if adjustments are worthwhile also from an economic point of view) delivers a target-oriented procedure to analyze the refrigeration plant behavior and to optimize the system effectiveness. The presented method finds possibly also application in other building energy systems, such as heat pumps, assuming sufficient and suitable reference values are available.

Possible drawbacks of the proposed method are on the one hand, that additional measured quantities are required in comparison to a conventional performance analysis. During the development of the method, however, care was taken to obtain the most relevant information about the refrigeration plant operation with the smallest possible amount of measuring equipment (also with considerations regarding state-of-the-art measuring concepts). On the other hand, the in-

troduced reference-based optimization potential index may seem inconsistent with conventional performance key figures definitions. The OPI compares a defined reference with the actual input while the output is assumed to be the same in both situations. Therefore, it cannot be mathematically combined to an overall system OPI. The OPI may also indicate that a subsystem performs unfavorably, while the neighboring subsystems still fulfill the technical requirements. However, the individual evaluation of subsystems is exactly the goal of the method, where each of them is assessed with the corresponding appropriate technical baseline. The absolute values of the OPI are less important, but rather if the adequate and acceptable limits are exceeded (technical requirements fulfilled or not). Thus, in all conscience and according to the obtained results, the proposed optimization potential index definitions are justifiable and it is possible to accept the mentioned drawbacks.

The present analysis of the field plant in refrigeration machine operation leads to the conclusion that the system including the hydraulic circuits is well designed and properly operated in general, especially in the warmer months over the year. The subsystem dry cooler performs most of the time in adequate or acceptable operation, except in October, where an optimization potential is present. The subsystem should therefore be monitored closely in the future, to determine whether this represents an outlier or if corrective measures have to be evaluated (e.g. optimize the cooler fans power consumption). Furthermore, all refrigeration machines investigated perform according to the technical standards during the warmer periods over the year. However, a noticeable increase in OPI is observed in the transition period, where generally an inadequate operation is present. Most likely, the refrigeration machines are not operating at the design point due to the reduced cooling demand, which can be also an indicator to make use of free cooling. The subsystem cold water storage & transport performs according to the technical standards, where in 97% of the time the technical requirements are fulfilled. Moreover, four out of seven cooling locations exhibit no to little optimization potential, while the remaining are not performing accordingly, especially in the transition period. The reason for the latter can finally not be determined, and consequently, the devices or control system settings of cooling location 1, 2, and 4 should be inspected for any defects or unfavorable control settings, respectively. If necessary, corrective measures can then be initialized (e.g. optimize the cold water distribution temperature level). In free cooling operation of the field plant, similar trends are observed, where both hydraulic circuits perform better as in refrigeration machine operation. Most likely, the reason is the reduced cooling demand in the colder months over the year, which results among others in a significantly reduced electrical power consumption of the auxiliary devices. The free cooling module reveals an acceptable operation and the performance is almost in steady-state over the

whole investigated time period. Consequently, no further actions are required. Overall, the electrical exergy input reveals typically the same magnitude as the thermal exergy and has therefore a significant effect on the field plant performance. From an energetic viewpoint, the electrical energy consumption is only a fraction of the thermal energy. This shows the importance of optimizing the operation of auxiliary equipment, e.g. with the application of variable speed drives, to ensure a most efficient plant operation and to reduce electricity costs.

In the present work technical data of 28 real field plants are acquired, from which 24 can be examined and analyzed with regard to their instrumentation. With this technical data and in some cases on site visits as well as further inputs from different actors in the industry, it is revealed that the majority of the field plants are moderately instrumented. Many measuring systems are designed in a way that a basic monitoring is possible and the operational safety is guaranteed. Consequently, the determination of possible optimization potentials is challenging. Through the contact with various companies, it was recognized that a wide range of knowledge in the respective fields is available. Furthermore, it can be stated that most actors in the industry show great interest in a retrofitting cost estimate for a target-oriented efficiency evaluation.

After assessing the measuring concepts of the field plants, the retrofitting costs to ensure the application of the proposed exergy-based evaluation method are determined. This represents a challenging task, as many factors, e.g. the accessibility of the measuring location, make the cost estimate for each plant unique to a certain extent. Nonetheless, a generalized estimate of the retrofitting costs was elaborated. From clarifications with measuring equipment manufacturers, it is determined that the retrofitting costs of electric meters, temperature sensors as well as data logging systems can be estimated on a lump sum basis independent of the size of the plant. Only the expense for heat meters is determined on the basis of a cost function with respect to the system cooling capacity. To the best of our knowledge, the elaborated individual expenses of the sensors allows to determine an upgrade cost estimate of any other refrigeration plant in the future. All cost estimates of components were validated in consultation with measuring equipment manufacturers. The average retrofitting expense is approximately CHF 18'100, which is rather elevated. Especially plants with several refrigeration machines and missing heat meters reveal elevated upgrade costs, as the latter have a strong financial impact. However, if field plants with a measuring concept close to the state of the art are considered, the average retrofitting costs are significantly reduced. A complete reinstrumentation should therefore be examined in detail for such field plants in order to allow the application of the proposed method.

8 Outlook and further need of research

Further investigations are needed regarding the determination of the cooling location exergy B_{CL}. As no measurements were available for the present study, an alternative approach was used for the subsystem CL in free cooling operation to determine the optimization potential index. To allow a consistent definition of the latter, the measurement of the temperature and the corresponding air humidity of the cooling location (e.g. air-handling unit, cooling coils, etc.) should be taken into consideration, which includes the determination of the exergy of humid air. The latter incorporates an additional exergy fraction, which would have to be included as an input in the analysis. In the same context, as with the current development stage all coolers are handled as dry coolers, the air humidity and cooling water consumption of e.g. hybrid coolers should be taken into account in order to increase the accuracy of the proposed method in such plants. Moreover, measurement data of field plants with heat utilization should be collected in order to develop the corresponding key figures for such subsystems. Likewise, a hydraulic analysis could be integrated to the proposed method in order to evaluate the specific flow exergies and to consider occuring pressure losses in detail. Both investigations, however, would require an increased number of measuring locations and increase the retrofitting costs. Regarding the latter, it was recognized that the instrumentation of each individual refrigeration machine quickly generates elevated expenses due to the increased heat meter costs. As an approach to reduce the retrofitting expense, it could be evaluated to measure the cooling capacity combined at a manifold line and to evaluate all refrigeration machines together (e.g. when the same type and size for redundancy reasons are installed). This would be accompanied by a reduction in the level of detail of the analysis, which however, may be acceptable in certain cases. For all mentioned investigations a well-founded data basis is essential, also to recognize interrelationships between various refrigeration systems and to use them for further evaluations. In the same context, the significance of the method could be further increased by determining the reference values with statistically sound, representative measurements and with the help of experts.

To handle the research gaps mentioned above, it is suggested to contact the companies with the most promising refrigeration plants in a next step. Preferably, the systems with additional subsystems and low retrofitting efforts should be considered. The readiness for a retrofit and its costs should be clarified individually, where the investigations revealed that it could be achieved with an acceptable financial expenditure (approximately CHF 15'000 for retrofitting plus evaluation). These field plants would also cover a large refrigeration capacity range (25, 250, 867, 1320 and 5252 kW), which is desirable for upcoming investigations. It is also possible that in

some cases there is a great willingness to invest, and thus, also plants with suboptimal instrumentation may be retrofitted. In addition, other financing possibilities should be examined so that the investment costs are not borne solely by the companies. After a successful retrofitting of the instrumentation, the field plants should be measured and surveyed over a longer time period, ideally at least two years, in order to provide a sound data basis for the further development of the evaluation method. Parallel to this, the implementation and application of the method in new refrigeration systems should be promoted.

References

[1] International Energy Agency, Key World Energy Statistics 2020, `https://www.iea.org/reports/key-world-energy-statistics-2020`, (accessed on 28.09.2020) (2020).

[2] V. Vakiloroaya, B. Samali, A. Fakhar, K. Pishghadam, A review of different strategies for HVAC energy saving, Energy Conversion and Management 77 (2014) 738–754. `doi:10.1016/J.ENCONMAN.2013.10.023`.

[3] K. Shan, S. Wang, D. C. Gao, F. Xiao, Development and validation of an effective and robust chiller sequence control strategy using data-driven models, Automation in Construction 65 (2016) 78–85. `doi:10.1016/j.autcon.2016.01.005`.

[4] M. Santamouris, Cooling the buildings – past, present and future, Energy and Buildings 128 (2016) 617–638. `doi:10.1016/j.enbuild.2016.07.034`.

[5] Swiss Federal Office of Energy (SFOE), Energy Strategy 2050: Chronology, `https://www.bfe.admin.ch/bfe/en/home/policy/energy-strategy-2050/_jcr_content/par/tabs/items/tab/tabpar/externalcontent.external.exturl.pdf/aHR0cHM6Ly9wdWJkYi5iZmUuYWRtaW4uY2gvZW4vcHVibGljYGljYX/Rpb24vZG93bmxvYWQvODI5My5wZGY=.pdf`, (accessed on 28.09.2020) (2018).

[6] Swiss Federal Office of Energy (SFOE), Energy Strategy 2050 once the new energy act is in force, `https://www.bfe.admin.ch/bfe/en/home/politik/energiestrategie-2050.exturl.html/aHR0cHM6Ly9wdWJkYi5iZmUuYWRtaW4uY2gvZW4vcHVibGljYGljYX/Rpb24vZG93bmxvYWQvODk5Mw==.html`, (accessed on 28.09.2020) (2018).

[7] Swiss Federal Council, Energy Act (EnA), `https://www.admin.ch/gov/en/start/documentation/votes/Popular%20vote%20on%2021%20Mai%202017/Energy-Act.html`, (accessed on 28.09.2020) (2017).

[8] T. Lang, C. Werner, M. Stettler, V. Prochaska, R. Dumortier, Auslegeordnung und Vorgehensvorschlag Energieeffizienz in der Klimakälte, Tech. rep., EnergieSchweiz (2015).

[9] M. Krütli, C. Hablützel, F. Tillenkamp, Systeme für die Beurteilung der Energieeffizienz

von Klimakälteanlagen, IEFE Energy Papers 2 (2016). `doi:10.21256/ZHAW-1183`.

[10] L. Brenner, F. Tillenkamp, M. Krütli, C. Ghiaus, Optimization potential index (OPI): An evaluation method for performance assessment and optimization potential of chillers in HVAC plants, Applied Energy 259 (2020). `doi:10.1016/j.apenergy.2019.114111`.

[11] L. Brenner, F. Tillenkamp, C. Ghiaus, Exergy performance and optimization potential of refrigeration plants in free cooling operation, Energy 209 (2020) 118464. `doi:10.1016/j.energy.2020.118464`.

[12] L. Brenner, S. Steiger, B. Shehu, M. Schneider, F. Tillenkamp, Exerate Proof of Concept: Exergie-Ansatz zur Beurteilung der Energieeffizienz von Klimakälteanlagen, Tech. rep., Swiss Federal Office of Energy (SFOE), Bern (Jan 2020). `doi:10.21256/ZHAW-20206`.

[13] Siemens, Kältetechnik, Tech. rep., Siemens, Frankfurt am Main (2017).

[14] İ. Dinçer, M. Kanoğlu, Refrigeration Systems and Applications, Wiley, Chichester, 2010. `doi:10.1002/9780470661093`.

[15] S. Wang, Handbook of Air Conditioning and Refrigeration, McGraw-Hill Education, New York, 2000.

[16] M. J. Moran, H. N. Shapiro, D. D. Boettner, M. B. Bailey, Fundamentals of engineering thermodynamics: SI version, Wiley, New York, 2010.

[17] A. Brunner, M. Kriegers, V. Prochaska, F. Tillenkamp, Klimakälte heute - Kluge Lösungen für ein angenehmes Raumklima, Faktor Verlag, Zürich, 2019.

[18] İ. Dinçer, M. A. Rosen, Exergy: Energy, Environment and Sustainable Development, Elsevier, Amsterdam, 2013.

[19] Y. A. Çengel, M. A. Boles, Thermodynamics: an engineering approach, McGraw-Hill, Boston, 2005.

[20] J. M. Gordon, K. C. Ng, Cool Thermodynamics, Cambridge International Science Publishing, Cambridge, 2001.

[21] P. Byrne, R. Ghoubali, Exergy analysis of heat pumps for simultaneous heating and cooling, Applied Thermal Engineering 149 (2019) 414–424. `doi:10.1016/j.applthermaleng.2018.12.069`.

[22] Swiss Society of Engineers and Architects (SIA), Lüftungs- und Klimaanlagen - Allgemeine Grundlagen und Anforderungen (SIA 382/1), 2014.

[23] Mechanical Engineering Industry Association (VDMA), Energieeffizienz von Kälteanlagen. Teil 2: Anforderungen an das Anlagenkonzept und die Komponenten (VDMA 24247-2), 2011.

[24] Mechanical Engineering Industry Association (VDMA), Energieeffizienz von Kälteanlagen. Teil 7: Regelung, Energiemanagement und effiziente Betriebsführung (VDMA 24247-7), 2011.

[25] H. Park, J. S. Lee, W. Kim, Y. Kim, The cooling seasonal performance factor of a hybrid ground-source heat pump with parallel and serial configurations, Applied Energy 102 (2013) 877–884. `doi:10.1016/j.apenergy.2012.09.035`.

[26] S. Kim, Y. Jeon, H. J. Chung, Y. Kim, Performance optimization of an R410A air-conditioner with a dual evaporator ejector cycle based on cooling seasonal performance factor, Applied Thermal Engineering 131 (2018) 988–997. `doi:10.1016/j.applthermaleng.2017.12.012`.

[27] M. Becker, T. Köberle, D. Pfeiffer, D. Rettich, EMeBKa : Entwicklung und exemplarische Anwendung von Methoden zur energetischen Bewertung von Kälteanlagen im laufenden Betrieb, Tech. rep., Hochschule Biberach, Institut für Gebäude- und Energiesysteme, Biberach (2016). `doi:10.2314/GBV:87199531X`.

[28] M. Sorrentino, G. Rizzo, A. Trifiro, F. Bedogni, A Model-Based Key Performance Index for Energy Assessment and Monitoring of Telecommunication Cooling Systems, IEEE Transactions on Sustainable Energy 5 (4) (2014) 1126–1136. `doi:10.1109/TSTE.2014.2334365`.

[29] M. Sorrentino, G. Rizzo, F. Genova, M. Gaspardone, A model for simulation and optimal energy management of Telecom switching plants, Applied Energy 87 (1) (2010) 259–267. `doi:10.1016/j.apenergy.2009.06.019`.

[30] J. Gordon, K. Ng, H. Chua, C. Lim, How varying condenser coolant flow rate affects chiller performance: thermodynamic modeling and experimental confirmation, Applied Thermal Engineering 20 (13) (2000) 1149–1159. `doi:10.1016/S1359-4311(99)00082-4`.

[31] L. Zhao, W. Cai, X. Ding, W. Chang, Model-based optimization for vapor compression refrigeration cycle, Energy 55 (2013) 392–402. `doi:10.1016/J.ENERGY.2013.02.071`.

[32] H. Fritschi, F. Tillenkamp, R. Löhrer, M. Brügger, Efficiency increase in carbon dioxide refrigeration technology with parallel compression, International Journal of Low-Carbon Technologies (feb 2016). `doi:10.1093/ijlct/ctw002`.

[33] C. Park, H. Lee, Y. Hwang, R. Radermacher, Recent advances in vapor compression cycle technologies, International Journal of Refrigeration 60 (2015) 118–134. `doi:10.1016/J.IJREFRIG.2015.08.005`.

[34] G. Lorentzen, Revival of carbon dioxide as a refrigerant, International Journal of Refrigeration 17 (5) (1994) 292–301. `doi:10.1016/0140-7007(94)90059-0`.

[35] J. Nickl, G. Will, H. Quack, W. Kraus, Integration of a three-stage expander into a CO2 refrigeration system, International Journal of Refrigeration 28 (8) (2005) 1219–1224. `doi:10.1016/J.IJREFRIG.2005.08.012`.

[36] B. Zhang, L. Chen, L. Liu, X. Zhang, M. Wang, C. Ji, K.-I. Song, Parameter sensitivity study for typical expander-based transcritical CO_2 refrigeration cycles, Energies 11 (5) (2018) 1279. `doi:10.3390/en11051279`.

[37] J. Baek, E. Groll, P. Lawless, Piston-cylinder work producing expansion device in a transcritical carbon dioxide cycle. Part I: experimental investigation, International Journal of Refrigeration 28 (2) (2005) 141–151. `doi:10.1016/J.IJREFRIG.2004.08.006`.

[38] V. Gonçalves, J. A. R. Parise, A study on the reduction of throttling losses in automotive air conditioning systems through expansion work recovery, in: International Refrigeration and Air Conditioning Conference, 2008, p. 2416.

[39] A. Subiantoro, K. T. Ooi, Economic analysis of the application of expanders in medium

scale air-conditioners with conventional refrigerants, R1234yf and CO2, International Journal of Refrigeration 36 (5) (2013) 1472–1482. `doi:10.1016/J.IJREFRIG.2013.03.010`.

[40] H. K. Ersoy, N. Bilir Sag, Preliminary experimental results on the R134a refrigeration system using a two-phase ejector as an expander, International Journal of Refrigeration 43 (2014) 97–110. `doi:10.1016/J.IJREFRIG.2014.04.006`.

[41] G. Pottker, P. Hrnjak, Effect of the condenser subcooling on the performance of vapor compression systems, International Journal of Refrigeration 50 (2015) 156–164. `doi:10.1016/J.IJREFRIG.2014.11.003`.

[42] G. Pottker, P. Hrnjak, Experimental investigation of the effect of condenser subcooling in R134a and R1234yf air-conditioning systems with and without internal heat exchanger, International Journal of Refrigeration 50 (2015) 104–113. `doi:10.1016/J.IJREFRIG.2014.10.023`.

[43] J. Navarro-Esbrí, F. Molés, Á. Barragán-Cervera, Experimental analysis of the internal heat exchanger influence on a vapour compression system performance working with R1234yf as a drop-in replacement for R134a, Applied Thermal Engineering 59 (1-2) (2013) 153–161. `doi:10.1016/J.APPLTHERMALENG.2013.05.028`.

[44] X. Wei, G. Xu, A. Kusiak, Modeling and optimization of a chiller plant, Energy 73 (2014) 898–907. `doi:10.1016/J.ENERGY.2014.06.102`.

[45] S. R. Thangavelu, A. Myat, A. Khambadkone, Energy optimization methodology of multi-chiller plant in commercial buildings, Energy 123 (2017) 64–76. `doi:10.1016/j.energy.2017.01.116`.

[46] E. Al-Bassam, R. Alasseri, Measurable energy savings of installing variable frequency drives for cooling towers' fans, compared to dual speed motors, Energy and Buildings 67 (2013) 261–266. `doi:10.1016/j.enbuild.2013.07.081`.

[47] B. Mu, Y. Li, J. E. Seem, B. Hu, A Multivariable Newton-Based Extremum Seeking Control for Condenser Water Loop Optimization of Chilled-Water Plant, Journal of Dynamic Systems, Measurement and Control, Transactions of the ASME 137 (11) (nov 2015). `doi:10.1115/1.4031051`.

[48] Y. Yang, B. Wang, Q. Zhou, Air Conditioning System Design using Free Cooling Technology and Running Mode of a Data Center in Jinan, Procedia Engineering 205 (2017) 3545–3549. `doi:10.1016/J.PROENG.2017.09.924`.

[49] K. Dong, P. Li, Z. Huang, L. Su, Q. Sun, Research on free cooling of data centers by using indirect cooling of open cooling tower, Procedia Engineering 205 (2017) 2831–2838. `doi:10.1016/J.PROENG.2017.09.902`.

[50] M. Schweiker, M. Shukuya, Comparative effects of building envelope improvements and occupant behavioural changes on the exergy consumption for heating and cooling, Energy Policy 38 (6) (2010) 2976–2986. `doi:10.1016/J.ENPOL.2010.01.035`.

[51] V. Bonetti, G. Kokogiannakis, Dynamic Exergy Analysis for the Thermal Storage Optimization of the Building Envelope, Energies 10 (1) (2017) 95. `doi:10.3390/en10010095`.

[52] R. Sangi, D. Müller, Exergy-based approaches for performance evaluation of building energy systems, Sustainable Cities and Society 25 (2016) 25–32. `doi:10.1016/J.SCS.2016.04.002`.

[53] E. Saloux, A. Teyssedou, M. Sorin, Development of an exergy-electrical analogy for visualizing and modeling building integrated energy systems, Energy Conversion and Management 89 (2015) 907–918. `doi:10.1016/J.ENCONMAN.2014.10.056`.

[54] S. Dubey, S. Solanki, A. Tiwari, Energy and exergy analysis of PV/T air collectors connected in series, Energy and Buildings 41 (8) (2009) 863–870. `doi:10.1016/J.ENBUILD.2009.03.010`.

[55] R. Mishra, G. Tiwari, Energy and exergy analysis of hybrid photovoltaic thermal water collector for constant collection temperature mode, Solar Energy 90 (2013) 58–67. `doi:10.1016/J.SOLENER.2012.12.022`.

[56] A. Fudholi, M. Zohri, G. L. Jin, A. Ibrahim, C. H. Yen, M. Y. Othman, M. H. Ruslan, K. Sopian, Energy and exergy analyses of photovoltaic thermal collector with ∇-groove, Solar Energy 159 (2018) 742–750. `doi:10.1016/J.SOLENER.2017.11.056`.

[57] S. Agrawal, G. Tiwari, Energy and exergy analysis of hybrid micro-channel photovoltaic thermal module, Solar Energy 85 (2) (2011) 356–370. `doi:10.1016/J.SOLENER.`

2010.11.013.

[58] M. Razmara, M. Maasoumy, M. Shahbakhti, R. Robinett, Optimal exergy control of building HVAC system, Applied Energy 156 (2015) 555–565. `doi:10.1016/J.APENERGY.2015.07.051`.

[59] B. Fan, X. Jin, X. Fang, Z. Du, The method of evaluating operation performance of HVAC system based on exergy analysis, Energy and Buildings 77 (2014) 332–342. `doi:10.1016/j.enbuild.2014.03.059`.

[60] Z. Du, X. Jin, B. Fan, Evaluation of operation and control in HVAC (heating, ventilation and air conditioning) system using exergy analysis method, Energy 89 (2015) 372–381. `doi:10.1016/J.ENERGY.2015.05.119`.

[61] X. Fang, X. Jin, Z. Du, Y. Wang, The evaluation of operation performance of HVAC system based on the ideal operation level of system, Energy and Buildings 110 (2016) 330–344. `doi:10.1016/J.ENBUILD.2015.11.020`.

[62] Y. Bi, X. Wang, Y. Liu, H. Zhang, L. Chen, Comprehensive exergy analysis of a ground-source heat pump system for both building heating and cooling modes, Applied Energy 86 (12) (2009) 2560–2565. `doi:10.1016/J.APENERGY.2009.04.005`.

[63] E. Saloux, M. Sorin, A. Teyssedou, Assessing the exergy performance of heat pump systems without using refrigerant thermodynamic properties, International Journal of Refrigeration 93 (2018) 1–9. `doi:10.1016/J.IJREFRIG.2018.06.005`.

[64] P. Hu, Q. Hu, Y. Lin, W. Yang, L. Xing, Energy and exergy analysis of a ground source heat pump system for a public building in Wuhan, China under different control strategies, Energy and Buildings 152 (2017) 301–312. `doi:10.1016/j.enbuild.2017.07.058`.

[65] D. Wu, B. Hu, R. Wang, Performance simulation and exergy analysis of a hybrid source heat pump system with low GWP refrigerants, Renewable Energy 116 (2018) 775–785. `doi:10.1016/J.RENENE.2017.10.024`.

[66] K. Menberg, Y. Heo, W. Choi, R. Ooka, R. Choudhary, M. Shukuya, Exergy analysis of a hybrid ground-source heat pump system, Applied Energy 204 (2017) 31–46. `doi:10.1016/J.APENERGY.2017.06.076`.

[67] X. Xu, D. Clodic, Exergy Analysis on a Vapor Compression Refrigerating System Using R12, R134a and R290 as Refrigerants, in: International Refrigeration and Air Conditioning Conference, 1992, pp. 231–240.

[68] J. Ahamed, R. Saidur, H. Masjuki, A review on exergy analysis of vapor compression refrigeration system, Renewable and Sustainable Energy Reviews 15 (3) (2011) 1593–1600. doi:10.1016/J.RSER.2010.11.039.

[69] P. Gullo, B. Elmegaard, G. Cortella, Advanced exergy analysis of a R744 booster refrigeration system with parallel compression, Energy 107 (2016) 562–571. doi:10.1016/J.ENERGY.2016.04.043.

[70] R. Roy, B. K. Mandal, Thermodynamic Analysis of Modified Vapour Compression Refrigeration System Using R-134a, Energy Procedia 109 (2017) 227–234. doi:10.1016/J.EGYPRO.2017.03.050.

[71] N. Bilir Sag, H. Ersoy, A. Hepbasli, H. Halkaci, Energetic and exergetic comparison of basic and ejector expander refrigeration systems operating under the same external conditions and cooling capacities, Energy Conversion and Management 90 (2015) 184–194. doi:10.1016/J.ENCONMAN.2014.11.023.

[72] L. Geng, H. Liu, X. Wei, Z. Hou, Z. Wang, Energy and exergy analyses of a bi-evaporator compression/ejection refrigeration cycle, Energy Conversion and Management 130 (2016) 71–80. doi:10.1016/j.enconman.2016.10.016.

[73] M.-H. Yang, R.-H. Yeh, Performance and exergy destruction analyses of optimal subcooling for vapor-compression refrigeration systems, International Journal of Heat and Mass Transfer 87 (2015) 1–10. doi:10.1016/J.IJHEATMASSTRANSFER.2015.03.085.

[74] J. Zhang, Q. Xu, Cascade refrigeration system synthesis based on exergy analysis, Computers & Chemical Engineering 35 (9) (2011) 1901–1914. doi:10.1016/J.COMPCHEMENG.2011.02.015.

[75] J. Harrell, J. Mathias, Improving Efficiency in a Campus Chilled Water System Using Exergy Analysis, ASHRAE Transactions 115 (1) (2009) 507–522.

[76] S. C. Hui, H. Y. Wong, Exergy analysis of cooling towers for optimization of HVAC

systems, in: Proceedings of the Hunan-Hong Kong Joint Symposium, Changsha, China, 2011, pp. 41–51.

[77] W. Fratzscher, V. M. Brodjanskij, K. Michalek, Exergie - Theorie und Anwendung, Deutscher Verlag für Grundstoffindustrie, Leipzig, 1986.

[78] A. Bejan, Advanced Engineering Thermodynamics, Wiley, 1997.

[79] N. Lior, N. Zhang, Energy, exergy, and Second Law performance criteria, Energy 32 (4) (2007) 281–296. `doi:10.1016/j.energy.2006.01.019`.

[80] G. Wall, Exergy tools, in: Proceedings of the Institution of Mechanical Engineers, Part A: Journal of Power and Energy, Vol. 217, SAGE PublicationsSage UK: London, England, 2003, pp. 125–136. `doi:10.1243/095765003606011399`.

[81] R. Sangi, D. Müller, Application of the second law of thermodynamics to control: A review, Energy 174 (2019) 938–953. `doi:10.1016/J.ENERGY.2019.03.024`.

[82] A. Bejan, G. G. Tsatsaronis, M. J. Moran, Thermal design and optimization, Wiley, New York, 1996.

[83] A. P. Simpson, A. E. Lutz, Exergy analysis of hydrogen production via steam methane reforming, International Journal of Hydrogen Energy 32 (18) (2007) 4811–4820. `doi: 10.1016/j.ijhydene.2007.08.025`.

[84] H. D. Baehr, S. Kabelac, Thermodynamik, Springer, Berlin, Heidelberg, 2012. `doi: 10.1007/978-3-642-24161-1`.

[85] M. Ozturk, Energy and exergy analysis of a combined ground source heat pump system, Applied Thermal Engineering 73 (1) (2014) 362–370. `doi:10.1016/J.APPLTHERMALENG.2014.08.016`.

[86] T. Morosuk, G. Tsatsaronis, Advanced exergetic evaluation of refrigeration machines using different working fluids, Energy 34 (12) (2009) 2248–2258. `doi:10.1016/J.ENERGY.2009.01.006`.

[87] T. Bai, J. Yu, G. Yan, Advanced exergy analyses of an ejector expansion transcritical CO2 refrigeration system, Energy Conversion and Management 126 (2016) 850–861. `doi:10.1016/J.ENCONMAN.2016.08.057`.

[88] Z. Erbay, A. Hepbasli, Application of conventional and advanced exergy analyses to evaluate the performance of a ground-source heat pump (GSHP) dryer used in food drying, Energy Conversion and Management 78 (2014) 499–507. `doi:10.1016/j.enconman.2013.11.009`.

[89] J. Chen, H. Havtun, B. Palm, Conventional and advanced exergy analysis of an ejector refrigeration system, Applied Energy 144 (2015) 139–151. `doi:10.1016/j.apenergy.2015.01.139`.

[90] T. Morosuk, G. Tsatsaronis, C. Zhang, Conventional thermodynamic and advanced exergetic analysis of a refrigeration machine using a Voorhees' compression process, Energy Conversion and Management 60 (2012) 143–151. `doi:10.1016/J.ENCONMAN.2012.02.021`.

[91] G. Tsatsaronis, Strengths and Limitations of Exergy Analysis, in: Thermodynamic Optimization of Complex Energy Systems, Springer Netherlands, 1999, pp. 93–100. `doi:10.1007/978-94-011-4685-2_6`.

[92] D. Schmidt, Low exergy systems for high-performance buildings and communities, Energy and Buildings 41 (3) (2009) 331–336. `doi:10.1016/J.ENBUILD.2008.10.005`.

[93] O. B. Kazanci, M. Shukuya, B. W. Olesen, Exergy performance of different space heating systems: A theoretical study, Building and Environment 99 (2016) 119–129. `doi:10.1016/J.BUILDENV.2016.01.025`.

[94] O. B. Kazanci, M. Shukuya, B. W. Olesen, Theoretical analysis of the performance of different cooling strategies with the concept of cool exergy, Building and Environment 100 (2016) 102–113. `doi:10.1016/J.BUILDENV.2016.02.013`.

[95] S. Eisenhauer, T. Hauck, M. Arnemann, Systematische Erstellung und Anwendung messtechnischer Konzepte zur energetischen Untersuchung von Kälteanlagen, in: DKV-Tagung, Dresden, 2015.

[96] S. Rohrer, C. Hablützel, F. Tillenkamp, M. Schneider, Einsparpotential bei der hydraulischen Einbindung von Kältemaschinen, Tech. rep., Zurich University of Applied Sciences ZHAW (2018).

[97] M. Ducoulombier, M. Sorin, A. Teyssedou, Thermodynamic bounds for food deep chilling tray tunnel operation, International Journal of Thermal Sciences 46 (2) (2007) 172–179. `doi:10.1016/J.IJTHERMALSCI.2006.05.001`.

[98] H. Torío, D. Schmidt, Annex 49 final report: Energy Conservation in Buildings and Community Systems (ECBCS) - Low exergy systems for high-performance buildings and communities, Tech. rep., Fraunhofer IBP, Stuttgart (2011).

[99] M. Shukuya, Exergy: theory and applications in the built environment, Springer, London, 2013. `doi:10.1007/978-1-4471-4573-8`.

[100] Choice of a reference state for exergetic analysis, Energy 15 (2) (1990) 113–121. `doi:10.1016/0360-5442(90)90048-7`.

[101] V. Bonetti, Dynamic exergy analysis for the built environment: fixed or variable reference?, in: Proceedings of the 9th Exergy, Energy and Environment Symposium, FESB, University of Split, Split, Croatia, 2017, pp. 924–939.

[102] B. Kílíc, Exergy analysis of vapor compression refrigeration cycle with two-stage and intercooler, Heat and Mass Transfer 48 (7) (2012) 1207–1217. `doi:10.1007/s00231-012-0971-4`.

[103] K. Zhang, Y. Zhu, J. Liu, X. Niu, X. Yuan, Exergy and energy analysis of a double evaporating temperature chiller, Energy and Buildings 165 (2018) 464–471. `doi:10.1016/j.enbuild.2017.12.055`.

[104] A. Yataganbaba, A. Kilicarslan, İ. Kurtbaş, Exergy analysis of R1234yf and R1234ze as R134a replacements in a two evaporator vapour compression refrigeration system, International Journal of Refrigeration 60 (2015) 26–37. `doi:10.1016/J.IJREFRIG.2015.08.010`.

[105] V. Martinaitis, J. Bielskus, K. Januševičius, P. Bareika, Exergy efficiency of a ventilation heat recovery exchanger at a variable reference temperature, Mechanics 23 (1) (2017) 70–77. `doi:10.5755/j01.mech.23.1.17678`.

[106] M. G. Alpuche, C. Heard, R. Best, J. Rojas, Exergy analysis of air cooling systems in buildings in hot humid climates, Applied Thermal Engineering 25 (4) (2005) 507–517. `doi:10.1016/J.APPLTHERMALENG.2004.07.006`.

[107] Y. Zhou, G. Gong, Exergy analysis of the building heating and cooling system from the power plant to the building envelop with hourly variable reference state, Energy and Buildings 56 (2013) 94–99. `doi:10.1016/J.ENBUILD.2012.09.041`.

[108] M. G. Baldi, L. Leoncini, Effect of Reference State Characteristics on the Thermal Exergy Analysis of a Building, Energy Procedia 83 (2015) 177–186. `doi:10.1016/J.EGYPRO.2015.12.208`.

[109] P. Gonçalves, A. R. Gaspar, M. G. da Silva, Comparative energy and exergy performance of heating options in buildings under different climatic conditions, Energy and Buildings 61 (2013) 288–297. `doi:10.1016/J.ENBUILD.2013.02.023`.

[110] K. Sartor, P. Dewallef, Exergy analysis applied to performance of buildings in Europe, Energy and Buildings 148 (2017) 348–354. `doi:10.1016/J.ENBUILD.2017.05.026`.

[111] A. Koca, H. F. Oztop, T. Koyun, Y. Varol, Energy and exergy analysis of a latent heat storage system with phase change material for a solar collector, Renewable Energy 33 (4) (2008) 567–574. `doi:10.1016/j.renene.2007.03.012`.

[112] M. Pons, On the Reference State for Exergy when Ambient Temperature Fluctuates, International Journal of Thermodynamics 12 (3) (2009) 113–121. `doi:10.5541/IJOT.1034000246`.

[113] M. Pons, Exergy Analysis and Process Optimization with Variable Environment Temperature, Energies 12 (24) (2019) 4655. `doi:10.3390/en12244655`.

[114] G. Evola, L. Marletta, Exergy and thermoeconomic optimization of a water-cooled glazed hybrid photovoltaic/thermal (PVT) collector, Solar Energy 107 (2014) 12–25. `doi:10.1016/j.solener.2014.05.041`.

[115] R. Sangi, D. Müller, Implementation of a solution to the problem of reference environment in the exergy evaluation of building energy systems, Energy 149 (2018) 830–836. `doi:10.1016/J.ENERGY.2018.02.098`.

[116] Z. Wei, R. Zmeureanu, Exergy analysis of variable air volume systems for an office building, Energy Conversion and Management 50 (2) (2009) 387–392. `doi:10.1016/j.enconman.2008.09.010`.

[117] Mechanical Engineering Industry Association (VDMA), Energieeffizienz von Klimakäl-teanlagen. Teil 8: Komponenten - Wärmeübertrager (VDMA 24247-8), 2011.

[118] H. Wang, Empirical model for evaluating power consumption of centrifugal chillers, Energy and Buildings 140 (2017) 359–370. doi:10.1016/J.ENBUILD.2017.02.019.

[119] B. P. Rasmussen, B. Shenoy, Dynamic modeling for vapor compression systems, Part II: Simulation tutorial, HVAC&R Research 18 (5) (2012) 956–973. doi:10.1080/10789669.2011.582917.

[120] A. Afram, F. Janabi-Sharifi, Review of modeling methods for HVAC systems, Applied Thermal Engineering 67 (1-2) (2014) 507–519. doi:10.1016/J.APPLTHERMALENG.2014.03.055.

[121] A. Afram, F. Janabi-Sharifi, Black-box modeling of residential HVAC system and comparison of gray-box and black-box modeling methods, Energy and Buildings 94 (2015) 121–149. doi:10.1016/J.ENBUILD.2015.02.045.

[122] B. P. Rasmussen, Dynamic modeling for vapor compression systems, Part I: Literature review, HVAC&R Research 18 (5) (2012) 934–955. doi:10.1080/10789669.2011.582916.

[123] T. A. Reddy, D. Niebur, K. K. Andersen, P. P. Pericolo, G. Cabrera, Evaluation of the suitability of different chiller performance models for on-line training applied to automated fault detection and diagnosis (RP-1139), HVAC and R Research 9 (4) (2003) 385–414. doi:10.1080/10789669.2003.10391077.

[124] F. W. H. Yik, V. K. C. Lam, Chiller models for plant design studies, Building Services Engineering Research and Technology 19 (4) (1998) 233–241. doi:10.1177/014362449801900407.

[125] W. Stoecker, J. Jones, Refrigeration and air conditioning, McGraw-Hill, New York, 1982.

[126] Y.-C. Chang, C.-Y. Chen, J.-T. Lu, J.-K. Lee, T.-S. Jan, C.-L. Chen, Verification of Chiller Performance Promotion and Energy Saving, Engineering 05 (01) (2013) 141–145. doi:10.4236/eng.2013.51a020.

[127] J. M. Gordon, K. C. Ng, H. T. Chua, Centrifugal chillers: Thermodynamic modelling and

a diagnostic case study, International Journal of Refrigeration 18 (4) (1995) 253–257. `doi:10.1016/0140-7007(95)96863-2`.

[128] K. C. Ng, H. T. Chua, W. Ong, S. S. Lee, J. M. Gordon, Diagnostics and optimization of reciprocating chillers: Theory and experiment, Applied Thermal Engineering 17 (3) (1997) 263–276. `doi:10.1016/s1359-4311(96)00031-2`.

[129] B. Foliaco, A. Bula, P. Coombes, Improving the Gordon-Ng Model and Analyzing Thermodynamic Parameters to Evaluate Performance in a Water-Cooled Centrifugal Chiller, Energies 13 (9) (2020) 2135. `doi:10.3390/en13092135`.

[130] T. S. Lee, W. C. Lu, An evaluation of empirically-based models for predicting energy performance of vapor-compression water chillers, Applied Energy 87 (11) (2010) 3486–3493. `doi:10.1016/j.apenergy.2010.05.005`.

[131] T. S. Lee, K. Y. Liao, W. C. Lu, Evaluation of the suitability of empirically-based models for predicting energy performance of centrifugal water chillers with variable chilled water flow, Applied Energy 93 (2012) 583–595. `doi:10.1016/j.apenergy.2011.12.001`.

[132] M. W. Browne, P. K. Bansal, Steady-state model of centrifugal liquid chillers, International Journal of Refrigeration 21 (5) (1998) 343–358. `doi:10.1016/S0140-7007(98)00003-6`.

[133] E. Rodriguez, B. Rasmussen, A comparison of modeling paradigms for dynamic evaporator simulations with variable fluid phases, Applied Thermal Engineering 112 (2017) 1326–1342. `doi:10.1016/J.APPLTHERMALENG.2016.10.131`.

[134] C. J. Hermes, C. Melo, A first-principles simulation model for the start-up and cycling transients of household refrigerators, International Journal of Refrigeration 31 (8) (2008) 1341–1357. `doi:10.1016/j.ijrefrig.2008.04.003`.

[135] B. Li, A. G. Alleyne, A dynamic model of a vapor compression cycle with shut-down and start-up operations, International Journal of Refrigeration 33 (3) (2010) 538–552. `doi:10.1016/J.IJREFRIG.2009.09.011`.

[136] Y. Yao, W. Wang, M. Huang, A state-space dynamic model for vapor compression refrigeration system based on moving-boundary formulation, International Journal of Refriger-

ation 60 (2015) 174–189. `doi:10.1016/J.IJREFRIG.2015.07.027.`

[137] H. Pangborn, A. G. Alleyne, N. Wu, A comparison between finite volume and switched moving boundary approaches for dynamic vapor compression system modeling, International Journal of Refrigeration 53 (2015) 101–114. `doi:10.1016/J.IJREFRIG.2015.01.009.`

[138] S. A. Kalogirou, Applications of artificial neural-networks for energy systems, Applied Energy 67 (1-2) (2000) 17–35. `doi:10.1016/S0306-2619(00)00005-2.`

[139] P. Jiang, Q. Zhou, X. Shao, Surrogate Model-Based Engineering Design and Optimization, Springer Tracts in Mechanical Engineering, Springer, Singapore, 2020. `doi:10.1007/978-981-15-0731-1.`

[140] A. S. Şahin, Performance analysis of single-stage refrigeration system with internal heat exchanger using neural network and neuro-fuzzy, Renewable Energy 36 (10) (2011) 2747–2752. `doi:10.1016/j.renene.2011.03.009.`

[141] Y. C. Chang, Sequencing of chillers by estimating chiller power consumption using artificial neural networks, Building and Environment 42 (1) (2007) 180–188. `doi:10.1016/j.buildenv.2005.08.033.`

[142] J.-H. Kim, N.-C. Seong, W. Choi, Modeling and Optimizing a Chiller System Using a Machine Learning Algorithm, Energies 12 (15) (2019) 2860. `doi:10.3390/en12152860.`

[143] The Mathworks Inc., Natick, Massachusetts, MATLAB version 9.4.0.813654 (R2018a) (2018).

[144] F. P. Incropera, D. P. Dewitt, T. L. Bergman, A. S. Lavine, Principles of heat and mass transfer, John Wiley & Sons, Hoboken, NJ, 2014.

[145] H. Jin, J. Spitler, A parameter estimation based model of water-to-water heat pumps for use in energy calculations programs, ASHRAE Transactions 108 (1) (2002) 3–17.

[146] G. Soave, Equilibrium constants from a modified Redlich-Kwong equation of state, Chemical Engineering Science 27 (6) (1972) 1197–1203. `doi:10.1016/0009-2509(72)80096-4.`

[147] I. Bell, M. L. Huber, M. O. McLinden, E. W. Lemmon, NIST Reference Fluid Thermodynamic and Transport Properties Database (REFPROP) Version 9 - SRD 23, National Institute of Standards and Technology (2013). `doi:10.18434/T4JS3C`.

[148] A. E. Ozgur, A. Kabul, O. Kizilkan, Exergy analysis of refrigeration systems using an alternative refrigerant (hfo-1234yf) to R-134a, International Journal of Low-Carbon Technologies 9 (1) (2014) 56–62. `doi:10.1093/ijlct/cts054`.

[149] S. Ruder, An overview of gradient descent optimization algorithms (Sep 2016). `arXiv:1609.04747`.

[150] M. T. Hagan, M. B. Menhaj, Training Feedforward Networks with the Marquardt Algorithm, IEEE Transactions on Neural Networks 5 (6) (1994) 989–993. `doi:10.1109/72.329697`.

[151] M. T. Hagan, H. B. Demuth, M. H. Beale, O. De Jesus, Neural Network Design, Oklahoma State University, Stillwater, OK, 2014.

[152] M. M. Hydeman, P. Sreedharan, N. Webb, S. Blanc, Development and Testing of a Reformulated Regression-Based Electric Chiller Model, ASHRAE Transactions 180 (2) (2002).

[153] A. Arora, B. Arora, B. Pathak, H. Sachdev, Exergy analysis of a Vapour Compression Refrigeration system with R-22, R-407C and R-410A, International Journal of Exergy 4 (4) (2007) 441. `doi:10.1504/IJEX.2007.015083`.

[154] F. Yu, K. Chan, Chiller system performance benchmark by data envelopment analysis, International Journal of Refrigeration 35 (7) (2012) 1815–1823. `doi:10.1016/J.IJREFRIG.2012.07.003`.

[155] M. Krütli, F. Tillenkamp, Statistik zum Bestand von Klimakälteanlagen, IEFE Energy Papers 6 (1) (2017). `doi:10.21256/zhaw-1357`.

[156] Federal Office for the Environment, Übersicht über die wichtigsten Kältemittel, Tech. rep., FOEN (2017).

[157] European Parliament, Regulation (EU) No 517/2014 of the European Parliament and of the Council of 16 April 2014 on fluorinated greenhouse gases and repealing Regulation (EC) No 842/2006, 2014.

[158] A. Mota-Babiloni, J. Navarro-Esbrí, Á. Barragán, F. Molés, B. Peris, Drop-in energy performance evaluation of R1234yf and R1234ze(E) in a vapor compression system as R134a replacements, Applied Thermal Engineering 71 (1) (2014) 259–265. `doi:10.1016/J.APPLTHERMALENG.2014.06.056`.

[159] R. Ben Jemaa, R. Mansouri, I. Boukholda, A. Bellagi, Energy and exergy investigation of R1234ze as R134a replacement in vapor compression chillers, International Journal of Hydrogen Energy 42 (17) (2017) 12877–12887. `doi:10.1016/J.IJHYDENE.2016.12.010`.

List of figures

List of tables

A Appendix

A.1 Refrigerants

Another essential component of the refrigeration machine is the working fluid, the refrigerant.

...heat transport within the cycle and is chosen depending on the appli-

st of existing refrigerants is long and Tab. A.1 shows the most impor-

Table A.1 – List of the most important refrigerants (not conclusive, state November 2017) [156].

Übersicht über die wichtigsten Kältemittel (Liste nicht abschliessend) Stand November 2017

Rechtlicher Status der Kältemittel gemäss Anhang 2.10 ChemRRV	Kategorie		Kältemittel	GWP[1]	Sicherheits-gruppe[2]	Bemerkungen
Ozonschicht-abbauende, verbotene Kältemittel	FCKW (chlorhaltig, perhalogeniert)		R11	4750	A1	Verbot für Neu ...
			R12	10900	A1	
			R502 (Gemisch)	4657	A1	
			R13B1	7140	A1	
	HFCKW (chlorhaltig, teilweise halogeniert)	Reinstoff Kältemittel	R22	1510	A1	
		Gemische (Blends) überwiegend R22 enthaltend	R401A (1639)	1152	A1	
			R402A (7650)	2755	A1	
			R402B (7651)	2416	A1	
			R405A (-840)	3152	A1	
			R409A (-856)	1555	A1	
In der Luft stabile Kältemittel, begrenzt anwendbar in neuen Anlagen und Geräten	FKW / HFKW (chlorfrei)	Reinstoff Kältemittel	R23	14500	A1	
			R32	675	A2[4]	
			R134	1430	A1	
			R125	3500	A1	
			R143	4470	A2[4]	
		Gemische (Blends)	R404A	3920	A1	
			R407C	1770	A1	
			R407F	1525	A1	
			R410A	2090	A1	
			R413A	2050	A2	
			R417A	2350	A1	
			R422A	3140	A1	
			R422D	2730	A1	
			R437A	1655	A1	
			R507A	3950	A1	
		Gemische mit HFO (Blends)	R445A	1356	A1	
			R449A	1397	A1	
			R450A	601	A1	
			R513A	631	A1	
Zulässige Kältemittel unter Vorbehalt der Einhaltung der Sicherheits-anforderungen	Natürliche Kältemittel	Reinstoff Kältemittel	R170 (Ethan)	6	A3	
			R290 (Propan)	3	A3	
			R717 (NH₃)	0	B2[4]	
			R718 (H₂O)	0	A1	
			R744 (CO₂)	1	A1	
			R600 (Isobutan)	3	A3	
			R1270 (Propen)	2	A3	
		Gemische (Blends)	R290/R600	3	A3	
			R290/R170	3	A3	
			R723 (31 (NH₃)	5	A[3]	
	HFO (teilhalogenierte Fluor-Olefine)		R1234yf	4	A2[4]	
			R1234ze	7	A2[4]	

1 ... (GWP) über einen Zeithorizont von 100 Jahren ... Werte (ausser natürliche Kältemittel R717 ...) aus IPCC AV (2007) ... ...html ... Werte für Gemische/Blends ...

2 Sicherheitsgruppe gemäss SN EN 378-1:2017

3 R723 ist in der SN EN 378-1:2017 nicht erfasst siehe Angabe des Herstellers.

4 Neue Sicherheitsgruppe gemäss SN EN 378-1:2017

265/2006-01765/01/25/11/03/M474-1699

tant ones according to the Federal Office for the Environment (not conclusive, state November 2017) [156]. Some of the refrigerants, mostly chlorofluorocarbons (CFC's) and hydrochlorofluorocarbons (HCFC's), have superior thermodynamic and handling properties, but were forbidden for new refrigeration plants due to their high ozone depletion (ODP) and global warming potential (GWP). Nowadays, in air-conditioning refrigeration, the following refrigerants are typically used [17]:

- Hydrofluorocarbons (HFC's):
    - R134a,
    - R407C,
    - R410A,
    - R32.
- Natural refrigerants:
    - R717 (ammonia),
    - R290 (propane),
    - R744 (CO_2).
- Hydrofluoroolefins (HFO's):
    - R1234yf,
    - R1234ze.

Since the HFC's exhibit an increased GWP, the European Council introduced the regulation No. 517/2014 on flurinated greenhouse gases [157]. The goal is to gradually reduce the HFC's placed on the EU market down to one fifth (21%) of today's sales volumes by 2030 (phase-down process). Therefore, several studies were carried out regarding the performance of HFO's in refrigeration machines [104, 148, 158, 159]. All investigations revealed a similar or only a slightly lower thermodynamic performance of the HFO's in comparison with R134a, and thus, the authors state that R1234yf and R1234ze are appropriate alternative refrigerants. However, HFO's are not stable in air and slightly flammable. As a consequence, appropriate safety measures are required when they are deployed.

A.2 Evaluation of exergy transfer by mass flow in terms of heat flow and temperatures

In the introduced evaluation system, the control volumes are chosen in a way, that the exergy transfer between subsystems occurs only by mass flow. The net exergy flow rate $\dot{B}$ over the system boundary is expressed by:

$$\dot{B} = \dot{m}_{in}b_{in} - \dot{m}_{out}b_{out} = \dot{m}(b_{in} - b_{out}) \tag{A.1}$$

where the incoming and outgoing mass flow rate is identical (mass balance). Assuming incompressible flow (liquid in the hydraulic circuits) and identical flow cross sections, and thus, same velocity at the in- and outlet, as well as no elevation change, the kinetic and potential exergy differences are negligible. Together with Eq. 3.5, Eq. A.1 can be rewritten as follows:

$$\dot{B} = \dot{m}[(h_{in} - h_0) - T_0(s_{in} - s_0)] - \dot{m}[(h_{out} - h_0) - T_0(s_{out} - s_0)]$$
$$= \dot{m}[(h_{in} - h_{out}) - T_0(s_{in} - s_{out})] \tag{A.2}$$

It is assumed that the the entropy change $\mathrm{d}s$ between the in- and outlet is dominated by heat exchange, where for an incompressible substance it is expressed with [16]:

$$\mathrm{d}s = \frac{\mathrm{d}u}{T} \tag{A.3}$$

The change in internal energy $\mathrm{d}u$ can be substituted with the product of specific heat capacity c and temperature change $\mathrm{d}T$ [16]. Assuming a constant specific heat capacity (e.g. small temperature differences), the integration between the in- and outlet state yields:

$$s_{in} - s_{out} = \int_{out}^{in} \frac{1}{T}\mathrm{d}u = \int_{out}^{in} \frac{c}{T}\mathrm{d}T = c\ln\left(\frac{T_{in}}{T_{out}}\right) \tag{A.4}$$

where T_{in} and T_{out} denote the in- and outlet temperature, respectively. The enthalpy difference between the in- and outlet can be described by [16]:

$$h_{in} - h_{out} = c(T_{in} - T_{out}) + \underline{v(p_{in} - p_{out})}^{\,\ll c(T_{in} - T_{out})} \tag{A.5}$$

where v is the specific volume, p_{in} the inlet and p_{out} the outlet pressure. The second term on the right-hand side is usually negligible small compared to the first term [16], and therefore,

neglected in the following. Applying Eq. A.4 and A.5 in Eq. A.2 yields:

$$\dot{B} = \dot{m} \left[c(T_{in} - T_{out}) - T_0 c \ln \left(\frac{T_{in}}{T_{out}} \right) \right] \qquad (A.6)$$

where the latter equation can be rewritten in the following form:

$$\dot{B} = \dot{m} c (T_{in} - T_{out}) \left[1 - T_0 \frac{\ln \left(\frac{T_{in}}{T_{out}} \right)}{T_{in} - T_{out}} \right] = \dot{Q} \left(1 - \frac{T_0}{\overline{T}} \right) \qquad (A.7)$$

Therefore, the exergy transfer by mass flow can be expressed in terms of the exergy transport by heat with the heat flow rate $\dot{Q}$ and the logarithmic mean temperature $\overline{T}$. The latter is defined as:

$$\overline{T} = \frac{T_{in} - T_{out}}{\ln \left(\frac{T_{in}}{T_{out}} \right)} \qquad (A.8)$$

Under the mentioned conditions, it is not necessary to evaluate the specific flow exergy of the in- and outlet. The transferred heat as well as the temperatures can be measured with commercially available heat meters, which are most likely installed in typical refrigeration plants, e.g. to monitor the cooling load.

A.3 Pseudo code of the exergy-based evaluation approach

Algorithm 1: Main file *n01_main_file.m*

Input: –

Output: Structures (i.e. arrays) with all the computed quantities (OPI, exergy, etc.)

Create structures with empty timetables;

```
%Read and store measurement data
```
Call function *f01_readData*;   `%see algorithm 3`

```
%Compute quantities (OPI, exergies, etc.)  in each subsystem
```
Call function *f10_OPI_CL_RM*;   `%see algorithm 5`
Call function *f11_OPI_CST_RM*;   `%see algorithm 6`
Call function *f12_OPI_RM*;   `%see algorithm 7`
Call function *f13_OPI_DC_RM*;   `%see algorithm 8`
Call function *f14_OPI_CL_FC*;   `%see algorithm 9`
Call function *f15_OPI_CST_FC*;   `%see algorithm 10`
Call function *f16_OPI_DC_FC*;   `%see algorithm 11`
Call function *f17_OPI_FC*;   `%see algorithm 12`

Algorithm 2: ANN model training *n10_train_ANN.m*

Input: Structure with all available measurements in SI units

Output: Trained artificial neural network (feed forward shallow network) model

```
%Set data to NaN when no cooling load and compressor power
 consumption is present (no running refrigeration machine).
```
for *Measurement 1 → size(Measurement)* **do**

    if $\dot{W}_{CPR}$ *or* $\dot{Q}_E$ *is zero* **then**

        Set compressor electrical power to NaN;

        Set evaporator heat flow rate to NaN;

        Set refrigeration machine secondary side temperatures to NaN;

    end

end

Remove NaN values from data set;

```
%Set up and train ANN model according to subsection 3.2.2.4.
```
Define ANN structure;

Set ANN parameters;

Train ANN;

```
%Test model
```
Compute compressor electrical power $\dot{W}_{CPR,ANN} = f(\dot{Q}_E, T_{C,in}, T_{C,out}, T_{E,in}, T_{E,out})$;

Compute model performance indicators;   `%Eq. 3.78 to 3.81`

Algorithm 3: Function *f01_readData.m*

Input: Raw measurement data

Output: Structure with all available measurements in SI units

Define and store measurement interval;

`%Compute and store measurements in SI units according to Tab. 3.1 and 3.3`

Compute and store electrical power of compressors and auxiliary devices;

Compute and store heat flow rates of condenser, evaporator, free cooling and cold water
   distribution;

Compute and store temperatures;

Algorithm 4: Function *f02_log_temp.m*

Input: Inlet and outlet temperatures

Output: Logarithmic mean temperatures

Calculate logarithmic mean temperature;   `%Eq. 3.7`

Algorithm 5: Function *f10_OPI_CL_RM.m*

Input: Structure with existing timetables (measurements, calculated exergies and key figures)

Output: Structure extended with new timetables (calculated exergies and key figures of
         subsystem CL in refrigeration machine operating mode)

`%Calculate cold water distribution exergies for every cooling location`

for *CL1 → CL7* **do**

    Compute cold water distribution logarithmic mean temperatures $\overline{T}_D$, $\overline{T}_D^*$ and $\overline{T}_D^{acc}$ by calling

    function *f02_log_temp* (see algorithm 4);   `%Eq. 3.26 and 3.28`

    Compute actual cold water distribution exergy B_D;   `%Eq. 3.25`

    Compute reference cold water distribution exergy B_D^*;   `%Eq. 3.27`

    Compute acceptable cold water distribution exergy B_D^{acc};

end

`%Calculate optimization potential index`

Compute OPI_{CL};   `%Eq. 3.24`

Compute OPI_{CL}^{acc};

Algorithm 6: Function *f11_OPI_CST_RM.m*

Input: Structure with existing timetables (measurements, calculated exergies and key figures)

Output: Structure extended with new timetables (calculated exergies and key figures of
        subsystem CST in refrigeration machine operating mode)

```
%Calculate actual evaporator exergies for every refrigeration
 machine
```
for *RM1 → RM5* **do**

    Compute evaporator logarithmic mean temperature $\overline{T}_E$ by calling function *f02_log_temp* (see
       algorithm 4);   `%Eq. 3.31`

    Compute actual evaporator exergy B_E;   `%Eq. 3.30`

end

```
%Calculate exergies of auxiliary devices
```
Compute actual circulating pump exergy $B_{el,CP,CST}$;   `%Eq. 3.32`

Compute reference circulating pump exergy $B^*_{el,CP,CST}$;   `%Eq. 3.34`

Compute acceptable circulating pump exergy $B^{acc}_{el,CP,CST}$;

```
%Calculate reference and acceptable evaporator exergies
```
Compute subsystem CST exergy losses $B_{L,CST}$;   `%Eq. 3.35`

Compute reference evaporator exergy B^*_E;   `%Eq. 3.33`

Compute acceptable evaporator exergy B^{acc}_E;

```
%Calculate optimization potential index
```
Compute OPI_{CST};   `%Eq. 3.29`

Compute OPI^{acc}_{CST};

Algorithm 7: Function *f12_OPI_RM.m*

Input: Structure with existing timetables (measurements, calculated exergies and key figures)

Output: Structure extended with new timetables (calculated exergies and key figures of
        subsystem RM)

Load trained ANN's;

```
%Calculate compressor electrical power for every refrigeration
 machine
```
for *RM1 → RM5* **do**

    Compute condenser logarithmic mean temperature $\overline{T}_C$ by calling function *f02_log_temp* (see
       algorithm 4);   `%Eq. 3.13`

    Compute reference condenser temperatures;   `%Eq. 3.17`

    Compute acceptable condenser temperatures;

    Compute reference compressor electrical power $\dot{W}^*_{CPR}$ with ANN;

    Compute acceptable compressor electrical power $\dot{W}^{acc}_{CPR}$ with ANN;

end

$\vdots$

⋮

```
%Calculate compressor electrical exergies for every refrigeration
 machine
```
for *RM1 → RM5* **do**

> Compute actual compressor electrical exergy B_{CPR};   %Eq. 3.22
>
> Compute reference compressor electrical exergy B_{CPR}^*;   %Eq. 3.23
>
> Compute acceptable compressor electrical exergy B_{CPR}^{acc};

end

```
%Calculate optimization potential index
```
Compute OPI_{RM};   %Eq. 3.21

Compute OPI_{RM}^{acc};

Algorithm 8: Function *f13_OPI_DC_RM.m*

Input: Structure with existing timetables (measurements, calculated exergies and key figures)

Output: Structure extended with new timetables (calculated exergies and key figures of subsystem DC in refrigeration machine operating mode)

```
%Calculate condenser exergies for every refrigeration machine
 (use computed condenser temperatures from algorithm 7)
```
for *RM1 → RM5* **do**

> Compute actual condenser exergy B_C;   %Eq. 3.12
>
> Compute reference condenser exergy B_C^*;   %Eq. 3.16
>
> Compute acceptable condenser exergy B_C^{acc};

end

```
%Calculate exergies of auxiliary devices
```
Compute actual circulating pump exergy $B_{el,CP,DC}$;   %Eq. 3.14

Compute reference circulating pump exergy $B_{el,CP,DC}^*$;   %Eq. 3.18

Compute acceptable circulating pump exergy $B_{el,CP,DC}^{acc}$;

Compute actual dry cooler fan exergy $B_{el,DC}$;   %Eq. 3.15

Compute reference dry cooler fan exergy $B_{el,DC}^*$;   %Eq. 3.19

Compute acceptable dry cooler fan exergy $B_{el,DC}^{acc}$;

```
%Calculate optimization potential index
```
Compute OPI_{DC};   %Eq. 3.11

Compute OPI_{DC}^{acc};

Algorithm 9: Function *f14_OPI_CL_FC.m*

Input: Structure with existing timetables (measurements, calculated exergies and key figures)

Output: Structure extended with new timetables (calculated exergies and key figures of

subsystem CL in free cooling operating mode)

```
%Calculate cold water distribution exergies for every cooling
 location (use computed cold water temperatures from algorithm 5)
```
for *CL1 → CL7* **do**

   Compute actual cold water distribution exergy B_D;   %Eq. 3.46

   Compute reference cold water distribution exergy B_D^*;   %Eq. 3.49

   Compute acceptable cold water distribution exergy B_D^{acc};

end

```
%Calculate optimization potential index
```
Compute OPI_{CL};   %Eq. 3.57

Compute OPI_{CL}^{acc};

Algorithm 10: Function *f15_OPI_CST_FC.m*

Input: Structure with existing timetables (measurements, calculated exergies and key figures)

Output: Structure extended with new timetables (calculated exergies and key figures of

subsystem CST in free cooling operating mode)

```
%Calculate exergies of auxiliary devices
```
Compute actual circulating pump exergy $B_{el,CP,CST}$;   %Eq. 3.48

Compute reference circulating pump exergy $B_{el,CP,CST}^*$;   %Eq. 3.51

Compute acceptable circulating pump exergy $B_{el,CP,CST}^{acc}$;

```
%Calculate actual free cooling exergy CST side for later use
```
Compute free cooling module logarithmic mean temperature CST side $\overline{T}_{FC,CST}$ by calling

   function *f02_log_temp* (see algorithm 4);   %Eq. 3.54

Compute actual free cooling module exergy CST side $B_{FC,CST}$;   %Eq. 3.53

```
%Calculate optimization potential index (with computed cold water
 distribution exergies in algorithm 9)
```
Compute OPI_{CST};   %Eq. 3.45

Compute OPI_{CST}^{acc};

Algorithm 11: Function *f16_OPI_DC_FC.m*

Input: Structure with existing timetables (measurements, calculated exergies and key figures)

Output: Structure extended with new timetables (calculated exergies and key figures of
      subsystem DC in free cooling operating mode)

```
%Calculate free cooling exergies DC side
```
Compute free cooling logarithmic mean temperature DC side $\overline{T}_{FC,DC}$ by calling function

  f02_log_temp (see algorithm 4);   `%Eq. 3.38`

Compute reference free cooling temperature DC side $T^*_{FC,DC}$;   `%Eq. 3.42`

Compute acceptable free cooling temperature DC side $T^{acc}_{FC,DC}$;

Compute actual free cooling exergy DC side $B_{FC,DC}$;   `%Eq. 3.37`

Compute reference free cooling exergy DC side $B^*_{FC,DC}$;   `%Eq. 3.41`

Compute acceptable free cooling exergy DC side exergy $B^{acc}_{FC,DC}$;

```
%Calculate exergies of auxiliary devices
```
Compute actual circulating pump exergy $B_{el,CP,DC}$;   `%Eq. 3.40`

Compute reference circulating pump exergy $B^*_{el,CP,DC}$;   `%Eq. 3.44`

Compute acceptable circulating pump exergy $B^{acc}_{el,CP,DC}$;

Compute actual dry cooler fan exergy $B_{el,DC}$;   `%Eq. 3.39`

Compute reference dry cooler fan exergy $B^*_{el,DC}$;   `%Eq. 3.43`

Compute acceptable dry cooler fan exergy $B^{acc}_{el,DC}$;

```
%Calculate optimization potential index
```
Compute OPI_{DC};   `%Eq. 3.36`

Compute OPI^{acc}_{DC};

Algorithm 12: Function *f17_OPI_FC.m*

Input: Structure with existing timetables (measurements, calculated exergies and key figures)

Output: Structure extended with new timetables (calculated exergies and key figures of
      subsystem FC)

```
%Calculate reference and acceptable free cooling exergies CST
 side
```
Compute reference free cooling temperature CST side $T^*_{FC,CST}$;   `%Eq. 3.56`

Compute acceptable free cooling temperature CST side $T^{acc}_{FC,CST}$;

Compute reference free cooling exergy CST side $B^*_{FC,CST}$;   `%Eq. 3.55`

Compute acceptable free cooling exergy CST side exergy $B^{acc}_{FC,CST}$;

```
%Calculate optimization potential index (use computed actual free
 cooling exergies CST side from algorithm 10)
```
Compute OPI_{FC};   `%Eq. 3.52`

Compute OPI^{acc}_{FC};

FOLIO ADMINISTRATIF

THESE DE L'UNIVERSITE DE LYON OPEREE AU SEIN DE L'INSA LYON

NOM : BRENNER   DATE de SOUTENANCE : 24.02.2021

Prénoms : Lorenz Hermann

TITRE : Exergy-based performance assessment and optimization potential of refrigeration plants in air-conditioning applications

NATURE : Doctorat   Numéro d'ordre : 2021LYSEI014

Ecole doctorale : ED162 MEGA (Mécanique, Énergétique, Génie civil, Acoustique)

Spécialité : Thermique énergétique

RESUME :
Une grande partie de la consommation d'énergie dans les bâtiments est due aux systèmes de chauffage, de ventilation et de climatisation. Entre autres systèmes, les systèmes de réfrigération font l'objet de mesures d'amélioration de l'efficacité. Néanmoins, les conditions opérationnelles réelles de ces installations et leurs performances doivent être connues, ainsi que tout potentiel d'optimisation éventuel, avant que des améliorations puissent être réalisées. Les analyses exergétique et énergétiques ont été largement utilisées pour évaluer la performance des systèmes de réfrigération. Entre autres, l'efficacité exergétique est utilisée comme indicateur pour déterminer la performance du système, mais les valeurs réalisables dans la pratique sont inconnues. Par conséquent, ce travail propose une méthode d'évaluation pratique des systèmes de réfrigération basée sur une analyse exergétique et des normes techniques comme base de référence. L'identification des améliorations possibles est pertinente dans la pratique, car les mesures qui améliorent l'efficacité du système permettent probablement d'éviter de fréquentes déficiences pendant l'usage. Avec l'*optimization potential index* (OPI) introduit dans cet ouvrage, les améliorations réalisables par rapport à l'état de l'art de la technologie et la performance sont identifiées d'un seul coup d'œil, quelle que soit la complexité du système. En divisant l'installation en différents sous-systèmes, chacun peut être évalué individuellement. Les non-spécialistes peuvent facilement déterminer l'état de fonctionnement du système et ensuite, si nécessaire, lancer une analyse détaillée ainsi que des contre-mesures appropriées. De plus, la modélisation est considérée comme une méthode appropriée pour déterminer des valeurs de référence si aucune n'est disponible selon les normes techniques. Parmi les différentes techniques de modélisation, les modèles *artificial neural network* révèlent les meilleures performances pour l'application présentée. L'application, la fonctionnalité et l'objectif de la méthode présentée sont illustrés par deux cas numériques et sur une installation réelle. La recherche révèle un fonctionnement approprié de l'installation étudiée en général, où trois des sept espaces conditionnés ont des problèmes de performance. La raison devrait être identifiée dans une étude détaillée ultérieure. Dans l'ensemble, l'apport d'exergie électrique auxiliaire est du même ordre que l'apport d'exergie thermique. Cela souligne l'importance de réduire la consommation d'énergie électrique au minimum, car elle constitue le facteur principal dans le coût d'exploitation des installations de réfrigération et permet également d'augmenter la performance du système. En outre, les concepts de mesure des systèmes réels sont analysés et les coûts de mise à jour correspondants pour l'application de l'approche présentée sont identifiés. Il est démontré qu'une mise à jour de l'instrumentation peut être rentable, si l'installation frigorifique comprend déjà un concept de mesure proche de l'état de la art.

Mots-clés : méthode d'évaluation du potentiel d'optimisation, analyse exergétique, installations de réfrigération à compression de vapeur, *optimization potential index*, OPI, *free cooling*.

Laboratoire de recherche : CETHIL (Centre d'Énergétique et de Thermique de Lyon)

Directeur de thèse : Christian GHIAUS

Président de jury : Ursula EICKER

Composition du jury : Adrian BADEA, Patrice JOUBERT, Frank TILLENKAMP
Invité : Ruello RUBINO